The Effect of Hydration on Enzyme Activity and Dynamics

A thesis
submitted in partial fulfilment
of the requirements for the Degree of
Doctor of Philosophy in Biological Science at the
University of Waikato by

Murielle Lopez

The University of Waikato
Te Whare Wānanga o Waikato

2008

ABSTRACT

Water has long been assumed to be essential for biological function. To understand the molecular basis of the role of water in protein function, several studies have established a correlation between enzyme activity and hydration level. While a threshold of hydration of 0.2 *h* (grams of water per gram of dried protein) is usually accepted for the onset of enzyme activity, recent works show that enzyme activity is possible at water contents as low as 0.03 *h* (Lind *et al*., 2004). Diffusion limitation in these experiments was avoided by monitoring enzyme-catalyzed hydrolysis of gas-phase esters. However, since water is also a substrate for the enzyme used in these experiments, they cannot be used to probe the possibility of activity at zero hydration. However, the pig liver esterase and *C. rugosa* lipase B are able to catalyse alcoholysis reactions in which an acyl group is transferred between an ester and an alcohol. Therefore, by following this reaction and using a gas phase catalytic system, we have been able to show that activity can occur at 0 g/g. These results led to the question of the accuracy of determinations of very low water concentrations; i.e., how dry is 0 g/g? Although gravimetric measurements of the hydration level do not allow us to define the anhydrous state of the protein with sufficient sensitivity, using ^{18}O-labeled water, we have been able to quantify the small number of water molecules bound to the protein after drying, using a modification of the method of Dolman *et al*. (1997). Testing different drying methods, we have been able to determine a level of hydration as low as 2 moles of water per mole of protein (equivalent to 0.0006 *h* in the case of pig liver esterase) and have shown that in the case of the pig liver esterase, activity can occur at this hydration level.

At the molecular level, if the hydration level affects activity, we can expect an effect on the protein dynamics. Neutron scattering spectra of hydrated powders, for instance, show that diffusive motions of the protein increase with the hydration (Kurkal *et al*., 2005) To address the question of the protein motions involved in the onset of enzyme activity at low hydration, we performed neutron scattering experiments on a pico-second time scale on dried powders. Preliminary results show a dynamical transition at hydration levels as low as 3 *h*. Molecular

dynamic simulations have also been used in this study to access the dynamics of the active site.

Overall, the results here show that pig liver esterase can function at zero hydration, or as close to zero hydration as current methods allow us to determine. Since the experimental methodology restricts this work to a small number of enzymes, it is unlikely that it will ever be possible to determine if all enzymes can function in the anhydrous state: however, the results here indicate that water is not an obligatory requirement for enzyme function.

RÉSUMÉ

L'existence d'une activité enzymatique résiduelle après lyophilisation de produits alimentaires a été à l'origine de la plupart des études portant sur l'effet de l'hydratation sur l'activité enzymatique. Ces travaux ont abouti à l'éclaircissement du rôle de l'eau au niveau moléculaire dans la fonction des protéines. Plusieurs études ont en effet révélé l'existence d'une corrélation entre le taux d'hydratation de l'enzyme et son activité. Le paradigme d'une hydratation minimale de 20% (g/g) requise pour l'initiation de l'activité enzymatique a longtemps prévalu alors que de récents travaux ont montré que l'activité était possible à des taux d'hydratation de 3% (g/g). La diffusion des substrats en absence d'eau ou de solvants organiques a été rendue possible par l'émergence de systèmes catalytiques en phase gazeuse. Cette avancée technologique pose aujourd'hui la question de l'activité enzymatique en milieu anhydre. Lind *et al*. (2004) ont étudié l'hydrolyse d'esters volatiles par l'estérase de foie de porc et la lipase B de *C. rugosa*. Cette réaction, impliquant l'eau comme un des substrats, ne permettait pas de tester la possibilité d'une activité enzymatique en conditions anhydre. Or, ces deux enzymes peuvent également catalyser l'alcoolyse qui implique le transfert d'un groupement acyle entre un alcool et un ester. Par conséquent, le suivi de cette réaction en phase gazeuse nous a permis, dans le cadre de ce doctorat, d'élucider cette problématique. Toutefois, quelle est la signification de 0% (g/g) d'hydratation au niveau moléculaire? Les mesures d'hydratation gravimétriques ne permettent pas en effet de certifier une protéine sèche de façon absolue. L'utilisation d'eau enrichie en oxygène 18 et de la méthode de quantification des molécules d'eau développée par Dolman *et al*., (1997) a permis l'estimation, avec une grande précision, du nombre de molécules d'eau liées à la protéine après un séchage intensif. La corrélation entre l'hydratation et l'initiation de l'activité enzymatique a permis d'établir que seulement deux molécules d'eau par molécule de protéine pourraient induire une activité.

Le taux d'hydratation, l'initiation de l'activité et la dynamique des protéines ont été corrélés par l'existence d'une transition dynamique moléculaire. Les spectres de diffusion de neutron sur des poudres hydratées ont montré que les

mouvements diffusifs des protéines augmentaient avec l'hydratation (Kurkal *et al*., 2005). Toutefois, les mécanismes impliqués dans le déclenchement de l'activité enzymatiques restent flouent. Pour tenter de résoudre ces questions, nous avons réalisé des expériences de diffusion de neutron à de faibles taux d'hydratation et à différentes échelles de temps (ps et ns). Des résultats préliminaires ont montré l'existence d'une transition dynamique à des taux d'hydratation de 3 % (g/g). L'approche de dynamique moléculaire au niveau local du site actif a également été étudiée grâce la simulation de dynamique moléculaire.

PREFACE

The research for this thesis was conducted as part of an international collaboration to study the relationship between protein dynamics and enzyme activity. The group leaders are Prof. Roy Daniel, Prof. John Finney and Prof. Jeremy Smith, who provide expertise on enzyme catalysis, protein-water interactions, and molecular dynamics simulations, respectively. Due to the collaboration between groups, the research is obviously divided, with each group primarily contributing to their area of expertise. My role in the collaboration was primarily related to the gas phase activity studies of several enzymes, to enable comparison with the dynamic data. I was also involved in the optimisation of enzyme assay procedures.

In many parts of this thesis, my own work has been placed in the context of the overall research effort. Where this has occurred, a clear distinction is made as to who conducted each part of research. It is felt that the presentation of the work in this context is necessary to enable the rationale for the conclusions to be evident. In Chapter Two, Stephen Cooke, a specialist at Waikato University, assisted with the mass spectrometer analyses. I did the water molecule quantification as well as the sample preparation and processing. Chapter III and IV were all my own work. Chapter V and VI are the results of a collaborative work between Waikato University, UCL (London, UK) and the CMB (Heidelberg, Germany). The neutron scattering data were analysed by collaborators although I was present and assist the sample loading and analysis at both I.L.L. and F.R.M. II, while the sample preparation was all my own work. The molecular dynamics simulations, described in chapter V, were carried out by myself at the CMB institute (Heidelberg, Germany) during my short term EMBO Fellowship.

ACKNOWLEDGMENTS

I would first like to thank my supervisor, Roy Daniel, who offered me the opportunity to work on this exciting project and to live this wonderful experience in New Zealand. I also thank him for the encouragement and patience he has shown throughout this study. I would like to thank my second supervisor, Rachel Dunn, for her continual guidance in science as well as in physical training. I am also very grateful to Colin Monk, for his technical assistance on a daily basis even during weekends. I would like to thank David Clement, my workmate and friend, for his great advices. I must thank Moeava Tehei, who first motivated me to join the group and who made me eager to learn more about protein dynamics. I also would like to thank all my lab mates for making the laboratory an entertaining and friendly environment.

I am also grateful to the many people in the Chemistry Department who let me use their equipments. In particular, I would like to thank Chris Hendy for his expertise in isotopic labelling and letting me use the vacuum line. Also a great thank to Steve Cooke who performed the mass spectrometry analysis and gave me the literature about isotopes.

I would also like to thank the Marsden Fundation for the Study Award, and the E.M.B.O. for the short termed fellowship award, which made my visit to CBM at IWR, Heidelberg, possible. Also to be thanked are Jeremy Smith, who invited me in his group to learn some Molecular Dynamics simulation basis, and Vandana Kurkal-Siebert for the time and the guidance she offered me there.

I would like to address a special thank to my parents. I would like to thank my dad for his pride and his financial support. Then I would like to thank my mom for her encouragements and great psychological support. I also would like to thank my friends Wade Tozer, Bundschu Alena, Lee-Anne Rawlinson, Rochelle Soo, Bogdan Costescu and others…for their love and support.

TABLE OF CONTENTS

LIST OF FIGURES

LIST OF TABLES

LIST OF ABBREVIATIONS

As	Specific enzyme activity (nmol.min^{-1}.mg^{-1})
A.S.A	Accessible surface area
Aw	Water activity
BSC	Backscattering spectrometer
BSA	Bovine Serum Albumin
CRL	*Candida rugosa* Lipase
DSC	Differential Scanning Calorimetry
EISF	Elastic Incoherent Structure Factor
FID	Flam ionization detector
GC	Gas Chromatography
h	Water content (g H_2O.g^{-1} dried protein)
HS	Headspace
Lip 1 or 3	Isoenzyme of C. rugosa lipase B encoded by the genes *lip 1* or *lip 3*, respectively
MD	Molecular Dynamics
MQ water	Water purified with a Millipore® system
MS	Mass Spectrometry
MSD	Mean Square Displacement
n-OG	n-Octyl Glucopyranoside
NMR	Nuclear Magnetic
PDB	Pee Dee Belemnite
PLE	Pig Liver Esterase
$_P$NPB	*para*-Nitro-phenyl butyrate
$_P$NP	*para*-Nitro-phenol
QENS	Quasi-Elastic Neutron Scattering
RH	Relative Humidity
SMOW	Standard Mean Ocean Water
Tg	Glass transition temperature
TOF	Time of Flight
V-SMOW or PDB	V stands for Vienna SMOW or PDB

CHAPTER I: INTRODUCTION

Water is widely assumed to be essential for life. Although water is the main constituent of all living organism, is this assumption well founded? The most obvious reason for this assumption is that life is not found in the absence of water. In addition, water is the only liquid inorganic solvent available at ambient temperature. Solvents are needed for biochemical reactions to occur. They provide a fluid medium for the reactants to circulate and interact. They also allow the interaction of important bio-molecules such as enzymes with other molecules or chemicals. Enzymes, the catalysts of biological systems, are remarkable molecular devices that determine the pattern of chemical transformation. They accelerate reactions by factors of at least a million, reactions that would not occur at a perceptible rate without enzymes: they are the machinery of life. So, it is no surprise that life is dependent upon water on earth. But at a molecular level, is water essential to life? Is there a potential for some other solvent to replace it, or are the special properties of water absolutely required?

In enzyme catalysis, water may play different roles. Water is found in and around the protein. The properties of water molecules that interact with the protein were shown to exhibit different properties and thus to play a major role on bio-molecules. These water or 'structural' water molecules were found to have a different role related to their location (Gronenborn and Clore, 1997 ; Williams *et al.,* 1994). The 'internal' water molecules that are found in deep clefts and cavities of the protein are viewed as an integral structural element of the protein (Franks, 1993 ; Gronenborn and Clore, 1997). They are also found to be important in stabilizing the native state of the protein through hydrogen bonding with the protein (Baker and Hubbard, 1984 ; Meyer, 1992). 'Surface' water has been found to play a major role in protein function. Another important role of water in enzyme catalysis is that water offers a diffusion medium to the substrates and products for their free circulation. The absence of such media is a limiting factor to the enzyme activity but also to the study of the effect of low hydration on the catalytic activity. There is evidence that many enzymes become active only once a 'threshold' hydration of the enzyme surface has been reached, typically *ca*. 0.2

$gH_2O.g^{-1}$ protein (for lysozyme) or a mole ratio of water : protein of greater than 150. For most small globular proteins this leads to 30–50% coverage of the surface, and coverage of most of the polar groups on the protein surface. Finally, the involvement of water in enzyme catalysis might be in two different ways. Firstly, water might be a reactant of the reaction itself. However, it is not the case of all reactions, as in the case of the ester transesterification catalysed by many lipases and esterases. Water is also involved in the thermodynamics of the reaction. In fact, the energy released upon water displacement would lower the energy of activation barrier of the enzyme.

It is widely accepted that dried enzymes are inactive and rigid. Studying the roles of the water of hydration with respect to enzyme activity and dynamics is technically challenging. However, as the techniques are improved, our understanding of the role of water in relation to enzyme activity and dynamics might change. For instance, even though a threshold of 0.2 g $H_2O \bullet g^{-1}$ protein is widely accepted for the onset of activity, the question is still not fully resolved. The first approach was to rapidly mix substrate and enzyme in solution, followed by lyophilisation, and finally to measure the modification of the resulting powder composition due to enzymatic activity. However, a drawback with this technique is that it may be providing information on product release rather than catalysis, and it is likely to be strongly diffusion limited. The use of enzymes in organic media has been another approach to a better understanding of the role of water in enzyme activity. A number of publications indicate that activity may be possible at very low hydration (Valivety *et al*., 1992 ; Graber, Bousquet-Dubouch, Lamare *et al*., 2003 and Lind *et al*., 2004). But the possibility that solvent molecules might replace water at the protein surface complicates the interpretation of results. Gas phase catalysis systems offer the advantage of good hydration control and the absence of diffusion limitation. Graber, Bousquet-Dubouch, Lamare *et al*. (2003) and Lind *et al*. (2004) used this system to study the effect of hydration on enzyme kinetics. As shown in our laboratory with the pig liver esterase, enzyme activity has been observed at water content as low as 0.03 g $H_2O \bullet g^{-1}$ protein (Lind *et al*., 2004). A gas/solid bioreactor was developed to be able to investigate the enzyme activity in a near anhydrous environment. However, this study posed the question of the dryness of the supposedly anhydrous protein.

If the hydration dependency of the activity and dynamics has been well characterised, the correlation between dynamics and activity remains relatively unexplored. Although it has been shown that certain proteins cease to function below the dynamical transition and that the dynamical transition is caused by the diffusive motions arising from the interaction between the protein and water, recent work at low water content questions this idea. If an increase of the activity with hydration is correlated with an increase of the protein softness, the onset of the activity in the case of the pig liver esterase at low hydration does not match with the appearance of diffusive motions (Kurkal *et al*., 2005).

The intent of this work is to investigate whether enzyme activity is possible in anhydrous or near-anhydrous conditions, and to investigate the effect of such hydration on the dynamics of enzymes. The clarification of the way that water interacts with bio-molecules may suggest the possibility of life without water. It is not surprising to find life depending upon water on Earth because of its abundance. But what would have evolved in a different environment? If this project brings up more philosophical questions, it also provides answers to industrial needs. Indeed, it requires the investigation of new techniques such as the use of catalyst in a gas/solid bioreactor, which might be useful in industry areas such as bioremediation.

1. *Protein hydration: definition*

The hydration water usually corresponds to the surface water. Thus, to investigate the hydration process, some authors have tried to differentiate between the different "types" of water. In the liquid phase, water molecules interact with each other to give a well defined network in which each water molecule will ideally be surrounded by four hydrogen-bonded neighbours (Franks, 1993). The presence of proteins will break this structure to create new water-protein interactions leading to another hydrogen-bonded network at the protein surface. Thus, some physical properties of water are disturbed creating different types of water. Eisenberg and Kauzmann (1969) only differentiated between the "bound water" and the "bulk water" when they looked at thermodynamic properties. While in another review, Gronenborn and Clore (1997) described two types of water: internal and surface water, where internal water is defined as the water providing specific structural interactions, or located in internal cavities, and the surface water is defined as very mobile water. Cooke and Kuntz, (1974) and Kuntz and Kauzmann, (1974) looked more specifically at the water-protein interactions, and distinguished three kinds of water molecules: those reasonably tightly bound involved in protein structures like enzyme active sites, others with a low mobility, and finally, a third category of water presenting similar properties to bulk water. These definitions apply to protein in solution. Careri and Peyrard (2001) discussed about weakly hydrated powders and the water molecules bound to the protein by hydrogen bonds to charged and polar sites of the protein. These authors highlighted the existence of a critical water content for the proton conductivity, which coincides with that observed for the onset of biological activity, and thus the relevance of water dynamics to protein function.

1.1. Water activity and relative humidity

The amount of water bound to the protein is likely to depend on the amount of water available for the hydration. For instance, it is observed that when the amount of water in the environment of the protein is increased the amount of hydration water is increased as well (Bull, 1944). Therefore, quantifying the water

in the immediate environment of the protein is relevant to the investigation of the hydration process.

Water activity and relative humidity are often used to indicate the amount of water in the immediate environment of proteins.

When water interacts with solutes and surfaces, it is unavailable for other hydration interactions. The term 'water activity' describes the amount of water available for hydration of proteins.

$$a_w = \lambda_w \bullet X_w = p/p_0$$

a_w = water activity

λ_w = activity coefficient of water

x_w = mole fraction of water in the aqueous fraction

p = partial pressure of water above the material

p_0 = partial pressure of pure water at the same temperature

The relative humidity is an indication of the moisture content of the air. It is defined as the ratio of water vapour density to the saturation water vapour density usually expressed in percentage:

$$RH = \frac{Actual\,vapor\,density\,(g/m^3)}{Saturated\,vapor\,density\,(g/m^3)} \bullet 100$$

It is also approximately the ratio of the actual to the saturation vapour pressure and so it can be expressed as the percentage of water activity:

$$RH \approx a_w \bullet 100$$

The hydration of a protein is often expressed in terms of the relative humidity it has been exposed to. However this presupposes that the hydration isotherm of all proteins is the same, which is not the case (Bull, 1944).

1.2. Expression of protein hydration

In turn, the amount of water bound to the protein can be directly expressed as grams of water per gram of dry protein, or h. However, it is only a gravimetric measure and does not reflect the effect of water on the protein properties.

$$h = m_w / m_{dp}$$

m_w: mass of bound water (g)

m_{dp}: mass of dry protein (g)

The hydration is also often expressed as a percentage of hydration (w/w). It is equal to:

$$\% \ hydration = \frac{w_w}{w_p}$$

where w_w is the weight of water and w_p the total weight of the protein. Thus, the values obtained are slightly different from the percentage, which would result from the simple multiplication of *h* by 100.

In fact, the effect of hydration on the protein is likely to depend upon the percentage of the protein surface covered. Enzyme activity has been observed under the monolayer coverage. In addition, it is known that in the hydration process residues are sequentially hydrated primarily as a function of their polarity (Rupley and Careri, 1988). The type of the residue hydrated might be relevant for activity. Indeed, the same value of *h* for proteins of different size will correspond to a different surface coverage (Table I-1).

Table I-1: Relationship between protein hydration and percentage surface coverage, compared with lysozyme (Dunn and Daniel, 2004).

	percentage surface coverage at:				
protein M_r (and accessible surface area[b], A_s)	$h = 0.02$ (H_2O : protein mole ratio)	$h = 0.10$ (H_2O : protein mole ratio)	$h = 0.20$ (H_2O : protein mole ratio)	$h = 0.4$ (H_2O : protein mole ratio)	$h = 0.6$ (H_2O : protein mole ratio)
5000 (A_s = 2823 Å^2)	3.0% (5.6)	15% (27.8)	31% (56)	59% (111)	89% (167)
14 250 (lysozyme) (A_s = 5670 Å^2)	4.1% (16)	21% (79)	41% (158)	84% (317)	126% (475)
30 000 (A_s = 9299 Å^2)	5.2% (33)	27% (167)	54% (333)	109% (667)	162% (1000)
60 000 (A_s = 14 799 Å^2)	6.7% (66)	33% (333)	67% (667)	134% (1333)	202% (2000)

[a] The percentage coverage was calculated assuming the surface coverage of a water molecule of 1.5 Å^2. The mole ratio of water : protein is also given in parentheses.
[b] The accessible surface area was calculated taking the accessible surface area of lysozyme as 5670 Å^2 (Golton 1980), and assuming an identical surface area/radius for the other proteins, and that they are spherical, monomeric, and with a volume approximately equal to 1.27 (Mr) Å^3.Da^{-1} (Creighton 1993). The figures are thus indicative and comparative only.

The table above shows considerable differences between the surface coverage. Larger percentages of surface coverage are reached in larger proteins compared to smaller proteins at the same hydration. This is explained by the fact that proteins are folded in a way that minimizes their interaction with the surroundings. However, most protein interiors make contact with the solvent. In addition, as indicated by the etymology of the word protein, proteins have different shapes and are not completely spherical. Thus, the estimate of the protein

surface coverage underestimates the protein surface that interacts with the solvent (Gates, 1979). It is usual to quantify the protein surface by the accessible surface area (A.S.A.), defined as the locus of the centre of a solvent molecule as it rolls along the protein surface making the maximum possible contact. It is calculated from atomic co-ordinates of high-resolution and well-refined crystal structures (Lee and Richards, 1971). The A.S.A. has been directly related to the hydrophobic free energy (Chothia, 1974; 1975). An acceptable approximation of the accessible surface is however offered for roughly spherical proteins by a power factor of the molecular weight as described by the following formula (Miller *et al*., 1987):

$$A_s = 6.3 \bullet Mr^{0.73}$$

A_s = Accessible surface area

Mr = Molecular weight

Teller (1976) proposed a model to estimate the A.S.A. buried on protein association. It should be noted that the 'accessible surface area' determination is a matter of some debate related largely to assumptions made about the 'radius' of the 'rolling solvent' water molecule and the assumed reticular density of the solvent molecules 'packing' in this surface. For instance, early work assumed a solvent radius of 1.4 Å taken as half of the water-water closest approached distance in ice. However, this distance is more like 3.0 Å in liquid water. Assuming water to be more like liquid than ice, thus a value of 1.5 Å might be better (Finney *et al*., 1979). In the Table above, a value of 2.2 Å has been used. Another problem is that water can act as either a donor or acceptor of hydrogen bonds. Depending on the case, the distance from the 'surface' of the protein groups will be different, thus a constant radius of the rolling solvent could introduce further uncertainties. The accessible surface area measured depends as well on the reticular density value of the water molecules 'packed' into the surface area. This value for liquid water is about 50 % of that of a close rearrangement of water molecules would have (Finney, 1975; 1978 ; Gellatly and Finney, 1982)).

In this thesis, the hydration level has been expressed as *h* or moles of water per mol of protein when these can be derived from the published measures.

1.3. Control and measurement of hydration

The hydration process is the incremental addition of water to dry macromolecules. To study this process, an essential preliminary step is to remove

the water. Dry protein powders can be obtained by a variety of methods, for example, by freeze-drying (Seligmann and Farber, 1971). To reach the desired hydration, the protein powder is then equilibrated under a controlled relative humidity (Bull, 1944).

A specific relative humidity can be selected by addition of different agents able to reduce water vapour concentration. For instance, sulphuric acid, glycerol or saturated salt solutions are mixed with water to reduce its activity. These agents being only in the liquid phase, they dilute the water and hinder escape of water molecules into the air. The system therefore adjusts to equilibrium where there are fewer water molecules in the air than there would be over a pure water surface. The RH is therefore lower than 100%.

Saturated salt solutions are convenient because a variety of salts can regulate a wide hydration range from 6.7 to 100 % (Greenspan, 1977 ; Hutcheon *et al.,* 1994). Below 3 % RH, desiccants such as phosphorus pentoxide (Henry *et al.,* 1967) are normally used. They either decrease the RH by trapping the water or reacting with it. The weakness of the first kind of desiccant is the uncertainty of the protein hydration level achieved (Valivety, Halling, Peilow *et al.,* 1992). A dramatic acid-base effect of molecular sieves on enzyme activity has also been described (Fontes *et al.,* 2002). In both cases, the purity grade influences their efficiency in drying. A level of zero hydration has for instance been reported by Dolman *et al.* (1997) with a high purity grade of phosphorous pentoxide.

Table I-1 Relative Humidity over different saturated salt solutions or desiccants at 25 C measured or taken from the CRC handbook (a) and the water adsorption measured for PLE and lipase B.

Saturated Salt Solution or Desiccant	*RH (%)*	*PLE hydration level (h)*	*Lipase B hydration level (h)*
P_2O_5	0.02	0	0
LiBr	6.5	0.034	0.046
LiCl	10.3	0.046	0.056
KAc	22.5 [a]	-	-
$MgCl_2$	31.8	0.073	0.102
COOK	43.2 [a]	-	-
NaBr	57.1	0.141	0.172
KI	68.9 [a]	-	-
NaCl	75.0	0.201	0.297
$ZnSO_4$	88.5 [a]	0.301	0.515
KSO_4	97.3 [a]	-	-
H_2O	100	0.822	-

The saturated salt solutions, although quite reliable, need to be handled with care. Some of them are toxic or partially volatile and might interact with the protein. It is then recommended to test them before use. The saturated salt solutions used here were commonly used in the laboratory and no colouring of the protein or protein denaturation was observed. In addition, the relative humidity reached depends on the temperature, thus to get reproducible data the temperature has to remain constant (O'Brien, 1948) during the equilibration period, which may be several days. Finally, depending on the length of the experiment, it is also necessary to make sure that the solution remains saturated. Once the hydration level established by isopiestic equilibration of protein powders is reached, the uptake of water is usually measured by gravimetric methods or Karl Fisher titration (AQUASTAR, Tech Notes).

2. *Protein thermodynamic properties affected by hydration*

A limited number of reviews are available that describe the techniques used to study the properties of pure water or water interacting with proteins (Kuntz and Kauzmann, 1974 ; Rupley and Careri, 1991 ; Rupley *et al.*, 1983 ; Rupley *et al.*, 1980).

Thermodynamics is the science involved in the relationships between work and heat. In the water-protein interaction, two forces drive the binding energy (or Gibbs free energy): the enthalpy and the entropy. The enthalpy represents the internal energy of a system while the entropy describes its disorder. The binding energy can be measured by the Gibbs free energy changes (ΔG) between unbound and bound water through this equation:

$$\Delta G = \Delta H - T\Delta S$$

ΔG = Gibbs free energy changes

ΔH = Enthalpy changes

T = Temperature

ΔS = Entropy changes

The free energy associated to the excess of hydration of protein is directly observed on melting profiles and is correlated to the melting temperature (Mitra and Chattoraj, 1978).

2.1. Free Energy

Gibbs free energy is the thermodynamic potential for a system under the constraints of constant temperature and constant pressure. The free energy of hydration is determined by sorption isotherms, which are a measure of the weight of water absorbed by a protein sample as a function of the partial pressure of water in the vapour phase at constant temperature (Bull and Breese, 1968).

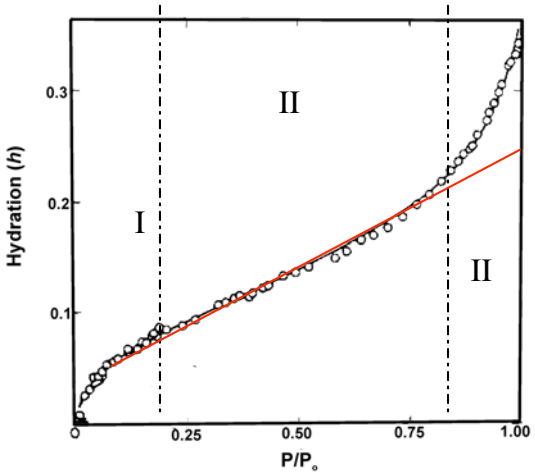

Figure I-1: D_2O sorption isotherm obtained for lysozyme at 27 °C as a function of RH from Dunn and Daniel (2004).

The sorption isotherm of proteins has a sigmoid shape showing a three step process as described by Rupley and Careri (1991) for lysozyme. Typically, the first step (I) starts by a "knee" in the sorption isotherm at 0.05 *h* describing the strong interaction of water with the charged groups of the protein surface. Following this is a plateau, between 0.1 and 0.25 *h*, which reflects the accumulation of water onto polar sites (II). Finally, the "upswing' above 0.25 *h* (III), indicates the completion of the hydration process by water condensation onto the weakest points of interaction.

Another characteristic of protein isotherms is that they typically exhibit hysteresis due to a poorly defined equilibrium.

The sorption isotherms can also be performed in organic media (Halling, 1990). The comparison with those performed in water shows that at low water content (a_w< 0.4) adsorption isotherm are similar. Thus, the presence of organic solvent has a little effect on the tightly bound water.

2.2. Enthalpy

The enthalpy is a thermodynamic state function usually measured as heat transferred to or from a system at constant pressure. The enthalpy changes are determined from the temperature dependence of the sorption isotherm.

Measurements of enthalpy have shown that at 0.2 *h* or higher hydration, the value of the enthalpy reached by a protein solution is equal to that of pure

water, while at lower hydration it is higher (Berlin *et al*., 1970 ; Rupley *et al*., 1980). Liltorp *et al*. (2001) showed, for instance, that lysozyme surface water has higher enthalpy than the "bulk" liquid.

The heat of denaturation can also be extracted from differential thermal analysis (D.T.A) (Steim, 1965). Although protein stability will not be discussed, the temperature at which a protein is denatured is useful to know when discussing protein function.

2.3. The heat capacity

The heat capacity is the amount of heat required to raise the temperature of an object or substance one degree. It specifies the temperature dependency of the enthalpy and entropy functions. The heat capacity isotherm can be measured for a full range of system composition and is sensitive to changes in the chemistry of water. Yang and Rupley (1979) studied the heat capacity changes in the lysozyme-water system and showed four different regions.

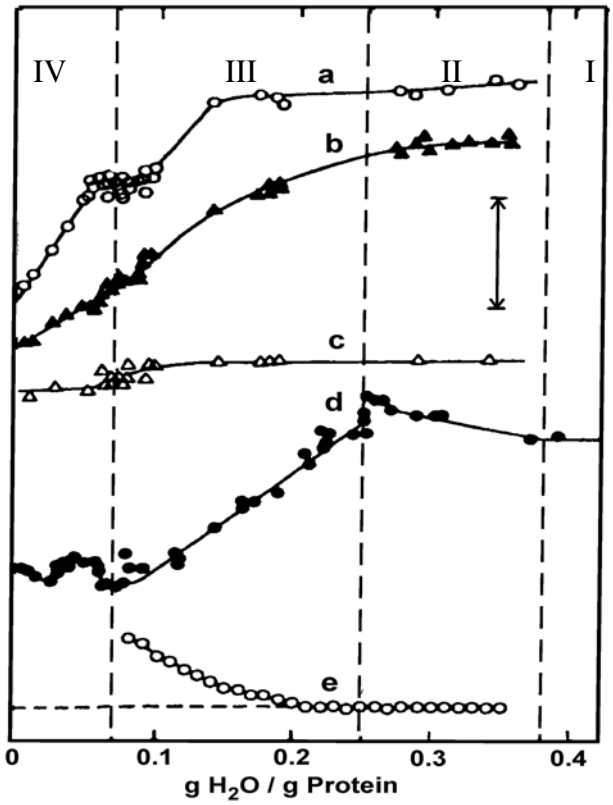

Figure I-2:Effect of hydration on lysozyme. Time-averaged properties, from top to bottom, the curves are: (a) carboxylate absorbance (1500 cm^{-1}); (b) amide I shift (1660 cm^{-1}); (c) OD stretching frequency (2570 cm^{-1}); (d) apparent heat capacity; (e) diamagnetic susceptibility (Careri *et al.,* 1980 ; Rupley and Careri, 1991 ; Yang and Rupley, 1979).

When the apparent heat capacity is expressed as a function of the hydration (Figure I-3), a stepwise hydration process can be observed as in the case of sorption isotherm. The correlation between several methods helped interpretation of these results. Infrared spectroscopy (curves a and b) helped for instance to correlate the rise and fall of the apparent heat capacity at a protein hydration of 0.05 *h* as a proton transfer from carboxylic acid to basic protein groups. The continuous change within region III was inferred to be the binding of water at amide I and carboxylate sites. The second rise and fall observed at the juncture between region III and II was seen as a transition associated with the condensation of water at the weakest binding sites of the protein surface. Then the apparent heat capacity tends to reach the value of dilute solution. At 0.38 *h*, this value is reached and the apparent heat capacity is constant.

3. *Effect of hydration on protein structure and dynamics*

Some introductory concepts on the effect of hydration on structure and dynamics can be found in reviews or text book (Eisenberg, 1990 ; McCammon and Harvey, 1987).

3.1. Hydration water dynamics

3.1.1. Water molecules at the protein surface

A number of reviews are available that discuss the different techniques used to describe these water-protein interactions at the protein surface and how these techniques complement each other to give us a complete picture of the protein hydration (Bernini *et al.,* 2004 ; Franks, 1993 ; Phillips and Pettitt, 1995). Svergun *et al.,* (1998) observed the hydration of three different proteins by X-ray and neutron experiments, and proposed the existence of a first hydration shell with an average density of 10% larger than that of the bulk. These results were further explained by MD simulations (Merzel and Smith, 2002 ; Smith, Merzel *et al.,* 2002). These authors found an increase of 15% of the density of the first hydration shell. They found out that only 5% involved significant changes in the average water structure and the other two thirds were attributed to the geometrical effect of the protein surface. In fact, as the protein surface is approached, the angles between the water dipoles and the protein surface normal are lower and the dipoles align more parallel to each other. At the protein surface, denser regions are found in depressions, and the hydrogen atoms are found closer to the protein surface than the oxygen, showing the effect of the protein topology on the water structure. The difference observed in the first hydration shell was also seen in the water dynamics. Russo *et al*. (2004) with a model protein system performed MD simulations and quasi-elastic scattering (QENS) experiments in two different conditions: first, in infinite diluted conditions where hydration water dynamics are dominated by the bulk water relaxation or diffusion time scale; second, a high protein concentration was used to observe the dynamics of the first hydration shell. It was observed that water molecules of the first hydration shell undergo

slower dynamics than in the bulk, with 'supercooled' diffusion behaviour and a suppression of the rotational motions, while the bulk water molecules possess faster translational dynamics and rotational motion. Bon *et al*. (2002) derived a model for the behaviour of water molecules from hydrated lysozyme triclinic crystals from combined structural and dynamical data. In this model no part of the solvent was behaving as the bulk. Water molecules were found to reorient themselves. Near the protein surface, these reorientational motions are ten times slower than in bulk. Near ordered parts of the protein surface, the reorientational motions are very well defined. Water molecules are also able to jump from their hydration sites to neighbouring sites. The water molecules further away from the protein surface have a confined long-range translational motion. The residence time of water molecules from different hydration layers is affected (Makarov *et al*., 2000).

A hydration site description provides a precise and convenient means to describe the variation of water properties. The study of Henchman and McCammon, (2002) showed for instance that the more a water molecule is buried, then the more its number of neighbours decreases. The buried water molecules are isolated, while the bulk-like water molecules have five neighbours Another remark was that the more buried they are, the greater the number of water-protein hydrogen bonds whereas the closer they are to the bulk, the more water-water hydrogen bonds are found. The dipole moment is found to be largest and more ordered inside the protein structure, because the protein holds the water in place. Moving towards the bulk, this magnitude decreases and the direction of the dipole moment becomes disordered. The residence time is found to increase the more buried the water molecules are. The water molecules jump between sites, with most traffic involving water molecules exchanging with the bulk. There is also movement across the surface: inside the protein jumps are unlikely to occur.

3.1.2. Buried water molecules

Protein function depends on a very specific 3D structure, which is stabilized by non covalent forces such as hydrogen bonds (Franks, 1993). Many authors have tried to quantify and localize these water molecules (Denisov and

Halle, 1995 ; Denisov *et al*., 1995 ; Kudryavtsev *et al*., 2000 ; Modig *et al*., 2004 ; Williams *et al*., 1994).

Those water molecules making mainly water-protein hydrogen bonds are favorable to protein stability (Takano *et al*., 1997). Another good example of the stabilizing effect of bound water is the case of the human dihydrofolate reductase (*h*DHFR) (Meiering and Wagner, 1995). This enzyme forms a binary complex with methotrexate (MTX) and a ternary complex with NADPH. In a NOE's (Nuclear Overhauser Effect) experiments these authors detected five bound water molecules in the first complex and six in the second one. The two first water molecules localized outside the active site form multiple hydrogen bonds between loops and/or secondary structural elements and stabilize the ternary fold of the enzyme. Two other waters, which are localised in the active site, have a different function; the first one bridging the MTX to the protein while the other links the first water molecule to the protein. A third water molecule of the active site would be involved in the protein surface protonation. And finally, the last water molecule, present only in the ternary complex, would hydrogen bond the cofactor to the protein.

Buried water molecules seem to play an important role in protein function. An interesting finding for lipid-binding proteins is that they possess large binding cavities filled with water molecules exchanging with a dynamic two orders of magnitude slower than that of bulk water. These water molecules have been implicated in the strength, the specificity and the kinetics of lipid binding (Modig *et al*., 2004). A more consistent piece of literature is however available on the role of water molecules in bacteriorhodopsin and has been reviewed by Kandori (2000). Water in the case of this protein would participate through a hydrogen-bond network to the induction proton pathway. Several experiments have shed light on the presence of water molecules in the shift base region. The chloride ions are also stabilized, in the case of the chloride pump of the halorhodopsin, by weak hydrogen-bonds (Shibata *et al*., 2004).

3.2. Protein motions

Dynamics is the science that studies the correlation between forces and motion. In the case of protein dynamics, two kinds of forces are involved. First,

the "strong" forces exerted by covalent bonds, which maintain the polypeptide chain, but which are unchained during protein function. Secondly, the "weak" forces, whose energies are similar to thermal energy at usual temperature, play a major role in governing atomic motions in macromolecules. They include hydrogen bonding, electrostatic and Van Der Waals interactions, as well as pseudo-forces arising from the hydrophobic effect (McCammon and Harvey, 1987)

Internal motions confer on the protein its flexibility, which is widely accepted as a requirement for activity. This flexibility arises from the primary structure of proteins and the conformation of the peptide bond. This bond involves the condensation of the α-carboxyl group of the first amino acid with the α-amino group of the following one. The resulting polypeptide chain (refer Figure I-4) is made up of a regularly repeating main chain (backbone) and distinctive side chains (R1, R2, R3…). The bond between the carbonyl carbon atom and the nitrogen atom of the peptide unit is not free to rotate because this link has partial double-bond character. If the peptide unit of the main chain is rigid (dihedral angle ω_2) and planar, there is a large degree of freedom on either side of this peptide unit (dihedral angles ϕ_2 and ψ_2). The rigidity of the peptide bond enables proteins to have well-defined three-dimensional forms. The freedom of rotation on either side of the peptide unit is important because it allows proteins to fold in many different ways. Also, all of the side chains, except glycine, have one or more single bonds about which internal rotation can occur.

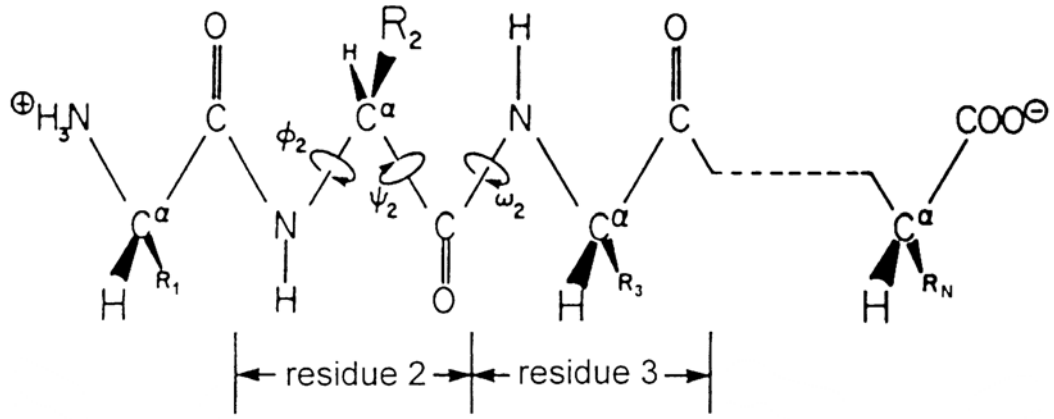

Figure I-3: Structure of a polypeptide chain. The covalent bonds and bond angles are rather rigid, but sizable rotations can occur around certain bonds. The dihedral angles ϕ_i, ψ_i and ω_i, measure the torsion around the bonds in the backbone of residue i. The labels R_i represent the side chains. Reproduced from McCammon and Harvey (1987).

Nonetheless, protein motions are constrained by higher degrees of conformational rearrangement, which induces the formation of some compacted protein units, folding their interacting groups into relatively close proximity while others protein units will have an extended structure. These component fragments also exhibit fluctuations from their lowest energy conformation over a wide range of structural variations from individual atomic vibration to significant tertiary unfolding or "denaturation". Kossiakoff (1985) talked about "regional melting" to describe substantial structure deformation usually caused by hydrogen bond breaking and about "protein breathing" to describe transient local redistribution. This distinction is relevant in the choice of the technique of investigation.

However the classification of the protein motions might be more or less complicated depending on the authors. For instance, Toussignant and Pelletier (2004) described three classes of internal protein motion as a function of their time scale, amplitude and energy variation. The first class corresponds to the local motions on a time scale range of 10^{-15}-10^{-1}s. It includes motions such as atomic fluctuation, side chain motion, loop motion and terminal arm motion. The second class is represented by rigid body motion (10^{-9}-1s). In this case, a small part of the protein moves in relation to another, affecting the energy barrier at the transition state. And the third class, large-scale motions, involves the same kind of motions as in the second class but that occur on a greater time scale (10^{-7}-10^{4}s). Daniel, Dunn *et al*. (2003) in their review, distinguished between fast fluctuations and soft

modes in respect to their time scale. The table I-2 below gives a good summary of the range of time scales and the amplitudes of protein motions.

Table I-2 Time scale and amplitude of protein motions.

Time scale (s)	Amplitude (Å)	Motions
10^{-15}-10^{-12}	0.001-0.1	Bond stretching Angle bending Constraint dihedral motion
10^{-12}-10^{-9}	0.1-10	Unhindered surface side chain motion Loop motion Collective motion
10^{-9}-10^{-6}	1-100	Folding in small peptides Helix coil transition
10^{-6}-10^{-1}	10-100	Protein folding

3.3. Effect of hydration on protein motions

This will be further discussed in the introduction of the chapter on the effect of hydration on enzyme dynamics (Chapter V). However, a more general view here is based on the review of Doster and Settles (2005). Liquids possess short-range and long-range translational diffusion; their molecular displacements are continuous and isotropic. For proteins, short-range motions correspond to molecular diffusion, while long-range ones are ordered. Thus, internal displacements are discontinuous, rotational and anisotropic. Water acts as a plasticizer to protein motions by increasing the protein conformational space, the friction and the effective barrier height. Upon dehydration, an infinite viscosity is observed that corresponds to a glassy state where the absence of intermediate and long-range diffusion is observed. A dynamical transition has been described when studying the mean square displacement of protein atoms as a function of the temperature. This transition seems to occur at the glass transition temperature (Tg) of the solvent. Below this temperature, proteins behave as solids; they are rigid and possess only rotational transition of the side chains. Above Tg, protein motions are rubber-like. Water introduces fluctuations; it decreases the entropy destabilizing the native state of the protein. Then, the effect of water on protein

dynamics is seen on a picoseconds time scale, where the hydrogen bonds are broken and formed. Therefore, there are two types of protein displacements, torsional and continuous ones, and water assisted motion. The latter is composed of fast hydrogen bond fluctuations and slower small-scale displacements.

In the same way, Dellerue *et al*. (2001) combined quasi-elastic neutron scattering and MD simulations to characterize the diffusive motions of different parts of hydrated C-phycocyanin. They made two important observations on the internal protein dynamics. First, there is a marked difference between the dynamics of the side chains and the backbone. The mean square displacement (MSD) being smaller for the backbone and its relaxation behaviour showing a diffusive regime reached at higher q2 range than for the side chain, the protein dynamics picture is found as a "hard" backbone and "soft" side chains. Second, there is a smooth decrease of mobility moving towards the interior of the protein, showing a 'radially softening' of the dynamics. Zanotti *et al*. (1999) studying the influence of hydration on protein internal dynamics showed that water-protein interactions at the protein surface affect the dynamics in a global manner. They observed a progressive induction of mobility as the water content increased from the periphery to the protein interior.

4. *Effect of hydration on enzyme activity*

Enzymes, as any proteins, require a very specific 3D structure to function. Protein folding produces a surface that maximises or minimizes perturbation protein-water interactions in such a way as to minimise the final free energy of the protein. Thus, water plays a determinant role in protein structure and function (Franks, 1993 ; Rupley and Careri, 1988). In the case of enzymes, the limiting step of activity is the formation of an intermediate state. Indeed, a chemical reaction is accompanied by a free energy change given by:

$$\Delta G = \Delta G^0 + RT \log \frac{[P]}{[S]}$$

Where [S] is the concentration of substrate; [P] is the concentration of the product; R is the gas constant; T the temperature and ΔG^0 is the free-energy change under standard conditions. The substrate S is transformed into the product P through a transition state S_a that has a higher free energy than either S or P. The

Gibbs free energy of activation ΔG_a is equal to the difference in free energy between the transition state and the substrate. The reaction rate V is proportional to ΔG_a:

$$V = v[S_a] = \frac{kT}{h}[S]e^{-\Delta G_a/RT}$$

k is Boltzmann's constant and *h* is the Plank constant.

Enzymes accelerate reactions by decreasing ΔG_a, the activation barrier. The enzyme-substrate complex formed creates a new reaction pathway whose transition state is lower than in the reaction without enzyme (Stryer, 1999).

In other words, an enzyme-catalysed reaction is affected by all the events able to decrease the height of the energy barrier or enable the barrier re-crossing (Hammes-Schiffer, 2002 ; Toussignant and Pelletier, 2004). These authors discussed the ways that protein motions can affect the enzyme activity. They distinguished between promoting motion, which decrease the height of the energy barrier, and dynamical motion that allows the energy barrier re-crossing. A change in the enzyme rate in organic media, for instance, has been observed by Affleck, Xu *et al.* (1992), when a few water molecules were added to the solvent. Another example, is the work done on lysozyme hydrated powder that has highlighted the requirement for substrate mobility at the protein surface for activity (Rupley *et al.,* 1980). The case of the bacteriorhodopsin illustrates as well the role of water in protonic conduction. Water molecules inside the proton pump would participate to the proton conduction pathway through a hydrogen-bonding network (Kandori, 2000). The binding of substrate may also induce a hydration variation as in the case of the human DHFR (*h*DHFR), where some specific water molecules are found to stabilize the formation of the complex enzyme-substrate-cofactor (Meiering and Wagner, 1995).

Given the different ways in which water may affect the catalytic rate, the role of water as a substrate or a product of the reaction is an important factor to take into account. This may be as a component of the reaction, for example, with hydrolysis reactions, or it may be in respect of free-energy considerations of the specific enzyme reaction involved (Kornblatt and Kornblatt, 1997). However, in other cases, water might be an inhibitor (Graber, Bousquet-Dubouch, Lamare *et al.,* 2003). This water is likely to be located at or near the active site, with potentially only small amounts of water involved.

In vivo, solvent water provides a fluid medium for the diffusion of substrate and product. Replacing water in this respect is challenging. Different systems have been envisaged and will be discussed below. As the techniques are improved, our understanding of the role of water in relation to enzyme activity might change.

4.1. Solid system: dry enzymes

One of the earliest approaches to investigate the effect of hydration on enzyme activity was to rapidly mix substrate and enzyme in solution, followed by lyophilisation and finally to measure the modification of the resulting powder composition due to enzymatic activity. Drapon (1985) has reviewed the work done on such systems. For instance, it was observed that the β-amylase requires a water activity of 0.65-0.7 for activity, when the protein sorption isotherm is found to deviate from the linear region. However, upon the addition of a hygroscopic substance to the reaction mixture activity was observed at a lower $a_{w.}$ Water confers to the reactants and the enzyme some mobility which might be required for activity. This was supported by the observation that activity could be detected at lower a_w when the substrate was a liquid. Studying the enzyme as a function of a_w has also shown two important facts: enzyme activity increases with increasing a_w and tends to a limit that increases as well with higher a_w.

The effect of water on the kinetic parameters has also been reviewed and shows that the V_{Max} increases linearly with a_w, while the K_M decreases as a function of a_w until an optimum is reached around 0.3-0.4 a_w, then it rises again. It was also observed that at lower water content, the optimum temperature was increased.

The correlation between the water sorption and enzyme activity have also revealed that enzyme activity could occur at a lower water content than expected. For instance, Drapon (1985) reported the case of the lipase studied by himself in (1972) or an esterase studied by Duden (1971), which were found to be active at a water activity of 0.025 and 0.1, respectively.

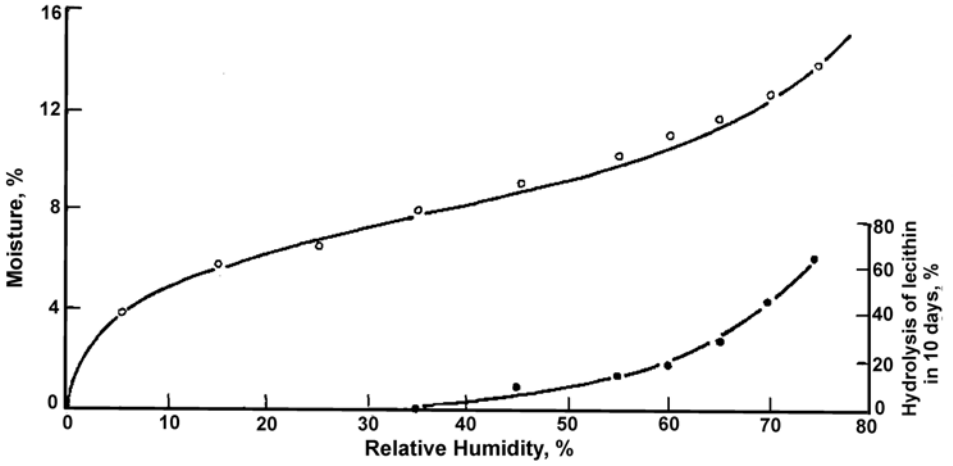

Figure I-4: Sorption isotherm of a mixture of barley malt flour and lecithin (open circles) and its phospholipids-hydrolytic activity as a function of relative humidity of the surrounding atmosphere. The degree of splitting after 10 days of storage was taken as a measure of activity (Acker, 1962).

In the case of the Barley malt flour, it has been shown that a moisture content of about 9% is required for hydrolysis to start (Figure I-5). It should be noted that these results are for a mixture of protein with other compounds. Studies done with pure protein indeed seem to agree that a threshold of 0.2 g $H_2O \bullet g^{-1}$ protein is required for the onset of the activity (Rupley and Careri, 1988). Some studies did not show this threshold but have been cited as though they did, as for urease (Skujins and McLaren, 1967). It also can be observed that enzyme activity increases with water activity. A drawback of this technique overall is that it may be providing information on product release rather than catalysis, since the enzyme-substrate complex will form faster in the solution before freeze-drying than in its solid form, and diffusion limitation seems inevitable (Drapon, 1985 ; Stevens and Stevens, 1979).

4.2. Organic media

When looking at alternative media to water to mediate the diffusion of products and substrates, the use of organic solvents has been investigated. The main difficulty is that enzymes are not usually soluble in organic solvents, and if they are they usually become denatured. However this problem is dealt with by suspending the enzyme powder with stirring or sonication. Although unexpected,

it has been found that many enzymes are active in organic media. One explanation would be that enzymes in organic solvent are unable to radically change their native conformation upon transition from water due to their kinetic barriers and therefore remain in an active conformation (Zaks and Klibanov, 1988).

A distinction has to be made between polar and non-polar organic solvents. Klibanov (1989) explained that enzymes retained a better activity in hydrophobic solvent, as the hydrophilic ones would strip the water away from the protein. He also pointed out that the interaction between the solvent and the enzyme's essential water is far more important than that between the solvent and the enzyme itself. Organic solvents present multiple advantages. Firstly, reactions that are not favoured in water may be enhanced in such media. Lipase and esterase-catalysed acylations, for instance, have a higher rate in dioxane as compared to water (Hacking *et al.,* 1999). Secondly, it has been found that enzymes retain the ionization state they acquired in the solution they have been freeze-dried from. This phenomenon is called the pH memory effect. Therefore, enzyme activity in organic solvents can be greatly enhanced by its incubation at its optimal pH prior to freeze-drying (Castillo *et al.,* 2006 ; Klibanov, 1989 ; Zacharis *et al.,* 1999). Because enzymes are rigid in non-polar organic media, it is also possible to improve their activity by molecular imprinting (Russell and Klibanov, 1988; Braco *et al*., 1990; Martinelle et *al*., 1995; Mingaro *et al*., 1995; Gonzalez-Navarro and Braco, 1997; Rich *et al*., 2002; Fishman and Cogan, 2003). This technique consists of trapping the enzyme in its active conformation by freeze-drying it with a substrate analogue. Finally, the thermostability of enzymes is considerably increased in dry organic media, which allows study at higher temperature just as is the case for dry enzyme powders (Klibanov, 1989 ; Zaks and Klibanov, 1988).

In the case of hydrophilic solvents, other factors may be involved in the activity. Kim *et al*. (1999) found for instance a linear relationship between the intrinsic activation energy of the subtilisin-catalysed transesterification and the polarity of the organic solvent. However, Parker *et al*. (1995) compared the enzyme hydration level reached in non-polar organic media and that in air. If the adsorption of the strongly bound water to protein is hardly affected by the low dielectric medium, that of the loosely bound water is significantly reduced in non-

polar organic media. Thus the formation of a complete monolayer is thermodynamically unfavourable in organic media.

To study the hydration effect some authors just added water to organic solvent and determine the amount of water bound to the protein in organic solvent by the Karl Fisher titration. Others determined the amount of water through a sorption isotherm knowing the thermodynamic water activity of the solvent used. Valivety, Halling *et al*. (1992) have observed, for instance, enzyme activity at water activity as low as $a_w \geq 0.0001$. Ma *et al*. (2002) also shed light on the water activity dependence of enzyme activity in organic media. For example, *C. rugosa* lipase expressed the highest acyl transfer rate at a_w=0.11 (this probably corresponds to about 0.05 *h*). Below this optimum level, if water was added to a solvent, the enzyme activity increased with the amount of water added. So enzyme activity in this case increases with hydration. Another surprising fact is that for some enzymes, fewer water molecules than thoses needed to give a monolayer coverage are required for the onset of enzyme activity. For instance, chymotrypsin needs only 50 water molecules to be active while a monolayer coverage of its surface would require 500 water molecules (Affleck, Xu *et al.,* 1992). Although water sorption isotherm of proteins in water-solvent mixtures have been found similar to those of proteins exposed to water vapour (Lee and Kim, 1995), solvent properties such as its dielectric constant affect the enzyme activity and dynamics (Guinn *et al.,* 1990). Affleck, Haynes *et al.,* 1992 suggested that slower motions observed, as the dielectric constant, when this constant is lower would explain differences in the enzyme stereospecificity. It was also observed that the initial addition of water would partly rigidify the enzyme and that further addition of water would coincide with an increase of the enzyme mobility and an increase of the activity (Partridge *et al.,* 1998).). A drawback of the use of organic solvent is that solvent molecules may have an effect on substrate solvation and affect the enzyme catalysis rate (Martinelle and Hult, 1995). It was suggested that solvent properties seem to affect the substrate's binding rather than the catalytic step (Garcia-Alles and Gotor, 1998).

"Essential" water molecules are thought to act as a lubricant or plasticizer providing the enzyme molecule with the flexibility necessary for enzyme catalysis (Poole and Finney, 1983). Water's role as a lubricant stems from its ability to form hydrogen bonds with functional groups of the protein, which therefore are

bound to each other, thereby "unlocking" the structure. Hence, other compounds with a high propensity for forming hydrogen bonds should act in a similar manner.

4.3. Gas phase system

The best alternative to water as a diffusion media, avoiding the potential complications in organic solvent is probably gas. The introduction of enzymes into a gas phase system presents several advantages. Firstly, enzymes are less sensitive to diffusion limitation as the diffusivities in the gas phase are much higher. Gas phase reactors offer also the possibility to monitor the relative humidity of the immediate enzyme environment. In addition, with the dehydrated form of enzymes being more resistant to thermo-inactivation, it allows studies at higher temperature (Lamare *et al.,* 2001 ; Lamare and Legoy, 1993 ; 1995). Finally, the absence of an organic solvent, and the use of a closed system, facilitates the direct determination of the hydration of the enzyme. However, it is very much limited by the availability of enzymes that have gaseous substrates and products.

A few enzymes using volatile substrates have been described in the literature. Alcohol oxidase, for instance, has been used to study the effect of water activity on the enzyme thermostability and activity. This work showed that the protein stability was increased at lower hydration while the activity increased with the water activity. Interestingly, the activity of this enzyme takes place at water content below the monolayer coverage (Barzana *et al.,* 1987).

Yang and Russell (1996; 1995) studied the effect of temperature and hydration on alcohol dehydrogenase activity and stability in a continuous gas phase reactor. These authors concluded that enzyme activity and stability require a temperature-independent level of hydration, which is closely related to the proportion of the protein that is hydrophilic. They also performed water adsorption isotherms in the presence of non-polar organic molecules and showed that water adsorption is affected to a small degree by a more polar substrate such as acetone. It should be noted that this enzyme requires a non-volatile coenzyme.

Haloalkane dehalogenase, used for the bioremediation of pollutant halogenated vapour emission, is another good example of enzymes able to

catalyse gas phase reactions. Once again, the effect of hydration on enzyme activity was investigated. In the case of this enzyme, it was found that dropping the relative humidity from 100% to 80 % induced a loss of activity of 50 %. These authors reported as well the importance of the protein ionization state for the gas phase activity (Dravis *et al.,* 2000). Erable *et al*. (2004) found a critical water activity of 0.4 for this enzyme to become active but the optimum conditions were a_w=0.9 at 40 °C and pH 9.

A complete kinetic characterization of the alcoholysis catalysed by *Candida antarctica* lipase B has also been possible with a gas/solid system (Bousquet-Dubouch *et al.,* 2001). The same team investigated the influence of organic components (Letisse *et al.,* 2003) and water (Graber, Bousquet-Dubouch, Lamare *et al.,* 2003) on the alcoholysis rate. The alcoholysis reaction has been found to obey a ping-pong bi-bi mechanism with a dead end inhibition by the alcohol substrate. Figure I-5 describes this mechanism. The first step of the reaction is the deacylation of the ester substrate (S1) by the enzyme (En) leading to the release of the alcohol product (P1) and to the formation of an acyl-enzyme intermediate (Enx). Then, the alcohol substrate (S2) is acylated and the ester product is released (P2). It is a pin-pong mechanism because the enzyme shuttles between a free and a substrate-modified intermediate state. The bi-bi mechanism refers to the fact that the binding of the substrates and the release of the products are ordered. Water acts as a competitive inhibitor of the first step, which is the dissociation of the methyl propionate, but has no effect on the acylation step. They showed that at very low water activity, only the alcoholysis reaction occurs.

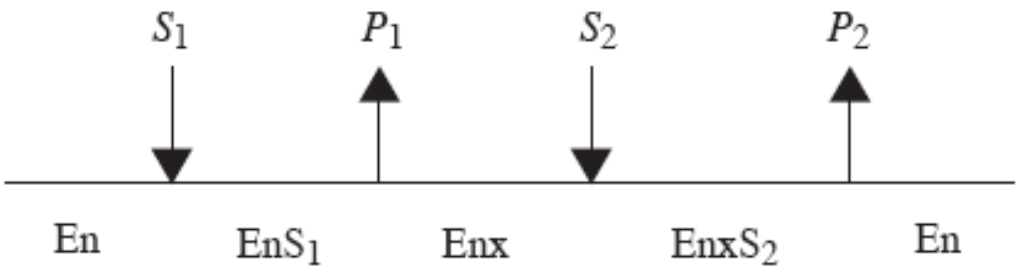

Figure I-5: Diagram of the alcoholysis reaction mechanism (Yang *et al.,* 2005).

As shown in our laboratory with pig liver esterase, enzyme activity has been observed at water content as low as 0.03 g H_2O*g^{-1} protein (Lind *et al.*, 2004).

Overall, these findings tend to contradict earlier findings of a requirement for a threshold hydration of $h \geq 0.2$ for activity, but all share a failure to conclusively determine the enzyme hydration at low hydration levels. Even the best determinations tend to rest on the assumption that a given dehydration method will produce a completely "dry" enzyme.

4.4. Protein dynamics and enzyme activity

The catalytic power of enzymes comes in part from their ability to bring together substrate and enzyme. Enzymes are also highly specific. Fisher was one of the first who tried to explain this specificity with the “lock and key” model in 1894. In this model the complementary shapes of the substrate and the enzyme enables their association. Although this model was a partial explanation of some mechanisms, it has been found inadequate for most enzymes. In 1958 Koshland proposed another solution: the “induced fit” model. Here the interaction between the substrate and the enzyme induces a continuous conformational rearrangement of the catalytic site to adapt to the substrate. In many cases crystallography has provided direct evidence for the existence of these different enzyme conformations, in the presence and the absence of substrate. An essential aspect of the induced fit model is enzyme flexibility, and it is now widely accepted that flexibility is required for catalytic activity. Flexibility was described by Zaccai (2000) as the deviation from the linear behavior of the mean square displacement of the protein atoms as a function of temperature. Rasmussen *et al*. (1992) supported this idea when studying ribonuclease A activity below the dynamical transition. The lack of activity below the transition, although they were not able to measure it, would be explained by the rigidity of the protein. Then, the substrates would not be able to fit the active site pocket.

Some thermodynamical insights have to be introduced here. The temperature dependence of ligand binding to myoglobin would be explained by the existence of different protein substates. These substates correspond to local minima in the potential energy landscape of different native conformations of

proteins. Thus, transition between the substates may occur if kinetic energy is sufficient. The anharmonic motions may involve confined continuous diffusion and/or jump diffusion between potential energy wells (Kneller and Smith, 1994 ; Rasmussen *et al.,* 1992). Internal protein motions can affect the catalytic rate in two ways. First, by influencing the height of the free energy barrier, which implies a modification of the equilibrium between the transition state and the reactants and products. Second, by influencing the capacity of re-crossing the barrier.

If most enzymes are inactive in low water media because of their rigidity (Ferrand, Dianoux *et al.,* 1993 ; Ferrand, Petry *et al.,* 1993 ; Ferrand, Zaccai *et al.,* 1993, for some enzymes, the onset of activity might be more complex. Lipases and esterases present for instance a better transesterification rate in organic solvent than in water (Hacking *et al.,* 1999). Daniel *et al*. (1998) were able to measure enzyme activity in cryo-solvent at very low temperature and performed an investigation of the enzyme dynamics at these temperatures. Their work showed that enzyme activity was possible below the dynamical transition. Rasmussen *et al*. (1992) also hypothesized that below the dynamical transition, water molecules bound in the active site would become so rigid that they could not be displaced easily by substrate and thus, activity would not be possible. Again, this hypothesis was ruled out by Daniel *et al*. (1998). The low temperature work has allowed the correlation between protein dynamics and activity. However, the interaction between the protein and water seems to play an important role as well. Demmel *et al*. (1997), for instance, correlates the dynamical transition to the O-O distance of the hydrogen bond. They observed an increase of the fraction of longer and weaker bonds as the temperature increased. Reat *et al.,* 2000 showed as well that in cryo-solvents of different compositions and melting points the atomic dynamics was relatively independent of the melting point of the solvent, while in pure water, the protein dynamics respond strongly to its melting point.

5. *Enzyme models*

5.1. Candida rugosa lipase B (EC 3.1.1.3)

Candida rugosa lipase is one of the most frequently used enzymes in biotransformation and has been well documented (Benjamin and Pandey, 1998 ; Dominguez de Maria *et al*., 2005). This enzyme has the advantages of being secreted, readily available commercially, not needing any cofactor, and being stable in organic media.

5.1.1. Purification and characteristion

Candida rugosa secretes a number of exolipase isoforms that are encoded by a lipase 'minigene family' designated *lip 1* to *lip 7*. The genes *lip 1* and *lip 2* encode for a mature protein of 534 residues with a putative signal peptide of 15 amino acids as shown by the cDNA sequence (Longhi *et al*., 1992). A biochemical characterisation of these proteins shows that there are four isoforms of *C. rugosa* lipase (CRL) with the same molecular weight of 60 kD (Rua *et al*., 1992). Two major CRL populations named LipA and LipB (encoded by *lip 3* and *lip 1* respectively) have been purified and differ only by the sugar attached to them (Rua *et al*., 1993). A further characterisation of *C. rugosa* lipase B by its substrate specificity and pI shows that there are two isoforms (Lopez *et al*., 2000). The isoenzyme composition of the enzyme these authors purchased from Sigma is 83% of lip 1 and 17 % of lip 3.

5.1.2. Kinetic specificity

C. rugosa lipase isoenzymes have a broad spectrum of specificities: they are substrate specific, positional specific (primary or secondary esters for instance), fatty acid specific, and stereospecific (Jensen *et al*., 1983). They catalyse a wide range of industrially important reactions such as hydrolysis and synthesis (Figure I-6). The sequence of the lid region is apparently responsible for the activity and specificity of *C. rugosa* lipase isoenzymes (Brocca *et al*., 2003). *C. rugosa* lipase B has both esterase and lipase activity, with its lipase activity

being stronger. In our studies, we have been focusing on the isoenzyme encoded by *lip 1*.

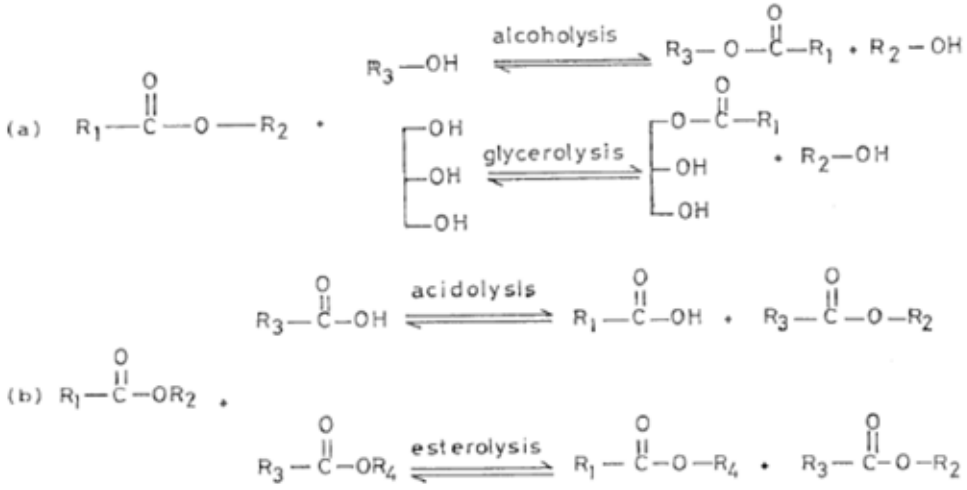

Figure I-6: Important reactions catalysed by CRLs (Benjamin and Pandey, 1998). (a) Trans-esterification involves the transfer of an acyl group to an alcohol or glycerol (glycerolysis). (b) Inter-esterification describes the transfer of an acyl group to a fatty acid (acidolysis) or a fatty acid ester (esterolysis).

5.1.3. Structure

C. rugosa lipase B is a single domain protein that belongs to the α/β hydrolase fold family. Its catalytic machinery has been characterised as a serine protease–like triad (SER-209, HIS-449 and GLU-341). The main variability between this enzyme and its family members is expressed by the sequence of three loops in the vicinity of the active site. The loop that differs the most is the flap between the residues 62 and 92. Another particularity of *C. rugosa* lipase B is that its activity is enhanced by a water-lipid interface. This phenomenon is called interfacial activation and includes a *cis* to *trans* isomerization of a proline residue of the flap to expose a large hydrophobic surface, which likely interacts with the lipid interface. This protein is N-glycosylated with a N-acetyl D-glucosamine residue on two sites ASN-314 and ASN-315 (Grochulski *et al.*, 1993). Another important structural feature of this enzyme is a unique binding site for the reaction intermediates (Grochulski *et al.*, 1994b).

Open (or active) and closed (or inactive) conformations of *C. rugosa* lipase B have been crystallised showing that its activation requires a rotation of the flap of almost 90 degrees to expose or exclude the active site from the solvent. The tunnel leading to the catalytic triad remains in both conformations. Although

water molecules can access it, the environment is quite hydrophobic. The oxyanion hole, which stabilises the oxyanion intermediate, is already pre-formed in the inactive conformation. In the closed conformation, a second N-acetyl-D-glucosamine residue on ASN-315, which is not ordered in the open conformation, seems to provide additional contact to stabilise the flap. Clearly, the conformational change from one conformation to the other involves a single loop (Grochulski *et al*., 1994).

5.1.4. Interfacial activation

C. rugosa lipase B was considered to be mainly inactive in the aqueous phase and active at a water-oil interface. Recently, it has been proposed that both the inactive and the active forms would coexist in the aqueous phase in a slow equilibrium. The activation in the aqueous phase would result from a dimerisation of the enzyme while at a water-oil interface; the opening of the flap is triggered by interaction with this interface (Turner *et al*., 2001).

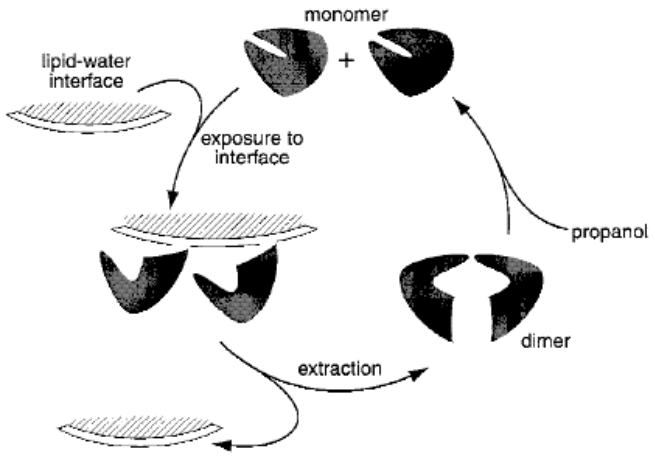

Figure I-7: Schematic representation of dimeric (active) and monomeric (inactive) forms of the lipase and the proposed mechanism of their interconversion (Turner *et al.*, 2001).

5.2. Pig Liver Esterase (EC 3.1.1.1)

The pig liver esterase (PLE also called proline-β-Naphthylamidase) is a carboxyl esterase, serine-dependant hydrolase that primarily catalyses the

hydrolysis of ester linkages between carboxylic acid groups and hydroxyl groups. It is located in the endoplasmic reticulum lumen of liver cells and is involved in the detoxification of xenobiotics and in the activation of ester and amide prodrugs. As with the lipase B, this enzyme does not need a co-factor for its catalytic activity, but exhibits a very low activity in organic solvents.

5.2.1. Purification and characterisation

The pig liver esterase is usually isolated from pig liver tissue, although one of the subunits of PLE has been recently cloned and expressed in the yeast *Pichia pastoris* (Lange *et al.,* 2001). Since the first purification of PLE in 1919 by Simonds, several authors improved the homogeneity of the preparation (Adler and Kistiakowsky, 1961 ; Falconer, 1946 ; Horgan, Stoops *et al.,* 1969 ; Levy and Ocken, 1969). Horgan, Stoops *et al.,* 1969 report a large-scale purification of homogenous PLE. The analysis of the physical properties of this enzyme showed some disparities in the molecular weight (Barker and Jencks, 1969) indicating a subunit composition.

The number of PLE subunits has been estimated to be between two and four depending upon the method of determination. Dudman and Zerner (1975) determined via gel filtration that the molecular weight of trimeric PLE was 206 ± 8 kDa (at 66 kDa per monomer). Barker and Jencks (1969) and Adler and Kistiakowsky (1961) ; Falconer (1946) ; Horgan, Dunstone *et al*. (1969) ; Horgan, Stoops *et al*. (1969) concluded that PLE was a dimeric enzyme of 168 and 163 ± 15 kDa, respectively. Other studies, as reviewed by Horgan, Dunstone *et al*. (1969), determined the molecular weight of dimeric PLE to be between 150-200 kDa by sedimentation coefficient and 70-82 kDa by gel filtration.

5.2.2. Kinetic properties

Active site titration with p-nitrophenyl dimethylcarbamate (NPDMC), bis-p-nitrophenyl phosphate (BNPP) and diethyl p-phenyl phosphate indicates the presence of two binding sites per molecules of enzyme.

While Krisch (1966) determined that the two active site centres were on different subunits, other authors concluded that both active sites were on the same monomeric unit since the monomeric PLE solutions displayed full activity and

substate activation (Adler and Kistiakowsky, 1961 ; Dudman and Zerner, 1975). Greenzaid and Jencks (1971) showed that one site catalysed hydrolysis of large substrates while the other one catalysed hydrolysis and methanolysis of smaller substrates. They also showed the formation of an acyl-enzyme intermediate and the release of the product alcohol, followed by the release of the product acid.

5.2.3. Structure

The X-ray crystallographic structure of the PLE is not known. Its secondary structure, as determined by optical rotary dispersion, consists of β-sheet, α-helix and random coil at levels of 80, 15 and 5%, respectively (Farb and Jencks, 1980).

Heymann and Junge (1979) investigated the heterogeneity of trimeric PLE isoenzymes using analytical sulphate electrophoresis. Three different subunits were separated and isolated from heterogeneous preparations of PLE, and their properties are displayed in Table I.3. The three subunits were designated α, β, and γ (where α and γ forms dominate) and were 58.2, 59.7 and 61.4 kDa, respectively. The three subunits differed only in primary amino acid sequence (no modification of the protein side chain) and behaved like an aliesterase, serine hydrolase and cholinesterase, respectively. They concluded that native PLE consisted of a diverse mixture of pure or hybrid variants of the three subunits.

However, Farb and Jencks (1980) discovered that the subunit combinations were not random. Instead, there was a favoured association between subunits of similar charge and specificity, where the substrate specificity and overall charge of each subunit was distinct due to small differences in their amino acid compositions. It was postulated that the primary function of the variants was to increase the substrate spectrum vulnerable to hydrolysis by PLE. This theory is in accordance with the function of many liver carboxylesterases – an enzyme that participates in the detoxification or metabolic activation of various ester- and amid-containing drugs, carcinogens and environmental pollutants.

Active site models are applied as an interpretive tool to predict stereospecificity for new substrate structure types. In the case of PLE, this role is important since this enzyme is widely used in organic chemistry due to its high stereoselectivity. The active site model proposes that substrates interact with two

polar binding sites, designated $P_{F(front)}$ and $P_{B(back)}$, and two hydrophobic sites, $H_{L(large)}$ and $H_{S(small)}$. The volumes of the P_F, P_B and H_S and H_L sites were first determined to be 2.0, 3.2, 6.0 and 40.5 $Å^3$ (Provencher *et al.,* 1993).

Further studies on the pocket dimensions of the four binding sites confirmed these values except for H_L which changed from 40.5 to 90 $Å^3$ (Provencher and Jones, 1994).

5.2.4. Structure of the human liver carboxyl esterase (*h*CE)

Although no structure is available for the pig liver esterase, its linear sequence has a good identity with the human liver esterase and both of them form a trimer. The *h*CE monomer is formed by 17 α-helix and 20 β-strands. It is divided into a catalytic, an αβ, and a regulatory domain. The catalytic domain contains the catalytic triad and a conserved high mannose N-linked glycosylation found at Asn-79. The αβ domain provides the bulk of the buried surface in the trimer. The regulatory domain is composed of α 10-12 and α-16, and two novel Ω loops. This region exhibits a higher thermal displacement and has been proposed to regulate the substrate binding and the product released. There are three ligand-binding sites. The active site, located at the base of the catalytic gorge, adjacent to it and separated from it with a thin wall of amino acids, there is the side door. The side door has been hypothesised to serve as a secondary substrate entrance and/or product release pore. The catalytic gorge is flanked by α-1 and α-10' motif. Adjacent to the gorge is the Ω1, Ω2 and α-10' form the Z-site. The Z-site is a surface-binding site that controls the trimer-hexamer equilibrium of the *h*CE (Bencharit *et al.,* 2006).

Table I-2: Identity of PLE with *h*CE. Sequence alignment realized with LALIGN program.

	PLE	*h*CE
Name	EST1_PIG precursor	EST1_HUM precursor
Number of AA	566	567
Sequence Identity of the whole sequence(%)		76.6
Sequence identity from AA 22 to 552 (%)		79

CHAPTER II: QUANTIFICATION OF WATER MOLECULES

1. *Introduction*

In many studies of the effect of hydration on enzyme activity the enzyme hydration is defined by the technique used rather than by direct measurement: the "dry" enzyme by the drying technique used, and the hydrated enzyme either by weight gain of this dry enzyme in the presence of water vapour, or simply by exposure to a given relative humidity and comparison to a hydration isotherm. Quite apart from the errors arising from the assumptions implicit in these techniques, at low hydration they are entirely unsatisfactory. From one author to the other, the drying method, and so the drying state they refer to, is different. At zero or very low water content, the properties of the protein are likely to be considerably affected, firstly because, in the hydration process, the first water molecules that interact with the protein are the most tightly bound and secondly because it is likely that at low hydration, enzyme properties will vary sharply with hydration. Therefore, knowing the amount of water molecules bound to the protein with a good sensitivity is an essential requirement to interpret the results at low water content.

1.1. Drying methods available

In most of the techniques used to quantify this tightly bound water, drying the protein completely to obtain a "zero" value is a prerequisite. Solvent water is easily removed by freeze-drying but still about 12% of residual water remains (Seligmann and Farber, 1971), although with a new freeze-drier, a level of 5% hydration can be reached. Freeze-drying is usually used as a first step. To further dry the protein, the relative humidity of its environment can be controlled using for instance, a saturated salt solution, a desiccant (O'Brien, 1948) or a dry gas such as dry nitrogen (Lamare and Legoy, 1995). The lowest hydration level reached with salt solutions, in the case of our proteins, is about 3 %, so once

again, a lot of water molecules remain. A comparative study of the efficiency of various desiccants on drying has shown that magnesium perchlorate and phosphorus pentoxide were the best (Greenspan, 1977). Dry nitrogen should have a relative humidity close to zero; however, the headspace needs to be continuously renewed. Therefore, desiccants can be used in combination with other methods to improve the drying efficiency. It is possible to heat the lyophilized protein, so long as it is under its temperature of denaturation. Vacuum drying can also be used in conjunction with the desiccant and the temperature.

1.2. Measurement of the tightly bound water

Isengard (2001) reviewed some methods to determine the water content in food, and most of these methods can be applied to proteins. The water content can be directly quantified with a gravimetric method after physical extraction from the protein. For instance, the protein can be equilibrated with a hygroscopic substance, such as phosphorus pentoxide or a molecular sieve, in a confined environment. The loss in water of the protein sample is then determined by the weight difference before and after the equilibration. The efficiency of this technique depends on the hygroscopic substance and on the equilibrium, and the accuracy is based on the assumption that the drying method will yield a completely anhydrous protein. It is in fact unlikely that all the water molecules will be removed. However, the use of an oven or a vacuum can improve the extraction of the water molecules. A large protein sample is required to detect small mass changes. In the same manner, it is possible to quantify indirectly the water molecules through sorption isotherm. The uptake of water of a dry protein sample is measured as a function of the water activity (Bull, 1944). Once again, the equilibrium as well as the accuracy of the scales is a limiting factor. Most of the scales available have four decimal places. Smith, Shirazi *et al*. (2002) used a gravimetric/calorimetric method to determine the water sorption isotherm of lyzozyme. They measured the mass change and the corresponding heat flow in a thin film exposed to a gas. The mass sensor is a quartz microbalance. The resonant frequency of a quartz plate resonator is inversely proportional to the thickness of the quartz plate. If this thickness is increased by the deposition of material on the surface of the resonator, its frequency will decrease. The heat flow

from the sample to the surroundings is measured as a function of time and the total heat associated is determined by integration over time. The advantage of this method is the high precision of the quartz microbalance, which can measure mass changes of ± 2 ng/cm^2, as well as the determination of thermodynamic parameters. However, six hours of conditioning were required to minimize the effect of prior history of the film sample on the observed mass and heat flow changes when an actual run began. Thermogravimetric (TGA) and differential thermal analysis (DTA) can also be used for the determination of the amount of bound water. The mass loss of the sample as well as its thermal events, are simultaneously recorded. For instance, de la Casa *et al*. (1998) found approximately 220 water molecules bound per molecule of lyophilized lipase B of *C. rugosa*. The DGA-DTA technique is also useful to distinguish between a strongly and a more weakly bound water.

Another direct quantification of the water content can be obtained with the Karl Fischer titration. In this case, the water does not need to be extracted. It is based on a two-step reaction. In the first step, an alcohol is esterified with sulphur dioxide; to obtain a quantitative reaction, a base to yield alkyl sulphite neutralizes the ester. In the second step, the alkyl sulphite is oxidised by iodine to give alkyl sulphate in a reaction that requires water; the base, again, provides for a quantitative reaction. The consumption of iodine is measured. A draw back of this technique is that water must get in direct contact with the chemical reagents, a fact that may cause problems with insoluble samples. This technique has been used extensively for the study of enzyme hydration in organic media (Affleck, Xu *et al*., 1992).

May *et al*. (1991) compared gravimetric, Karl Fischer titration and thermogravimetric (TG) profiles in the determination of the moisture content. For each method, ten replicates were analysed. The Karl Fischer titration and the TG measurements are found to give about 1% more moisture in the samples than the gravimetric methods. This difference can be explained by the fact that the gravimetric method measures only one type of bound water while the other methods are able to quantify all the bound water. Moreover, a gravimetric measurement requires 200 mg of protein sample while the Karl Fisher titration gives a better estimation with only 40 mg and TG with only 2 mg. The TG

method can be coupled to mass spectrometry to differentiate between the water content of the sample and the water evolved from thermal decomposition.

The physical properties of water can be used for its quantification. For instance, dielectric spectroscopy methods measure the water tumbling and can detect water quantitatively in different clusters if they are held by different averaged hydrogen bond strength. In fact, the water dipole attempts to continuously reorient in an applied oscillating electromagnetic field. Depending on the frequency, the dipole may move in time to the field, lag behind it or remains apparently unaffected. When it lags behind the field, it means that there are interactions between the dipole and the field leading to a heat energy loss. In water, the ease of this movement depends on the strength and extent of the hydrogen bond network. In free liquid water it is usually observed at GHz frequencies whereas for more restricted "bound" water it occurs at MHz frequencies and in ice at kHz (long radio-wave). The dielectric loss is determined over a wide range of frequencies (kHz-Ghz). A slow tumbling (~ ns) usually characterizes the tightly bound water while a fast tumbling (~ ps) characterizes the loosely bound water. The drawback of these techniques is that only freely movable water can be measured accurately, as crystallized or tightly bound water molecules cannot be re-orientated in the field in the same way. Different intermediate states exist, an aspect that must be covered by the calibration which must therefore be product specific (Isengard, 2001 ; Suzuki *et al.,* 1996).

Sei *et al.,* 2005 described cold-spray ionization (CSI) mass spectrometry (MS) as a reliable technique to characterize the number of water molecules bound to a macromolecule. It is a direct solution analysis method, a variant of electro-spray (ESI) MS operating at low temperature (ca -80 to 10 °C) but it is more sensitive.

The water ^{17}O water relaxation dispersion experiment is essentially due to structural water molecules buried within the protein structure but exchanging rapidly (Denisov and Halle, 1995 ; Lee and Kim, 1995 ; Modig *et al.,* 2004). Such experiments have revealed for instance, in the case of ubiquitin, absence of highly ordered internal water molecule (Denisov *et al.,* 1995).

Dolman *et al.* (1997) used isotopic labelling and mass spectrometry to measure low levels of bound water. The protein was labelled with either

deuterated water or ^{18}O-water and dried over P_2O_5. The enrichment of the sample in the rare isotope was then measured by mass spectrometry. The main advantages of the ^{18}O-labeled water technique are the accuracy of the measurement at very low levels and the slow oxygen-oxygen exchange on the time scale of the experiment. These authors were able to detect levels such as 4 ± 2 water molecules per molecule of lysozyme. However, ^{18}O labelling is costly. The deuterium labelling, based on the same principle, is less reliable because of the lability of the proton.

A complete dryness can only be ascertained within the limits of the best water detection/determination method. The methods based on the direct determination of the mass of water usually require a large amount of sample to be sensitive. The most sensitive to date is the determination of a ratio of moles of water per mol of protein by isotopic ratio determination. Thus, in turn, all water determination methods depend for their absolute accuracy on this zero value. This work focuses on the measurement of very low water content. Thus, the isotopic exchange with ^{18}O-labeled water method has been chosen, as it is the most sensitive method available to date. The method used by Dolman *et al*., (1997) was slightly modified and adapted to our project in an attempt to increase sensitivity.

1.3. General ideas on isotopes

The chemical element oxygen has three stable isotopes: ^{16}O, ^{17}O and ^{18}O, with natural abundances of 99.76, 0.035 and 0.2 % respectively. ^{16}O is the abundant element while ^{17}O and ^{18}O are the traces element. According to classical chemistry, the chemical characteristics of isotopes, or rather of molecules that contain different isotopes of the same element, are equal. To a large extent this is true. However, if a measurement is sufficiently accurate, we observe tiny differences in the chemical as well as the physical behaviour of isotopic compounds. This phenomenon is called isotope fractionation. The differences in physical and chemical properties of isotopic compounds are brought about by mass differences of the atom nuclei. The consequences are that heavier molecules have a lower mobility and have a higher binding energy. For instance $H_2{}^{18}O$ water has a lower vapour pressure and evaporates less easily than its lighter counterpart. Because of these two properties of natural isotopes, enrichment in the trace

element can be detected and measured through the estimation of the variations of the isotopic composition of the oxygen of water. Oxygen isotope analysis considers only the ratio of ^{18}O to ^{16}O.

1.3.1. Expression of the amount of isotope

The amount of isotope is usually expressed as a ratio to its counter part. The isotope ratio (R) is defined by the expression:

$$R = \frac{abundance\,of\ rare\ isotope}{abundance\,of\ abundant\,isotope}$$

While the isotope concentration (C) is defined, in the case of water, with:

$$C = \frac{[H_2{}^{18}O]}{[H_2{}^{18}O] + [H_2{}^{16}O]} = \frac{{}^{18}R}{1+{}^{18}R}$$

Where ^{18}R is the abundance ratio of the oxygen 18 and $[H_2O]$ is the concentration of water molecules containing either the oxygen 16 or 18.

If the rare isotope concentration is very large, as in the case of labelled compounds, the rare isotope concentration is given in *atom %*.

$$atom\% = C \times 100$$

1.3.2. Use of δ value and isotope reference

Isotope ratios are generally not reported as absolute numbers. The main reason is that mass spectrometers are not sensitive enough to detect very small variations of these ratios in two samples. Another reason is that the necessity of international comparison requires the use of references to which the samples have to be related. Therefore, isotope abundance is generally reported as a deviation of the isotope ratio of a sample A relative to that of a reference sample or standard, r:

$$\delta_{A/r} = \frac{R_A}{R_r} - 1\,(\times 10^3)$$

For the specific oxygen isotopes:

$${}^{18}\delta = \frac{({}^{18}O/{}^{16}O)_A}{({}^{18}O/{}^{16}O)_r} - 1 \times 10^3$$

1.3.3. Tracer concentration, amount of tracer

The amount of tracer or isotope concentration is defined by:

$$[H_2{}^{18}O] = \frac{Amount\ of\ H_2{}^{18}O}{Amount\ of\ water} = \frac{H_2{}^{18}O}{H_2{}^{16}O + H_2{}^{18}O} = \frac{{}^{18}R(H_2O)}{1+{}^{18}R(H_2O)}$$

The rare isotope cannot simply serve as tracer; it has to be distinguished from a base value. Therefore, the tracer concentration is defined as the deviation of the rare isotope concentration from a base level.

$$[H_2{}^{18}O] - [H_2{}^{18}O_{base}] = {}^{18}R_r\{{}^{18}\delta - {}^{18}\delta_{base}\}$$

The amount of tracer, where W defines the amount of tracer:

$${}^{18}R_r\{{}^{18}\delta - {}^{18}\delta_{base}\} \bullet W = {}^{18}R_r \bullet \Delta^{18}\delta \bullet W$$

1.3.4. International standard

Originally, $^{18}O/^{16}O$ ratio of an arbitrary water sample was compared to that of average seawater. This Standard Mean Ocean Water (SMOW) in reality never existed. Measurements on water samples from all oceans by Epstein and Mayeda (1953) were averaged and referred to a truly existing reference sample, NSB1, that time available at the US National Bureau of Standards (NBS). In this way the isotope water standard, SMOW, became indirectly defined by Craig (1961) as:

$${}^{18}\delta_{NSB1/SMOW} = -7.94\ ‰$$

Various standards have been defined as ‰ for reporting the atomic composition of a sample. Oxygen and hydrogen stable isotope ratios are normally reported relative to the SMOW or the virtually equivalent VSMOW (Vienna-SMOW) while carbon isotope ratios are reported to the PDB (Pee Dee Belemnite) or its essentially equivalent VPDB (Vienna-PDB). This situation arises from the practical fact that neither the isotope measurements on water nor those on carbonates are performed on the original material itself but are made on the gaseous CO_2 reacted with it or derived from the sample.

Table II-1: The stable isotope of oxygen: practical data for the natural abundance, properties, analytical techniques and standards.

	^{16}O	^{17}O	^{18}O
Natural Abundance	0.9976	0.00038	0.00205
Reported as		$^{17}\delta$ or$\delta^{17}O$	$^{18}\delta$ or $\delta^{18}O$
In		‰	‰
Instrument		MS	MS
Analytical medium		O_2	O_2 or CO_2
International standard			VSMOW for water VPDB for carbonate
Absolute value			VSMOW: 0.0020052 VPDB: 0.0020672

1.3.5. The $^{18}O/^{16}O$ analysis of water

Since water poses many problems in the mass spectrometer, the $^{18}O/^{16}O$ ratio has to be transferred to a more suitable compound such as carbon dioxide gas. The most common sample preparation method for $^{18}\delta$ in water is the CO_2-H_2O equilibration in which about a millimole of CO_2 is brought into isotopic equilibrium with a few millimetres of sample water. An aliquot of the equilibrated CO_2 is then transferred to the mass spectrometer for $^{18}O/^{16}O$ measurement. The $^{18}\delta$ value for CO_2 equilibrated with the water sample is equal to the $^{18}\delta$ value of the water itself, where the $^{18}\delta$ refer to the international reference VSMOW. Therefore, the $^{18}\delta_{pdb}$ value obtained from the mass spectrometry analysis has to be corrected. The relation between VSMOW and VPDB-CO_2 is:

$$^{18}\delta_{x/VSMOW} = 1.04143\ ^{18}\delta_{x/VPDBg} + 41.43‰$$

2. *Materials and methods*

2.1. Materials

Crude extract of pig liver esterase (PLE) (EC 1.3.1.1.) (Sigma E3019) and high-grade phosphorus pentoxide (P_2O_5) (Aldrich, ≥ 99.9 atom %) were purchased from Sigma-Aldrich, New Zealand. PLE was further purified following the method described in chapter III.2.2.

^{18}O-labeled (^{18}O atom ≥95%) water was purchased from Cambridge Isotope Laboratories (CIL) in the USA.

Vacuum line of the chemistry department was used for the extraction of the oxygen 18.

The mass spectrometer used was a Geo 20-20 dual inlet from the Stable Isotope Unit of The University of Waikato. It has an integral manifold for the introduction of prepared gas samples. An automated CAPS is also attached for the determination of $^{13}C/^{12}C$ and $^{18}O/^{16}O$ from biogenic and inorganic calcite.

2.2. Method

2.2.1. Labelling of the protein

The hydration water of the protein has to be replaced by labelled water. To this end, 50 to 100 mg of enzyme powder is weighed in a pear-shaped flask. Most of the water content is removed by further drying over fresh, high grade P_2O_5 for three days at room temperature. This drying will be sufficient to reduce the water content to less than 1 mg/per 100 mg protein, so that the maximum error arising from any residual non-labelled water is very small (less than 1%). The protein powder is then equilibrated against 1 g of pure ^{18}O-labeled water for 2 to 3 days in a confined environment. Once a hydration level around 30-40 % (w/w) is reached, the labelled water is removed to stop the re-hydration process.

Then, the protein is dried using different methods and the amount of residual water is determined by measuring the residual ^{18}O. In this study, we have examined the effect of various parameters on the drying efficiency, for example, the use of different desiccants, the effect of temperature, the length of exposure of the enzyme to the desiccant, or the use of vacuum.

Before the mass spectrometer analysis the label has to be transferred to carbon dioxide, as explained earlier.

2.2.2. Transfer of the label from H_2O to CO_2

Once the protein is dried, its weight is determined by gravimetric analysis inside a glove box where the relative humidity is controlled below 5%. One millilitre of purified water (MQ water) is added. The flask is closed with a stopcock to ensure its isolation from the environment and to enable its connection to a vacuum line. First, the content of the flask is frozen in liquid nitrogen and then degassed on the vacuum line. This process is repeated three times to remove the air and the CO_2 present in the flask. After the last degassing, a standard amount of CO_2 is added. Incubation of the samples for at least 24 hours at 25°C with a slight agitation is required to allow the equilibration of the label from the hydration water with the added CO_2.

The CO_2 is then extracted from the sample flask to be analyzed by the mass spectrometer. The extraction line is composed of two cold traps, which are initially in liquid nitrogen. The protein sample is quickly frozen in liquid nitrogen and transferred to a slush bath. The slush bath is a mixture of 50 % ethanol and 50% *iso*-propanol in which liquid nitrogen is added to reach a temperature between -80 °C and -110 °C. Once the flask is connected to the extraction line, and isolated from the pump, the CO_2 travels from the sample to the first cold trap. Then, in the same manner, the first cold trap is placed in a slush bath to free the CO_2 from the first cold trap to the second one. Finally, the CO_2 is trapped into a CO_2 sample cell.

2.2.3. Mass spectrometer analysis

A mass spectrometer is able to separate atoms or rather ions with different mass and measure their relative abundances. A gas containing different isotopes of an element is ionized in the ion source. The positive ions are accelerated by high voltage and subsequently enter a magnetic field perpendicular to the electric field. The path of the ions becomes circular because of the Lorentz force. The circle radius depends on the ion mass: the ions of heavier masses follow the larger

circle. In this way the different isotopic ions become separated and can be collected. In these collectors, the ions loose their electric charge, causing small electric currents that can be measured. From the ratio of these currents the isotopic ratios of the original gases can be determined. For $^{18}O/^{16}O$ in CO_2, the isotopic composition is determined by the ratio of mass 45 and 46. It is difficult to measure the absolute isotope abundances to better than about 1%, but by comparing the abundances between a standard and a sample gas it is possible to determine the difference in isotope abundance to about 1 ppm. For this reason, isotopic abundances are expressed as differences using the delta value.

2.2.4. Determination of the mole ratio $H_2{}^{18}O$/protein

The mass spectrometer gives $^{18}\delta_{pdb}$, which corresponds, as previously explained, to the analysis of the carbonic gas. The isotope fractionation being different in water, this value has to be corrected with the relation between VSMOW and VPDB-CO_2.

For instance, for this set of data:

$$^{18}\delta_{x/VSMOW}=1.04143\ ^{18}\delta_{x/VPDBg}+41.43‰$$

Table II-2: Determination of the isotope ratio in samples.

Sample	d18Ovpdb(g)	d18Ovsmow	R	Averaged R control	Corrected R
MQ	4.01	45.61	0.002096659	0.002104693	
unlabeled	15.06	57.12	0.002119733		
Sample 1	485.17	546.70	0.003101442		0.000996749
Sample 2	520.43	583.42	0.003175073		0.00107038
Sample 3	491.23	553.01	0.003114096		0.001009403
MQ	4.51	46.12	0.002097687		

Each trial has two controls (Table II-2): a MQ water control and an unlabeled enzyme control. The MQ water control will be used to remove the background of natural level of ^{18}O-labeled water of the water while the unlabeled protein will be used to remove the background from the protein. The delta value of the controls has been averaged over all the trials and the standard deviation calculated. The average value is about 46.82 ± 0.3, the standard deviation being so low, that the averaged value could be used for each trial.

To calculate the amount of ^{18}O-labeled water, we first have to calculate the isotope ratio R of the sample:

$$R_s = (\frac{^{18}\delta}{1000} + 1) * R_r$$

Where R_r is the ratio $^{18}O/^{16}O$ in the international reference VSMOW and is equal to 0.0020052. The R value of the sample is then corrected by the averaged R value of the controls to remove the background of the system. The isotope concentration is then calculated from the isotope ratio.

$$C = \frac{[H_2{}^{18}O]}{[H_2{}^{18}O] + [H_2{}^{16}O]} = \frac{^{18}R}{1 + ^{18}R}$$

Where $R_s = {}^{18}R$. The concentration of ^{18}O water or ^{16}O water is not known. However, the amount of MQ water added has been weighed and the number of moles of total water can be calculated. :

$$n(H_2{}^{16}O) + n(H_2{}^{18}O) = n(H_2O)$$

If we consider a constant volume, then:

$$n(H_2{}^{18}O) = C * [n(H_2{}^{16}O) + n(H_2{}^{18}O)]$$

Table II-3: Example of water molecule quantification.

Sample	Isotope concentration C	mols of water	mols of 18O	mols of protein	mols 18O/mol of protein
MQ					
unlabeled					
Sample 1	0.000995757	0.055727778	5.55E-05	9.37E-07	59.22
Sample 2	0.001069236	0.055777778	5.96E-05	9.58E-07	62.25
Sample 3	0.001008385	0.055744444	5.62E-05	9.16E-07	61.37
MQ					

For instance, in the table above, the isotope concentration was determined previously and the moles of MQ water (column 3) is known from the determination of the weight of water added. Thus, number of moles of water with ^{18}O is calculated by multiplication of column 2 by column 3:

$$n^{18}O_{\text{sample 1}} = 0.000995757 * 0.055727778$$

Then, from the dry weight of the protein, the number of moles of protein is calculated. For the lipase B and PLE a molecular weight of 57095 and 60070 Da were used, respectively. Although the PLE is known to be a trimer, each monomer has its own active site. Therefore, I have treated PLE as a monomer,

and have used the averaged molecular weight of one monomer.

2.2.5. Validation of the method:

The standard deviation of the delta value obtained with the mass spectrometer has been calculated and is 0.33. The error of the measurement is then:

$$\frac{0.33}{46.82} * 100 = 0.7\%$$

Therefore the ^{18}O technique is potentially a very sensitive method.

The critical point of this experiment is the control of the hydration level during the experiment, and ensuring no loss of the label during the full processing of the samples. Can we repeat the experiment with a good accuracy and reproducibility? To answer these questions the reproducibility between the samples, and between different trials, was tested. Pig liver esterase (PLE) and lipase B were dried over P_2O_5 for two weeks at room temperature after being labelled. This experiment was repeated three times and each sample was prepared in two or three replicates. The results are presented in Table II-4 below.

Table II-4: Error of the measurement.

	Lipase B	**PLE**
Moles of ^{18}O/mol of protein	23.6 29 31.2 37.5 34.1 32.8 36.4 38.6	12.9 16.3 16.4 12.9 14.9 11.4 11.9
Average	32.9	13.8
Standard deviation	5.0	2.0
% error	15	14.7

Between 7 and 8 individual samples were analysed from all these experiments. All the values were averaged and a standard deviation from this average was calculated. The percentage of error is below 20% even if we add the 1% of error resulting from the mass spectrometer analysis. It is possible that some

of the error actually arises from small but real differences in hydration of the sample due to heterogeneity in the enzyme powder. However, the assumption will be made that these are all real experimental errors. Nevertheless, the reproducibility of this technique is good enough to be reliable and useful.

3. *Results*

3.1. Preliminary trials

Rachel Dunn performed preliminary trials. She used three proteins: lysozyme, pig liver esterase (PLE) and lipase B. The proteins were dried over P_2O_5 at 65°C for two weeks as described in the chapter V.1. Previous work in our laboratory (c.f. Chapter V.1) had suggested that the lowest protein hydrations might be achieved using this procedure. The results (Table II-5) indicate that a much lower hydration has been achieved with lysozyme, about one molecule of water per 5 molecules of enzyme, than with either PLE or lipase B, and that the hydration of these two is similar after this treatment.

Table II-5: Results obtained by Rachel Dunn after two weeks drying at 65°C.

		Mass of protein (mg)	***Lysozyme***	***PLE***	***Lipase B***
Moles of ^{18}O-water per mol of protein	Trial 1	~ 100	0.13		8.31
		~ 100	0.16		8.44
	Trial 2	~ 100	0.19	8.70	9.81
		~ 100	0.18	8.82	9.34
		~ 100		8.73	14.33
	Trial 3	102.5			7.96
		46.2			8.46
		55.8			7.07
Average			0.17	8.75	9.22
Standard deviation			0.02	0.05	2.08
% Error			13.89	0.58	22.60

The table above shows that 50 or 100 mg of protein give the same result. Thus we will be able to use a smaller amount of protein than usually expected. The results obtained with lysozyme are lower than those obtained by Dolman *et al*. (1997). These authors found a residual amount of water of 2.1 and 2.8 mol of water per mol of lysozyme. However, their drying method was probably not as efficient as ours, as they only dried the lysozyme for 72 hours over phosphorus pentoxide at room temperature.

3.2. Effect of different desiccants

Phosphorus pentoxide (P_2O_5) is widely used as desiccant to dry proteins. However, Trusell and Diehl (1963) found, when measuring the residual water in air, that anhydrous magnesium perchlorate ($MgOCl_4$) and barium oxide (BaO) were better desiccants. We used ^{18}O-labeled water to test which of these three desiccants would be the best to dry our enzymes. These measurements were done with the pig liver esterase. The method was the same as described in the methodology paragraph but in this case, after hydration to ~0.4 *h*, the enzyme was dried either with $MgOCl_4$, P_2O_5 or BaO.

3.2.1. One week drying

After re-hydration of the enzyme with the ^{18}O-labeled water, the enzyme was exposed to the appropriate desiccant for a week at room temperature. The table below gives the δ value obtained from the mass spectrometry analysis and the calculated mol of water per mol of protein, for each sample. The mass of protein used and the level of re-hydration of the protein with labelled water are specified too as they might be useful for the interpretation of the results. Two replicates were used for each desiccant.

Table II-6: PLE residual water determination after one week drying at room temperature.

Desiccant	P_2O_5	P_2O_5	$MgOCl_4$	$MgOCl_4$	BaO	BaO
Mass of protein (mg)	48.8	56.9	52.8	50.9	55.1	57.4
^{18}O-water hydration (*h*)	0.42	0.32	0.45	0.42	0.42	0.41
$^{18}\delta_{VSMOW}$	191.6	221.9	99.8	113.0	256.0	226.1
mol ^{18}O/ mol of protein	17.6	20.8	7.4	8.2	26.2	23.4

The mol ratio between ^{18}O-labeled water and the protein is the lowest when magnesium perchlorate ($MgOCl_4$) is used as desiccant. These results are in agreement with those of Trusell and Diehl (1963) who found that magnesium perchlorate was the best desiccant. However, in our study, barium oxide seems to be the less efficient. This could be explained by the use of higher grade of phosphorus pentoxide (P_20_5) in the case of our experiment. However, the lower apparent efficiency might be due to the fact that P_2O_5 loses efficiency after taking up water. It might have been necessary to renew it more often. In addition the apparent better efficiency of $MgOCl_4$ might be due to a loss of the label. Indeed, the $MgOCl_4$ does not react with water irreversibly and is supplied in hexa-hydrated crystal form.

3.2.2. Four weeks drying

The amount of residual water obtained after one week of drying is already quite low. However, this experiment was designed to answer the question of how far can we dry a protein rather than how much water is bound to it. In this aim, the PLE was dried for four weeks at room temperature. The results are presented in Table II-7 below.

Table II-7:PLE residual water determination after four weeks drying at room temperature.

	Sample 1	**Sample 2**	**Sample 3**	**Sample 4**	**Sample 5**
Desiccant	P_2O_5	P_2O_5	$MgOCl_4$	$MgOCl_4$	BaO
Mass of protein (mg)	36.8	45.1	30.8	35.6	42.3
^{18}O water hydration (*h*)	0.46	0.45	0.54	0.51	0.44
$^{18}\delta_{VSMOW}$	67.2	66.6	59.9	60.4	135.7
mol ^{18}O/ mol of protein	3.7	3.0	3.2	2.8	14.5

The results show that only a few water molecules are present even after four weeks of equilibration against the desiccants. Although $MgOCl_4$ still seems to be the best desiccant, the two desiccants tend to the same value: three moles of water per mol of protein. The result obtained for sample 5 is too high compared to the results obtained after a week. It is probably due to an external contamination and unfortunately the duplicate was lost.

3.2.3. Back exchange

In parallel with this experiment, we performed gravimetric measurements with large protein samples to check the weight loss with the different desiccants. Lysozyme was initially hydrated at a known relative humidity, and then gradually dried down using different drying methods.

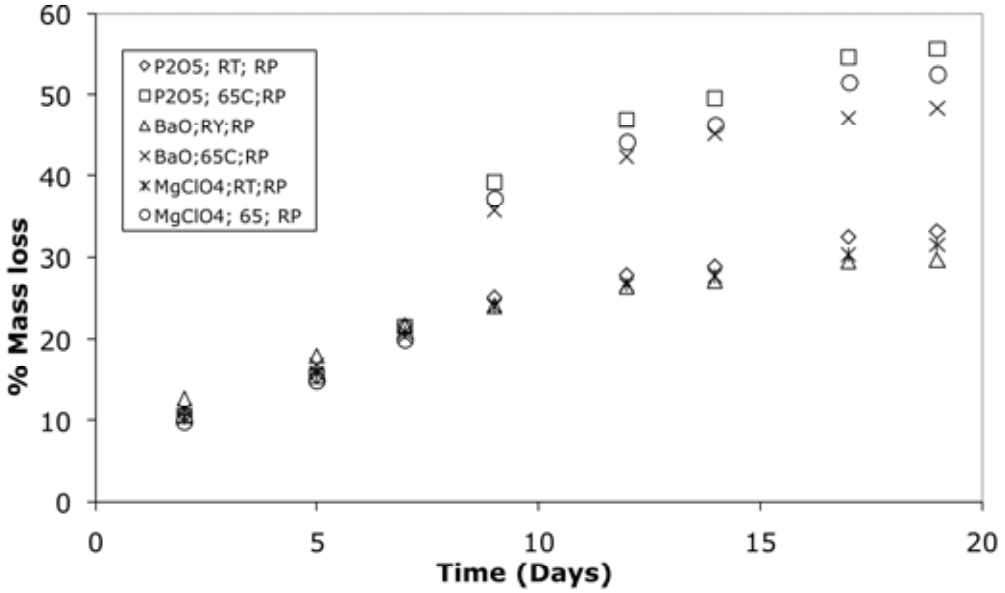

Figure II-1: Weight loss of lyzozyme under different drying conditions equilibrated over either phosphorus pentoxide (P_2O_5), barium oxide (BaO) or magnesium perchlorate ($MgOCl_4$). The temperature was set at room temperature (RT) or 65 °C and the pressure at room pressure (RP).

This graph (Figure II-1) shows that at 65°C, the weight loss is higher than at room temperature. The difference between the desiccants appears more marked at higher temperature. Although it is difficult to measure the gravimetric differences of these samples with a good confidence, the following ranking can be extracted:

$$P_2O_5 > MgOCl_4 > BaO$$

Although the gravimetric method is not accurate enough to make conclusive assumptions, these results do not completely agree with the ^{18}O measurements, where magnesium perchlorate ($MgOCl_4$) is found to have a better efficiency in drying. In fact, it comes in hexa-hydrated crystals. Trusell and Diehl (1963), in his experiments, used dried $MgOCl_4$ (dried at 250 °C under vacuum). So, one of our concerns was that the label could have been diluted by some residual water molecules bound to the desiccant. The same observation was made by Dolman *et al*. (1997); they compared the residual water content of lyzozyme after drying with P_2O_5, BaO and $MgOCl_4$ and found that there were fewer residual water molecules with BaO and $MgOCl_4$. They concluded that some label was lost with these two desiccants. However, no comparison of these desiccants, in terms of their efficiency, has been done. Unlike $MgOCl_4$, BaO reacts irreversibly with

water, so it is not clear why the use of this desiccant would induce a higher loss of the label than P_2O_5. Moreover, the amount of desiccant used for drying being in large excess compared to the amount of labelled water, the amount of label left after four weeks should be close to zero.

Another concern, which applies to all these desiccants, because of the time course of these experiments over weeks, is that the ^{18}O oxygen might be able to exchange with the oxygen of the desiccant or of the protein.

An experiment was designed to check the back exchange of labelled water molecules into the desiccant. It is a challenge to design such experiment, because it is difficult to know in which form the ^{18}O will back exchange and how to extract it. The main concern is about the dilution of the label with non-labelled water molecules coming from the $MgOCl_4$ crystals. The idea is that the amount of exchangeable water should be measurable by the quantification of the ^{18}O label extracted.

Between 6-12 g of desiccant were placed inside a pear shaped flask. Two micro-litres of ^{18}O-labeled water were added. (The P_2O_5 could not be tested in this way as its reaction with water releases heat.) Two replicates with BaO and $MgOCl_4$ were prepared as well as two controls with only the two micro-litres of labelled water. The flasks were closed and degassed on the vacuum line as described in the methodology chapter. In parallel, flasks with one millilitre of purified water (MQ) water were degassed to reproduce the conditions of the water quantification in the case of the protein samples. After two days of incubation at room temperature, the headspace of the sample is transferred into another flask with MQ water. This flask is degassed and CO_2 is added. After at least 24 hours incubation at 25 °C, the CO_2 was extracted and analysed on the mass spectrometer. The results are presented in Table II-8 below.

Table II-8: Residual ^{18}O-water content in desiccants.

Sample	$^{18}\delta_{SMOW}$	$nH_2{}^{18}O$
BaO	49.31	2.79E-07
BaO	46.71	-1.26E-08
$MgOCl_4$	49.70	3.22E-07
$MgOCl_4$	46.33	-5.39E-08
^{18}O water	833.89	8.82E-05
^{18}O water	877.51	9.28E-05
MQ water	46.82	0

The first remark is that the diluted ^{18}O controls gave the same value as those performed earlier with the protein samples. This is a good indication that all the labels have been transferred from the first to the second flask. No water control has been done but the averaged value obtained from the previous experiments has been used (46.82), which might explain the negative results obtained for some samples. This experiment shows that after two days, at most only 5% of the water molecules bound to the desiccant are released. 5% less water molecules were also quantified when magnesium perchlorate ($MgOCl_4$) and barium oxide (BaO) were used as desiccant rather than phosphorus pentoxide (P_2O_5) (Dolman *et al.,* 1997). For this reason, and because the effectiveness as desiccants of $MgOCl_4$ and BaO did not seem significantly better that P_2O_5, the latter has been generally used.

3.3. Effect of drying time

With the aim of completely drying the protein, we tried to increase the time of the equilibration of the protein with the desiccant, and the temperature. The protein was kept at room temperature or at 65°C. In the first series of experiments, the protein was hydrated with labelled water and then shifted directly over P_2O_5 to dry. The results of the water molecule quantification for the pig liver esterase (PLE) and lipase B are presented in the tables below. Although the results are presented in different tables, the experiments for PLE and lipase B were carried out simultaneously. The quantification has been done after 1, 2 or 4 weeks of equilibration with the desiccant. At least two replicates were performed

for each 'incubation' time. In addition, some of the incubation times were repeated to check the reproducibility of these experiments. In these tables, the mass of protein used and the re-hydration level with ^{18}O-labeled water before drying are indicated because a difference of these values between samples might affect the results. The results are the $^{18}\delta_{VSMOW}$ value obtained from the mass spectrometer analysis and the calculated water content given in mol of ^{18}O-water per mol of protein.

Table II-9: Results of the water molecule quantification bound to PLE with ^{18}O-labeled water at room temperature.

PLE	Sample	Mass of protein (mg)	Hydration (*h*)	$^{18}\delta_{VSMOW}$	moles ^{18}O/ mol of protein
1 week	1	52.9	0.26	283.9	29.8
	2	59.6	0.26	362.3	35. 2
	3	53.2	0.27	323.1	34.42
2 weeks	Trial1 1	92.2	0.22	224.5	11.9
	2	50.8	0.27	142.0	12.9
	Trial2 3	58.1	0.49	159.6	14.6
	4	61	0.28	186.3	11.4
	5	49.4	0.35	141.7	12.9
	Trial3 6	51.3	0.27	171	16.3
	7	48.3	0.28	164.9	16.4
4 weeks	1	48	0.48	110.9	9.0
	2	52.7	0.51	119.8	9.3

Table II-10: Results of the water molecule quantification bound to lipase B with ^{18}O-labeled water at room temperature.

Lipase B	Sample	Mass of protein (mg)	Hydration (*h*)	$^{18}\delta_{VSMOW}$	moles ^{18}O/ mol of protein
1 week	1	52.3	0.44	546.7	59.6
	2	53.6	0.4	583.4	62.7
	3	51.8	0.43	553.0	61.8
2 weeks	1	95.3	0.42	585.6	36.4
	2	106.2	0.41	684.4	38.6
	1	61.3	0.39	414.4	37.5
	2	53.1	0.41	334.2	34.1
	3	53	0.38	322.6	32.8
	1	53.9	0.44	244.9	23.6
	2	47.7	0.41	262.4	29
	3	38.6	0.44	234	31.2
4 weeks	1	62.2	0.59	359	32.3
	2	52	0.65	419.6	46.1

Tables II-9 and II-10 summarize the water content of the PLE and lipase B, respectively, after different drying times over P_2O_5. For two weeks, the experiment has been repeated three times in order to obtain meaningful statistics. As the time is increased, the number of mol of water per mol of protein decreases. Thus, drying is improved by an increase of the length of exposure to P_2O_5. The comparison of these results after 2 weeks at room temperature with those after two weeks at 65°C presented earlier, also confirmed that the higher temperature improves the drying. These results are also in agreement with the gravimetric measurement. An apparent exception is lipase B, where after 4 weeks of drying, the hydration is similar to that found after 2 weeks drying for one sample, and the other is higher. This may have arisen from a higher hydration level with ^{18}O-labeled water prior to drying compared to the other samples. The structure of the lipase B had collapsed into a paste, presumably hindering dehydration. Pure water was used for the re-hydration with the label instead of a saturated salt solution. These results indicate that each step of the experiment has to be controlled and

reproduced in the same manner to get meaningful results. Comparing the amount of water between the PLE and the lipase B, it is observed that for the same drying conditions, the lipase B has twice as many water molecules as the PLE. This is in a good agreement with the sorption isotherm obtained for these proteins (refer section III-3.1.4.1).

However, even under drastic conditions, it has not been possible to remove all the water molecules. To improve the drying methods, two possibilities are offered: increase the temperature or use a vacuum. An increase of the temperature was not desirable since it might result in denaturation, so the use of a freeze-drier to apply a vacuum was chosen. Moreover, in parallel to these experiments, the effect of identical drying conditions on enzyme activity was investigated. However, the enzymes used for the activity measurements were not re-hydrated prior to drying, as the protein was not labelled. As the enzyme used for the parallel activity measurements were from a stored freeze-dried powder, the water content should not be over a few %. Therefore the efficiency of drying by P_2O_5 is expected to be better than with the re-hydrated enzyme samples. Thus, the water content of the enzymes used for the enzyme activity may be lower than expected.

3.4. Effect of freeze-drying

In this series of experiments, the enzymes were freeze-dried prior to equilibration over phosphorus pentoxide (P_2O_5). The aim was to improve the drying of the enzymes to see if we could remove all the water molecules.

The protein was prepared in the same manner described in the methodology paragraph until the re-hydration of the enzyme with the labelled water. Then, once the desired hydration is reached, the enzyme is quickly frozen and shifted into a desiccator and connected to a freeze-dryer. The protein was removed after 12 or 24 h. The vacuum was released inside a glove box kept at a relative humidity level under 5%.

3.4.1. Sixteen hours of freeze-drying

The hydration level of the enzymes prior to freeze-drying is only about 30-40%, while a water content below 1% can be reached with a freeze-dryer used at

its optimum conditions (Seligmann and Farber, 1971). Thus, a short time under the freeze-dryer should remove most of the water. The samples are then placed over P_2O_5 for different times as done previously. These experiments were carried out only with the pig liver esterase (PLE). The results are summarized in Table II-11 below.

Table II-11: Mol of water per mol of PLE remaining after 12 hours freeze-drying followed by 1, 2 or 4 weeks of drying over P_2O_5.

Drying time over P_2O_5	Sample	Mass of protein (mg)	Hydration (*h*)	$^{18}\delta_{VSMOW}$	mol ^{18}O/ mol of protein
1 week	1	54.7	0.4	90.7	5.4
	2	37.7	0.4	77.35	5.5
2 weeks	1	47.9	0.39	78.6	4.6
	2	47.9	0.42	76.1	4.2
	3	47.5	0.4	75.0	4.1
4 weeks	1	44.2	0.39	66.0	3.0
	2	42.4	0.42	65.0	3.0
	3	46.5	0.4	66.8	3.0

After a week of exposure over P_2O_5, only approximately 5 water molecules are bound to the protein, which is less than half that found in the case of the experiments without freeze-drying. Once again, the increase of the length of exposure to the desiccant improves the drying; but the freeze-drying might have led to a loss of the label as underlined by Dolman *et al*. (1997). However, in their case it was the labelling of the protein which was done by freeze-drying, and not the drying. In addition they were measuring loss of deuterium by D_2O, the protons being more labile than the oxygen. They also did not discuss the fact that the freeze-drying might have improved the following drying step.

3.4.2. Twenty four hours freeze-drying

As in the previous experiments, all the samples were re-hydrated with labelled water and then freeze-dried. A control, with no drying over phosphorus pentoxide (P_2O_5), was analyzed for the quantification of ^{18}O directly after freeze-

drying. The results are presented in Tables II-12 and II-13 below for pig liver esterase (PLE) and lipase B, respectively.

Table II-12: Mol of ^{18}O per mol of PLE after 24 hours freeze-drying.

Further drying over P_2O_5	Sample	Mass of protein (mg)	Hydration (*h*)	$^{18}\delta_{VSMOW}$	Mol ^{18}O/ mol of protein
No drying over P_2O_5	1	48.6	0.4	90.65	6.12
	2	44.5	0.44	87.45	6.22
1 week	1	40.4	0.42	58.6	2.13
	2	47.5	0.44	61.1	2.19
	3	47.4	0.44	63.7	2.54
2 weeks	1	44.1	0.42	61.8	1.79
	2	44.6	0.44	57.7	1.74
	3	47.3	0.40	59.6	1.9

Table II-13: Mol of ^{18}O per mol of Lipase B after 24 hours freeze-drying.

Further drying over P_2O_5	Sample	Mass of protein (mg)	Hydration (*h*)	$^{18}\delta_{VSMOW}$	Mol ^{18}O/ mol of protein
No drying over P_2O_5	1	47.3	0.33	157.49	14.53
	2	66	0.26	149.88	14.03
	3	42.9	0.32	192.55	15.39
1 week	1	43.8	0.35	108.4	9.2
	2	51.7	0.33	115.1	9.28
	3	56.9	0.32	127.19	9.18

The number of mol of water molecules per mol of PLE is lower compared to the values obtained after 12 hours of freeze-drying. The sample with no drying over P_2O_5 shows the highest water content but still only a few water molecules are left. The efficiency of the desiccant was improved by the prior freeze-drying step. For the lipase B, the lower level reached tended to be around 9. This value was indeed reached by two different drying methods: with 24 hours freeze-drying plus one week drying over P_2O_5 at room temperature, and after two weeks at 65°C.

These might suggest that lipase B posses around 9 structural water molecules.

4. *Conclusions*

The graph below summarizes the experiments done on the quantification of water molecules. The first remark is that whatever the drying method, the number of water molecules bound to the enzyme decreases with increasing drying time. A second remark is that preliminary freeze-drying improves the efficiency of the final drying stage. This is underlined by the fact that increasing the length of the freeze-drying led to a further improvement of the drying. It is therefore clear that removal of the bulk water of hydration greatly facilitates the attainment of low hydration in subsequent drying steps; this is not surprising since it is well known that phosphorus pentoxide (P_2O_5) is most effective when "fresh", i.e. when dry. During the removal of the "bulk" water it becomes less effective in removing the last, tightly held, water molecules bound to the protein. Dolman *et al*. (1997), who first used ^{18}O-labeled water for the quantification of water molecules, observed an extensive loss of their label. However, their protein was lyophilized from a solution where bulk water was also present. In fact, bulk water will exchange more rapidly and may induce a higher loss of the label.

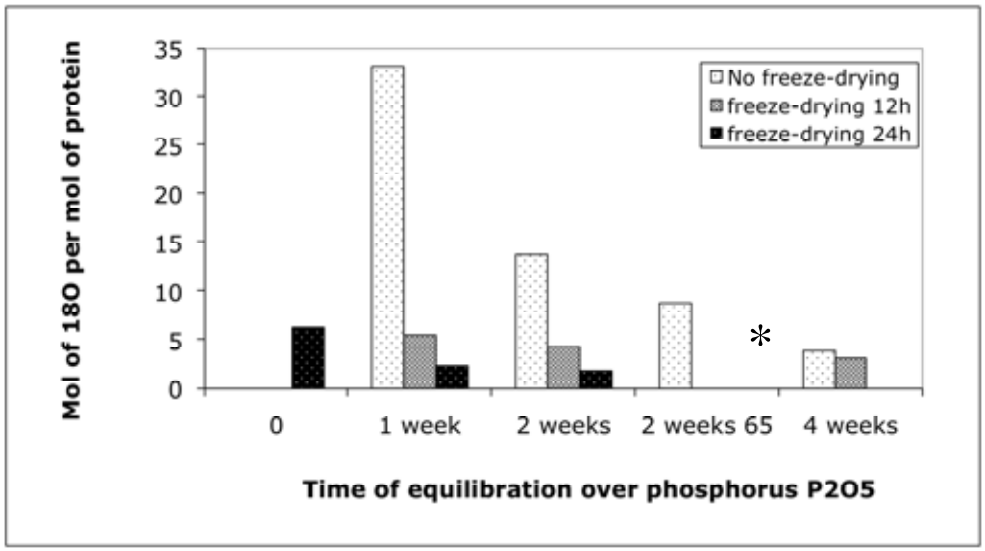

Figure II-2: Water quantification as a function of the drying time over P_2O_5 and with or without freeze-drying prior to drying. The x-axis shows the drying time over the desiccant while the y-axis represents the number of water molecules bound per molecule of protein.
** but see note in text, below*

The quantification of water molecules with ^{18}O-labelled water is relatively sensitive and reproducible. The high reproducibility is explained by the comparison of the sample to international standards and the care taken to the sample handling. Errors might indeed be induced by loss of the label during the experiment or a wrong estimation of the dry mass of the protein. Dolman *et al*. (1997) comparing several technique of water determination estimated the error of about ± 2 water molecules per mol of protein. Although it is probably the most sensitive technique available up to date to measure low level of water bound to a protein, this estimation is probably good but underestimated. In fact, all the techniques involve an estimation of the dry weight of the protein. The results presented here are based on the 'dry' weight of the enzyme minus the weight of ^{18}O-water bound. This correction still left the uncertainty of the weight of protein due to the sensitivity of the scale. For instance, in the case of an error of 1 mg in the dry weight determination would lead to an error of about ± 0.02 moles of water molecules per mol of protein on the water quantification. The differences observed between the results of the amount of water bound to the pig liver esterase after four weeks of drying show that the main source of error is the sample handling. In this case, the results would be more like 6 ± 3 water molecules per mol of protein. However, the samples investigated after four weeks of exposure to P_2O_5, have been re-hydrated to a too high a level, so they should be disregarded.

CHAPTER III: DEVELOPMENT OF THE SOLID/GAS BIOREACTOR

1. *Introduction*

Lind *et al*. (2004) found that the pig liver esterase was able to work at hydration levels as low as 3% (w/w) or ~ 0.03 *h*. However, since the experimental system was based upon a hydrolysis reaction, where water is a substrate, it was impossible to study enzyme activity at zero water content. To address the question of enzyme activity in near anhydrous conditions, we have used an alcoholysis reaction in a gas phase catalytic system. The rationale of the work described here is to validate my experimental set-up, to verify and extend previous work on the gas phase hydrolysis reaction system, to carry out preliminary determinations on the effect of various experimental parameters to optimize both hydrolysis and alcoholysis experimental systems, and to pilot studies on the more demanding alcoholysis reaction.

1.1. Improvement of the hydrolysis activity

The lifetime activity of an enzyme may be enhanced in two ways; increasing its stability during storage, as reviewed by Carpenter *et al*. (1997), or acting directly on the activity rate by the modification of the reacting media and/or of the enzyme (Lee and Dordick, 2002).

1.1.1. Excipients

Freeze-drying is perceived to be a gentle process for drying biological active substances. This is because enzymes, for instance, are more stable in their solid form. However, it has been shown that the low activity of enzyme powders observed in organic media might be correlated to an inactivation at the stage of freeze-drying (Ru *et al*., 1998). The stability of freeze-dried powders depends

critically on how the freeze-drying is carried out (Francks, 1993). n the same manner, in a gas/solid system, enzyme activity might be improved with better freeze-drying conditions. To prevent enzyme denaturation during freeze-drying, it is important to understand how this process works: it is composed of three steps.

First, an initial freezing step involves formation of ice nuclei. Depending on many factors, especially the cooling rate, super cooling may occur. Thus, ice formation may, in fact, take place well below 0 °C. The removal of water by freezing increases the solute concentration/viscosity until a saturation value is reached. At this stage, a glass transition takes place T_g' (glass transition temperature associated with maximum freeze concentration). The unfrozen water W_g at this temperature and the glass transition temperature of the dried product (T_g) are also important parameters and can be determined by differential scanning calorimetry. The initial freezing is then followed with a primary drying, in which the ice is separated from the solute by sublimation. The temperature of the sample is rather critical; if the temperature rises above $T_{g'}$, the ice would melt into the solute phase. Finally, the secondary drying step begins after all the frozen water has sublimed and thus can be facilitated by increasing the product temperature. The bound water is removed during this stage (Carpenter *et al*., 1997).

Slow freezing leads to large ice crystals, whereas fast freezing leads to fine ice crystals. The latter increased the interfacial area and led to denaturation. However, excessively rapid cooling rate will not be a problem by forming a glass state rather than ice. Freezing damage is also induced by addition of salt. In fact, the formation of precipitates at low temperature or the reduction of the pH of the unfrozen buffer might occur. Numerous cryo-protectants, such as sugars or polyols, for instance, act as protectors during the freezing steps. However, most of these cryo-protectants are ineffective during the drying steps. Only disaccharides seem effective during freezing and drying.

There are two main theories to explain the cryo-protectant effect of excipients. First, they would provide a glassy environment where the conformational flexibility of the protein and so unfolding is reduced. This theory is supported by the fact that the effectiveness of the preservative action of many excipients appears correlated to their glass transition temperature (Green and Angell, 1989). Another theory would be that the direct hydrogen bonding between

the excipient and the protein stabilized the protein structure and replaces water-protein interactions (Carpenter and Crowe, 1989).In addition to these main theories, a third one has been proposed, which involves the trapping of water in the complex formed by the protein and the excipient (Belton and Gil, 1994).

1.1.2. Volatile buffers

In low water media, the demonstration of a "pH memory" effect caused great interest for the enhancement of the enzyme activity. Enzymatic activity was found to be critically dependent on the aqueous pH before drying, even when there is no true aqueous phase under the assay conditions (Klibanov, 1989;Zaks and Klibanov, 1988).

'pH memory' has been attributed to a fixation of protein catalytic group ionization after drying of the biocatalyst preparation. The standard model for this fixation process is the maintenance of all the ionization states present before the freezing of the preparation. However, the ionisation state and so the enzyme activity in organic media might change if the buffer ions are removed as volatile components (Zacharis *et al*., 1999).

1.1.3. Bio-Imprinting

Among the various strategies developed to enhance the non-aqueous activity of an enzyme, molecular imprinting is a promising approach for *Candida rugosa* lipase B. Molecular imprinting consists of trapping an enzyme in its active conformation with a substrate analogue or an inhibitor. After freeze-drying of the enzyme-substrate analogue complex, the substrate analogue is removed. The enzyme, being rigid in the anhydrous state, retains its active conformation in organic solvent. The efficiency of this technique seems to depend on the enzyme. For instance, Russell and Klibanov (1988) were able to improve the subtilisin activity by 100 times while Slade (2000) was able to increase the activity of BSA only threefold. Braco *et al*. (1990) showed that not only could the enzyme activity be enhanced with this method, but the enzyme selectivity as well.

In the case of *C. rugosa* lipase B (CRL), the activity is greatly enhanced by oil/water interfaces. Its activation at interfaces is the result of an important

conformational rearrangement including the opening of a lid covering the active site. In this context, an interfacial activation-based molecular imprinting is induced, in the aqueous phase, by the binding of the lipase to a water/oil interface (Martinelle *et al.,* 1995 ; Rich *et al.,* 2002). The use of an amphiphile molecule as imprinter has been found to improve CRL activity (Gonzalez-Navarro and Braco, 1997 ; Mingarro *et al.,* 1995). Mingarro *et al.* (1995) also showed the importance of the nature of the amphiphile. The nature of the solvent used seems to have an impact as well on the efficiency of the imprinting. Fishman and Cogan (2003) found variations of the activation factor from 5 to 230 % depending on the dielectric properties of the solvent. However, bio-imprinting seems to be efficient for lipases even in solvent-free media (Gonzalez-Navarro and Braco, 1997).

It is not clear if either pH or bio-imprinter will affect activity in dry enzymes under a gas phase (as opposed to a dry liquid phase), but in principle there seems no reason why not.

1.2. Alcoholysis reaction

The alcoholysis reaction catalysed by lipases has been well described in organic media (de la Casa *et al.,* 2006 ; Valivety, Halling *et al.,* 1992, 1992 ; Valivety, Halling, Peilow *et al.,* 1992) and in the gas phase. Bousquet-Dubouch *et al.* (2001) studied the alcoholysis reaction of *Candida antarctica* lipase B in a gas/solid system and determined the mechanism of this reaction to be ping pong bi-bi. They also used this system to study the effect of water (Graber, Bousquet-Dubouch, Lamare *et al.,* 2003 ; Graber, Bousquet-Dubouch, Sousa *et al.,* 2003) on the alcoholysis reaction. They found out that water is a competitive inhibitor of the deacylation step. Propanol was also found to inhibit this reaction.

The ester synthesis mechanism in the case of PLE, has been proposed to involve an acyl-enzyme intermediate (Adler and Kistiakowsky, 1961).

2. *Materials and Methods*

2.1. Materials

2.1.1. Enzymes

Crude esterase extract from porcine liver was purchased from Sigma-Aldrich (E3019, Sigma).

Lipase/esterase from *Candida rugosa* (Lipomod™ 34P) was a gift from Biocatalysts.

Esterase from *Penicilium roqueforti* (Lipomod ™ 338P) was a gift from Biocatalysts.

Mixed esterase/lipase/protease from Porcine Pancreas (Lipomod ™ 224P) was a gift from Biocatalysts.

Mixed fungal esterase blend including *Penicilium roqueforti* (Lipomod™ 183P) was a gift from Biocatalysts.

Lipase SNS and lipase from *Pseudomonas* were extracts previously prepared in our laboratory.

2.1.2. Chemicals

Desiccants: high-grade phosphorus pentoxide (≥ 99.99%; Aldrich); magnesium chloride (99.99 %; Aldrich); barium oxide (97%; Riedel-de-Haen).

The esters methyl butyrate, propyl butyrate and ethyl butyrate were all of GC assays purity (Fluka).

Propanol (GC assays; Sigma)

MOPS titration buffer (≥ 99.5%; Sigma).

2.1.3. Equipment

2.1.3.1 Gas chromatograph

The gas phase chromatograph (Varian 3000) was equipped with a flame ionization detector (F.I.D.) and a slightly polar packed column (Chromosorb 101, Supelco). The carrier gas was dry nitrogen. The detector and injector temperature

were kept at 250 °C while the column was maintained at 170 °C.

The flow rates were 30 mL/min for the dry N_2 and H_2, and 300 mL/min for the dry air. The column was a glass column of about 30 cm length with a 0.8 cm diameter.

2.1.3.2 Bioreactor used for the hydrolysis reaction

The hydrolysis reaction was studied with a single tube system (Figure III-1). The protein was dissolved into MQ water or MOPS buffer (pH 6.5); 100 µL of this solution was applied to a glass fibre paper and freeze-dried. The protein was usually re-hydrated at room relative humidity overnight prior to initiation of the reaction. To start the reaction, 4 µL of ethyl butyrate were injected through a septum onto a second glass fibre paper. 100 µL - 500 µL of headspace were taken out at varying time intervals. The total headspace volume was approximately 8 mL.

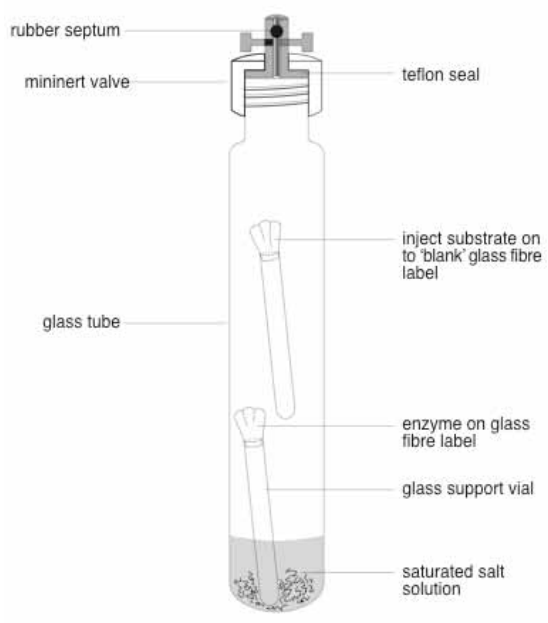

Figure III-1: System used to measure the hydrolysis reaction.

2.1.3.3 Bioreactor used for the alcoholysis reaction

The alcoholysis rate was measured in a dual-mininert system (Figure III.2) for the reasons discussed in section III-3.1.4.2. This system is composed of two tubes separated by a stopcock. One side contains the enzyme (usually 5 mg of

enzyme powder) while the other side contains the desiccant or saturated salt solution. The stopcock is kept open to allow the drying or hydration of the protein. Once the desired hydration level is reached, the stopcock is closed and the reaction is initiated by the injection of 4 μL of propanol and 4 μL of methyl butyrate onto a glass fibre paper. As before, the amount of product released by the enzyme was measured at different time intervals by removal of 100 μL of the headspace gas and analysed by gas chromatograph.

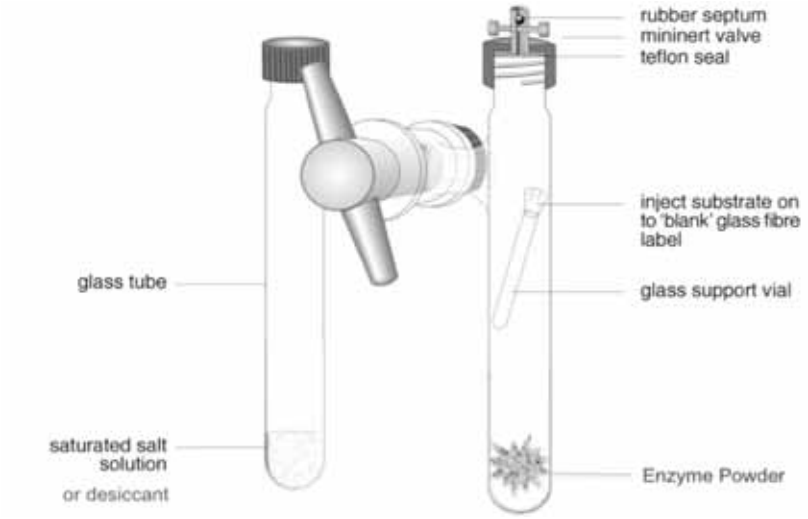

Figure III-2: Schema of the dual-mininert system

2.1.3.4 Syringes

0.5 and 5 μL SGE syringes were used for the injection of liquids and 100 and 500 μL gas tight Hamilton syringes were used for headspace injection.

2.2. Methods

2.2.1. Partial protein purification

2.2.1.1 C. rugosa lipase B

The *Candida rugosa* lipase B as supplied by Biocatalyst (Lipomod™ 34P) was purified using Fast Flow Q Sepharose (FFQ, Pharmacia Biotech). A column (~ 478 mL) was packed using a thick slurry of the resin, pre-washed and equilibrated with 300 mM then 30 mM MOPS-NaOH (pH 6.5) until the eluent pH

was consistently 6.5. The flow rate was maintained at 10 mL*min^{-1} using an AKTA system (Pharmacia, Biotech).

Twenty to thirty grams of *Candida rugosa* lipase B was dissolved in 900 mL of MQ water. Once the enzyme had dissolved, the protein solution was spun down at 8000 rpm for 15 min. The supernatant was then dialysed overnight. In the morning, the conductivity was checked to ensure it was below 5 mS. One hundred millilitres of MOPS-NaOH (300 mM; pH 6.5) were added to give a final buffer concentration of 30 mM while keeping the conductivity under 5 mS before loading onto the column.

Half of the enzyme solution was loaded onto the column. After loading of the enzyme, the column was washed with of 30 mM MOPS-NaOH until no protein was detectable in the eluent (usually about two column volumes). The column was then washed a second time with 0.1 M NaCl (prepared in equilibration buffer). The protein of interest was then eluted using a six-column volume linear salt gradient (from 0.1 to 0.75 M NaCl), and 50 mL fractions were collected. Carboxyl esterase activity was assayed with para nitro-phenol butyrate (*p*NP-butyrate, 25 mM) in MOPS-NaOH buffer (pH 6.5; 0.05 M) at 30 °C.

Active fractions were pooled and concentrated by ultrafiltration using an Amicon® YM10 membrane. For practical reasons, dialysis was preferred to diafiltration to desalt the protein. Dialysis tubing with a molecular weight cut off of 6000-8000 was used. Once the remaining salt concentration reached 1 mM or lower, the protein was freeze-dried.

2.2.1.2 Pig liver esterase (PLE) purification

PLE was purified using an identical method to that described for *C. rugosa* lipase B, except that the column buffer was set at pH 7.0 and the linear salt gradient was 0.1-0.5 M NaCl.

2.2.1.3 Other enzymes

Some of the crude extracts tested for the alcoholysis reaction (L224P, lipase SNS and lipase from pseudomonas) were purified further. The method used was similar to the one used for the pig liver esterase or lipase B described in the

previous chapter. The column used was the same as described above, while the buffer was 20 mM MOPS-NaOH at pH 7. And the linear salt gradient was between 0.1 - 0.5 M of NaCl.

2.2.2. Liquid-phase activity measurements

The esterase activity against pNP-butyrate was measured using a discontinuous assay. The assay mixture was composed of 885 µL of 50 mM MOPS (pH 6.5 or 7.0, for lipase B and PLE respectively), 5 µL of 1M $CaCl_2$ and 100 µL of 25 mM pNP-butyrate (dissolved in ethanol). The mixture was incubated at 30°C and the reaction was initiated by the addition of 10 µL of enzyme solution. After 10 min, the reaction was stopped by addition of 500 µL of copper phosphate stopping reagent. The stopping reagent was made up from stock solution of copper chloride ([$CuCl_2.2H_2O$]=28.5 g/L), sodium phosphate ([$NaH_2PO_4.12H_2O$]=68.5 g/L), sodium tetraborate ([$NaB_4O_7.10H_2O$]=19.1 g/L) and 10 mL Triton X-100. The reaction vial was centrifuged and the supernatant measured for absorbance at 400 nm. The absorbance at 400 nm of the *p*-nitrophenol was measured as a function of its concentration (Figure III-3) and used to determine the extinction coefficient of the product under the assay conditions.

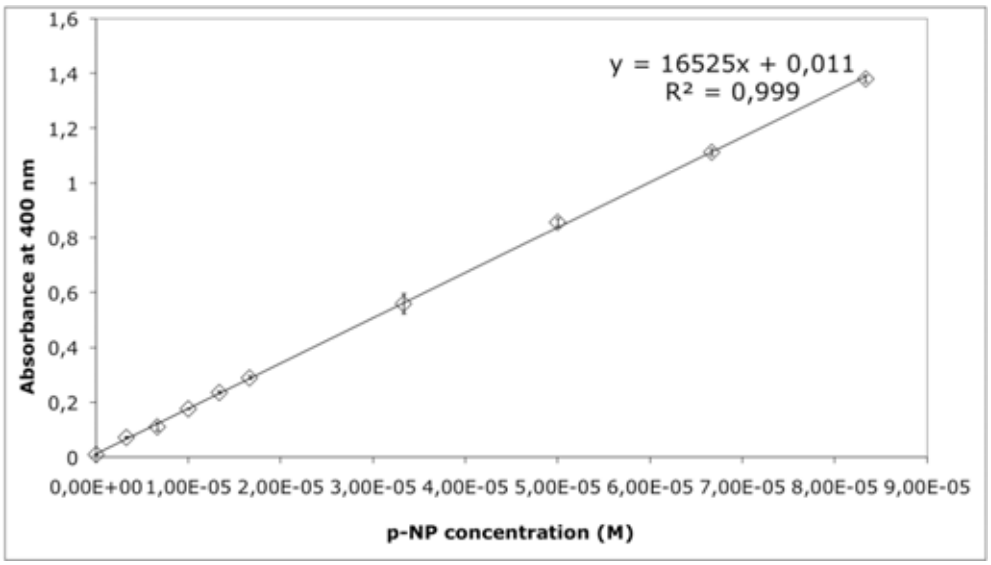

Figure III-3: Standard curve of *p*-nitrophenol for esterase activity determination. The linear regression is y = 16525 x + 0.0116 for the range of concentrations studied with a correlation coefficient of 0.9997.

2.2.3. Protein quantification

Protein concentrations above 0.5 mg*mL^{-1} were determined by the method of Biuret using bovine serum albumin (BSA 2 mg*mL^{-1}) as standard. The Biuret reagent was made up of 0.96 g/L of anhydrous cupric sulphate ($CuSO_4$), 4.81 g/L of sodium tartrate and sodium hydroxide (NaOH) 3%. Usually between 0.1-0.5 mL of the protein solution was added to 2.5 mL of the reagent. The absorbance was read at 545 nm after 30 min of incubation at room temperature. Figure III-4 shows the results obtained for BSA. Protein concentrations below 0.5 mg*mL^{-1} were determined by the far UV method described by Scopes (1994). The protein concentration of the eluent from the chromatography columns was monitored continuously at 215 and 280 nm.

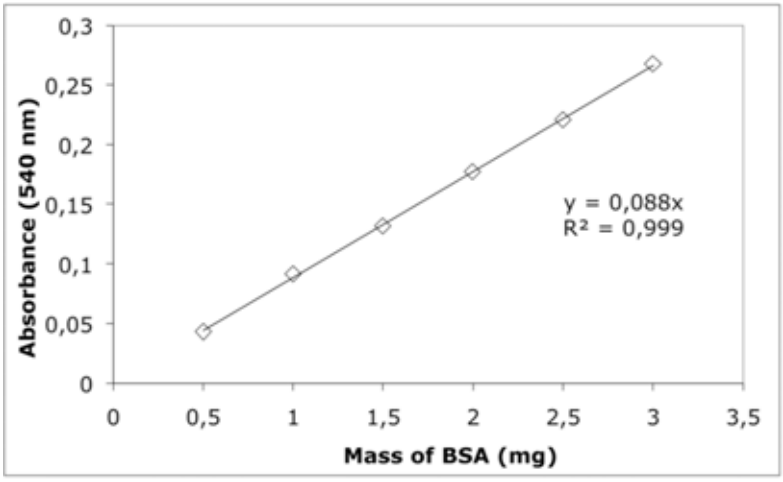

Figure III-4: Standard curve used to quantify the amount of protein in a solution with the Biuret reagent. The reference protein is BSA (Bovine Serum Albumin).

2.2.4. Drying methods

2.2.4.1 Hydrolysis

Unless specified otherwise, for the hydrolysis reaction, the lipase B was dissolved in MOPS (50 mM; pH 6.5) at a concentration of 5 mg/mL. 100 µL of the enzyme solution was aliquoted onto a glass fibre paper with a surface area of 1.5 cm^2. Once the paper had absorbed the solution, the glass fibre paper was freeze-dried. Before the experiment, the paper was rehydrated at room relative humidity (RH≈50-60 %) as a preliminary to adjusting to a specific hydration in

the experimental apparatus.

2.2.4.2 Alcoholysis

Usually 5 mg of purified enzyme powder or 30 mg of the crude extracts were introduced inside one of the sample tubes of the dual mininert system. For this series of experiments, the enzymes were dried sequentially over 10 days in the following manner.

- 2 days room temperature over silica gel
- 2 days room temperature over fresh high grade phosphorus pentoxide (P_2O_5)
- 5 days 65 ˚C over fresh high grade P_2O_5
- 1 day room temperature over fresh high grade P_2O_5

After the drying step over silica gel, P_2O_5 was added into the empty vial of the dual mininert system. This addition was carried out inside a glove box with a RH under 5%. Both tubes were sealed with a mininert® top, and the stopcock between them was then opened.

2.2.5. Hydration and sorption isotherm measurements

2.2.5.1 Enzyme hydration

100 mg of enzyme powders of lipase B and PLE were dried over high grade P_20_5 for a week at room temperature. The weight of protein obtained was considered, for these experiments, as the "dry weight" of the protein (but see chapter II). Then, the proteins were exposed to increased relative humidity (RH) using different saturated salt solutions. The enzyme was exposed one week at room temperature at each RH and the uptake of water was measured.

2.2.5.2 Sorption isotherm

For each RH, the enzyme hydration was calculated and expressed as a fraction of the dry weight, i.e., as *h*. The enzyme hydration was then reported as a function of RH.

2.2.6. Enzyme gas phase assays

2.2.6.1 Hydrolysis

Unless indicated otherwise, the glass fibre paper prepared as described above, and containing about 500 µg of *C. rugosa* lipase, was introduced into a glass vial of 9 mL (Figure III.1). A second "empty" glass fibre paper was also introduced. Then the vial was closed and sealed with a mininert® top as described in the material paragraph. 4 µL of ethyl butyrate were introduced through the septum with a 5 µL syringe and injected onto the "blank" glass fibre paper. The reaction followed is:

$$ethyl\ butyrate + water \Leftrightarrow ethanol + butyric\ acid$$

2.2.6.2 Alcoholysis

After the drying step, the stopcock was closed and the reaction initiated by the injection of both substrates in the same manner as described for the hydrolysis reaction. To prevent any contamination, different syringes are used for each substrate: 4 µL of propanol are added and then 4 µL of methyl butyrate.

$$Methyl\ butyrate + propanol \Leftrightarrow Methanol + \mathrm{Pr}opyl\ Butyrate$$

2.2.7. Quantification of the substrates and products

2.2.7.1 For the hydrolysis reaction

The hydrolysis of the ethyl butyrate into ethanol and butyric acid was followed by the measurement of the amount of ethanol and ethyl butyrate produced in the gas phase by gas chromatography (GC). Under our conditions, the butyric acid was not be detected by the gas chromatograph because the packing material of the column was not appropriate.

Standards curves of the substrates and products were performed for their quantification. The solutes were dissolved in water at different concentrations in three replicates, and 0.5 µL of the mixture are injected onto the GC. The amount of analyte (W_{GC}) injected onto the GC was calculated (Figure III-5):

$$W_{GC}(nmol) = C(nmol/mL) * 0.5 \bullet 10^{-3}(mL)$$

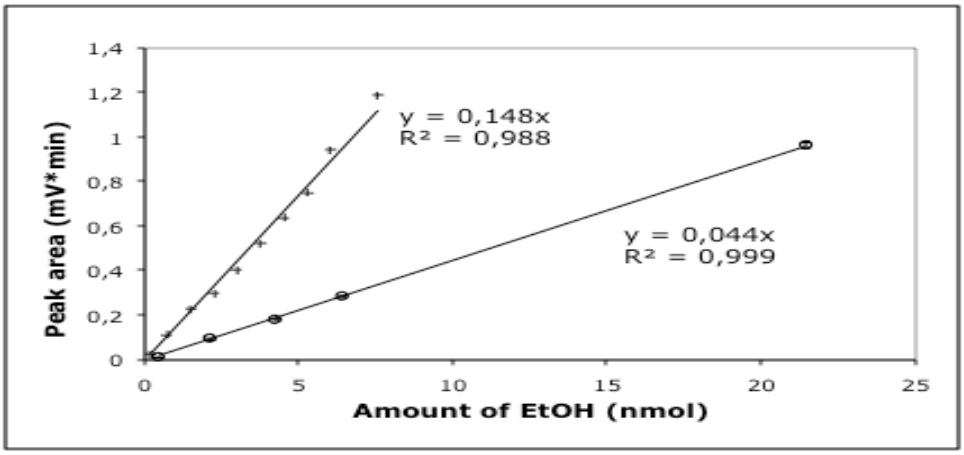

Figure III-5: GC standard curves of ethanol (○) and ethyl butyrate (+).

$$A = aW_{GC}$$

A is the peak area obtained with the gas chromatograph

$\mathbf{W_{GC}}$ is the amount of analyte injected onto the GC

a is the slope from the analyte's standard curve

The slopes of the standard curve give the sensitivity of the gas chromatograph for each analyte, which is assumed to be the same whether the analyte is injected in a gas or liquid form, since the analytes were volatile at the injector temperature.

To calculate the amount of analyte in the sample vial (W), it is necessary to take into account the volume of the headspace (HS) injected (100 µL) onto the GC as well as the volume of the vial (9 mL):

$$W_i = W_{GC} / 0.1 * 9$$

2.2.7.2 Standard curves used for alcoholysis

In the same manner, standard curves were performed for each substrate and product of the alcoholysis reaction. The results are presented in the figure below.

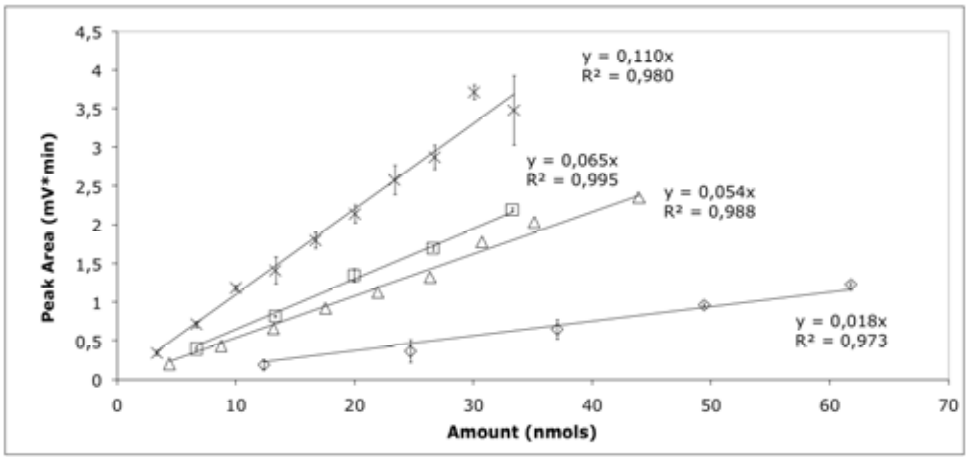

Figure III-6: Standard curves used for the quantification of methanol (◊); propanol (△); methyl butyrate (×) and propyl butyrate (□).

2.2.7.3 Correction of the raw data

In our experiments, we carried out consecutive analyses from the same sample vial. Although the partition coefficient remains constant, the peak area obtained for the second and subsequent aliquots may be reduced. In the absence of enzyme, for instance, taking successive aliquots from the same vial, would lead to a decline and eventually to a complete exhaustion of the total amount of analyte (Kolb and Ettre 1997.

In the same manner the amount of product and substrate in our vial is potentially underestimated. To correct the amount of product and substrate present in our vial, the following formula was used:

$$W_c = W_i + (W_{i-1}/9 * 0.1)$$

W_c: amount of analyte corrected

W_i: amount of analyte at the sampling i

W_{i-1}: amount of analyte at the previous sampling

$W_{i-1}/9*0.1$: amount of analyte extracted from the sample tube at the step W_{i-1}.

2.2.8. Hydrolysis improvement methods

2.2.8.1 The use of cryoprotectants

Stock solutions of sucrose, glycerol or sorbitol at a concentration of 100 mg/mL were prepared in water. Between 2.5 and 10 μL of the stock solution were

added to 100 µL of a stock solution of lipase B in MOPS buffer (50 mM; pH 6.5). The mixture was then aliquoted onto a glass fibre paper. The papers were freeze-dried and re-hydrated at room relative humidity and the hydrolysis reaction was measured as previously described.

2.2.8.2 The use of volatile buffers

MOPS buffer was used as a non-volatile buffer control. Sodium formate and ammonium hydrogen carbonate are two buffers where only one component is volatile; ammonium formate is a buffer where both of the components are volatile. These four buffers were tested over different concentration and pH. The pH was adjusted with either hydrogen chloride (HCl) or sodium hydroxide (NaOH). The assay mixture was prepared as described for the hydrolysis reaction.

2.2.8.3 Bio-imprinting

Following the methodology used by Gonzalez-Navarro and Braco (1997), we tested the activity of bio-imprinted lipase B in our solid/gas bioreactor. The enzyme was incubated for 5 min at 4 °C in MOPS buffer in the presence of the amphiphile n-octyl glucopyranoside (n-OG). The mixture was then applied to a glass fibre paper and freeze-dried. To remove the n-OG, the glass fibre paper was washed in three successive baths of benzene/ethanol (90:10). Another control with addition of sorbitol to the imprinted enzyme was performed. Sorbitol may prevent the denaturation of the imprinted enzyme. The glass fibre paper was air dried at room RH. Two controls were prepared; a non-imprinted enzyme and non-washed control; and a non-imprinted but washed the same way as the imprinted samples (e.g. washed in organic solvent). A third control without excipient was performed as well. Each sample was done in four replicates, and the hydrolysis activity in the gas phase was checked as previously described.

3. *Results*

3.1. Improvement of the hydrolysis reaction

The diffusivities in the gas phase are high and should cause fewer problems due to diffusion limitation than in the liquid phase. However, the amount of enzyme might have an impact on the kinetics. For instance, the amount of substrate and product in the gas phase, being limited by their vapour pressure, might not be in excess if the amount of enzyme becomes too high. Another problem is that the surface of the fibre paper where the enzyme is pulled down might become too small as the amount of enzyme is increased. Thus, the assay will be diffusion limited. Finally, the products, butyric acid and ethanol, may denature the enzyme if diffusion away from the enzyme is not rapid enough. For these reasons, initial rates might seem to be the most reliable.

Two preliminary experiments were carried out, first with very low amounts of enzyme and then with larger ones.

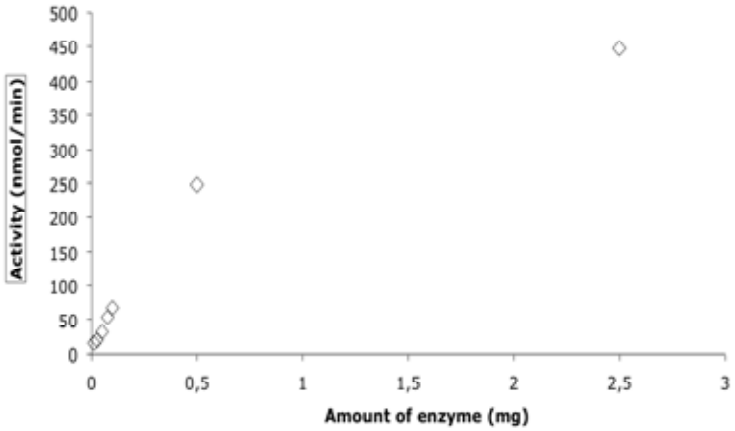

Figure III-7: Production of ethanol as a function of the amount of enzyme.

Different amounts of enzyme were added onto the same surface area of glass fibre paper and each rate measured over the first 15 minutes, when the amount of ethanol produced in the gas phase increased linearly with time. The resulting rates are represented as a function of the amount of enzyme in the graph above (Figure III-7). Between 0.01 and 0.5 mg of protein, the hydrolysis activity increases linearly with the amount of enzyme. At 0.5 mg and above the activity slows, and above 2.5 mg decreases (results not shown). The decrease of the

enzyme activity with increasing amounts of enzyme might be explained by different factors. Firstly, the inhibition of the products on the alcoholysis rate seems the simplest explanation. Small alcohols, such as propanol, have been shown to inhibit the alcoholysis of *Candida Antarctica* lipase B(Bousquet-Dubouch *et al*., 2001). Recent studies on methanolysis have also highlighted that an initial ratio higher than 1:1 between both substrates when methanol was a substrate, could inhibit the esterification. However, further addition of methanol later on in the reaction, could improve it (Nie *et al*., 2006). Secondly, the protein might be too packed onto the paper and prevent the diffusion of the substrates. And finally, the quantity of substrate in the headspace of the sample tube is limited by its vapour pressure but also by the vapour pressure of the product appearing with time. Thus, further production of ethanol might not be detected in the gas phase. However, the fact that the rate decreases at higher amount of enzyme indicates that diffusion limitation is probably the best explanation. Arising from these results, the amount of lipase B chosen for use for the investigation of the hydrolysis activity was 0.5 mg or less.

The amount of substrate and product in the gas phase was followed over time and extrapolated to t=0 where the amount of the products is assumed to be null (Figure III-8).

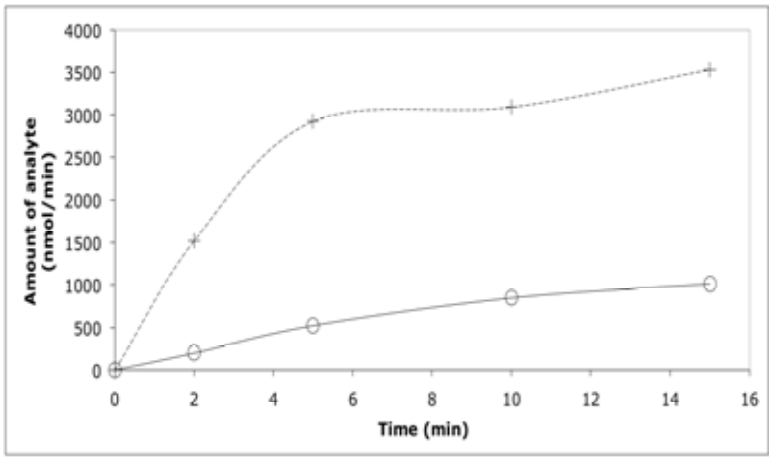

Figure III-8: Amount of ethanol (○) and ethyl butyrate (+) followed as a function of time by GC.

The amount of ethyl butyrate substrate in the gas phase increases until a maximum value. This is because it requires a few minutes for the substrate to evaporate and reach equilibrium with the gas phase. This results in a lag of a few

minutes before the gas phase of the analysis vessel is equilibrated with the added liquid substrate. However, since the amount of product increases linearly with time over the first five minutes, with no apparent lag, it seems that this has not significantly limited the enzyme activity. The total enzyme activity is determined by the slope of the linear regression line of the amount of ethanol produced with time, the trend line was chosen to cross the x axis at t=0. An average activity of 324 ± 31 nmol/min (specific activity approximately 648 nmol/min/mg) is observed under these conditions.

3.1.1. The use of cryo-protectant

Three different cryo-protectants were tested, two polyols (glycerol and sorbitol) and one disaccharide (sucrose), for their efficiency to protect lipase B against denaturation during the freeze-drying process. The gas phase activity of the resulting enzyme preparation was tested. Different amounts of cryo-protectants (also called excipients) were tested to find the minimum amount required to produce the optimum effect.

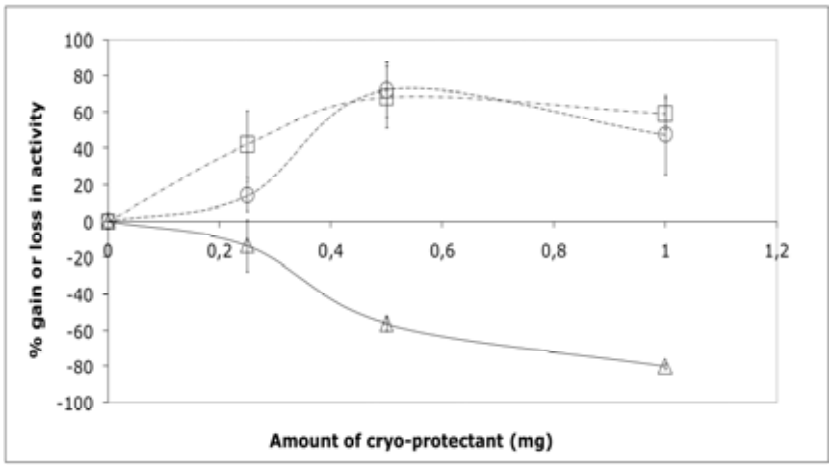

Figure III-9: Enzyme activity as a function of the amount of glycerol (△), sorbitol (□) or sucrose (○) with 0.5 mg of lipase B.

The zero point of the graph above shows the enzyme activity with no cryo-protectant. The glycerol has a negative effect on the rate, which is in disagreement with its low glass transition temperature (refer Table III.1). Sorbitol has a better effect than sucrose, but the difference is not significant. Small sugars and polyols may have an effect on the active site and explain an increase of activity. For

instance, some lipases are able to transform glycerol (Kim *et al*., 2007). However, the negative effect of glycerol on activity shows that this fact does not completely explain the effect of the excipients. Liao *et al*. (2002) showed that additives might preserve activity and/or the enzyme native state upon storage. They found a weak correlation between the enzyme-recovered activity on the aqueous phase and the preservation of the native state. This finding is important since as for our gas/phase assays, the enzyme is not in aqueous phase. Thus the preservation of the native state upon freeze-drying is crucial. Carbohydrate's effect on freeze-drying has nothing to do with their glass transition temperature (Tg) but with their ability to form hydrogen bond with the protein. The minimum mass ratio required for the protective effect would then correlate with the protein monolayer coverage. In molar terms this ratio is about 166.8 for sucrose and 313.42 for sorbitol. Sucrose and sorbitol give the same optimum at 0.5 mg which corresponds to an enzyme:cryo-protectant ratio of 1:1 by weight. The monolayer coverage of this enzyme by water molecules would be around 600 for a hydration level about 0.2 *h* (refer section V-2). Thus, the surface coverage of the cryo-protectants, being larger than a water molecule, probably approximates a monolayer. Disaccharides such as sucrose protect proteins against denaturation during both the freezing and the drying steps, which would explain the positive effect of sucrose. Another hypothesis advanced by Liao *et al*. (2002) is that the stabilisation of the secondary structure is correlate with the Tg, lower Tg leading to a limited stabilisation. The excipient Tg would not be the only important factor; another would be an excessive high Tg of the excipient as compared to the Tg of the same excipient in combination with the enzyme. These two last hypotheses do not agree with our results for sorbitol. It might be expected that the Tg of the protein-excipient mixture should be fairly close to that of sorbitol. An excess of the enzyme mobility resulting in denaturation found by Liao *et al*. (2002) may explain the negative effect they observed with glycerol.

Table III-1: Glass transition temperature of excipients (Liao *et al.*, 2002)

Excipient	Tg (°C)
Glycerol	- 99.9
Sorbitol	- 34.5
Sucrose	- 48.8
Trehalose	- 31.1

3.1.2. The use of volatile buffers

It has been observed in organic media that enzyme activity could be improved by incubation of the enzyme at its optimum pH prior to freeze-drying(Klibanov, 2001). The enzyme would be able to preserve its active conformation through the "pH memory" effect. This phenomenon might be explained by either the enzyme rigidity in organic media and/or the fact that after freeze-drying, some remaining salt would preserve its ionisation state.

The presence of salt in the enzyme powder is not desirable, as the hydration level would be affected. However, the possibility of the use of volatile buffer could overcome this problem by their evaporation during the freeze-drying process. In the following experiment, the effect of a non-volatile buffer on the enzyme activity was compared to two partially volatile buffers (sodium formate and ammonium hydrogen-carbonate) and one completely volatile (ammonium formate) at three different pHs and two different molarities.

Table III-2: Effect of different buffers on the pH memory.

Buffer	**Buffer concentration (mM)**	**Activity (nmol/min)**		
		pH 6.5	**pH 7.5**	**pH 8.5**
MOPS	4	67.3±6.9	34.3±4.8	48.3±11.8
	40	162.1±15.6	116.7±16.3	104.4±16.3
Ammonium Formate	4	38.4±12.6	19.8±3.4	41.9±n.d.
	40	80.3±6.5	122.6±11.7	79.8±35.0
Sodium Formate	4	34.6±17.1	21.4±1.9	29.1.±7.2
	40	113.9±8.4	105.4±12.0	97.4±3.1
Ammonium Hydrogen-carbonate	4	29.7±2.2	12.0±1.7	29.4± n.d
	40	63.2±5.9	90.1±13.3	62.1±15.3

The overall enzyme activity is lower than usual because these samples have been stored before use. In addition, since the room relative humidity (RH) varied between 50% and 60%, some differences might occur from one experiment to the other. The reference sample of reference is the one with MOPS (40 mM; pH 6.5). All the samples with a buffer concentration of 4 mM present a lower activity than those at 40 mM. Thus, all the buffers have a positive effect on the enzyme activity and the samples with low concentration of buffer do not have a buffering effect strong enough or have a weaker ionic strength. Samples at 400 mM have also been used but there is no improvement in activity compared to the samples at 40 mM (results not shown). A pH optimum shift is also observed depending on the buffer used. MOPS and sodium formate show an optimum activity at pH 6.5 while the two others give an optimum activity at pH 7.5. Among the "volatile buffers", the ammonium formate seems the best to retain a 'pH memory' effect. This result is rather atypical and goes against the idea that the 'pH memory' effect is due to the ionized state of the enzyme after freeze-drying. However, the change of shape due to the ionised state might remain upon freeze-drying. Overall, the best activity was with 40 mM MOPS, pH 6.5.

Table III-3: Effect of buffer (40 mM; pH 6.5) on enzyme activity.

Buffer	**MQ Water**	**MQ Water**	**MOPS**	**MOPS**	**Ammonium Formate**	**Ammonium Formate**
Excipient	None	Sorbitol	None	Sorbitol	None	Sorbitol
Activity (nmol/min)	11.7 ± 2.8	105.2 ± 7.4	63.1 ± 5.7	115.1 ± 9.0	37.4 ± 5.1	110.0 ± 11.9

A control experiment was also performed to verify the existence of a pH memory effect with lipase B in the gas phase. In this experiment, the activity was measured for an enzyme incubated in purified water before freeze-drying as compared with an enzyme dissolved in MOPS or ammonium formate. It is shown in Table III-3 that the presence of ammonium formate improves the activity by 3 times and MOPS by 6, but these are not additive. Thus, the enzyme activity is also improved with volatile buffer but the effect is not as important as the effect obtained with MOPS. However, in the presence of sorbitol, the different buffers do not show any differences as compared to water. Indeed, the rate obtained for water, MOPS and ammonium formate is equivalent. Thus, the improvement of the enzyme stability with the excipient would override the "pH memory". One should remark that the re-hydration of the samples at room RH might have led to a hydration level of lipase B between 0.1-0.2 *h*. Although enzymes are considered to be rigid at such hydration level, it would be expected to obtain better results at lower hydration.

3.1.3. Bio-imprinting

This method consists in locking the active conformation of an enzyme with a substrate-analogue or an inhibitor. In organic media, the enzyme being rigid, the active conformation is preserved. In the gas/solid bioreactor, the relative humidity (RH) of the enzyme environment can be controlled to be near anhydrous conditions. It is then expected that a freeze-dried powder of the enzyme-substrate analogue complex to remain rigid in such environment. The removal of the substrate analogue is a critical step as the organic solvents used are known to slightly destabilise the enzyme and that it has to be efficient. Excipients such as sorbitol are often added to the enzyme mixture to improve the enzyme stability.

However, the presence of such excipients is not desirable when studying the effect of hydration on the enzyme activity. Thus, the improvement of the enzyme activity with *n*-OG as bio-imprinter has been tested without the addition of excipient. The results are summarized in the table below.

Table III-4: Bio-imprinting assays.

	Not imprinted not washed	**Not imprinted (washed)**	**Bio-imprinted with *N*-OG (washed)**	**Not imprinted + Sorbitol**	**Bio-imprinted with *N*-OG + Sorbitol (washed)**
Activity (nmol/min)	91.9 ± 2.5	40.3 ± 4.5	28.5 ± 3.0	105.2 ± 7.4	124.9 ± 10.6
% gain or loss of activity		- 56.2 %	- 68.9 %	+ 15.34 %	+ 35.9 %

The results show that washing the enzyme in the organic solvent induces a loss of more than 50% of the enzyme activity. The bio-imprinting technique seems to induce a loss of 10% of the enzyme activity. It might be because the washing only partially removed the n-OG from the active site. However, in presence of sorbitol, there is an increase of 35% of the activity compared to a non-washed and non-imprinted control. This was the same improvement observed in the presence of the excipient without bio-imprinter (cf. cryo-protectant section). The bio-imprinter does not seem to work. There are two explanations; first, the enzyme was re-hydrated at room RH. Therefore, the conformational rigidity required may have been lost. Second, the loss of activity between a non imprinted but washed enzyme and a bio-imprinted enzyme might indicate that not all the imprinter was removed.

3.1.4. Effect of relative humidity (RH) on enzyme hydration and activity

Saturated salt solutions are used to control the relative humidity inside the sample tube and thus the enzyme hydration. These solutions were previously used to study the effect of hydration on enzyme activity (Lind et al. 2004).

3.1.4.1 Sorption Isotherm of lipase B and pig liver esterase

Sorption isotherms measure the uptake of water by proteins as the function of the relative humidity (RH) of their immediate environment. Knowing the sorption isotherm is useful to choose the right saturated salt solution to use to reach a desired enzyme hydration level. The sorption isotherms were measured for pig liver esterase (PLE) and lipase B.

Table III-5: Water uptake of lipase B and PLE when equilibrated over different saturated salt solution.

Saturated salt solution or desiccant	*RH above the saturated salt solution (%)*	*Lipase B mass uptake (mg)*	*PLE mass uptake (mg)*
P_2O_5	0.02	0	0
LiBr	6.5	4.3	1.9
LiCl	10.3	5.2	2.6
$MgCl_2$	31.2	9.4	4.1
NaBr	57.1	15.9	7.9
NaCl	75	27.4	11.2
$ZnSO_4$	88.5	47.5	16.8
H_2O	100	n.d.	45.9

The values of RH obtained here were experimentally measured with a RH probe (VASALA, Alltech) within a confidence of ± 2 %. The relative humidity values obtained experimentally are in good agreement with those found in the literature (Greenspan, 1977). The results show that the lipase B adsorbs at least as much water as PLE when equilibrated above the same saturated salt solutions. The water uptake of the lipase B at 100 % was not measured as the protein powder had collapsed into a paste. The sorption isotherms extracted from these results are presented in the graph below:

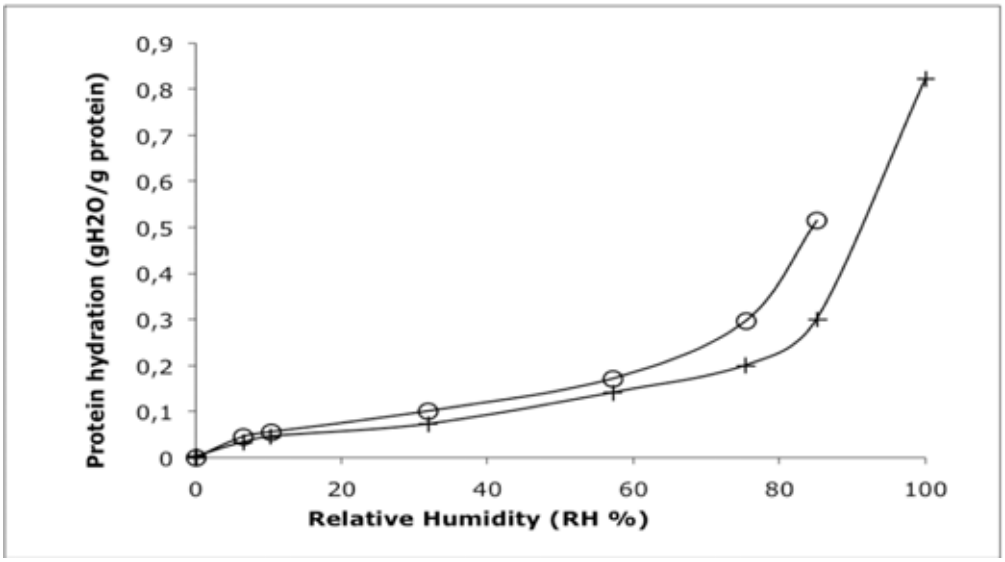

Figure III-10: The water uptake of Lipase B (○) and PLE (+) as a function of the relative humidity.

Both sorption isotherms show the expected sigmoid shape (include reference). The inflection of the curve obtained for lipase B occurs at lower RH than for PLE, consistent with the fact that lipase B is taking up more water than PLE at the same RH.

3.1.4.2 Effect of hydration on the lipase hydrolysis reaction

To study the effect of hydration on enzyme activity, the enzyme has to be equilibrated against saturated salt solutions and/or a desiccant to reach the desired hydration level. After freeze-drying, the glass fibre paper with the enzyme was equilibrated with a saturated salt solution to reach different levels of hydration. The samples were left to equilibrate for a week at room temperature. The hydrolysis activity was measured by gas chromatography as described above. One control without any saturated salt solution and/or desiccant was performed to test the effect of the incubation period above a salt solution. The hydration level was in this case estimated to the one obtained at room RH.

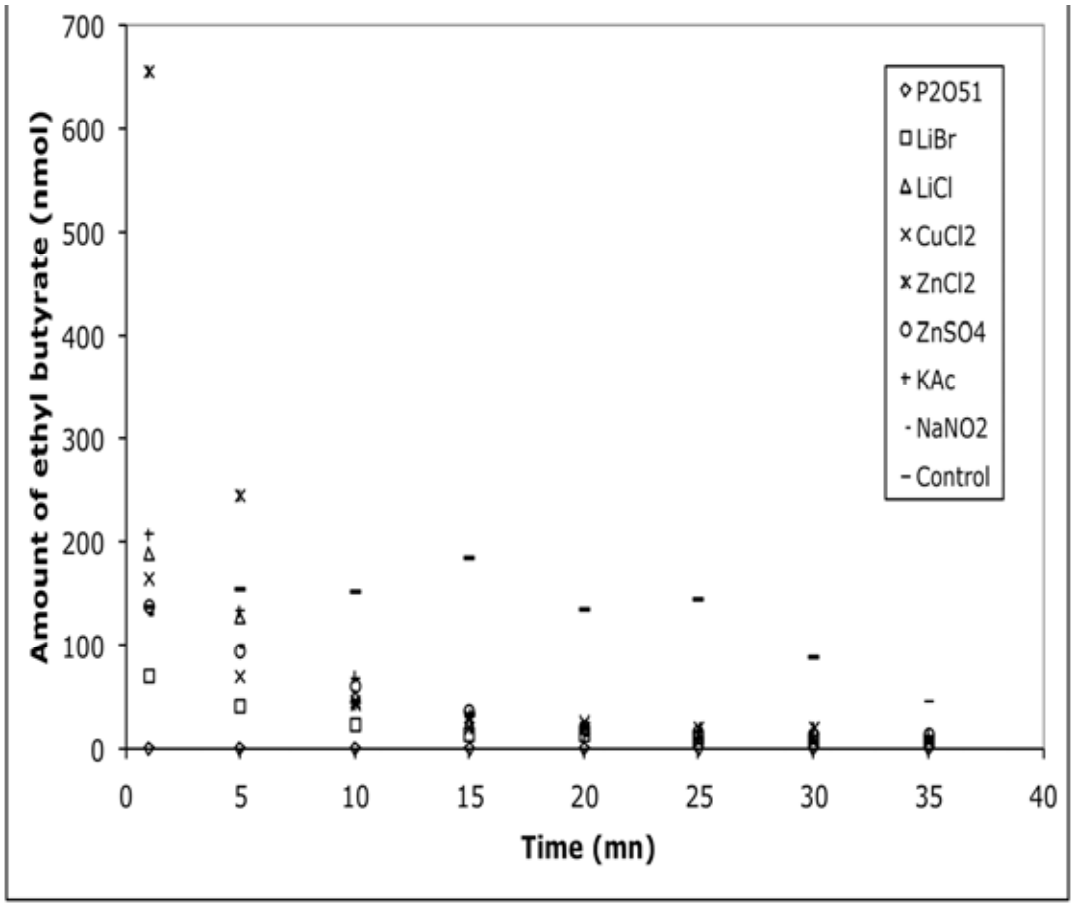

Figure III-11: Effect of saturated salt solutions on the amount of ethyl butyrate in the gas phase.

In this experiment the reaction was carried out under a gas phase exposed to the saturated salt solution. No ethanol production was observed and the amount of ethyl butyrate substrate in the gas phase (Figure III-11) decreased rapidly with time except in the absence of saturated salt solution. Thus, it was concluded that a side reaction occurred. The liquid phase appears to remove both the substrate and product from the gas phase. The amount of ethyl butyrate in the control sample (with no salt solution) remains relatively constant throughout the enzyme reaction. Thus, the detection of the analytes in the headspace is not possible in the presence of the saturated salt solution. As a result of this experiment, double mininert system was then substituted for the single system used up to this point as pointed out by the experiments done on the effect of hydration on enzyme activity (Chapter IV, section 3.1). This system is composed of two sample tubes separated by a stopcock. The saturated salt solution is placed in one tube, and the enzyme in the second one. Once the desired hydration is reached, the stopcock is closed and the reaction then initiated (cf. Figure III-2). In these studies, it was observed that

the enzyme activity was favoured when the enzyme was freeze-dried in the presence of excipients (Figure III-9). It was also found that pre-incubation of lipase B in buffer improves its activity through the 'pH memory' effect (Table III-5). The bio-imprinting method showed a little effect, although better effect might have been observed in anhydrous conditions. The positive effect of the pH memory or of a bio-imprinter is overridden by the use of excipient. Thus, the main difficulty seems to be the preservation of the enzyme stability over the assay as supported by the effect of the use of excipient.

The main focus of this work is the investigation of enzyme activity in near anhydrous conditions. To this end, it was necessary to move on to the alcoholysis reaction where water is not a substrate or a product. Work on the hydrolysis reaction has underlined the necessity of the use of a different experimental system when looking at the effect of hydration on the alcoholysis reaction. The detection of the products in the gas phase is in fact possible only in absence of a liquid phase. Alcoholysis rates are expected to be lower than hydrolysis ones, and near anhydrous conditions might lower these rates still further, so that the work above in trying to optimise gas phase reaction rates has been important. The next step was to study the gas phase alcoholysis reaction to optimise the measurement of these low rates.

3.2. Alcoholysis reaction

3.2.1. Preliminary enzyme screening

Lipases and esterases seem good candidates to study the effect of hydration on enzyme activity in a gas/solid system. Firstly, they are able to catalyse the alcoholysis reaction, where water is neither a substrate nor a product. Secondly, they do not require co-factors to work. Thirdly, studies in organic solvents or in the gas phase show that these enzymes are able to work at low water content. However, lipases and esterases are a large family of enzymes, and some of them seem better than others; it was therefore necessary to find out which enzymes would work the best in our system; since rates seemed likely to be low it was important to optimize our conditions. We tested some crude extracts of lipase we had in the lab as well as some enzymes known to have good activity at low

hydrations, such as *M. miehi* lipase (Valivety, Halling *et al.,* 1992), *C. rugosa* lipase B (Gonzalez-Navarro and Braco, 1997) and pig liver esterase (Gais *et al.,* 2001).

First, the enzymes or crude extracts were compared by their hydrolysis activity in the aqueous phase. We used a discontinuous assay with *para*-nitrophenyl butyrate substrate, as described in the section 2.2.2.

Table III-6: Hydrolysis activity against *p*NP butyrate in aqueous phase of different enzymes. The descriptions of the crude extracts are given in section 2.1.1.

Enzyme	***Specific Activity (µmol/min/mg)***	***Purity***
Esterase/Lipase/Protease from prcine pancreas (L224P)	7	Crude extract
Mixed fungal esterase blend including *P. roqueforti* (L187P)	189.1	Crude extract
Esterase from *P. roqueforti* (L338P)	112.9	Crude extract
Lipase/Esterase from *C. rugosa* (L34P)	284.3	Crude extract
Lipase SNS	17.6	Crude extract
Pseudomonas lipase	154	Crude extract
C. rugosa lipase B (CRL)	600	purified
Pig liver esterase (PLE)	254	purified

As expected, all the extracts had activity against pNP-butyrate; several of the crude extracts had a lower specific activity than the pure enzyme. The crude extract of *C. rugosa* lipase B (CRL) shows the best activity in comparison to the other crude extracts. The esterase mixtures from *P. roqueforti* (L187P and L338P) and the *Pseudomonas* lipase also have a good hydrolysis activity. Then, the SNS lipase has a very small hydrolysis activity. And finally, the lipase/esterase/protease mixture isolated from porcine pancreas has nearly no

activity. However, it is difficult to compare these extracts for their activity, as we do not have any information about their purity. In addition, we are interested in the alcoholysis reaction rate and not in the hydrolysis rate. And finally, the assay conditions were optimized for *C. rugosa* lipase B and not for the others. It was then necessary to compare these enzymes for the alcoholysis reaction in our bioreactor.

However, the selected enzyme should have the best alcoholysis rate. The alcoholysis rate was measured in the gas phase for each enzyme. As the enzyme preparations were quite crude, we had to add large amounts of enzyme powder into each sample tube. About 30 mg of powder was added. The protein powders were dried and used with no pre-treatment. The alcoholysis rate in the gas phase was measured in two replicates for each enzyme. This experiment was repeated twice for some enzymes.

Table III-7: Production of methanol (MeOH) and propyl butyrate (ProOBu) as a measure of alcoholysis rates obtained crude extracts of lipases and esterases in a solid/gas bioreactor.

Enzyme	***Specific Activity - assay 1 (pmol/min/mg)***		***Specific Activity - assay 2 (pmol/min/mg)***	
	MeOH	ProOBu	MeOH	ProOBu
Esterase/Lipase/Protease from porcine pancreas (L224P)	1110	124	1576	210
Mixed fungal esterase blend including *P. roqueforti* (L187P)	86	28	112	34
Esterase from *P. roqueforti* (L338P)	-	-	87	22
Lipase/Esterase from *C. rugosa* (L34P)	43	20	-	-
Lipase SNS	500	199	290	417
Pseudomonas lipase	520	2380	173	297
C. rugosa lipase B (CRL)	1750	70.8	-	-
Pig liver esterase (PLE)	0	407	-	-

The results in Table III-7 are difficult to interpret unequivocally because of the differences observed in the production rate of the two products. In fact, the alcoholysis reaction has two steps and these two steps have different rates. However, the propyl-butyrate being the final product released from the enzyme, should be a good indicator of the global reaction rate. The two assays show a fairly good agreement, with 5 enzymes giving the best results, namely PLE, CRL, the pseudomonas lipase, lipase SNS and L224P.

It is clear that the aqueous phase hydrolysis assays are very poor predictors of gas phase alcoholysis activity. The comparison shows that the enzymes, which have the best hydrolysis activity in the aqueous phase, tend to have the lowest alcoholysis rate in the gas phase. Some lipases and esterases seem more specific for this reaction. PLE shows no production of methanol but a large amount of propyl butyrate, which might be an indication of a leak. However, no propyl butyrate can appear without a complete transesterification. In addition, methanol is a small and volatile molecule more likely solvate the protein or escape because of a leak. Thus, based on the propyl butyrate rates, these results show that the pure PLE offered the best gas phase activity followed by the crude lipase SNS and the lipase from *Pseudomonas*. The mixture L224P from Porcine pancreas and *C. rugosa* lipase B has also a good activity. The relatively poor results obtained for the enzymes L187P and L338P could be explained by denaturation of the enzyme. In fact, as the drying conditions are quite harsh, a recovered enzyme activity was measured to insure the integrity of the enzymes after the gas phase assays. The enzymes were re-dissolved into water and the hydrolysis activity checked (Table III-8). We found that only 30-50% of the enzyme was active after drying. The recoveries would seem to suggest that L224P is a very good alcoholysis enzyme. However, the activity for the lipase L224P, lipase SNS and the lipase from pseudomonas is so low, the recovered activity is not too meaningful in these cases, although for the first of these this may be due to the large losses during the assay itself.

Table III-8: Recovered liquid phase esterase activity against *p*NP butyrate after gas phase alcoholysis assays.

Enzyme	***As before GC assay (µmol/min/mg)***	***As after GC assay (µmol/min/mg)***	***Recovered activity (%)***
Esterase/Lipase/Protease from prcine pancreas (L224P)	7	1	14.3
Mixed fungal esterase blend including *P. roqueforti* (L187P	189.1	96.5	51.0
Esterase from *P. roqueforti* (L338P)	112.9	34.9	30.9
Lipase/Esterase from *C. rugosa* (L34P)	16.6	16.5	93.7
Lipase SNS	284.3	149.2	52.5
Pseudomonas lipase	15.4	5.1	33.2

For these preliminary experiments, the powders were taken straight from the bottle. To determine the effect of any included salt or other materials, which may disturb the protein hydration, we dialyzed the powders and checked the alcoholysis activity (Figure III-12). The best enzymes from the previous experiments were tested as well as *Mucor miehi* lipase. Some of the best crude extracts were also further purified to determine enzymes with good alcoholysis activity. The purification of the lipase SNS, for instance, gave three fractions with activity against *p*NP-esters. These fractions were also tested for their gas phase alcoholysis activity.

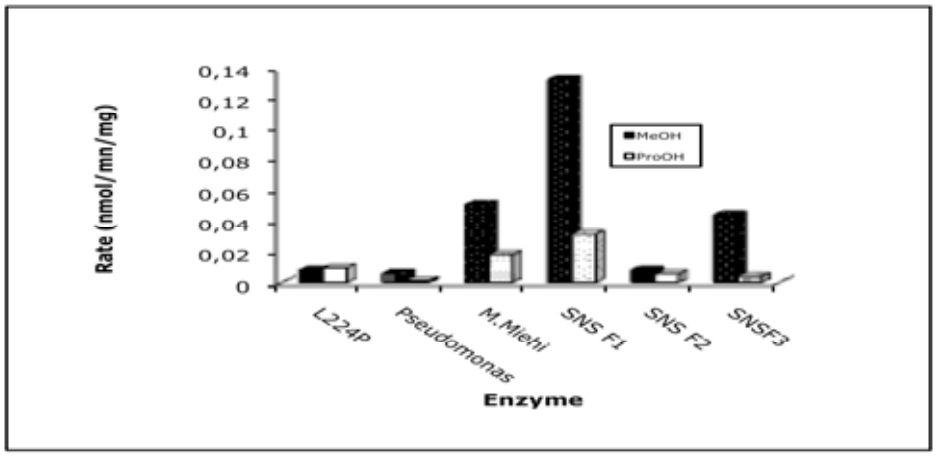

Figure III-12: Alcoholysis rate after dialysis.

As expected, the alcoholysis specific activities after dialysis were much lower than non-dialysed enzymes. The alcoholysis reaction of the SNS lipase seems concentrated in the first fraction. A 'pure' enzyme was added in this series of experiments: *M. miehi*. However, the alcoholysis rates of the purified fraction SNS 1 and *M. miehi* were still gave rates about 10 times lower than those obtained with the purified lipase B from *C. rugosa* and PLE. Thus only these last two enzymes were chosen for the investigation of the enzyme activity at low hydration.

3.2.2. Alcoholysis reaction of *Candida rugosa* lipase B

The alcoholysis reaction was further studied with *C. rugosa* lipase B in the gas/solid bioreactor at very low hydration. The enzyme was dried over P_2O_5 at 65 °C as described in the paragraph III.2.2.4.2., to give an expected hydration of about 9 water moles per mol of protein (or 0.003 *h*).

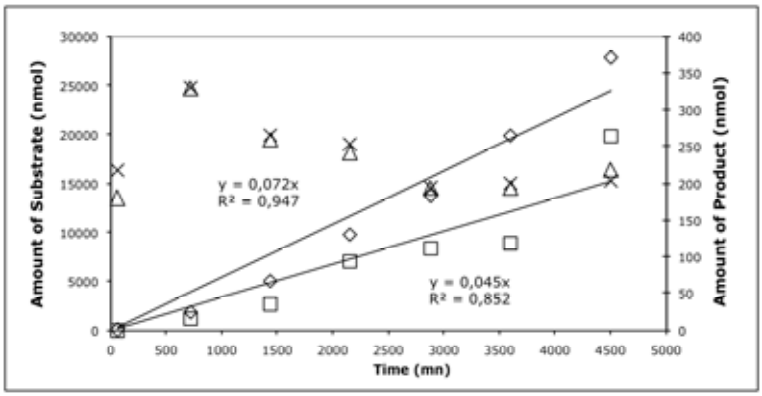

Figure III-13: Production of methanol (◊) and propyl butyrate (□) and disappearance of propanol (Δ) and methyl butyrate (×) as a function of time.

The amount of substrate is plotted on the left axis of Figure III-13 while that of the product are plotted on the right. The substrates are in excess compared to the products. One have to bear in mind that the amount of substrate in the gas phase is function of their vapour pressure and this might induce discrepancies between the molar ratios of the component resulting of the reaction and measured in the gas phase. Thus, molecules of substrate remaining on the glass fibre paper might replace gas phase molecules of substrate used by the enzyme. In addition, the amount of each component of the reaction is function of their vapour pressure in the mixture. The initial up and down of the amount of substrates is due to the time required to reach the equilibrium between liquid and gas phase. Often a stirrer is used to improve the equilibration step. The data for product increase does not show this because they are directly produced in the gas phase. The decrease of the amount of substrate following the "up and down" is due to their consumption by the enzyme. In addition, the vapour pressure of the substrates decrease as the products appears.

This experiment was performed with 5 mg of purified lipase B in six replicates to check the reproducibility (Table III-9).

Table III-9: Six replicate alcoholysis rates of C. rugosa lipase B in a solid/gas bioreactor.

	Methanol	**Propyl butyrate**
Rate (nmol/min)	0.0311	0.0271
	0.1788	0.1812
	0.0587	0.054
	0.0726	0.0453
	0.0755	0.092
	0.028	0.0242
Average	0.07412	0.07063
σ	0.05029	0.05424

Thus, in average, the methanol production is about 74 ± 50 pmol/min and the production of propyl butyrate is about 70 ± 54 pmol/min. The agreement between the products is good, but the reproducibility is relatively poor. This may be due to several factors. First of all, as the injection of the headspace is manual, the reproducibility is low compared to automated ones. However, the increase in the amount of product in the gas phase follows good straight lines (Figure III-13). Another possible explanation is that the amount of product in the gas phase is so low (only a few nanomoles), that we are working near the detection limits of the gas chromatograph, especially in the initial points of the time course. Indeed, only 5 nmol at most of product are injected onto the GC while its detection limit is about 1-3 nmols. Another explanation would be that with the hydration level of the enzyme powder being so low, and the dependence of rate on hydration potentially high, a small difference in the hydration level from one replicate to another could give a significant variation in the rate. Given that the powder preparations are unlikely to be homogeneous, this seems a likely cause. In addition the possibility of a back reaction would explain the non-reproducibility of the assays but also the slightly lower amount of propyl butyrate as compared to the amount of methanol.

3.2.2.1 Effect of buffer and substrates

Propanol has been found to inhibit the alcoholysis reaction of *C. antarctica* lipase B. Preliminary experiments have been done to check if another combination of substrates would improve the alcoholysis rate and thus improve the detection of the products.

Pr*oOH* + *MeOBu* ⇔ *MeOH* + Pr*oOBu* (Reaction 1)

Pr*oOBu* + *MeOH* ⇔ *MeOBu* + Pr*oOH* (Reaction 2)

Table III-10:Effect of different substrates on the alcoholysis reaction.

Products	**- MOPS**		**+ MOPS**	
	Assay 1 rate (nmol/min)	***Assay 2 rate (nmol/min)***	***Assay 1 rate (nmol/min)***	***Assay 2 rate (nmol/min)***
methanol	0.800	0.335	0.820	5.2679
propyl butyrate	0.051	0.222	0.392	2.396
propanol	0.239	0.488	0.084	0.301
methyl-butyrate	0.109	0.704	0.253	2.369

Only two replicates have been done, and given the variability it is difficult to do a quantitative comparison. However, some tentative qualitative conclusions can be drawn. There is no significant effect of the combination of substrates on the alcoholysis rate in the absence of MOPS. The second conclusion would be that the presence of buffer increases the alcoholysis rate, but may lower the reproducibility; and rates may be higher when methanol and propyl butyrate are the products. On the whole the experiment provided no evidence to support any change in the use of reaction 1 as the assay of choice.

3.2.2.2 Effect of desiccant

Phosphorus pentoxide became yellow in some reaction tubes after several days at 65°C. This might indicate reduced efficiency of this desiccant; two alternative choices were barium oxide (BaO) and magnesium perchlorate ($MgOCl_4$).

The experiment described in paragraph 3.2.2 was repeated, using the same

drying method but with different desiccants. The rate for the production of methanol and the propyl butyrate was determined. The experiment was performed in three replicates. The averaged rate obtained and the standard deviations are reported in Table III.8.

Table III-11: Effect of the desiccant on enzyme activity.

	BaO	***$MgOCl_4$***	***P_2O_5***
Rate of MeOH production (nmol/min)	0.059 ± 0.019	0.043 ± 0.022	0.109 ± 0.104
Rate of ProOBu production (nmol/min)	0.029 ± 0.007	0.010 ± 0.009	0.123 ± 0.124

The table above shows that better reproducibility is obtained with barium oxide and magnesium perchlorate, the highest activity is however with P_2O_5 and the lowest with $MgOCl_4$. These results are in agreement with the drying efficiency of the desiccant results observed in the Chapter II. The exception is the high alcoholysis activity observed with P_2O_5, explained by a loss in its efficiency after too long an exposure to 65 °C.

3.2.3. Alcoholysis reaction with pig liver esterase

3.2.3.1 Diffusion limitation

The diffusivities in the gas phase are high compared with those in solution. For example, the diffusion coefficient of ethanol in air is 40.4 cm^2/sec, compared with the diffusion coefficient of glucose in water, which is 0.63 cm^2/sec. However, in a solid/gas phase system we have to take into account the diffusivities of the reactants. This is because to detect the very low levels of activity expected at very low hydrations, large amounts of enzyme have had to be used, precluding the possibility of dispersal of the enzyme by, for example, immobilization, without an unacceptable loss of sensitivity in the system. So in our bioreactor, the enzyme is a static powder, in which protein-protein contacts

are potentially favoured. It is therefore possible that the amount of solid phase limits the accessibility of the substrates to the enzyme.

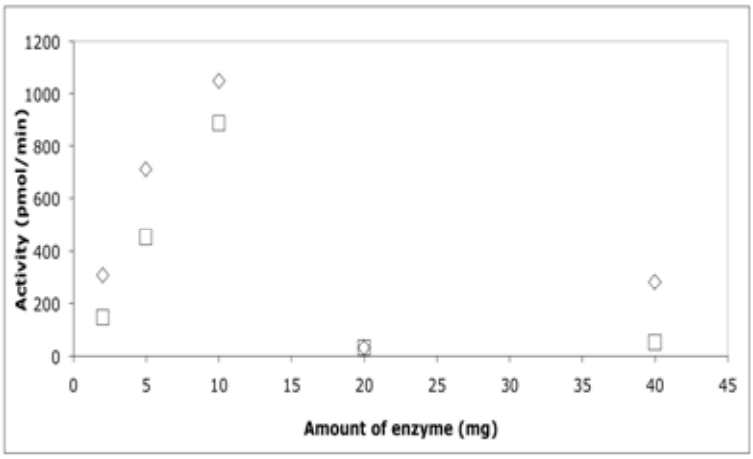

Figure III-14: Diffusion limitation of the substrates: production of methanol (◊) and propyl butyrate (□) as a function of the amount of enzyme powder.

The effect of the amount of enzyme on the total activity is presented in Figure III-14. Between 0 and 10 mg, the activity increases linearly with the amount of enzyme. Above 10 mg, the rate decreases dramatically. There are a number of possible reasons for this. The amount of enzyme powder pulled down into the sample tube might affect the reaction rate by increasing the "matrix effect". The matrix represents all the surfaces inside the sample tube able to adsorb gas phase compounds and decrease their concentration in the gas phase. Then, an increase of the volume of the matrix (volume of enzyme powder) will decrease the amount of substrate in the gas phase. This phenomenon occurs in fact for each amount of enzyme causing systematic errors. The actual effect must lie with diffusion limitation, since although the surface area is higher with more enzyme, the rate should be proportionately faster. One explanation might be that substrate vapour is not evolved fast enough to cope with utilisation but at the same time the extra surface area is mopping up product. In addition, the diffusion limitation of the substrate might occur because of the packing of the enzyme in its powder form. The latter fact explains a non-proportional correlation between the amount of enzyme and the surface occupied. Whatever the reasons for the rate decrease above 10mg enzyme, it is clear that the problem can be resolved by using less than 10mg per assay. The amount of 5 mg of enzyme powder was chosen for the following experiments as it gives a good rate with no diffusion

limitation for both enzymes. However, it clear that care must be taken in correlating/interpreting the results between different experiments in strictly quantitative terms.

3.2.3.2 The alcoholysis reaction in the gas phase

The alcoholysis reaction catalyzed by pig liver esterasr (PLE) requires an acyl-enzyme intermediate. The first step of this reaction corresponds to the binding of methyl-butyrate onto the enzyme, and the enzyme is then butylated. Then, in the second step, the 'butyl-enzyme' binds the propanol, which is in turn butylated. The two steps may have different rates. The binding of methyl butyrate may be larger or smaller than the uptake of propanol, and production of the final product, propyl butyrate, will be the best measure of the overall reaction rate, although it may display a lag phase. [Refer section IV-4 where the mole ratio product/protein will be discussed.]

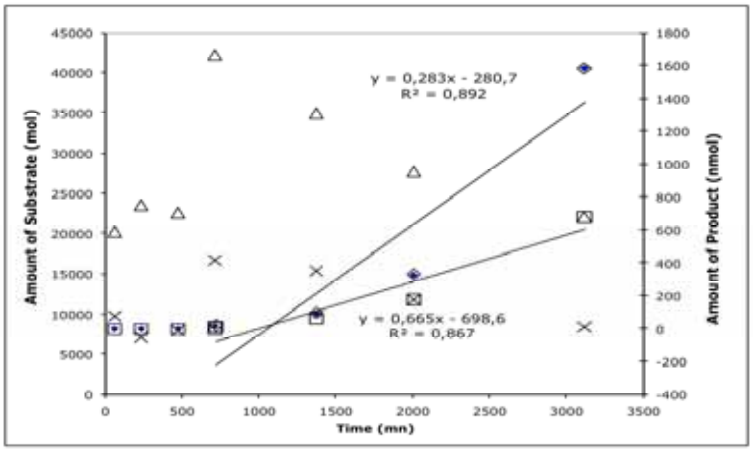

Figure III-15: Amount of substrates (propanol (△) and methyl butyrate (✕)) and products (methanol (◊) and propyl butyrate (□)) as a function of time.

Figure III-15 shows the amount of substrate on the left y-axis and the amount of product on the right y-axis. As in the case of the lipase B, the amount of substrate in the gas phase first increases and then decreases. The products seem to appear in the gas phase with a lag phase and then increase linearly with time. Something is going badly wrong, a leak perhaps? After checking all the system for leaks and because of the problems observed with the use of phosphorus pentoxide (P_2O_5) at 65°C, another experiment using PLE dried over P_2O_5 at room

temperature was carried out. The results are presented in Figure III-16.

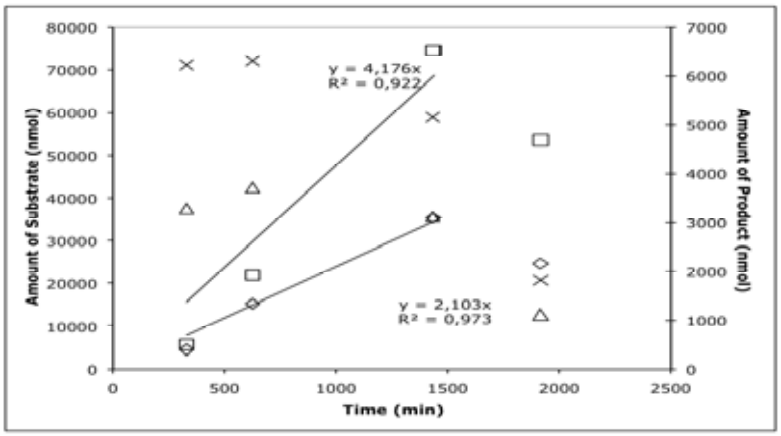

Figure III-16: Amount of substrates (propanol (△) and methyl butyrate (×)) and products (methanol (◊) and propyl butyrate (□)) as a function of time.

In this case, nearly no lag phase is observed in the appearance of the products. The amount of the product (methanol and propyl butyrate) appearing matches in the time scale the disappearance of the substrates (propanol and methyl butyrate). The enzyme activity is higher but it might be only because of a higher hydration level than in the previous experiment. It is pointed out here the difficulties for the interpretation of the results observed because of the drying method used. The low amount of products and the low reproducibility of the results lead us to start the investigation of enzyme activity at higher hydration but do not rule out the possibility of activity at very low water content.

3.2.3.3 Effect of substrates and buffer

It is a preliminary experiment to test if a different combination of substrates may have a positive effect on enzyme activity. It has been found for instance that methanol was able to stimulate serine protease like enzyme (Hutcheon et *al*. 1997). The pH memory is also investigated with the comparison between enzyme pre-incubated or not in MOPS (50 mM, pH 7) prior to freeze-drying. The reactions investigated were:

$$\text{Pr}oOH + MeOBu \Leftrightarrow MeOH + \text{Pr}oOBu \quad \text{(Reaction 1)}$$

$$\text{Pr}oOBu + MeOH \Leftrightarrow MeOBu + \text{Pr}oOH \quad \text{(Reaction 2)}$$

This experiment was carried out in duplicate. The rates of the products'

appearance are presented in Table III-12.

Table III-12:Rate product evolution for reactions 1 and 2 in presence or absence of MOPS.

Products	- MOPS		+ MOPS	
	Assay 1 rate (nmol/min)	***Assay 2 rate (nmol/min)***	***Assay 1 rate (nmol/min)***	***Assay 2 rate (nmol/min)***
Methanol	0.007	0.466	1.200	3.444
Propyl Butyrate	0.112	0.205	1.540	1.341
Propanol	0.466	0.171	0.0182	Lost
Methyl Butyrate	2.873	0.811	0.0161	lost

Given the level of experimental variability it is hard to draw conclusions. However in the case of the first reaction, the enzyme activity seems to be enhanced by the incubation in buffer before freeze-drying while in the case of the second reaction, the buffering of the enzyme prior to freeze-drying may have decreased the activity. In the absence of MOPS, the alcoholysis reaction might be enhanced when methanol is a substrate. Overall, in the presence of MOPS, the first set of substrates seems to have given the best results, although there is considerable variability in both sets of results. Given the desirability of a buffering presence, and in the absence of conclusive evidence of higher activity from "reaction 2", the first combination of substrates has thus been retained for subsequent experiments.

3.2.3.4 Effect of desiccant

As in the case of lipase B, the effect of the three desiccants barium oxide (BaO), magnesium perchlorate ($MgOCl_4$) and phosphorus pentoxide (P_2O_5) was tested. The drying step was carried out at room temperature and six replicates of each sample were performed to test the reproducibility. The results are summarized in Table III-13 below.

Table III-13:Effect of desiccant on the alcoholysis reaction catalysed by PLE.

	BaO	***$MgOCl_4$***	***P_2O_5***
Rate of MeOH production (nmol/min)	15.5 ± 2.84	13.7 ± 1.17	2.17 ± 0.52
Rate of ProOBu production (nmol/min)	3.92± 0.45	4.56 ± 0.5	5.12 ± 1.098

The production of methanol is higher for BaO and $MgOCl_4$ than for P_2O_5 while the production of propyl butyrate is similar for all desiccants. There is a large difference between the production of methanol and propyl butyrate with BaO and $MgOCl_4$, while the two product amounts are closer for P_2O_5.This is consistent with the fact that P_2O_5 (Figure II-1) has the best efficiency in drying. With lower hydration level (below 0.03 *h*), fewer water molecules are available to competitively inhibit the alcoholysis reaction by transforming the methyl butyrate into methanol and butyric acid. The solid/gas bioreactor used in these studies does not allow to distinguished between alcoholysis and hydrolysis (when using methanol as an indicator). However, the later results show that the rate of the ester production is probably more reliable than alcohol production to determine the overall alcoholysis rate.

4. *Conclusions*

The gas phase hydrolysis activity is improved by 70% after addition of excipient, by 10 times if the enzyme was pre-incubated at an optimum pH in MOPS through the 'pH memory effect'. Thus, the first conclusion on the investigation and optimisation of the catalytic potential of the solid/gas bioreactor is that enzyme activity might be improved using the same methods as those used in organic media. Although the bio-imprinting technique has not shown an enhancing effect, it should be remembered that the experiments here were not performed in dry conditions and that the washing step might have failed as

indicated by the loss of 10% of activity of the imprinted sample compared to a non-imprinted one. Additionally, the comparison between the use of glass fibre paper or free powder have suggested that a gain of activity might be obtained using an immobilised enzyme – but that this is likely to be inevitably accompanied by a loss of sensitivity to unacceptable levels in the specific case of our closed experimental system.

The investigation of the alcoholysis reaction in near anhydrous condition has revealed a number of experimental difficulties, including gas chromatograph detection limits (the detection limits of the GC requires that about 450 nmols to be produced in the headspace of the gas/solid bioreactor). Additionally, major reproducibility problems were encountered, and partly resolved, by improvement of the sealing properties of the bioreactor's stopcock, of the mininert top used, and of the gas tight syringes used. Attempts to improve enzyme pre-drying by using an elevated temperature (65°C) led to a colouring of the phosphorus pentoxide (P_2O_5). To prevent any possible side reactions arising from high temperatures, the drying over P_2O_5 was performed at room temperature. Despite these problems, enzyme activity at very low hydration has been clearly demonstrated although the lack of the reproducibility between some experiments indicates need for caution in comparing absolute data values between experiments.

CHAPTER IV: EFFECT OF HYDRATION ON ENZYME ACTIVITY

1. *Introduction*

The interest in studies about the correlation between enzyme activity and hydration level originally emerged from concerns about food preservation. A residual enzyme activity was observed in lyophilized food samples leading to their degradation. A value of 0.2 *h* is widely accepted as the threshold requirement of water for enzyme activity (Rupley *et al.,* 1983), however there are some disparities between enzymes. For the alcohol dehydrogenase, Yang and Russell (1996) found a value of 0.16 *h* while for lysozyme, the observation of activity starts at a hydration level of 0.2 *h* (Rupley *et al.,* 1980). These disparities seem to arise from the amount of water required to complete the hydration of the polar groups of the proteins, and/or the size of the proteins (see table I-1). In fact, the hydration is a three step process (Rupley and Careri, 1991 ; Rupley *et al.,* 1983), in which the charged groups are the first sites occupied by water at low hydration (under 0.07 g of water/g of protein or *h*). Then, between 0.07-0.25 *h*, water binds to polar groups and forms clusters at the protein surface. These clusters increase in size to continue the hydration process. At a value of 0.38 *h* a monolayer of hydration shell should be reached by completion of the hydration of the apolar residues, although this value is dependant on the total accessible surface area of the protein considered.

In contrast to the above findings, Valivety, Halling *et al.* (1992) detected significant activity at a hydration level of 0.0025 *h (8 moles of water per mol of protein)* with an immobilized lipase in organic solvents. Small errors in water determination by the Karl Fischer titration, as well as difficulties in obtaining the value for "dry" protein on which the hydration must be based, could have lead to large hydration errors. Studies conducted with enzyme powders show that enzyme activity is detectable in organic media below a hydration of 10 % (g of water per g of dry protein). However, the possible effect of the organic solvent itself on the properties of the enzyme makes interpretation of these findings (Gorman and Dordick, 1992) difficult in molar terms.

Gas/solid bioreactors have been developed and found to be a useful tool to study the effect of hydration on enzyme activity, although frequently set up and used for applications development (Lamare and Legoy, 1995 ; Letisse *et al.*, 2003). Lamare and colleagues have studied the effect of various parameters, such as water and organic compounds, on the alcoholysis reaction catalysed by *C. antarctica* lipase B (Bousquet-Dubouch *et al.*, 2001 ; Graber, Bousquet-Dubouch, Lamare *et al.*, 2003 ; Graber, Bousquet-Dubouch, Sousa *et al.*, 2003). They found that the alcoholysis reaction of *C. antarctica* lipase B obeys a ping-pong bi-bi mechanism that is competitively inhibited by water and organic compounds. They have been able to observe enzyme activity at water content below the monolayer coverage. They also showed that between a water activity of 0 and 0.5 (so a relative humidity level between 0 and 50%), the alcoholysis rate was increased as the water activity decreased. Unfortunately, the water content of the enzyme was not directly measured. Lind *et al.* (2004) also found that PLE and *C. rugosa* lipase B were able to catalyse the hydrolysis reactions at enzyme hydration levels as low as 3% (g of water per g of dry protein).

2. *Materials and Methods*

2.1. Materials

2.1.1. Enzymes

Crude extracts of esterases from Porcine liver (E3019, Sigma) and Lipase/esterase from *Candida rugosa* (Sigma-Aldrich, L1754) were further purified as described in the Chapter III.2.2.1.1.

2.1.2. Chemicals

Phosphorus pentoxide (P_2O_5) ≥ 99.99 % (Aldrich)

GC purity grade of methyl butyrate, propanol and propyl butyrate were purchased from Fluka.

2.1.3. Gas Chromatograph (GC)

The quantification of the substrates and products of the reaction mixture was described in the previous chapter. The experiments on the effect of hydration on activity utilised a Shimadzu (14-B) GC equipped with a flam ionisation detector (F.I.D.) The packing material (Poropack Q, mesh 80/100, Alltech) was slightly less polar than the one used in the previous chapter. In this case the column was maintained at 250°C while the injector and detector were at 300°C.

2.2. Methods

The alcoholysis reaction was studied in the same gas/solid bioreactor described in the previous chapter and the reaction followed was the same (see section III.2.2.).

2.2.1. Drying

The protein powder was dried over high-grade phosphorus pentoxide (P_2O_5). The degree of drying is controlled by variation of the time of the protein equilibration with phosphorus pentoxide and/or by shifting the system from room temperature to 60°C.

For the alcoholysis reactions, the following drying conditions were used:

- 1 week (7 days) drying over P_2O_5 at room temperature.
- 2 weeks (14-15 days) drying over P_2O_5 at room temperature.
- 2 weeks drying over P_2O_5 at 60 °C: in this case, the protein is gradually dried by equilibration of the protein over P_2O_5 for three days at room temperature followed by one week at 65°C. The P_2O_5 is renewed if necessary and the samples are cooled for 4 days at room temperature.
- 1 month (28-30 days) drying over P_2O_5 at room temperature.

2.2.2. Quantification of the substrates and products of the reaction

The quantification of the amount of substrate and products were

performed as described in the previous chapter. The standard curves were performed in ethanol for accuracy.

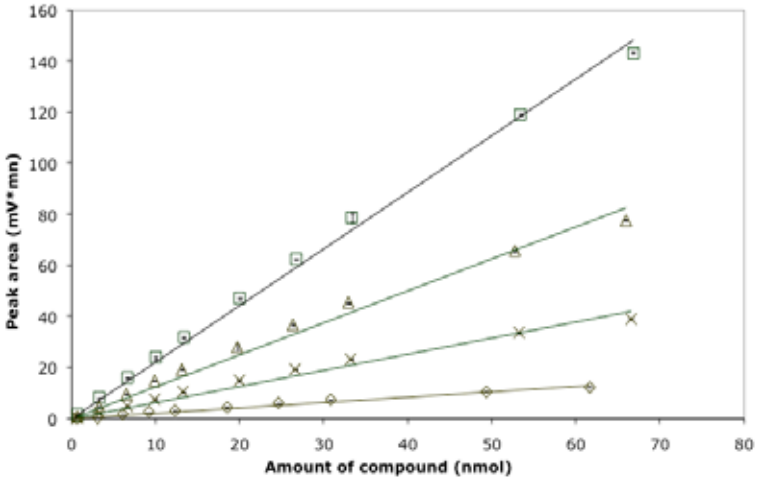

Figure IV-1: Standard curves used for the quantification of substrates and products of the reaction. Propanol (✕); methyl butyrate (△); methanol (◊) and propyl butyrate (□).

The coefficients obtained for the methanol and the propyl butyrate were 0.21 and 2.22 respectively. The coefficient for the propanol and the methyl butyrate were 0.3 and 1.25, respectively. The sensitivity of this GC was about ten times lower than the previous one.

3. *Results*

3.1. The alcoholysis reaction at about 0.1 *h*

The alcoholysis reaction was studied with lipase B and pig liver esterase (PLE). An initial check was performed with the enzyme powder stored in a desiccator over silica gel at 4 °C (with no further drying). These experiments were initially performed to make sure that the enzymes were able to carry out the alcoholysis reaction at higher hydration levels than those investigated.

3.1.1. Alcoholysis Reaction with *C. rugosa* Lipase B

The hydration level was estimated to be 0.094 *h* on the basis of weight loss after four days of drying with phosphorus pentoxide (P_2O_5) at room temperature (refer sorption isotherm).

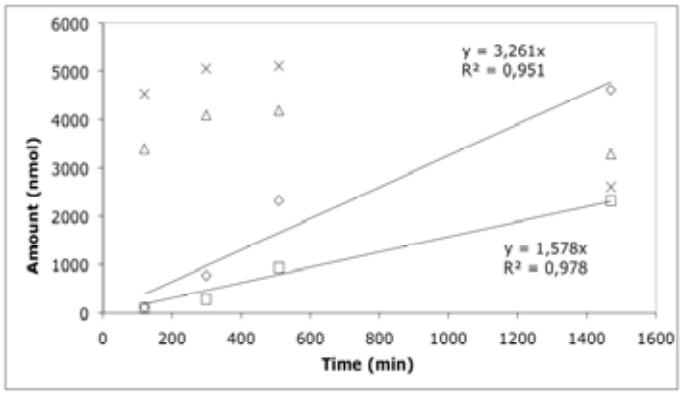

Figure IV-2: Alcoholysis reaction with *C. rugosa* lipase B: Amount of substrates (propanol (△) and methyl butyrate (✕)) and products (methanol (◊) and propy butyrate (□)) in the gas phase as a function of time.

Under the current experimental conditions, the amount of substrate in the gas phase remained constant. However, at the longest sample duration, the amount of product reached a level equivalent to that of the substrates. Thus, to prevent substrates depletion, the rates were measured over these initial points. This experiment was performed in five replicates to give the rate of production for propyl butyrate and methanol of 599 ± 202 pmol/min/mg and 1305 ± 413 pmol/min/mg, respectively.

3.1.2. Alcoholysis Reaction with pig liver esterase (PLE) at 0.1 *h*

3.1.2.1 Alcoholysis reaction as a function of time

For each experiment a series of controls were run: a blank with no enzyme and a denatured enzyme control. In both cases, it was verified that no products were released. From the quantification performed with our gas chromatograph the amount of substrates and products present in the headspace as a function of time could be studied. From this analysis, the rate of formation of the products could be determined.

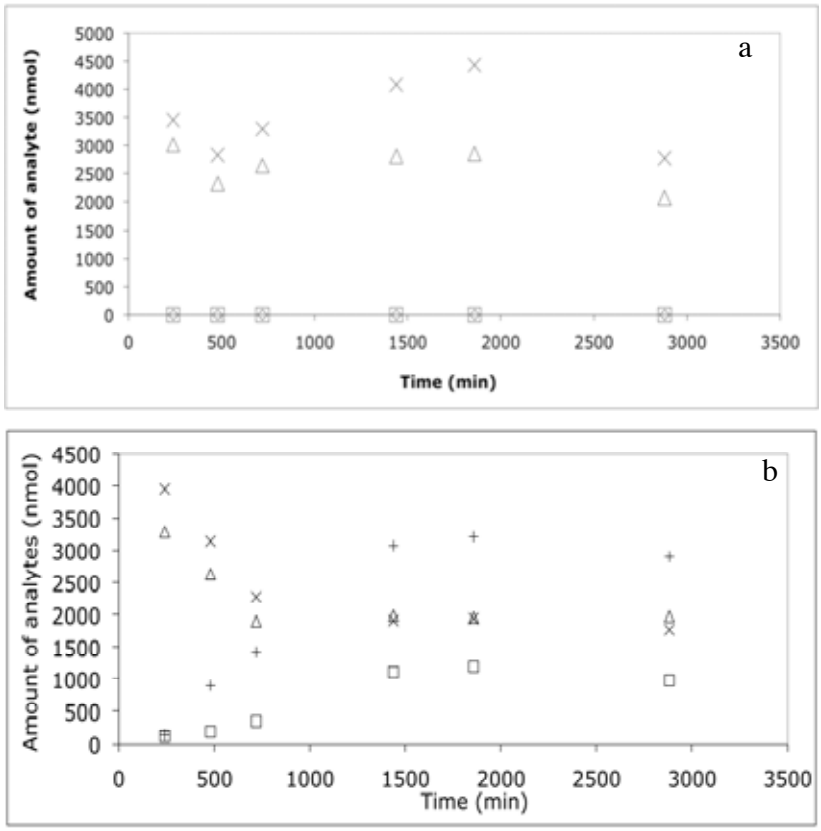

Figure IV-3: Transesterification of propanol (△) and methyl butyrate (×) into methanol (◊) and propyl butyrate (□) without enzyme (graph a) and with PLE (graph b).

The comparison of the substrate concentrations between the control and the sample showed that there was a consumption of substrates in the presence of enzyme. Thus, enzyme activity occurs. A comparison between the increase in the amount of product and the decrease of the substrate showed that substrate depletion might occur quickly under these conditions.

In these experiments, the PLE was taken straight from a storage bottle kept under vacuum at 4°C. Its hydration level was estimated with the sorption isotherm to be around 0.074 *h*. The sample showed a decrease in the concentration of both substrates and an increase in the concentration of both products as a function of time. In addition, the denatured control exhibits the same pattern as the no-enzyme control. The propyl butyrate production was found to be 1800 ± 200 and 8800 ± 600 pmol/min/mg for the methanol. The correlation between *h* and the number of moles of water per mol of protein is explained in Table IV-1:

Table IV-1:Correlation between the drying method, the water quantification and the hydration level of PLE

Drying/hydration method	***Water molecules quantified in Chapter II (moles ^{18}O/mol of protein)***	***Hydration (h)***
24 h freeze-drying + 1 week over P_2O_5	2.3	0.00076
16 h freeze-drying + 4 weeks over P_2O_5	3.0	0.00099
4 weeks over P_2O_5	3.3	0.00109
16 h freeze-drying + 2 weeks over P_2O_5	4.3	0.00143
16 h freeze-drying + 1 week over P_2O_5	5.4	0.00179
24 h freeze-drying	6.2	0.00206
2 weeks over P_2O_5 65 C	9	0.00299
2 weeks over P_2O_5	13.8	0.00459
1 week over P_2O_5	32.4	0.01078
LiBr (5% RH)	114	0.03795
Stored powder	239	0.07957

3.1.2.2 Alcoholysis reaction as a function of the amount of enzyme

The effect of diffusion limitation was studied in the previous chapter. However, as a new batch of PLE was used and the gas chromatograph was different, it was decided to check the effect of protein amount on the observed kinetics. This experiment was performed at a hydration level around ~ 0.08 *h* but it has to be viewed as a preliminary check.

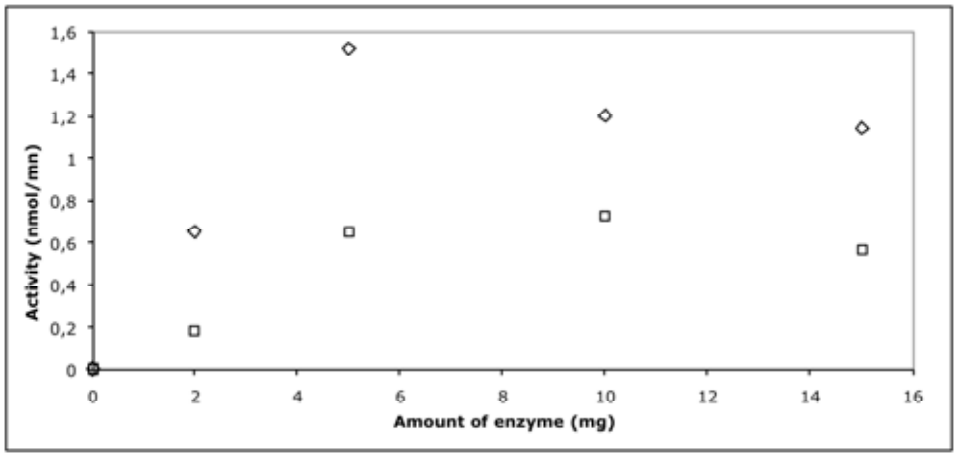

Figure IV-4: Effect of the amount of enzyme on methanol (◊) and propyl butyrate (□) production rate.

Different amounts of enzyme powder were aliquoted into the sample tube and the alcoholysis reaction rate was measured. An increase of the reaction rate was observed between 0 and 5 mg of enzyme powder. However, for the highest enzyme amounts the observed rate was seen to flatten or decrease, as shown in Figure III-14. These results tend to confirm those obtained in the previous chapter, i.e., that the optimum enzyme amount is about 5 mg, although the hydration level was different.

3.1.2.3 Rate of alcoholysis as a function of amount of substrate

Propanol is known to inhibit the alcoholysis reaction in the case of *C. antarctica* lipase B (Letisse *et al.*, 2003). Initially, it was decided to add 4 µL of each substrate in order to saturate the headspace. But if one of the substrates inhibited the reaction, it would be possible to improve the alcoholysis rate with different substrate ratios. As a preliminary experiment, different ratios of substrates were tested in order to find out whether any ratio would optimize the alcoholysis reaction.

Five different ratios of a propanol/methyl butyrate mixture were tested; 1:4 ;1:2;1:1;2:1 and 4:1 (V:V). About 20 µL of these mixtures were prepared and 8 µL were injected onto the glass fibre paper to initiate the reaction. The powdered PLE was taken straight from the bottle, without any special drying. The experiment was performed in duplicate.

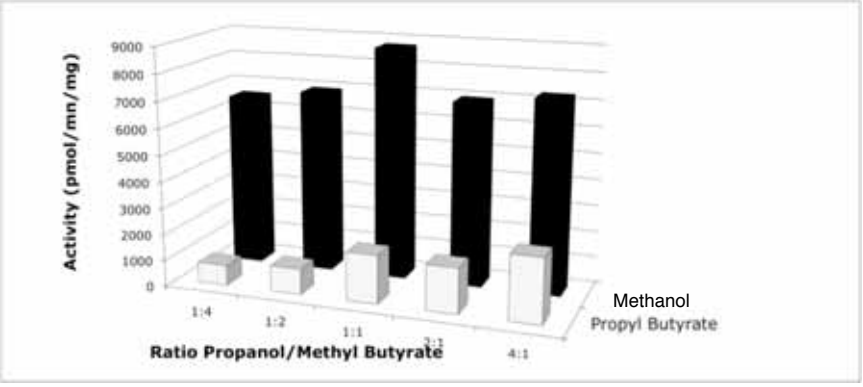

Figure IV-5: Effect of the ratio of the two substrates on the rate of production of methanol (black) and propyl butyrare (white).

The graph above showed that whatever the ratio was between the two substrates, the amount of methanol produced seemed somewhat less affected than propyl butyrate although a 1:1 ratio seemed optimal. An increase in the relative amount of propanol caused an increase of the rate of propyl butyrate production. The hydration level of the enzyme used here had been estimated (with the sorption isotherm) to be around 0.07 *h*, where hydrolysis reaction occurs and might compete with the alcoholysis reaction (Lind *et al*., 2004); thus the propyl butyrate rate should give a better indication of the alcoholysis reaction. The results therefore indicate that the highest ratio of propyl butyrate:methanol favoured the alcoholysis reaction. Lind *et al*. (2004) studied the hydrolysis of ethyl butyrate with a similar experimental system. The rates obtained for lipase B and PLE at a hydration level of 0.1 *h* were about 50 and 5000 pmol/min/mg respectively. The results above are thus in agreement with those obtained by Lind *et al*. (2004). The large amount of methanol produced might be due in this case to hydrolysis.

3.2. Alcoholysis reaction at 0.03 *h*

The comparison of the alcoholysis reaction at high hydration levels is difficult as it is in competition with the hydrolysis reaction. However, at 0.03 *h* hydration the hydrolysis reaction should be low enough to observe the alcoholysis reaction. The pig liver esterase (PLE) was equilibrated against a saturated solution of lithium bromide (LiBr) for a week at room temperature. The relative humidity reached above the saturated salt solution was about 6.5 %. An estimation of the

hydration level, based on the adsorption isotherm, gives a value of 0.034 *h* (or 114 mol of water per mol of protein).

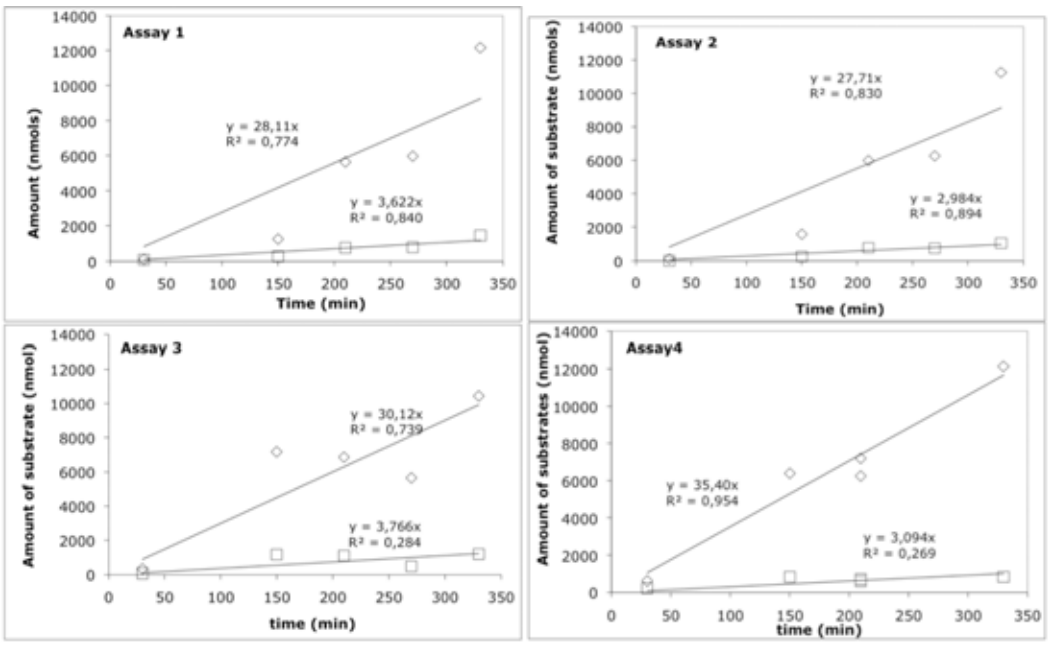

Figure IV-6: Amount of methanol and propyl butyrate produced as a function time with PLE at 0.03 *h* of hydration.

The amount of methanol present in the gas phase was about ten times higher than the amount of propyl butyrate. This was an indication that the hydrolysis reaction occurred. The rate obtained for the propyl butyrate and methanol were 673 ± 77 pmol/min/mg and 6068 ± 707 pmol/min/mg, respectively. The reproducibility was good, the error being under 12%.

3.3. Enzyme dried over phosphorus pentoxide (P_2O_5): activity between 0.01 *h* and 0.007 *h*

All the experiments described below were performed for both pig liver esterase (PLE) and lipase B, but no activity was detected for lipase B. This is in contrast to the results obtained in the previous chapter where some activity was observed with lipase B dried over high grade P_2O_5 for two weeks at 65 °C. There are two explanations possible for this discrepancy: firstly, although the enzyme used was purified in the same manner, the source of the enzyme was different (purchased from a different company with different grade of purity), which might have effected the isoenzyme purified; secondly, the detection limit of the gas

chromatograph used here was about 10 times lower than the one used in the previous chapter. As the observed activity with the dried lipase B was already quite low (3 nmol/min), any reduction in assay sensitivity may have made detection impossible.

3.3.1. One week at room temperature: activity at 0.01078 *h*

After one week drying over P_2O_5, the enzyme reaction was initiated as described in the methodology paragraph (refer section Chapter III.2.2). The amount of product released as a function of time was measured by gas chromatography and the results are presented below.

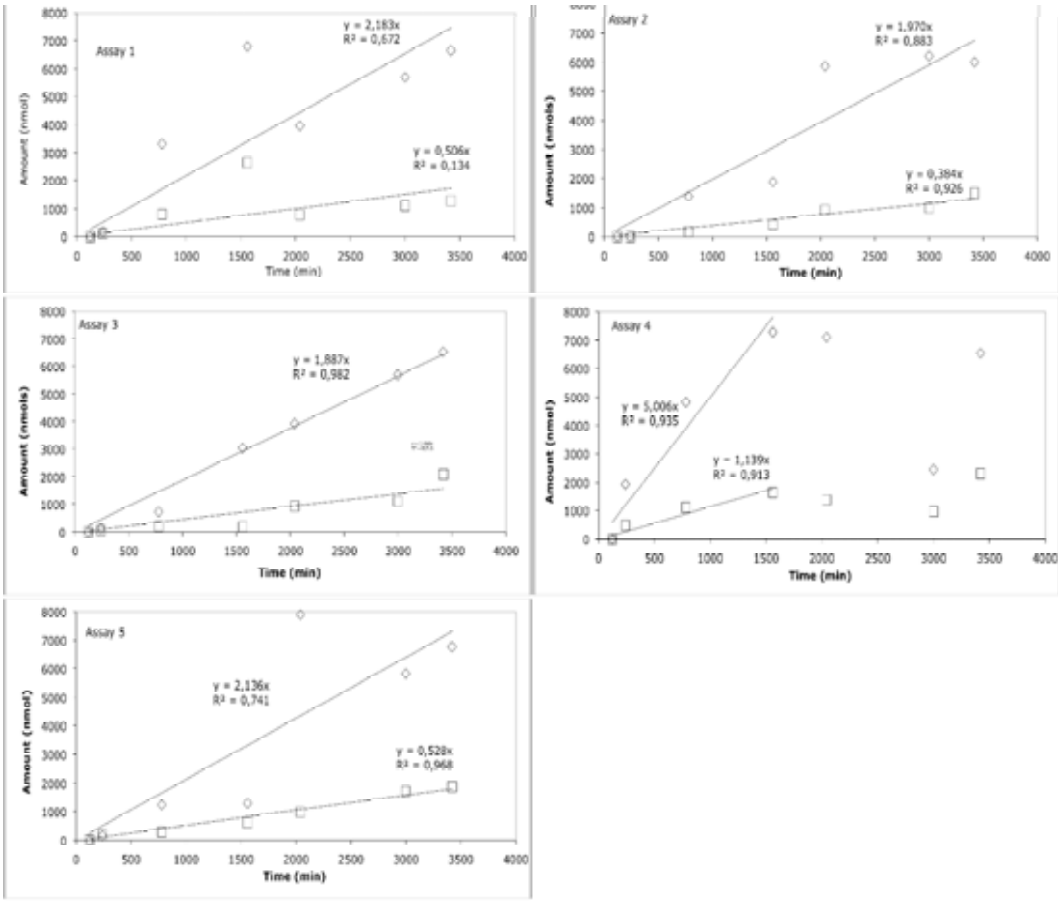

Figure IV-7: Production of methanol (◊) and propyl butyrate (□) in the gas phase as a function of time. PLE was dried for 1 week over phosphorus pentoxide at room temperature.

A large number of replicates had to be used for the quantification. For most of the samples, an initial rate could be determined from a linear fit to the early points of the time course. The rates obtained for each replicate were averaged and a standard deviation was calculated. Assay 4 was an outlier and not included in the calculations to give the final rates: 94 ± 11 for propyl butyrate and 407±98 pmol/min/mg for methanol.

3.3.2. Two weeks at room temperature: activity at 0.00459 *h*

In the same manner, we observed the enzymatic rate after two weeks drying over P_2O_5.

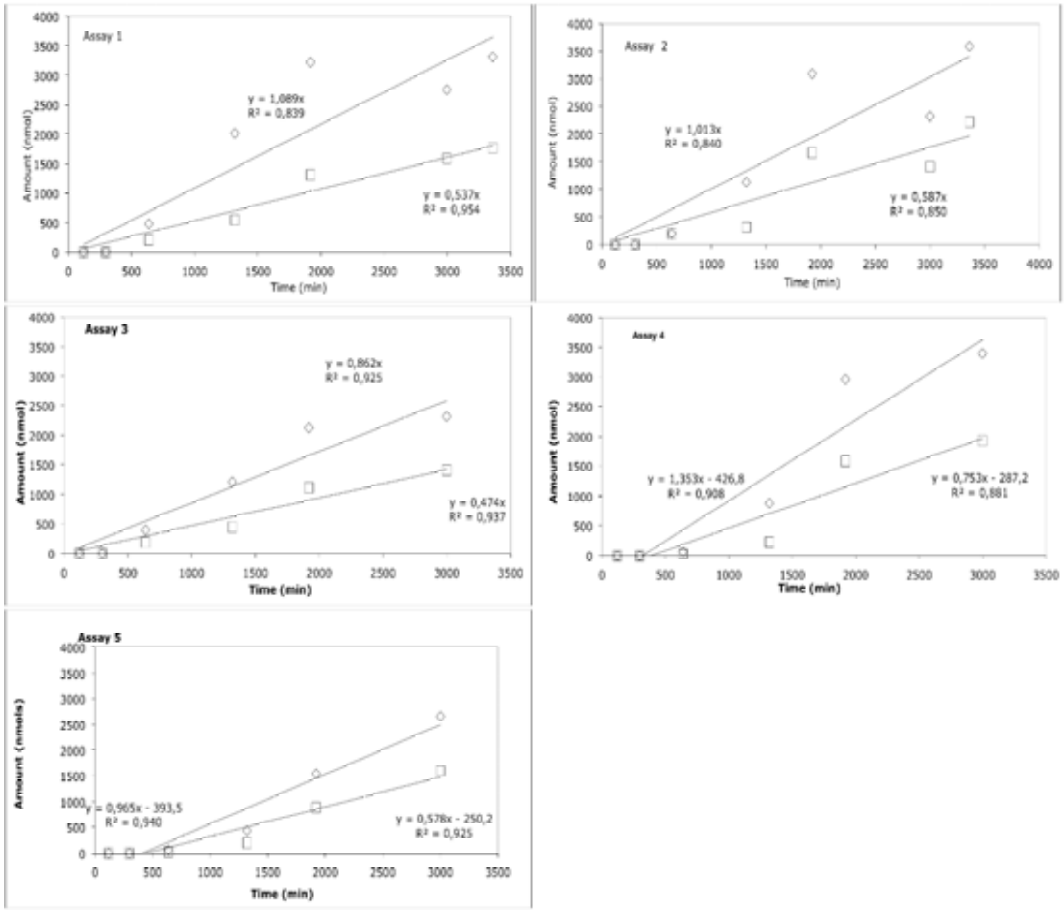

Figure IV-8: Production of methanol (◊) and propyl butyrate (□) in the gas phase as a function of time. PLE was dried during 2 weeks over phosphorus pentoxide at room temperature.

As observed in the graphs above, the products seemed to appear after a lag phase. While previously we could already detect some product before 300 min, here, the products were observed only after 700 min. It is quite possible that this lag was caused by non-specific absorption of the products to the enzyme itself, and that when these sites were saturated the product appeared in the gas phase. Given the potentially variable surface area between enzyme samples, this effect may not be consistent between samples. In any event when the product appeared it was evolved in a linear fashion, and the (minimum) rates could be calculated from these later points. For these samples, the initial rate of reaction was measured between the lag phase and the plateau. The rates for methanol production were 215.5 pmol/min/mg ± 30.5 and 124.5 pmol/min/mg ± 16.6 for the propyl butyrate. The rate for the production of propyl butyrate was higher than the one observed with a shorter drying period, which might indicate that the alcoholysis reaction is favoured (Graber, Bousquet-Dubouch, Lamare *et al.*, 2003), but was also promising in terms of enzyme activity in anhydrous conditions. The rate observed here for the production of methanol was lower than after one week of drying which may bear out the expectation that enzyme activity will decrease at lower hydration levels.

3.3.3. Two weeks at 65°C: activity at 0.00299 *h*

As explained in the methodology paragraph, the protein was sequentially dried over P_2O_5 at 65 °C and then re-equilibrated at room temperature before initiation of the enzyme activity.

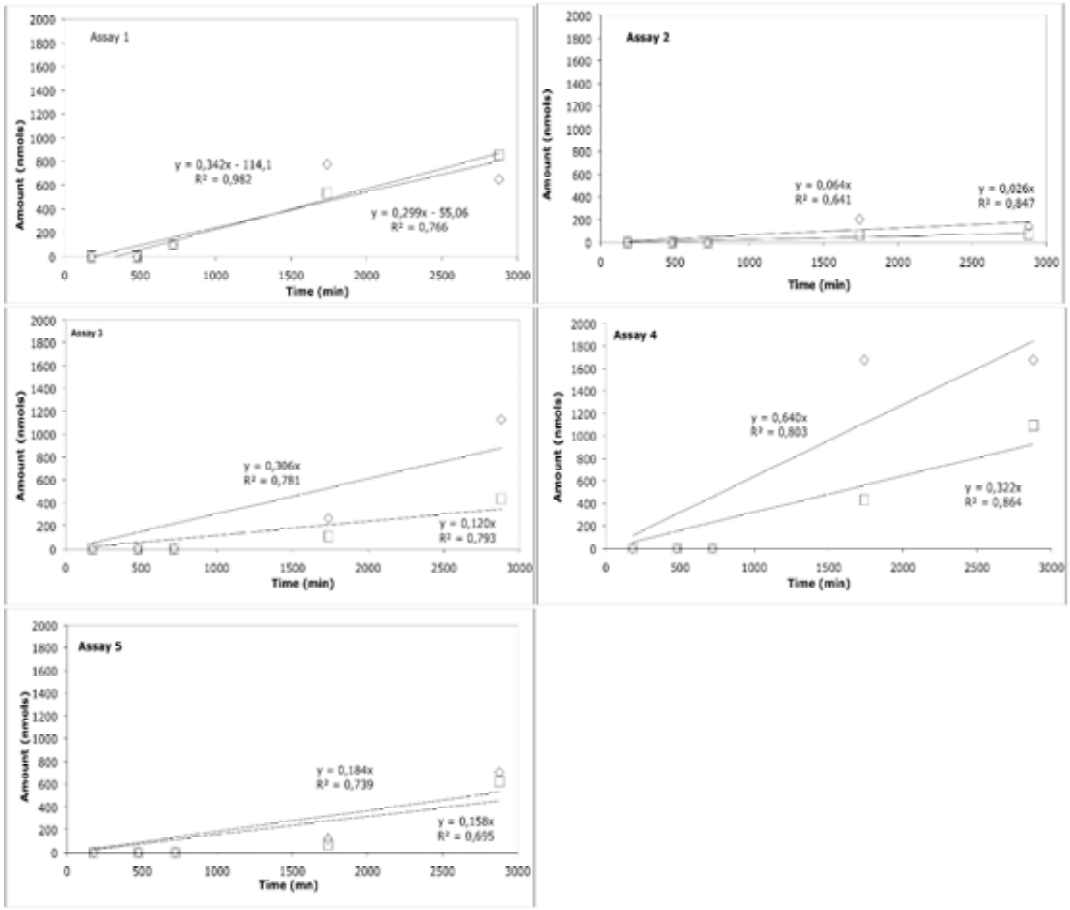

Figure IV-9: Production of methanol (◊) and propyl butyrate (□) in the gas phase as a function of time. PLE dried for 2 weeks at 65 °C over phosphorus pentoxide.

The same lag phase was observed, as with the pervious data, and the rates for enzymatic activity obtained were lower. The rate for propyl butyrate was 36.5 ± 24.3 pmol/min/mg (the methanol rate is 58.7 ± 43.0 pmol/min/mg).

3.3.4. Four weeks at room temperature: activity at 0.00109 *h*

For this series of assays the pig liver esterase (PLE) was dried over phosphorus pentoxide (P_2O_5) at room temperature for four weeks.

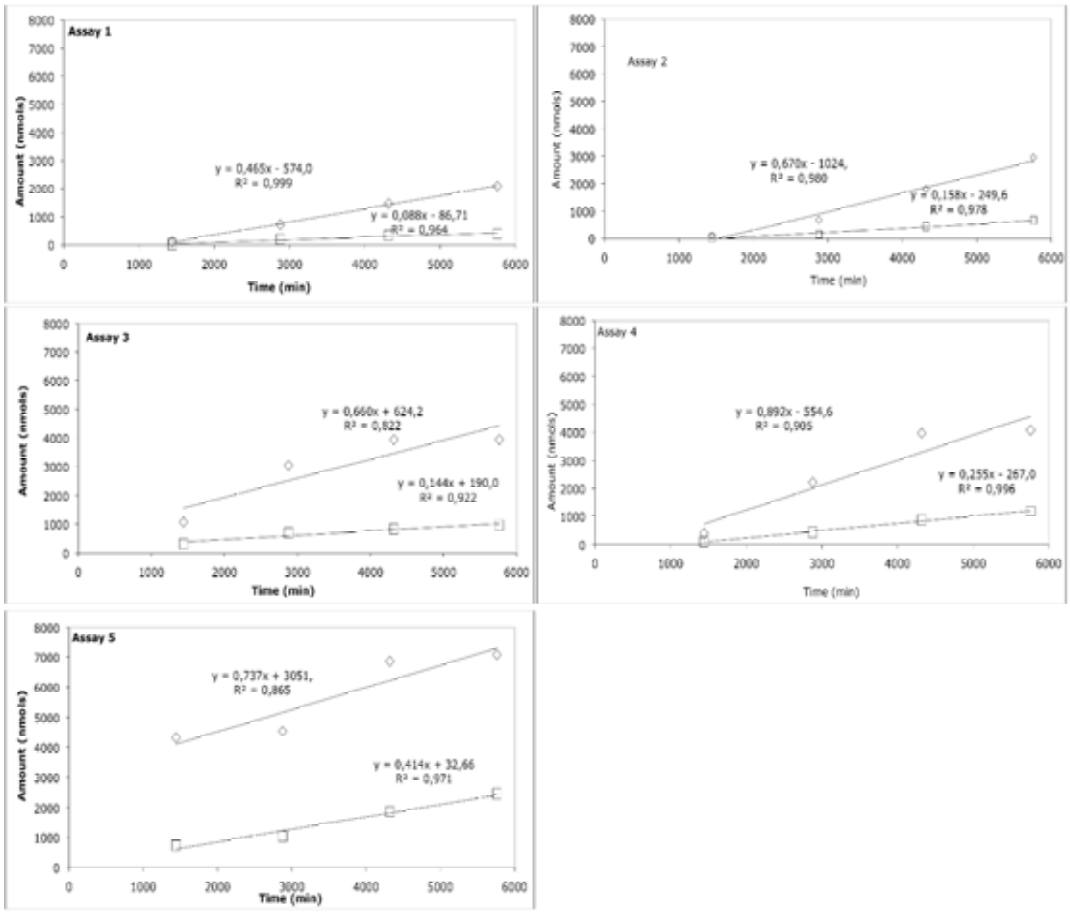

Figure IV-10: Production of methanol (◊) and propyl butyrate (□) in the gas phase as a function of time. PLE dried for 4 weeks at room temperature over phosphorus pentoxide.

The rate for the production of propyl butyrate was 42.4 ± 22.9 pmol/min/mg (and 137.0 ± 27.5 pmol/min/mg for methanol). The reproducibility for the rate of production of propyl butyrate was very low; nearly 50% of error for the propel butyrate rate but this error probably arose from the low rates values. In fact, these values were close to the detection limit of the gas chromatograph.

3.4. Enzyme freeze-dried prior to equilibration over P_2O_5

The enzyme used for the water molecule quantification performed with ^{18}O water was re-hydrated to 30% hydration and then dried over phosphorus pentoxide (P_2O_5). While previously, when the enzyme was not freeze-dried prior to exposure to P_2O_5 (refer section IV-3.3), the enzyme powder used for the measure of activity was directly shifted from a stored bottle to a desiccator over P_2O_5. Thus, the drying efficiency might have been improved in the activity

measurements as compared to the water molecule quantification experiments. In order to start with a protein of the same level of hydration and improve the drying over P_2O_5, the enzyme used for the quantification and the one used for the assays were re-hydrated with ^{18}O-labelled water and vacuum dried prior to exposure to P_2O_5.

It might be difficult to interpret the results since $H_2{}^{18}O$ may affect the reaction; D_2O commonly does.

3.4.1. Sixteen hours of freeze drying

After re-hydration with ^{18}O-labeled water, the enzyme was freeze-dried for 16 hours inside desiccators. The vacuum was released in a glove box where the relative humidity was controlled to remain under 5% of humidity. Then the enzyme was stored over high grade P_2O_5 and dried over different time periods. All the assays (with the exception of the samples dried for one week over P_2O_5) were performed at room temperature. In each case, five replicates were analysed. The results are presented in Figures IV-11 to IV-13.

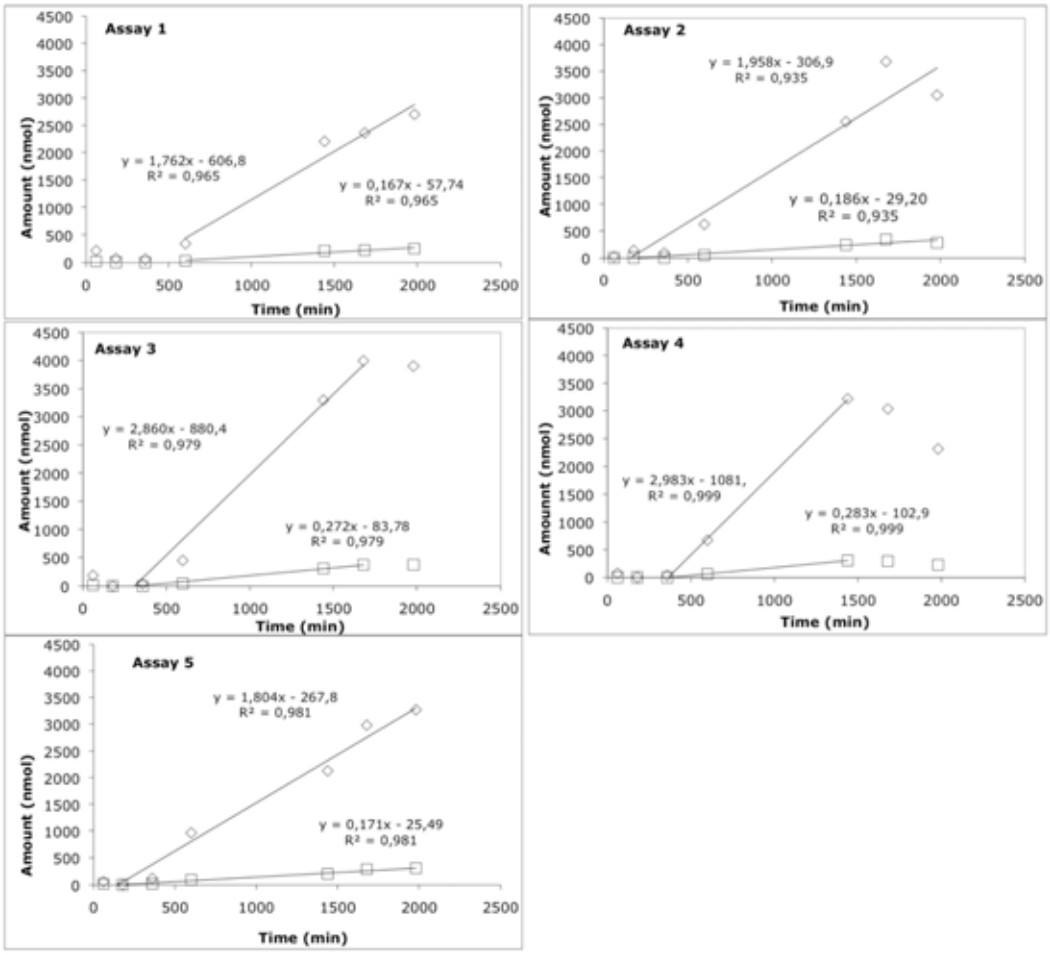

Figure IV-11: Activity at 0.00179 *h*. Propyl butyrate (□) and methanol (◊) production in the gas phase after 16 hours of freeze-drying and one week over P_2O_5 at room temperature.

The propyl butyrate rate was 51.3 ± 14.3 pmol/min/mg (and for methanol production was about 454.8 ± 106.9). A lag phase of about 300 minutes was still observed. The propyl butyrate production was rather low compared to that after one week drying without the freeze-drying step, while the methanol production was about the same. This would suggest that the second step of the transesterification was slower.

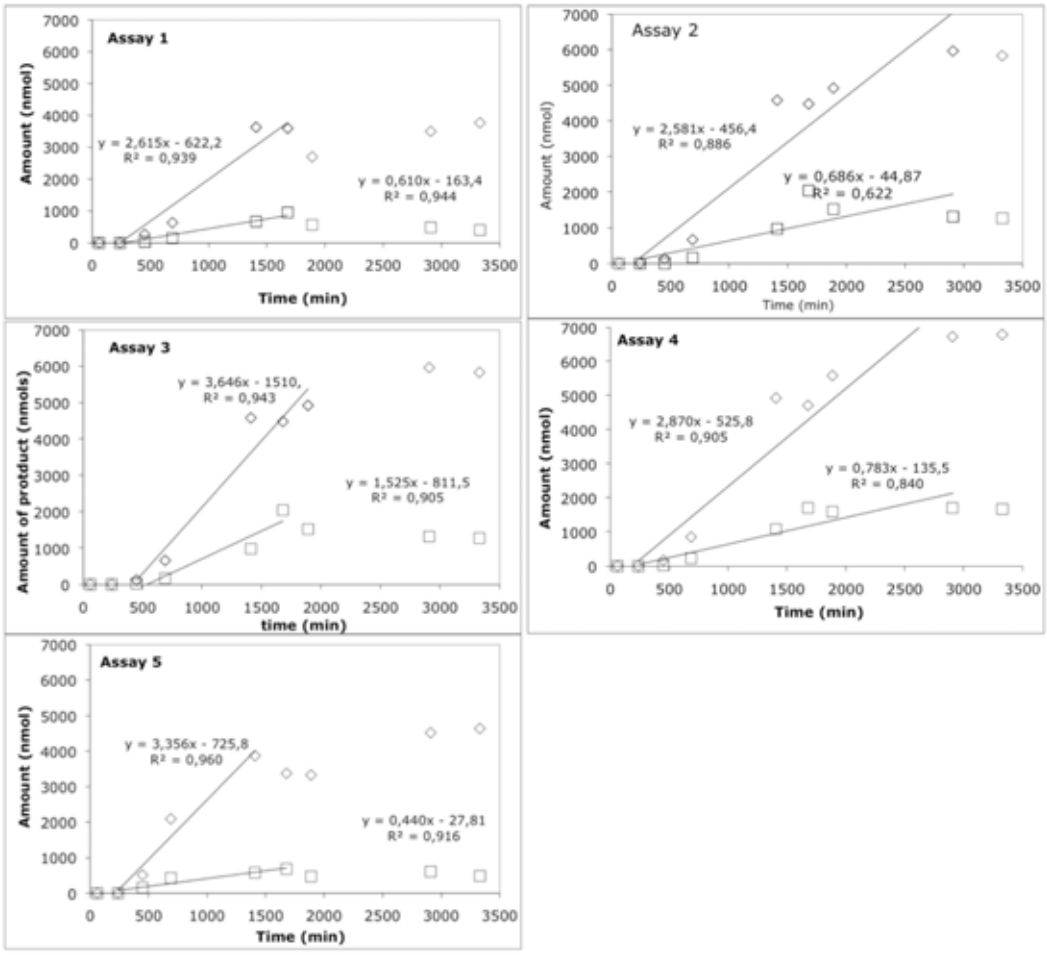

Figure IV-12: Activity at 0.00143 *h*. Propyl butyrate (□) and methanol (◊) production in the gas phase after 16 hours of freeze-drying and two weeks over P_2O_5 at room temperature.

The propyl butyrate production was 161.8 ±75.0 pmol/min/mg (and 602.8 ± 84.1 for the methanol). These results, as compared to those obtained after two weeks without freeze-drying, showed an equivalent amount of propyl butyrate.

This observation might be due to activation of the hydrolysis reaction. An activation of the hydrolysis reaction would mean a higher hydration level than expected, which does not seem plausible as vacuum was used to decrease the hydration level. Although it is possible that water uptake might have occurred during the release of the vacuum, this is relatively unlikely because the release of the vacuum was performed in a confined environment with a relative humidity controlled below 5% and a moisture trap was filtering the air coming through the desiccator.

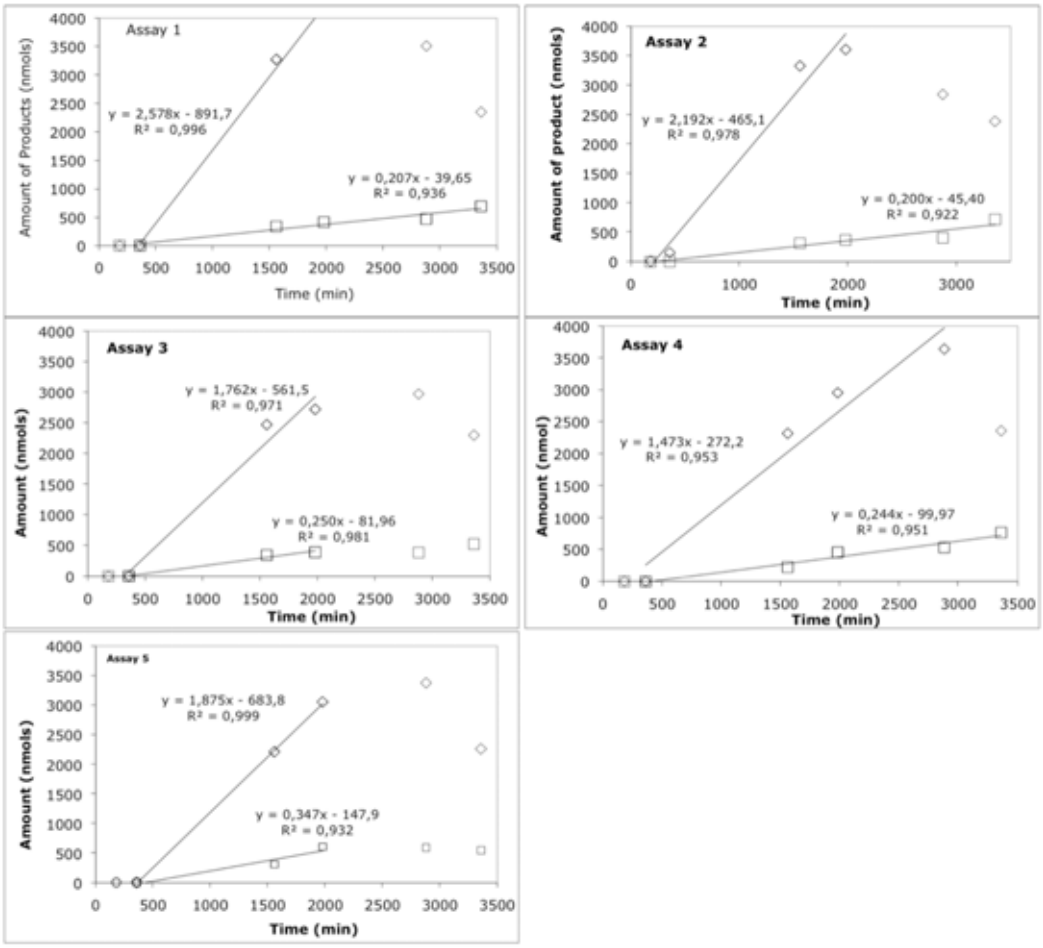

Figure IV-13: Activity at 0.00099 *h*. Propyl butyrate (□) and methanol (◊) production in the gas phase after 16 hours of freeze-drying and four weeks over P_2O_5 at room temperature.

The propyl butyrate production was about 50.0 ± 10.5 pmol/min/mg and 395.3 ± 75.8 for the methanol. Once again, the amount of methanol produced was about three times higher than compared to the amount of methanol after four weeks drying without freeze-drying, while the amount of propyl butyrate was about the same.

The enzyme activity was improved as well as the reproducibility. However, while the rate of methanol production was higher under these conditions, the rate of propyl butyrate production seemed to agree well with the results obtained before. One concern was the loss of ^{18}O-labeled water during freeze-drying by exchange with the environment. This would introduce an underestimation of the amount of water bound to the protein. Although the freeze-drier offered good vacuum conditions, contamination from external water may indeed have occurred. However, as explained in Chapter II, oxygen exchange is

slow and unlikely to be significant over the freeze-drying time. The release of the vacuum was another critical step for loss of label. It was performed under a controlled relative humidity of 5% and a moisture trap, composed of dry silica gel, filtered the air going through the desiccator. Thus, the loss of label here seems unlikely.

3.4.2. 24h freeze drying

This series of experiments analysed the enzyme activity of samples left on the freeze-drier for a longer time than paragraph 3.3. In order to answer to the question of a loss of label, control samples were removed from the freeze-drier and the activity was directly measured, while other samples were left for one week over P_2O_5.

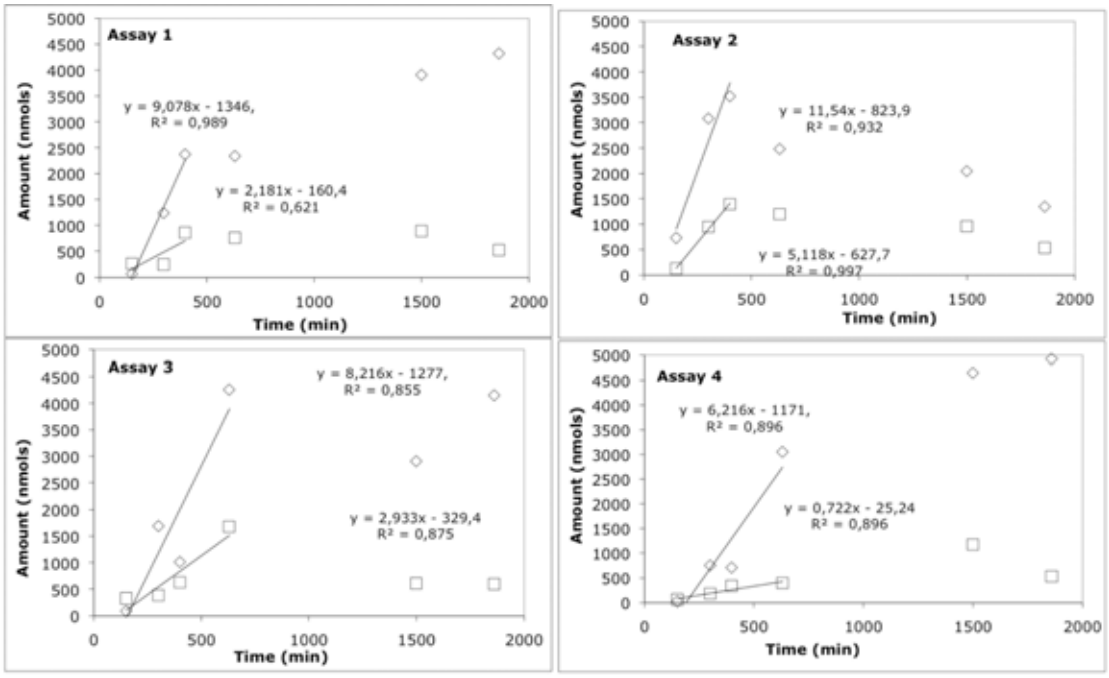

Figure IV-14: Activity at 0.00206 *h*. Propyl butyrate (□) and methanol (◊) production in the gas phase after 24 hours of freeze-drying and no drying over P_2O_5.

The methanol was produced with a rate of 1783 ± 390 pmol/min/mg and the rate for the propyl butyrate was 548 ± 317. These results were expected to be high because the freeze-drier was expected to leave a relatively high water content in the sample. However, water quantification performed on these samples showed that only about 6.2 water molecules per molecule of enzyme were still bound.

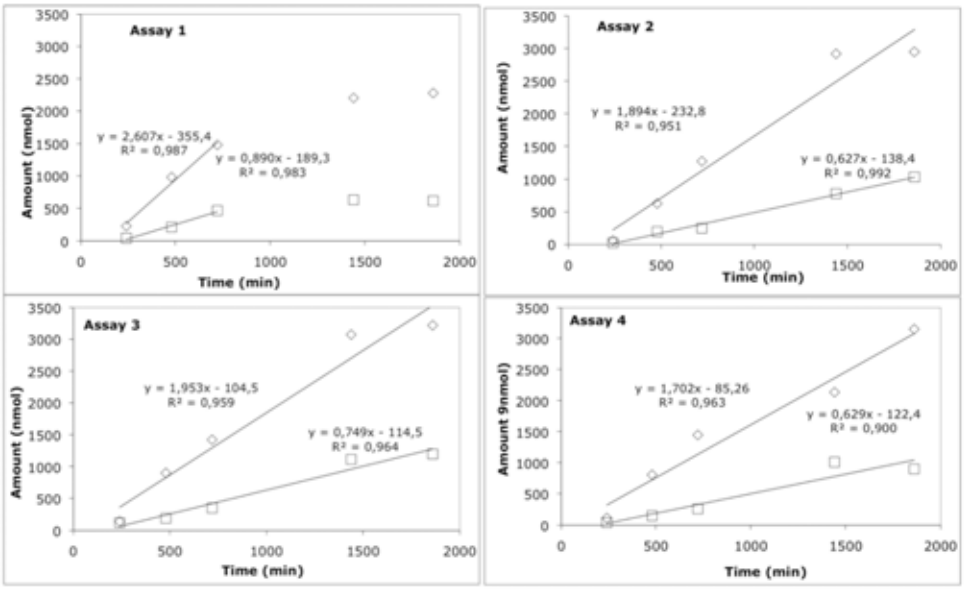

Figure IV-15: Activity at 0.00076 *h*. Propyl butyrate (□) and methanol (◊) production in the gas phase after 24 hours of freeze-drying and one week over P_2O_5 at room temperature.

After a week of exposure to P_2O_5, the methanol production rate was about 508 ± 33 pmol/min/mg and propyl butyrate one was 161 ± 21. These results agreed with those obtained after sixteen hours of freeze-drying.

A summary of the rates obtained for the methanol and propyl butyrate production with different drying methods are presented in the Figure IV-16.

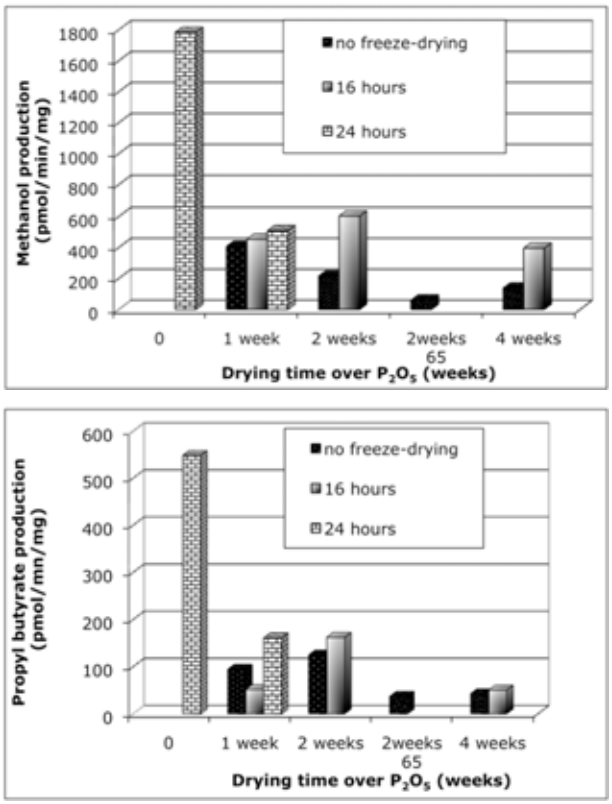

Figure IV-16: Methanol and propyl butyrate production as a function of the different drying time of PLE over P_2O_5 and with or without freeze drying prior to P_2O_5 exposure.

These results showed that freeze-drying improved methanol and propyl butyrate production in a general manner. This effect was marked for methanol especially when longer drying time over P_2O_5 were applied, while for propyl butyrate the effect of freeze-drying was small. The methanol production was expected to be favoured at high water content. The freeze-drying prior to drying improved the following drying steps but also could improve the protein stability over time. Thus the positive effect observed might have arisen from the improvement of the protein stability rather than a high hydration level.

3.5. Correlation of enzyme activity with hydration level

The use of a similar drying method for the quantification of water molecules bound to the enzyme and to measure its catalytic activity allowed the correlation between the hydration level and the enzyme activity.

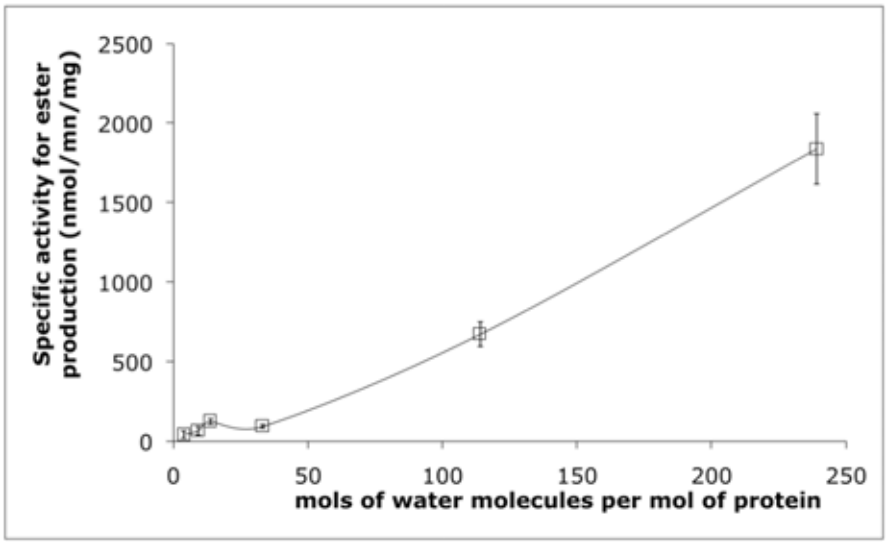

Figure IV-17:Propyl-butyrate production as a function of PLE hydration level.

The graph above represents the specific activity of pig liver esterase (PLE) for its ester product as a function of the enzyme hydration. An initial increase of the activity with hydration is observed and followed by a slight decrease. This was already observed by Affleck, Xu *et al*. 1992 in the case of subtilisin. These authors measured the subtilisin activity in organic solvents to which different amounts of water were added. From corresponding dynamic measurements, they explained this behaviour by a change in the protein flexibility.

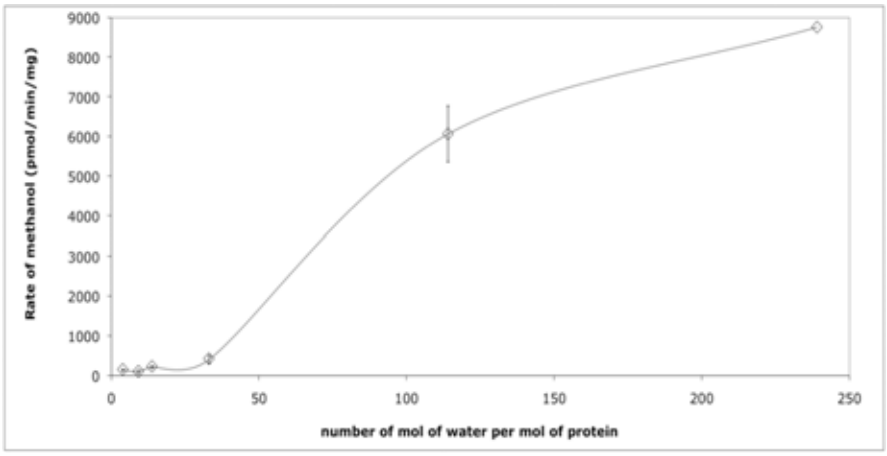

Figure IV-18: Production of methanol in the gas phase as a function of the hydration level.

As shown in Figure V-18, the rate of alcoholysis, as monitored by the rate of methanol production, increases with increasing hydration of the PLE. The amount of methanol produced does not increase linearly with the enzyme

hydration. Indeed, the enzyme activity increases slightly with hydration below 50 moles water/mol protein and then, its dependence on enzyme hydration becomes stronger. These results are in contradiction to those of Bousquet-Dubouch *et al*. (2001). This group observed a slight decrease of the alcoholysis reaction with *Candida antarctica* lipase B when the water activity was increased. Two main differences between their system and ours might explain this discrepancy. Firstly, they did not measure directly the hydration of the enzyme but the water activity of the gas entering the system. Secondly, they were able to discriminate between the alcoholysis reaction and the hydrolysis reaction using two different detectors. Another important difference is that PLE is used in the case of our experiments with methanol as a product of the reaction. In fact, PLE has been found to be activated by small alcohols (Greenzaid and Jencks, 1971)

All these results confirm that enzyme activity occurs well below 0.03 *h* of hydration. However, the water content of the enzyme used for the activity determinations is probably even lower than that of the enzyme used for the water quantification. In fact, in the last case, the enzyme was re-hydrated around 30 % with ^{18}O-labeled water and then, equilibrated over phosphorus pentoxide (P_2O_5) while the enzyme used for the activity measurement, was taken from a batch at about 10 % and then dried.

Another remark is that an enzyme hydration of 0% has not yet been reached with the drying methods previously used. Therefore, it was decided to freeze-dry the enzyme after re-hydration with ^{18}O-labeled water to improve the drying step over P_2O_5.

4. *Conclusion*

Table IV-2 summarizes the activity of pig liver esterase (PLE) obtained for the different drying methods as well as the water content measured with the ^{18}O-labelled water.

Table IV-2: Summary of the results of PLE activity as a function of hydration level.

Freeze-drying time (hours)	***Drying time over P_2O_5 (weeks)***	***Moles of water per mol of protein***	***Propyl-butyrate rate (pmol/min/mg)***	***Methanol rate (pmol/min/mg)***
None	1	33.1	93.9 ± 11.0	407 ± 98
	2	13.8	124.5 ± 16.6	215.5 ± 30.5
	2 at 65C	9.1	36.5 ± 24.3	58.7 ± 43.0
	4	3.8	42.4 ± 22.9	137.0 ± 27.5
16	1	5.5	51.3 ± 14.3	454.8 ± 106.9
	2	4.3	161.8 ±75.0	602.8 ± 84.1
	4	3.0	50.0 ± 10.5	395.3 ± 75.8
24	0	6.2	547.8 ± 317.4	1782.7 ± 390.5
	1	2.3	160.7 ± 20.7	508.1 ± 33.5
	2	1.8		Lost

The activity measurements do not match the amount of water molecule remaining after drying, especially for the samples freeze-dried prior to drying. However, there is a correlation between the enzyme activity and the length of exposure of PLE to P_2O_5. One explanation for these results could be a loss of label upon freeze-drying. However, the better activity observed with the freeze-dried samples could result from less denaturation of the enzyme over time. As discussed earlier, the loss of label seems unlikely, thus the second hypothesis is more probable. In the case of the non freeze-dried samples, the methanol rate decreases as the time of exposure increase apart for the sample dried at 65°C. It is not so evident for the propyl butyrate rate. This fact might be explained by a hydration dependency of the first step of the reaction while the second step would be hydration independent at low water content.

The rates of methanol and propyl butyrate production are low. One of our concerns was that the rates observed were due to product release rather than activity. Thus the ratio of moles of product per mol of enzyme over the time course of the experiment was calculated. The results are presented in Table IV-3.

Table IV-3: Moles ratio of the products per mol of protein as a function of the hydration level

Moles of water molecules per mol of protein	***Moles of methanol per mol of protein***	***Moles of propyl butyrate per mol of protein***
239 ± 2	110.5	23.2
114 ± 2	109.4	12.2
30 ± 2	85.6	19.7
12 ± 2	45.2	26.18
9 ± 2	12.3	7.7
3 ± 2	47.7	14.8

Thus, for each hydration studied, it was verified that the enzyme was able to perform several turn over. Although the rates may have been obtained under non-saturation of substrate, it does not affect the key objective/conclusion of this work, which is to show whether activity can occur in near-anhydrous conditions. Methanol has been found to enhance serine-protease through a solvation effect. However, the low availability of methanol in the case of our experiments makes it unlikely.

These results question the interpretation of role of water hydration on enzyme activity. Water affects enzyme activity in many ways. Although the role of water as a reactant or as a diffusion medium for the products and substrates of the reaction can be eliminated by the use of a gas phase transesterification catalytic system, water may still have played an important role in respect of free energy considerations. For instance, water molecule displacement upon substrate binding may induce a rise in entropy leading to a more favourable reaction (Kornbaltt and Kornblatt, 1997). Another possibility still not ruled out by these results is the role of water in the internal structure of a protein. However, surface water that interacts directly with the protein was thought up today to play a major role in protein function. The activity at water content as low as 3 or 2 water molecules per molecule of protein implies that not even a full coverage of the charged group is required for enzyme activity. In addition, the 'essential' water molecules are likely to be found near the active site rather than at the protein surface (refer Chapter V).

CHAPTER V: EFFECT OF HYDRATION ON ENZYME DYNAMICS

1. *Neutron scattering*

The use of this technique to study the protein dynamics has been reviewed (Gabel *et al.,* 2003 ; Zaccai, 1999). Neutron scattering experiments usually probe the global dynamics of proteins on a picosecond-nanosecond time scale. Neutrons provide an ideal tool for the study of almost all forms of condensed matter. Firstly, they are readily produced at a moderated nuclear research reactor and spallation source. Secondly, they are non-destructive and can penetrate deeply into matter. Thermal energy neutrons have wavelengths close to 1 Å, matching inter-atomic distances. Experiments using neutron radiation, therefore, provide simultaneously information on the amplitudes and energies of atomic motions. These are the reasons why neutron scattering experiments have been extensively used to study protein dynamics. In addition, the sensitivity of neutrons to hydrogen and oxygen atoms positions and fluctuations, as the different cross-section of hydrogen atom and its isotope deuterium, facilitate water dynamics studies.

The temperature dependence of the internal motion of proteins has been studied with different techniques such as neutron scattering, Mossbauer spectrometry or molecular dynamics simulation. These studies have revealed a change in the slope of the temperature dependence of the average mean square displacement of atoms in proteins within the temperature range 170-240 K. It is referred to as the "protein dynamical transition" (Doster *et al.,* 1989 ; Hayward and Smith, 2002 ; Parak and Knapp, 1984). Below the transition, the hydrated protein behaves as a harmonic solid with essentially only vibrational motions while above the transition; there is a striking dynamical transition arising from the excitation of non-vibrational motions. This change in dynamics resembles that seen in the liquid-glass transition.

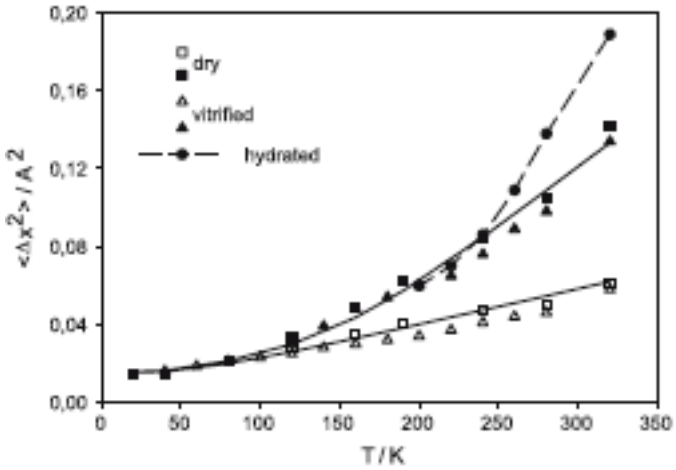

Figure V-1: Total and vibrational mean square displacements (IN13) derived from a cumulant analysis of the elastic scattering function of D_2O-hydrated myoglobin, h = 0.35 (full dots), dehydrated myoglobin (squares) and glucose-vitrified myoglobin (triangles). The full lines in the dry case were derived assuming the EISF and the correlation time for methyl group rotation (Doster, 2008).

Neutron scattering experiments carried out on dried and hydrated powders of lysozyme have shown that the protein dynamical transition is not observed on dried samples, however upon addition of glycerol or water, the anharmonicity is recovered (Tsai *et al*. 2000).

Thus, the protein dynamical transition seems solvent-dependent. To explain the solvent dependency of the dynamical transition, Tournier *et al*. (2003) studied the effect of water on the dynamical transition using molecular dynamics (MD) simulations. They used a dual heatbath method in which the protein and the solvent were held at different temperatures, to determine the driving forces behind the protein transition. They found that the protein dynamical transition was dependent on the solvent and is most pronounced in the outer parts of the protein. They also clarified the properties of the solvent responsible for inducing the dynamical transition. Thus, water translational diffusion may drive the protein dynamical transition (Wood *et al*., 2008). It also has been suggested that the protein solvation shell would play a major role in the temperature dependence of protein solution dynamics (Tournier *et al*., 2005). In fact, experiments on xylanase in water : methanol mixtures have shown that the onset of the dynamical transition moves to lower temperatures with increasing methanol concentration. The dynamical transition temperature is correlated to the melting temperature of the solvent on the pico-second time scale. However, this transition temperature appears at lower temperature on a nano-second timescale than that of the melting

point of the cryo-solvent used. This was explained as an experimental artefact. MD simulations confirmed the shift of the protein dynamical transition to higher temperatures as a consequence of a higher-resolution instrument. Thus, on a pico-second time window, slower motions would not be seen (Becker *et al.,* 2004 ; Daniel *et al.,* 1999 ; Daniel, Finney *et al.,* 2003). In neutron scattering of dry and hydrated myoglobin (Doster *et al.,* 1989) two temperature transition were observed at 180 K and 240 K and assigned to two molecular processes: torsional jumps of side-chains between states of different energy and water-induced collective motion. The latter were not observed in the dry sample. The protein dynamics might be more complex than those described by the dynamical transition. These result was confirmed by Roh *et al.,* (2006 and 2005), who studied the effect of hydration on the dynamics of lysozyme. In addition to these two onsets of anharmocitiy described by Doster, they observed three different relaxation processes on the pico-nano second dynamics. Firstly, the low temperature onset of anharmonicity at 100 K was attributed to methyl group fluctuations and was found not dependent on the hydration level. Then, a fast relaxation dynamics corresponding to fast conformational fluctuations were also distinguished from a slow relaxation process corresponding to larger scale motions. Thus below the dynamical transition, the motions would not be purely vibrational. These two processes are hydration dependent. An increase of the enzyme hydration was found to rapidly enhance the fast relaxation process leading then to the activation of the slow relaxation. The activation of the slow process would be responsible of the dynamical transition. In the case of lysozyme, the dynamical transition seems to occur only above 0.2 *h* and to be correlated to the onset of the activity. Our group has already performed and published neutron scattering and enzyme activity experiments with pig liver esterase (Kurkal *et al.,* 2005 ; Kurkal-Siebert *et al.,* 2006 ; Lind *et al.,* 2004) with the aim of correlating the effect of hydration on the activity and dynamics of the enzyme. These results have shown in a solid/gas bioreactor that this enzyme was able to be active under 0.03 *h*, and that at all the hydrations studied, diffusive motions were observed on a pico-second timescale. This work does not rule out the requirement of quasi-elastic scattering for enzyme activity. However, it was not possible with the hydrolysis reaction to study enzyme activity at lower hydration. Now that the activity has been probed at very low water content (refer Chapter IV), some

dynamical features might be revealed on a different time scale. In this work we have performed neutron scattering experiments on pig liver esterase (PLE) samples on IN16 to probe the motions on a ns timescale. Another question arises as well with the water molecule quantification - how dry were our dried samples. To answer this question, samples with two different drying methods were prepared and measured with a time of flight spectrometer at FRM II (Tof-Tof).

1.1. Theory of neutron scattering

A background to the theory and techniques of neutron scattering can be found in Fanchon *et al*. (2000) ; Fitter *et al*. (2006) ; Kostorz and Lovesay (1979).

1.1.1. The neutron

A full understanding of the neutron scattering techniques requires the knowledge of some basics of the neutron particle. Table VI-1 gives the characteristic of the neutron such as its mass or its magnetic momentum. The neutron not being charged, it interacts weakly with matter and can penetrate deeply. In addition, its spin corresponds to a magnetic momentum sensitive to the magnetic field of unpaired electrons. The coupling neutron-nuclear magnetic moment allows the study of the order and the dynamics of these moments.

Table V-1:Properties of the neutron.

Mass (kg)	***Charge***	***Spin***	***Magnetic momentum (m_N)***
$1.675*10^{-27}$	Null	1/2	-1.913

To measure the interaction of the neutron with matter, some values have to be defined. Firstly, the momentum of the neutron described by de Broglie's equation:

$$\mathbf{p} = \hbar\mathbf{k}$$

Where $\hbar$ is Plank's constant divided by 2π and $\boldsymbol{k}$ is the wave vector $|\boldsymbol{k}| = 2\pi/\lambda$. The wavelength of the neutron λ is:

$$\lambda = \frac{h^2}{2m_n\lambda^2} = 2k_BT$$

Where k_B is the Boltzmann's constant and T is the neutron moderator temperature. Another important value, is the energy of the neutron, which is equal to:

$$E = \frac{\hbar^2\mathbf{k}^2}{2m_n}$$

m_n is the mass of the neutron.

1.1.2. Neutron interaction with matter

In a scattering experiment the neutron undergoes a change in momentum after interacting with matter. This means that neutron has a change in direction and/or velocity. The momentum changes can be described by the scattering vector, $\boldsymbol{Q}$, defined as the vector difference between the incoming and scattered wave vectors:

$$\mathbf{Q} = \mathbf{k}_1 - \mathbf{k}_0$$

Where $\boldsymbol{k}_0$ and $\boldsymbol{k}_1$ are the incident and scattered wave vector respectively. Beside a change of direction, the magnitude of $\boldsymbol{k}$ can also change as energy between the incident neutron and the sample are exchanged. The law of energy conservation can be expressed as:

$$E = E_1 - E_0 = \hbar^2\frac{\mathbf{k}_1^2}{2m_n} - \hbar^2\frac{\mathbf{k}_0^2}{2m_n} = \hbar\omega$$

The neutron interacts with the nucleus of atoms. This interaction is likely to depend on the effective cross sectional area that an atom presents to neutron and then scatters or absorbs. A scattering cross-section, σ, is the probability of neutron-atom interaction and is equal to:

$$\sigma_S = 4\pi b^2$$

$\boldsymbol{b}$ is the scattering length. The interaction neutron-atom depends on the number of nucleons and their energy level, which makes light atoms as hydrogen visible. Two isotopes of the same elements have, as well, a different interaction. For instance, H and D have a very different cross-section.

The magnetic moment of the neutron interacts with the magnetic field arising from the spins and orbital momentum of magnetic exchanges. The spin dependence of the scattering cross section is expressed in the existence of a

coherent and an incoherent cross section. They are characterized by the coherent and incoherent scattering length b. The coherent scattering length is the analogue to the atomic form factor, f, in X-ray. The spherical waves that interfere scattered by the nuclei give information on the collective behaviour of the nuclei. The incoherent scattering corresponds to an isotropic background, which must be subtracted from the raw data, and gives information on the motion of single atoms investigated via studying the changes in energy of the scattered beam.

The exchange of energy will also give precious information on the dynamics of the sample. When no energy is exchanged, $\hbar\omega = 0$, the scatter is said to be elastic and inelastic when $\hbar\omega \neq 0$. The elastic scattering gives a description of all atoms. The dynamical phenomena over a time range between 10^{-13}-10^{-7}s can be investigated through the inelastic scattering but also through the quasi-elastic, which involves small energy exchanges with a spectral disposition peaked at zero. The incoherent spectrum of a scattering experiment is then divided into three categories. The elastic scattering (ESN), which probes the self-probability of distribution of hydrogen atoms; the quasi-elastic (QENS) is typically a Lorentzian centred on $\hbar\omega = 0$ and arises from diffusive motions in the sample; the inelastic scattering arises from vibrations.

1.1.3. Quasi-elastic and Inelastic Neutron Scattering

These techniques explore the atomic and molecular motions in space on length scales of the order the wavelength of the neutron (10^{-12}-10^{-9} m). The energy range investigated is 10 -10^{-5} meV and the wave-vector transfer values $\boldsymbol{Q}$ for elastic scattering are typically within the region of 0.3 Å^{-1} with $\boldsymbol{Q} = \frac{4\pi}{\lambda}\sin\frac{\varphi}{2}$ and φ being the scattering angle.

The dynamic structure factor $S(\boldsymbol{Q},\omega)$ is calculated from a typical dynamical process. The spectra in the QENS experiment is analysed in the energy domain corresponding to the maximum centred at 0 and $\hbar\omega \neq 0$. While in the time domain, it corresponds to the relaxation of the dynamical function. In the case of the atomic self-diffusion, the relaxation function (intermediate structure factor) has a single exponential time decay for small $\boldsymbol{Q}$:

$Is(Q,t) \sim \exp(-\Gamma t)$ with $\Gamma = 1/\tau = D_s Q^2$ and τ being the time decay constant and D_s the self-diffusion coefficient. This transforms in the energy

domain to a Lorentzian function of width 2Γ. For larger scattering vector, Γ depends on the geometric and dynamics details of the diffusive process. For a particle at rest, $\Gamma = 0$ and $S(\boldsymbol{Q},\omega)$ is a sharp elastic line δ(ω) at $\hbar\omega = 0$.

When a monochromatic beam is sent on a sample, it is scattered. The observation of the scattering is made under a total scattering angle 2θ, and a solid angle $d\Omega$. A double cross-section is then defined by:

$$\frac{d^2\sigma}{d\Omega d\omega} = \frac{k}{k_0}\frac{\sigma}{4\pi}S(\boldsymbol{Q},\omega)$$

Where the ratio k/k_0 characterise the scattering process, σ is the total cross section and $S(\boldsymbol{Q},\omega)$ in the Van Hove scattering function.

1.1.4. The Van Hove Scattering Function

S(Q) is the static scattering factor and corresponds to the energy integrated scattering intensity. While $S(\boldsymbol{Q},\omega)$, the scattering function , is momentum and energy dependant. The static structure factor is defined for pairs of atoms (i,j) by:

$$S(\boldsymbol{Q}) = N^{-1}\sum_{i=1}^{N}\sum_{j=1}^{N}e^{-i\boldsymbol{Q}(r_i - r_j)} = N^{-1}\left|\sum_{i=1}^{N}e^{i\boldsymbol{Q}r_i}\right|^2$$

Where N is the number of identical atoms, r are the positions occupied by the nuclei and are pairs of particles. If motion are observed, then $S(\boldsymbol{Q})$ becomes time dependent and the intermediate scattering function is obtained:

$$I(\boldsymbol{Q},t) = N^{-1}\sum_{i=1}^{N}\sum_{j=1}^{N}\left\langle e^{-i\boldsymbol{Q}r_i(0)}e^{i\boldsymbol{Q}r_j(t)}\right\rangle$$

The brackets here indicate the thermal average. Operators r_i, are vectors over physiological temperatures and energy ranges corresponding to QENS. Finally, the Fourier Transform (FT) of the correlation function derived by Van Hove give for the coherent scattering $S(\boldsymbol{Q},\omega)$ and incoherent $S_s(\boldsymbol{Q},\omega)$:

These relations describe the conditional probability per unit volume to find an atom at a position r_j at a time t if this or anther atom has been at r_i at previous time.

$$S(\boldsymbol{Q},\omega) = (2\pi^{-1})\int_{-\infty}^{+\infty}\int_{-\infty}^{+\infty}G(r,t)e^{i(Qr-\omega t)}drdt$$

$$S_s(\boldsymbol{Q},\omega) = (2\pi^{-1})\int_{-\infty}^{+\infty}\int_{-\infty}^{+\infty} G_s(r,t)e^{i(Qr-\omega t)}drdt$$

Where $G(r,t)$ and $G_s(r,t)$ are the correlation function for the coherent and incoherent scattering respectively.

The conditions are:

$$\hbar\omega << \frac{1}{2}k_BT \quad and \quad \frac{(\hbar Q)^2}{2M} << \frac{1}{2}k_BT$$

1.1.5. The Elastic Incoherent Structure Factor (EISF)

The EISF describes the behaviour of the correlation function at a very long time. The correlation function can split into its asymptotic values: its time-dependant limit ($G'_s(r, t)$) and its long-time limit ($G_s(r, \infty)$) with $G_s(r, t) = (G_s(r, \infty)) + (G'_s(r, t)$. The FT of this relation gives:

$$S_s(\boldsymbol{Q},\omega) = S_s^{el}(\boldsymbol{Q})\delta(\omega) + S_s^{in}(\boldsymbol{Q},\omega)$$

$S_s^{el}(\boldsymbol{Q})\delta(\omega)$ is a pure elastic line and arises from the diffraction of the neutron at infinite time and $S_s^{in}(\mathbf{Q},\omega)$ is the inelastic component. Thus, the EISF provide structural information on localized single-particle motions by the determination of the elastic intensity (Bée, 1992). At a relative high resolution, the measure of the elastic and inelastic integrals gives:

$$EISF = \frac{I^{el}}{I^{el} + I^{in}} = \frac{AS_s^{el}(\boldsymbol{Q})}{A\int_{-\infty}^{+\infty} S_s(\boldsymbol{Q},\omega)d\omega}$$

Where A is the normalization factor including the Debye-Waller factor.

1.2. Methododology

Two different neutron scattering experiments in this project were carried out at the ILL (Grenoble, France) on a backscattering spectrometer (IN16) in July 2005, at FRM II (Garching, Germany) with TOFTOF, a time of flight spectrometer in May 2006. However, the results of this second experiment have not yet been analysed.

1.2.1. Sample preparation

Pig liver esterase (150 units/mg, EC 3.1.1.1) was obtained from Sigma, and further partially purified using Fast Flow Q Sepharose. The enzyme was hydrogen/deuterium exchanged by twice dissolving the protein in 99.9% D_2O at 10 mg/ml, for 20 hours at 4 °C, and then lyophilised. A completely anhydrous enzyme powder was prepared by extensive drying in the aluminium sample cell. The lyophilised powder was initially packed into the sample holder in a glove box where the relative humidity was below 5% to prevent back exchange. The sample was then placed in a desiccator, over phosphorus pentoxide, for one week at room temperature. From previous gravimetric studies it was found that the resulting hydration after such treatment was less than 1%. Finally the sample was rapidly (< 60 seconds) sealed in a low humidity environment to reduce any adsorption of water. To prepare protein powders at higher hydrations, the original enzyme powder was hydrated to successively higher hydrations by equilibration with the appropriate saturated salt solution. The salts used to prepare the saturated solutions were dissolved in D_2O several times, and rotary evaporated to near dryness, so as to exchange as much of the water of crystallization as possible. The saturated salt solutions were then prepared in deuterium oxide. Lithium bromide and zinc sulphate were used to reach the hydration levels of 3% and 50%, respectively. One should remark that the relative humidity reached with saturated salt solutions prepared in D_2O are usually slightly lower than those prepared in normal water. As for the dry sample, the deuterium-exchanged protein was loaded into the sample cell inside the glove box, then, the protein was equilibrated for a week at room temperature with the appropriate saturated salt solutions. These samples were run on IN 16 at ILL.

The samples run on TOFTOF were prepared on the same manner but differed by the hydration level. One was dried over silica gel to reach a hydration level about 1.5% and the second one was dried for 7 days under phosphorus pentoxide (P_2O_5), initially at 65 °C overnight, then at room temperature. Samples at 3 and 50% were also performed.

1.2.2. Measurements on IN 16 at ILL (Institut Laue-Langevin, Grenoble, France)

In the back scattering (BSC) technique, the analyzers reflect neutrons with well-defined final energy, E_f, to the detectors. Complete analysis of the energy spectrum is performed by varying the energy of the incident neutrons around this value E_f. The BSC spectrometers are designed for inelastic scattering experiments with very high-energy resolution ($\delta E \sim 0.9$ μeV) and moderate momentum transfer resolution. BSC is more useful for problems in which the energy width of the scattering does not vary significantly with Q, such as self-diffusion or tunnelling motions. A resolution of the order of 1 μeV is also necessary for the investigation of long-range diffusive motions, such as those occurring in bio-molecules on timescale longer than 10 ps. The primary spectrometer of IN16 (Figure V-2) uses neutron optical focusing. As a consequence IN16 has a higher flux than IN10 and maintains perfect backscattering condition in the primary spectrometer at the expense of Q-resolution.

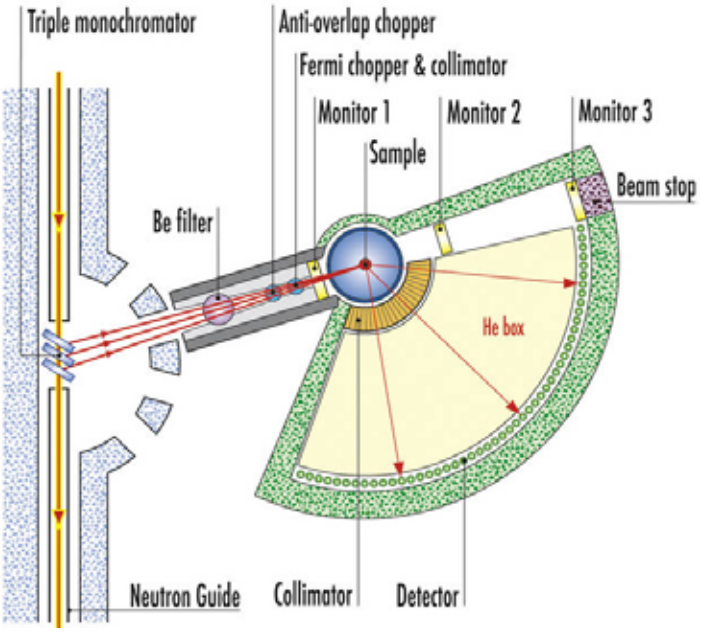

Figure V-2: Representation of the Backscattering spectrometer IN16 from I.L.L. (Grenoble, France).

The incident neutron wavelength was 6.27 Å. All data were collected with the sample holder oriented at 135° relative to the incident beam. The samples were contained in aluminium flat-plate cells, of 0.4 mm thickness. Spectra were

measured with a temperature ramp starting at 120 K and increasing to 300 K in steps of 10 K every half an hour. The measured transmission for all the samples was 0.96 indicating that multiple scattering was negligible. The detectors were calibrated by normalizing with respect to a standard vanadium sample. The cell scattering was subtracted, taking into account attenuation of the single-scattered beam. Finally, the scattering was normalized with respect to the scattering at the lowest measured temperature, and the lowest measured scattering vector, Q.

1.2.2.1 Quasi-elastic scattering

Vandana Kurkal-Siebert, who is part of J.C. Smith collaborating team, treated the raw data as explained below. An alternative approach used for obtaining $\langle u^2 \rangle$ is directly from the elastic peak, by summing S_{inc} over a range of small q values so as to obtain the integrated elastic intensity $S_{INT}(T)$. Assuming that $\boldsymbol{Q}$ is small enough over the integration range used so that Equation 1 still holds, then $S_{INT} = \langle u^2 \rangle$. This method has an advantage that it does not rely on fitting the low $\boldsymbol{Q}$ region of the scattering data, this being often a difficult task owing to noise in the data. Again, the scattering intensities were normalized to those at 120 K.

The determination of the quasi-elastic scattering intensity as a function of temperature was performed by integration of the difference between the spectrum of the sample, and the normalized vanadium spectrum.

Equation 1:

$$S_{INT}^{Quasi}(q_{mean},E,T) = \int_0^E S_{sample}(q_{mean},E,T) - S_{vanadium}(q_{mean},E,T)dE$$

Equation 1 is valid only in the quasi-elastic region. Since vanadium is a pure elastic scatterer, $S_{INT}^{Quasi}(q_{mean},E,T)$ is the quasi-elastic scattering of the sample. The quantity $S_{INT}^{Quasi}(q_{mean},E,T)$, was calculated by summation of the differences between the intensities of the sample and vanadium in the energy range $0 < E < 0.5$ meV and normalized to those at 120 K. The clear distinction between the quasi-elastic and inelastic region is rather difficult. However, the quasi-elastic region was chosen such that it does not include inelastic intensity. Moreover, changing the quasi-elastic energy range from $0 < E < 1$ meV to $0 < E < 0.5$ meV did not alter the results.

1.2.2.2 Mean-square displacement (MSD) and the environmental force constant

The dynamic structure factor $S(Q,\omega)$ is obtained by the Fourier transform of the intermediate scattering function $I(Q,t)$ and is given by:

Equation 2

$$S_s(Q,\omega) = \frac{1}{2\pi}\int_{-\infty}^{+\infty} dt e^{-i\omega t} I(Q,t)$$

Equation 3

$$I_s(Q,t) = \frac{1}{N}\sum_{\alpha=1}^{N} \left\langle\ e^{-iQR_\alpha(0)} e^{iQR_\alpha(t)}\ \right\rangle$$

Where α labels individual atoms whose positions are specified by their time-dependent position vector operators $R_\alpha(t)$. The elastic scattering $S(Q,0)$ was calculated by integrating $S(Q,\omega)$ over the instrumental full width at half maximum energy resolution. The mean-square displacement of the system from $S(Q,0)$ was obtained from the Gaussian approximation which makes use of the following cumulative expansion.

Equation 4

$$\left\langle e^{-iQ,R_\alpha(0)} ei^{Q,R_\alpha(t)} \right\rangle = e(-1/2)\left[\ Q(R(t) - R(0))^2\ \right]$$

Neglecting the terms in the exponent of Equation 4 of order higher than Q^2, the intermediate scattering function can be written, with the exponent averaged over all directions of $F(Q, t)$ as

Equation 5

$$F(Q,t) = \frac{1}{N}\sum_{\alpha}\ e^{-(Q^2/6)\left\langle (R_\alpha(t)-R_\alpha(0))^2 \right\rangle}$$

The elastic scattering is determined by the t→∞ limit of F, i.e., from Equation 3.

Equation 6

$$F(Q,t) = \frac{1}{N}\sum_{\alpha}\ e^{-(Q^2/6)\left\langle u_\alpha{}^2 \right\rangle}$$

Where $\langle u^2 \rangle$ is the t→∞ mean-square displacement of atom α. Equation 4 involves a sum of Gaussians. Therefore, even when the Gaussian approximation is valid for individual atoms at low Q, because of the fact that a sum of Gaussians is itself not a Gaussian, S(Q,ω) will not have a Gaussian form. There will, therefore, be a non-Gaussian contribution to the measured scattering due to motional heterogeneity, i.e., due to the fact that distribution of the mean-square displacements exists in proteins. Neglect of this non-Gaussian contribution

corresponds to the following approximation,

Equation 7

$$\frac{1}{N}\sum_{\alpha=1}^{N} e^{\left(-\langle u_\alpha^2\rangle Q^2/6\right)} \approx e^{\left(-\langle u_\alpha^2\rangle Q^2/6\right)}$$

Where $\langle u^2\rangle$ is the mean-square displacement averaged over the atoms in the protein. The approximation in equation 4 is valid for Q→0. Hence the elastic scattering in the limit of Gaussian approximation at temperature T is given by:

Equation 8

$$S_s = (Q,0,T) = Ae^{\left(-\frac{Q^2}{6}\langle u^2\rangle\right)}$$

Where A is a constant and $\langle u^2\rangle = [R(t)-R(0)]^2$, the mean-square displacement and not the mean-square fluctuations, $[R(t)-R_{mean}]^2$, which is the value usually used in the Debye-Waller factor in the harmonic approximation. The mean-square fluctuation in a one-dimensional harmonic approximation corresponds to half the mean-square displacement, i.e., $\langle u^2\rangle = [R(t)-R_{mean}]^2$.

A plot of $lnS_{inc}\ (Q, \omega, T)$ vs Q^2 was fitted with a straight line in the linear regime of Q^2 ($0.8 < q < 1.4$ Å^{-1}), the slope of which yields $\langle u^2\rangle$. As the scattering was normalized with respect to the 120 K intensities, the $\langle u^2\rangle$ determined is equal to where $\langle u^2\rangle_T$-$\langle u^2\rangle_{120}$ is the absolute mean-square displacement at temperature, T. The force F is the variation of potential energy f over a length Δl i.e. $F\Delta l = -\Delta V$. The rigidity of a given environment is reflected in the force exerted on an atom when it moves away from its equilibrium position. The mean environmental force constant ⟨k⟩ (in N/m), the force exerted per unit displacement can be calculated from the derivative of $\langle u^2\rangle$ versus T using the relation:

Equation 9

$$\langle k\rangle = 2k_B/(d\langle u^2\rangle/dT) = 0.00276/(d\langle u^2\rangle/dT)$$

With $\langle u^2\rangle = 6\langle x^2\rangle$, where $\langle x^2\rangle$ is the mean-square fluctuations. $\langle k\rangle$ corresponds to mean force constant for a set of harmonic oscillators. These are valid in the harmonic regime. Above the dynamical transition temperature, the measured $\langle k\rangle$ corresponds to a force constant in a quasi-harmonic approximation.

1.2.3. Measurements on Tof-Tof Forschungneutronenquelle Heinz Maier Leibnitz (FRM II), (Garching, Germany)

Time-of-flight instruments are composed of a primary spectrometer, producing the pulsed monochromatic beam, and of a secondary spectrometer, containing the sample table, the flight path and the detectors. The path between the sample and the detector is sufficiently long for measuring the time of flight of the scattered neutron, which is directly connected to the energy change in the sample. The time, τ, to 'flight' over a distance L, from the sample to the detectors, is given by:

$$\tau = \frac{L}{v}$$

The knowledge of the velocity of the incoming neutron v_0, and the measurement of τ, allows to determine the energy transfer, $h\nu$, according to:

$$h\nu = \frac{m}{2}(v^2 - v_0^2) = \frac{mL^2}{2}\left(\frac{1}{\tau^2} - \frac{1}{\tau_0^2}\right)$$

Where τ_0 is the time-of-flight of neutrons scattered elastically. The angular position of the detectors and the TOF measurement permit the analysis of both the momentum transfer $\boldsymbol{Q}$ and the energy transfer $\hbar\omega$. TOFTOF is a time of flight spectrometer supplied with cold neutrons, which is optimized for high flux (neutron flux: 1.10^{10} n/cm^2/s) and low background. The incident wavelength of TOFTOF is 1.5-1.6 Å and its elastic energy resolution is between 5 μeV-5 meV.
The samples were contained in aluminium flat-plate cells, of 0.3 mm thickness. Spectra were measured with a temperature ramp starting at 120 K and increasing to 400 K in steps of 10 K every half an hour.

1.3. Results

1.3.1. Results from ILL

The mean-square displacement, $\langle u^2 \rangle$ as a function of temperature calculated using Equation 1 is shown in Figure V-3 for three different hydrations. Only four days of beam time were allowed for this project, so it was not possible

to run more hydrations. Each sample was analysed over 24 hours and 24 hours were required for the vanadium control. Spectra were measured with a temperature ramp starting from 120 K to 300 K in steps of 10 K per hour.

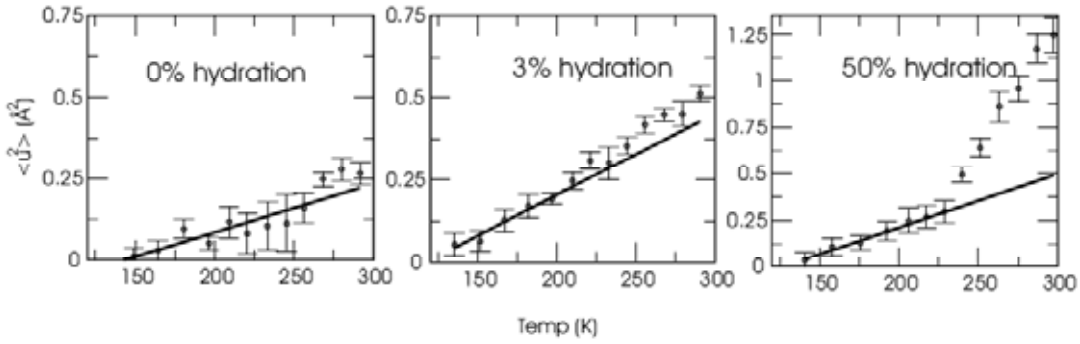

Figure V-3:$\langle u^2 \rangle$ of PLE as a function of the temperature for the three hydrations measured and calculated from raw data collected with IN16 (ILL, Grenoble)

For the "fully hydrated" control, (50% hydration), a dynamical transition is observed between 230-240 K for the pig liver esterase (PLE). The change in slope is quite steep. As previously observed with IN 5 (Kurkal *et al*., 2005), a very small change in the slope is observed for 0% and 3% hydration. The smaller amplitude (flatter slope) observed at lower hydrations, is consistent with an increase of the rigidity of the system as the hydration level decreases. Then, a dynamical transition well below the monolayer coverage (50 % of hydration) is confirmed. For the sample hydrated at 3%, this transition occurs around 250K, while for the 0% one, it occurs between 250 and 270 K. The change in the dynamical behaviour occurs at higher temperature with lower hydration levels. These results support the idea that water decreases the energy barriers between local minima required for the onset of diffusive motions.

Because of their energy resolution, IN16 probes motions on a nano-second timescale while IN5 probes motion on a pico-second timescale. In Figure V-4, the results obtained with the two different spectrometers are compared.

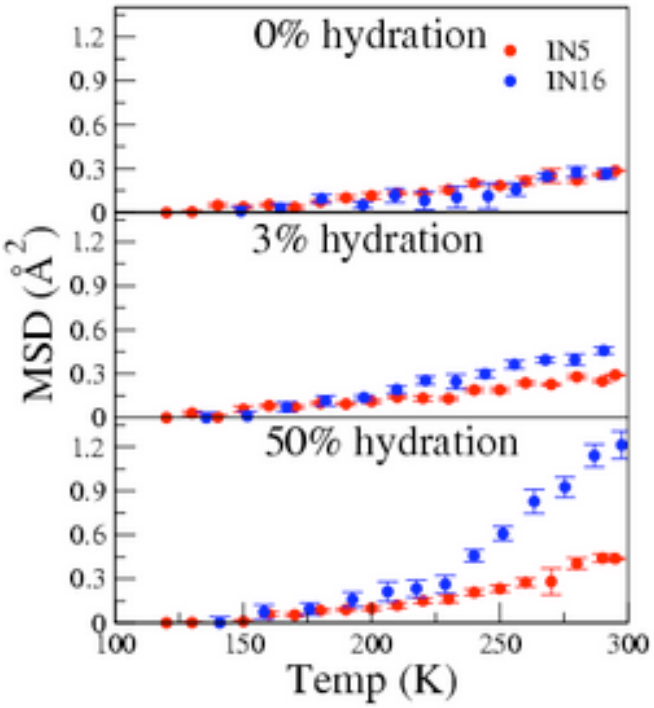

Figure V-4: MSD of PLE at different hydrations as a function of the temperature measured by two different spectrometers IN16 and IN5 (ILL, Grenoble)

The temperature dependency of the mean square displacement (MSD), as measured with IN16, gives a steeper change in slope above the dynamical transition temperature than the slope change observed with IN5. The change in slope observed with IN16 occurs at a lower temperature than observed with IN5. Daniel, Finney *et al*. (2003) concluded that the dynamical transition is time-scale dependent as well as temperature-dependent. Thus, two kinds of motions are observed; fast motions observable on a pico-second time-scale and activated at higher temperature, and larger amplitude motions observed on the nano-second time-scale activated at a lower temperature. The results presented here clearly show the effect of the energy resolution on the mean-square displacement (MSD). IN16 has a finer resolution and thus incorporates slower motions into the MSD. Thus, the MSD observed with IN16 is higher. At 0%, the data seem to coincide and suggest the only presence of fast vibrational motions in the sample. However, taken individually, a very small transition is observed. At 3% of hydration, the differences are clear, thus the presence of fast vibrational motion is clear. The temperature, at which the dynamical transition occurs, as well as the amplitude, is in both cases hydration dependent.

1.3.2. Results from FRMII

It was expected to run the drier samples at a higher temperature than 300 K and to have an intermediate hydration sample between 0 and 3%. Tof-tof is a time of flight spectrometer, which has about the same resolution than IN5. We would then have obtained information on the nano-second time scale dynamics.

Non-isothermal transitions of lyophilised protein, as seen by differential scanning calorimetry, decrease with increasing moisture content (Fujita and Noda, 1981). Bell *et al*. (1995) found values such as 161°C for a dry somatotropin recombinant and 65 °C at 28% moisture. Gentili *et al*. (1997) described an irreversible melting temperature for *C. cylindracea* lipase of 86°C upon which the enzyme is partially or totally deactivated. In solution, C. rugosa lipase B has a temperature of denaturation of 324.3 K (Shnyrov et *al*., 1998). Thus it can be expected for lipase B and PLE to remain active above 350 K (77 °C) when dried, while most of the dynamics studies stop at 400 K (127°C). This fact might explain why a dynamical transition has not been observed before. The aim of this work was then to investigate the dynamics of PLE up to 400 K to confirm that a transition occurs above 295 K. Some attempts to measure the temperature of denaturation of lipase B and PLE with differential scanning calorimetry at different hydration have been done without success. A sample was also dried to reach a hydration level of 1.5% (g of water per g of dry protein). Although the resolution might not be good enough, it would have been expected to have a transition between 250 and 295 K. This result would have been more meaningful in the case of the absence of a transition in the dry sample. The neutron scattering data still need to be treated by our collaborators.

1.4. Conclusions

These results show that the global dynamics of PLE observe both harmonic and anharmonic behaviour even at “zero” hydration. Water molecule quantification has indeed revealed that still about 3 water molecules per mol of enzyme were present in our samples (see section II-3). These results also state that the absence of anharmonic behaviour observed in most systems cannot be yet correlated to the absence of water. Firstly because most proteins investigated were not completely dried. Secondly, because they probably investigated the

temperature dependency of the dynamics well below the temperature of denaturation of dry proteins.

However, these results confirm a hydration dependency of the temperature at which the dynamical transition occurs and of the amplitude of motions.

The discrepancies in the temperature at which the transition occur as a function of the time scale investigated confirm that the dynamic behaviour of a protein is time dependent. Thus, fast and slow motions have the same hydration dependency.

2. *Molecular dynamic simulations*

2.1. Introduction

Enzyme activity at low hydration has always been a concern in food preservation where a residual enzyme activity was sometimes observed after drying. Nowadays, workers try to understand the molecular basis of the role of water in protein function. Towards this aim, several studies have established a correlation between enzyme activity and hydration level. While a threshold of hydration of 0.2 *h* is usually accepted for the onset of enzyme activity, recent works show that enzyme hydrolysis is possible at water contents as low as 0.03 *h* protein (Lind *et al.,* 2004). Pig liver esterase and *C. rugosa* lipase B are able to catalyze alcoholysis where water is not involved as a reactant of the reaction. Therefore, by following this reaction and using a gas phase catalytic system, we have been able to show that activity can occur in anhydrous or near anhydrous conditions. Although gravimetric measurements of the hydration level do not allow us to define the anhydrous state of the protein with sufficient sensitivity, using ^{18}O-labeled water, we have been able to quantify the small number of water molecules bound to the protein after drying. These preliminary experiments showed that 8 moles of water per mole of protein would be enough for the onset of the lipase B activity (refer Table VI-1). Hydration affects protein function and dynamics. Neutron scattering spectra show that diffusive motions of the protein increase with the hydration (Zanotti *et al.,* 1999). This behaviour is correlated with the increase of enzyme activity. But, no correlation can be done with the onset of the activity (Kurkal *et al.,* 2005). So what are the motions involved in the

onset of enzyme activity at such hydration? To address this question, we have performed molecular dynamics simulations on one of our models: *Candida rugosa* lipase B at hydration levels where enzyme activity has been observed.

C. rugosa lipase B is a single domain protein that belongs to the α/β hydrolase fold family. Its catalytic machinery has been characterized as a serine protease –like triad (SER-209, HIS-449 and GLU-341). The main variability between this enzyme and its family members is expressed by the sequence of three loops in the vicinity of the active site. The loop that differs the most is the flap between the residues 62 and 92. Another feature of *C. rugosa* lipase B is that its activity is enhanced by a water-lipid interface (Turner *et al.,* 2001). This phenomenon is called interfacial activation and includes a *cis* to *trans* isomerisation of a proline (PRO-92) residue of the flap to expose a large hydrophobic surface, which likely interacts with the lipid interface. This protein is *N*-glycosylated with a *N*-acetyl D-glucosamine residue on two sites (ASN-314 and ASN-315) (Grochulski *et al.,* 1993). Another important structural feature of this enzyme is a unique binding site for the reaction intermediates (Grochulski *et al.,* 1994b).

Both the open (or active, refer figure V-5) and closed (or inactive, refer figure V-6) conformations of *C. rugosa* lipase B have been crystallized showing that its activation requires a rotation of the flap of almost 90 degrees to expose or exclude the active site from the solvent (Grochulski *et al.,* 1994).

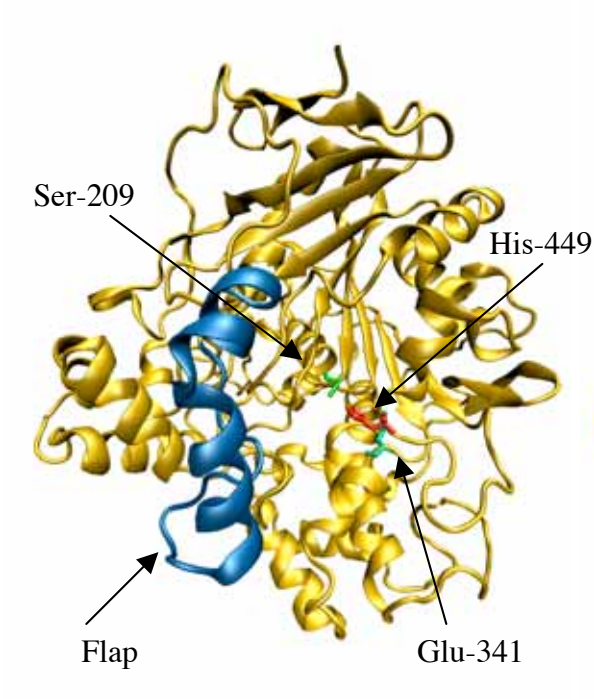

Figure V-5: 'Open' form of *C. rugosa* lipase B.

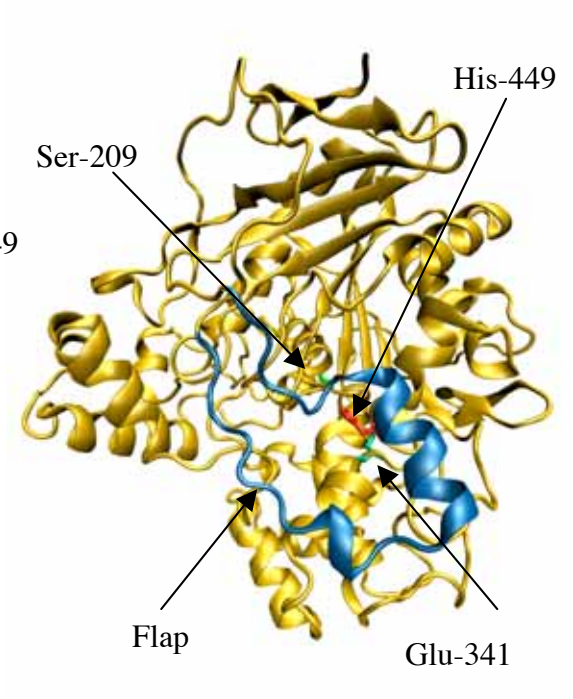

Figure V-6: 'Close' form of *C. rugosa* lipase B.

The figures above show that the flap covers the active site in the closed conformation. From MD simulation, we will extract information of how the structure of the enzyme in the vicinity of the water changes with time, and quantify and localize the water molecules required for activity. Simulations will be carried out with *Candida rugosa* lipase B to investigate how these water molecules modify the protein dynamics.

2.1.1. Basis of MD simulations

Some introductory concepts on MD simulations are available in (Leach, 2001) and (Karplus and Petsko, 1990). Molecular dynamics is the science of simulating the motions of a system of particles. MD simulations begin with the knowledge of the energy of the system as a function of the atomic coordinates. The potential energy surface determines the relative stabilities of the different possible stable or metastable structures. The forces acting on the atoms of the system, which are related to the first derivatives of the potential with respect to the atom positions, can be used to calculate the dynamic behaviour of the system by solving Newton's equations law of motion for the atoms as a function of time. Simulations cover the same time scale and amplitude range of motions as neutron

scattering. Because they provide individual particle motions as a function of time, they can be probed far more easily than experiments and complement them to answer detailed questions (Karplus and Petsko, 1990).

Molecular dynamics (MD) simulations often complement the understanding of the macromolecular dynamics by providing information that is not accessible by the neutron scattering experiments. This computational method calculates the time dependant behaviour of a molecular system. To investigate a biological system which involves many atoms, molecular mechanics is usually used. This method is based on the Newton's second law of motion:

$$F_i = m_i \bullet a_i$$

Where $\boldsymbol{F_i}$ is the force exerted on a particle of mass $\boldsymbol{m_i}$ and acceleration $\boldsymbol{a_i}$. Integration of the equations of motion yields a trajectory that describes the position, velocities and acceleration of the particles as they vary with time.

2.1.2. Theory

In molecular modelling, the Born-Oppenheimer approximation is usually assumed. It states that the dynamics of the electron react as their nuclei. So the electron and the nuclei can be treated separately. Thus, the energy of a molecule in its ground electronic state is considered as a function of its nuclear coordinates only. The way in which energy varies with coordinates is referred to as the potential energy surface.

As described previously, MD simulation consists of the numerical, step-by-step, solution of the equation of motion:

$$\frac{d^2 x_i}{dt^2} = \frac{F_{x_i}}{m_i}$$

This equation describes the motion of a particle $\boldsymbol{i}$ of mass $\boldsymbol{m_i}$ along the coordinates ($\boldsymbol{x_i}$) with $\boldsymbol{F_i}$ being the force on the particle in that direction. It is obviously important to specify the position of the atoms in the system to a modelling program. There are two common ways in which this can be done. The most straightforward approach is to specify the Cartesian coordinate (x,y ,z) of all the atoms present. The alternative is to use internal coordinates, in which the position of each atom is described relative to other atoms in the system.

Nevertheless, these calculations are computationally consuming and some

approximations have to be done. CHARMM (Brooks *et al.,* 1983) is a research program developed at Harvard University for the energy minimisation and dynamics simulation of proteins, nucleic acids and lipids in vacuum, solution or crystal environments. The CHARMM potential energy function, for instance, calculates the energy as a sum of bonded (or internal) terms and a sum of non-bond terms. The energy E is a function of the atomic position, R, of all the atoms in the system.

$$V(R) = E_{bonded} + E_{non-bonded}$$

$$E_{non-bonded} = E_{van-der-waals} + E_{electrostatic}$$

$$E_{bonded} = E_{bonb-stretch} + E_{angle-bend} + E_{rotate-along-bond}$$

The bonded terms are defined by the contribution of the bond stretching, the angle bending and the rotation along the bond, while the non-bonded terms represent the contribution of the van der Waals and electrostatic interactions in the energy.

2.1.3. Setting up and Running a MD simulation

First, it is necessary to establish an initial configuration to the system. The protein structure is then often used. It is necessary to assign initial velocities to the atoms. This can be done though the Maxwell-Boltzmann equation which provides the probability that an atom *i* of mass m_i has a velocity v_{xi} in the *x* direction at the temperature *T*:

$$p(v_{xi}) = \left(\frac{m_i}{2\pi k_B T}\right)^{1/2} \exp\left[-\frac{1}{2}\frac{m_i v_{xi}^2}{k_B T}\right]$$

It represents a Gaussian distribution, which can be obtained using a random number generator. The initial velocities are often adjusted so that the total momentum of the system is zero. Once the system is set up, then the simulation can commence. At each step, the force on each atom must be calculated by differentiating the potential function. The force is straightforward to calculate for two atoms interacting under the Lennard-jones potential:

$$f_{ij} = \frac{r_{ij}}{|r_{ij}|}\frac{24\varepsilon}{\sigma}\left[2\left(\frac{\sigma}{r_{ij}}\right)^{13} - \left(\frac{\sigma}{r_{ij}}\right)^{7}\right]$$

The force between the two atoms is equal in magnitude and opposite in direction and applies along the line connecting the two nuclear centres, in accordance to Newton's third law. It is necessary to calculate the force between each atom pair just once. The first stage of a MD simulation is the equilibration. The purpose of this phase is to bring the system at equilibrium from the starting configuration. During this phase, different parameters such as the temperature are monitored. The parameters used to characterize whether equilibrium has been reached include the kinetic, potential and total energies, velocities, temperature and pressure. The total energy should remain constant while the kinetic and the potential energy would be expected to fluctuate in the microcanonical ensemble. The component of the velocities should describe a Maxwell-Boltzmann distribution and kinetic energy should be equally distributed among the three directions *x,y* and *z*. Next, the entire system is minimized. Only then, the production phase starts.

2.1.3.1 Energy minimization

It is impossible to visualise the potential energy surface of a molecule. Molecular modelling is interested in minimum energy arrangements of the atoms that correspond to stable states of the system. A minimization algorithm can be used to localize these minimum points of the energy surface. There are two groups of minimization algorithms, those that use derivatives of the energy with respect to the coordinates, and those that do not. For instance, in this study, the steepest descents and the conjugated gradient methods were used. They are first-order minimization methods, which gradually change the coordinates of the atoms as they move closer and closer to the minimum point. The steepest descent method moves in direction parallel to the net force. Having defined the direction along which to move it is then necessary to decide how far to move along the gradient. Consider the two-dimensional energy surface, the gradient direction from the starting point is along the line indicated. In the conjugate gradient method, the gradients at each point are orthogonal but the directions are conjugated.

2.1.3.2 Integration method

The particle changes energy whenever the particle changes its position. The equation of motion is then integrated using a finite difference method, where the motions of all particles are coupled together under the influence of a continuous potential. All the algorithms used assume that the position and the dynamics properties can be approximated as a Taylor series expansion. The Verlet algorithm, for instance, uses the positions and the accelerations at time *t* and the position from the previous step (*t*-δt) to calculate the new position (*t*-δt):

$$r(t + \delta t) = 2r(t) - r(t - \delta t) + \delta t^2 a(t)$$

Where ***r*** describes the position and ***a*** the acceleration of the particle. The velocities do not explicitly appear in the Verlet algorithm but can be calculated. The Verlet velocity method gives positions, accelerations and velocities at the same time and does not compromise position.

2.2. Method

2.2.1. Dynamics production

The crystal structures of the open and closed conformations of *C. rugosa* lipase B were taken from the Protein Data Bank. The structures are resolved to 2.06 Å and 2.1 Å respectively. In these structures, three *N*-acetyl-glucosamine residues covalently bound to the enzyme were removed prior the simulation. All the crystal waters were maintained. A box of water was built around the protein. After removal of the water molecules overlapping the protein and the crystal waters, the interaction energy between the protein and each water molecule was calculated on the basis of van-der-Waals and electrostatic interactions. The water molecules were then sorted as a function of their interaction strength. Those with the highest strength were kept. To look at the dynamics at very low hydration, we decided to keep only the amount of water molecules where activity has been observed or of a biological relevance (Table V-2).

Table V-2 Number of water molecules added to a molecule of lipase B, corresponding hydration level and biological relevance of the choice of the number of water molecules added.

Number of simulated water molecules	***Corresponding Hydration (h)***	***Biological relevance***
0	0	Dry protein control
4	0.0013	
8	0.0025	Activity observed in gas phase
15	0.005	
22	0.007	Activity observed in gas phase
50	0.015	
100	0.03	Hydrolysis activity observed in gas phase
158	0.05	Strong protein:water interactions
317	0.1	
475	0.15	
634	0.2	Threshold usually accepted as necessary for the onset of activity
1110	0.35	
1586	0.5	Fully hydrated control

All the structures were minimized using the steepest descent method followed by a conjugated-gradient method. The MD simulations were carried out with a 50 ps time step at 298 K with CHARMM force field (Bernard R. Brooks, 1983) version 31b2 using all-atom parameter set 22 (MacKerell, 1998). The velocity-verlet integrator was used in conjunction with the TPCONTROL command. The coordinates and trajectories were recorded each 50 ps for all the atoms over 1ns.

2.2.2. Analysis

2.2.2.1 Mean Square Displacement (MSD)

The analyses were performed only on the open conformation of *C. rugosa* lipase B, as the opening of the flap must occur at higher time scale.

The first dynamic parameter we analysed is the mean square displacement (MSD), which is a measure of the average distance that the atoms travel and it is defined by:

$$\mathrm{MSD} = \langle |\mathbf{r}(t) - \mathbf{r}(0)|^2 \rangle$$

The time dependency of the mean square displacement (MSD) of the protein was studied for each hydration. This parameter was calculated for all the atoms of the protein as well as those of flap and those of the active site.

The MSD was then averaged over the 1 ns dynamic and plotted as a function of hydration. Once again, the hydration dependency of the MSD was calculated for the different part of the enzyme (i.e. whole protein, flap and active site).

2.2.2.2 Autocorrelation function

As the opening of the flap seems to be the major event of the lipase activity, and even though it is occurring at higher time scale, we looked at the tendency of the occurrence of this event. We calculated the autocorrelation function of the distance between the flap and the active site.

The autocorrelation function (ACF) will describe the correlation of this distance with itself at different points in time over the 1 nano-second trajectory and is defined by:

$$R(t,s) = \frac{E[(X_t - \mu)(X_s - \mu)]}{\sigma^2},$$

X_t is the value of the process at time t,

μ is the mean of X_t

σ^2 is the variance of X_t

E is the expected value operator.

The distance flap-active site is determined between the centre of mass of the active site and the centre of mass of the flap. The center of mass **R** of a system of particles is defined as the average of their positions $\mathbf{r}_i$, weighted by their masses m_i:

2.3. Results

2.3.1. The Mean Square Displacement (MSD)

The time dependency of the mean square displacement of the whole protein has been plotted for all hydrations (Figure V-7).

2.3.1.1 MSD as a function of time

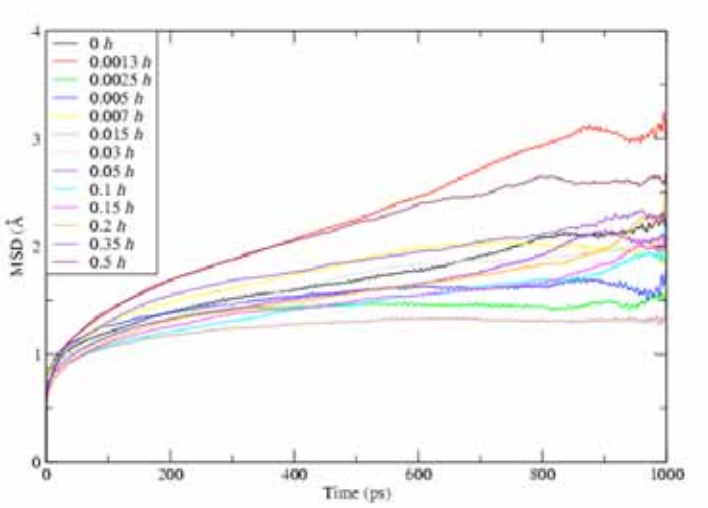

Figure V-7: MSD of *C. rugosa* lipase B as a function of time at different hydration levels.

The MSD increases slightly with time for all hydrations, except maybe for 0.015 *h*. The highest hydration shows the highest increase of the MSD. However, the MSD with time of the hydrogen of the protein hydrated at 0.0013 *h* observed the same increase of as for the highest hydration. Thus, there is no clear correlation between the hydration level and the MSD. This may be due to the poor convergence of the trajectories. Multiple MD trajectories would be required to achieve statistical convergence. If we look only at the atoms of the flap, the dynamics seems to be more affected by the hydration level (Figure V-8). In this

case, the two highest hydrations have the highest increase of the MSD with time while the others hydration seem to have the same behaviour. Figure V-9 shows the MSD of the active site as a function of time. Once again, there is no dependency on the hydration level of the MSD. It is however interesting to see that we have three groups. The first group has no increase of the MSD with time. The second one, where we can find all the hydrations level above 0.1 *h*, with a small increase of the MSD. And the third one, composed of only one curve, with the highest increase of the MSD.

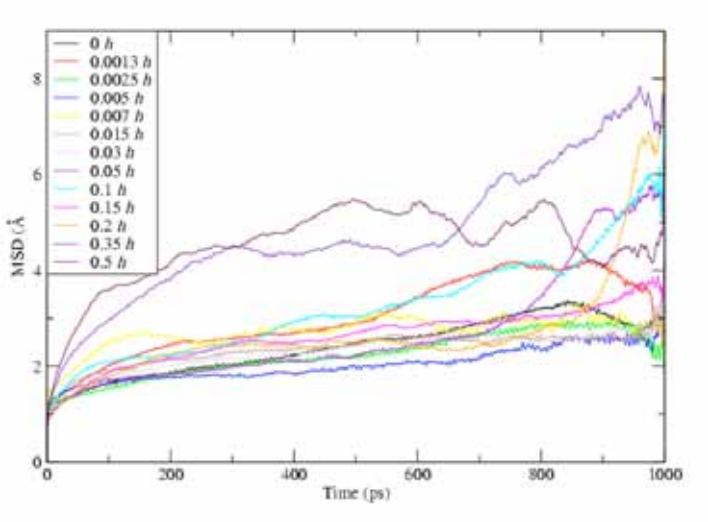

Figure V-8: MSD of the flap of the protein as a function of time for all the hydration studied.

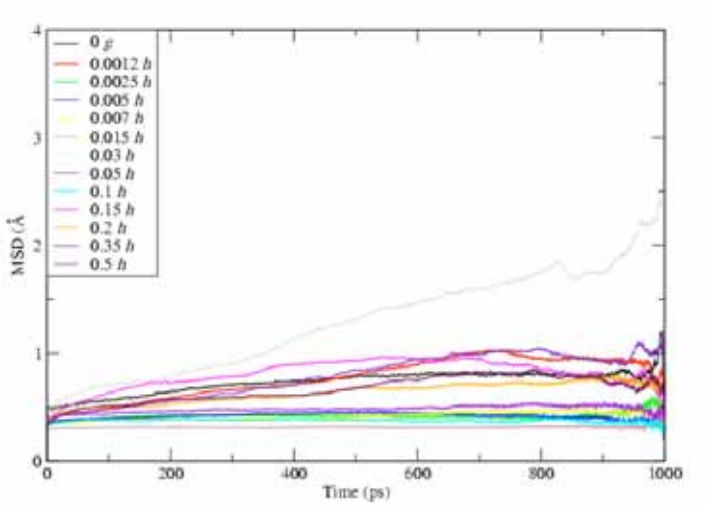

Figure V-9: MSD of the catalytic triad of the lipase B as a function of time for all the hydrations studied.

From these results, it can be concluded that the active site is probably the most sensitive to the hydration level as the effect of the addition of water is observed at a smaller amount than for the flap. It also appears that this process show three steps. Thus, the active site, which is in the core of the protein, would be the most affected by the hydration level.

2.3.1.2 MSD as a function of hydration

The mean square displacement as a function of hydration has also been calculated for the different parts of the protein (Figure V-10 and V-11). The comparison of the structure of the open and closed conformations has shown that the $\alpha_{b3,2}$ helix travels a distance of 19 Å to become the part of the flap that is the most extended toward the solvent. So it is not surprising that the flap has the highest MSD. The analysis of the MSD of the whole protein as a function of hydration (dark curves) shows that the global dynamics increase with hydration between 0.1 and 0.5 *h*. Under this value, the correlation between the MSD and the hydration value is lost. From thermodynamic studies, we know that below a hydration level of 0.1 *h*, water molecules condense onto the strongest interaction sites of the protein surface. It is therefore likely that the MSD will depend on the location of the interaction water:protein rather than on the number of interactions. In the case of the atoms of the flap (red curves), the MSD increased considerably above 0.2 *h*. This is in agreement with a high activation of the enzyme activity. It is also in agreement with the threshold usually admitted for the onset of activity. In fact, all enzymes for which the activation process required a loop movement would not be able to work under such hydrations. As in the case of the whole protein, below 0.2 *h* the correlation between the hydration level and the MSD is lost. The active site (green curves) shows a very small MSD and very stable at high hydration. As for the flap, below a hydration level of 0.2 *h*, the MSD value is not correlated to the hydration level and can reach higher values than those at high hydration levels.

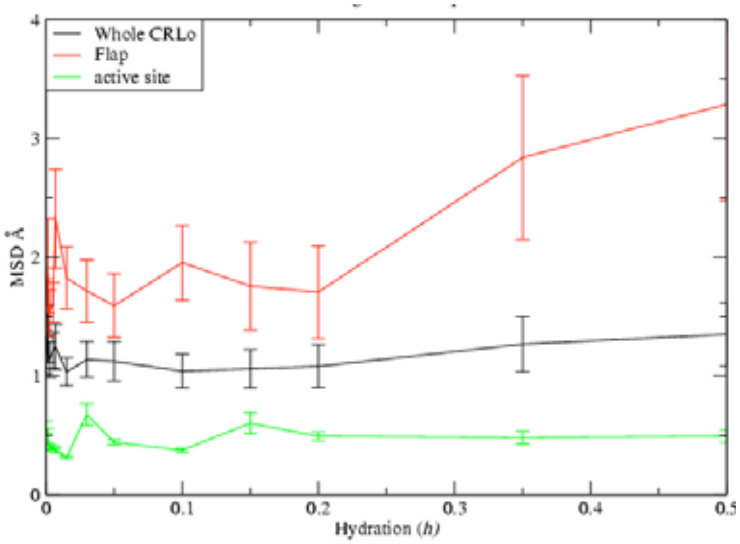

Figure V-10:MSD of the lipase B, its flap or of its catalytic triad as a function of hydration averaged over 200 ps.

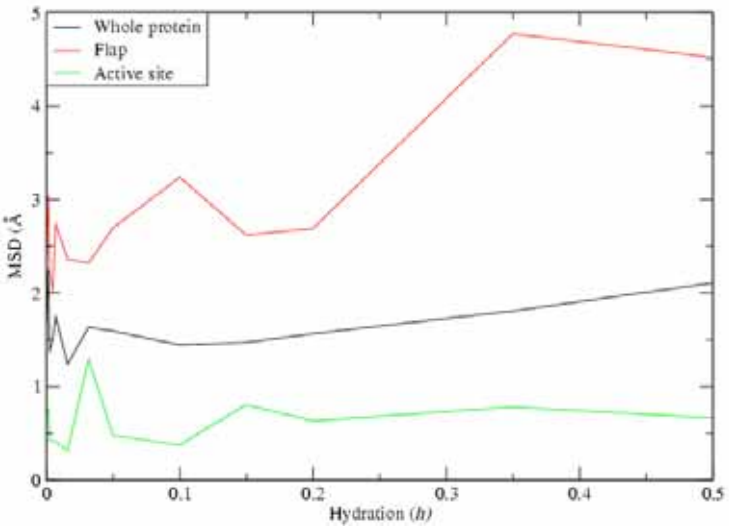

Figure V-11: MSD of the lipase B, its flap or of its catalytic triad as a function of hydration averaged 1 ns.

2.3.2. Autocorrelation function

The autocorrelation function has been plotted for all hydrations (Figure V-11). We would expect this function to oscillate and decrease with time as the flap moves away from the active site. We do not have this feature but it is noticeable that the oscillation of the function increases with the hydration level. It is therefore important to remark that we are not looking at a transition from open to closed conformation and *vice versa*, since this transition occurs at a different time scale. However, we can see the tendency of this motion.

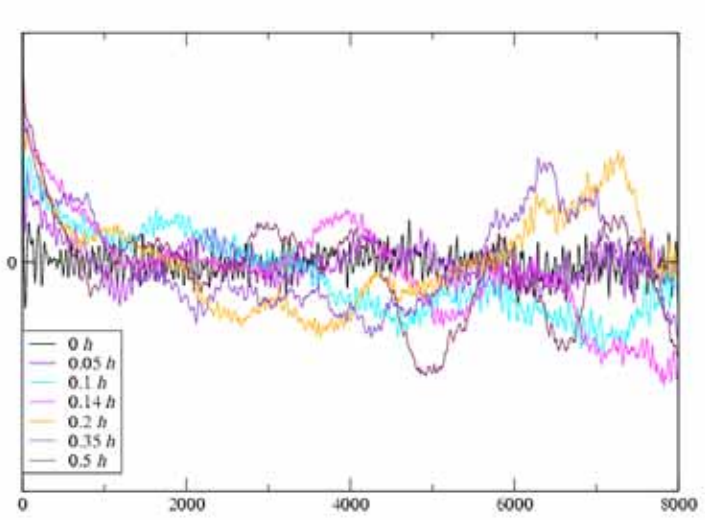

Figure V-12: Autocorrelation function of the distance between the centre of mass of the active site and the centre of mass of the flap in the case of the open lipase B for different hydrations

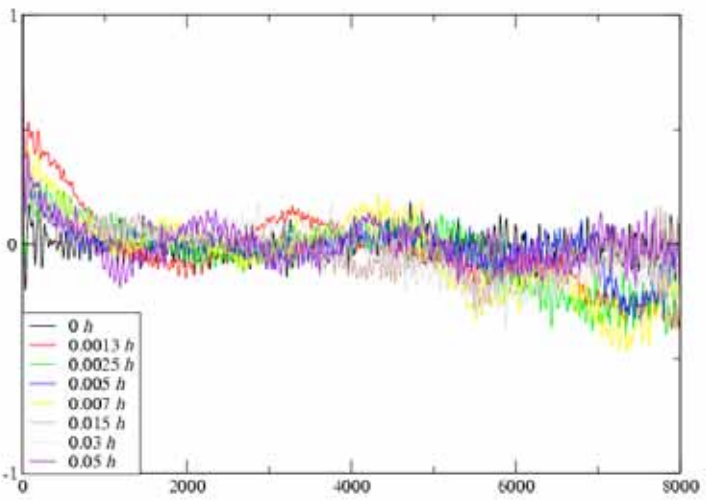

Figure V-13: Autocorrelation function of the distance between the center of mass of the active site and the center of mass of the flap in the case of the open lipase B for hydrations levels below 0.05 *h*.

From the Figures V-11 and V-12 that the correlation function gets larger and higher amplitudes as the hydration levels increase. The correlation function at 0 *h* is flat while some motions seem to appear already at a hydration level of 0.0013 *h*. These results indicate a strong correlation between the hydration level and the opening of the flap.

The lowest hydration molecules are represented below (figure V-14 to 17) at the end of the production run.

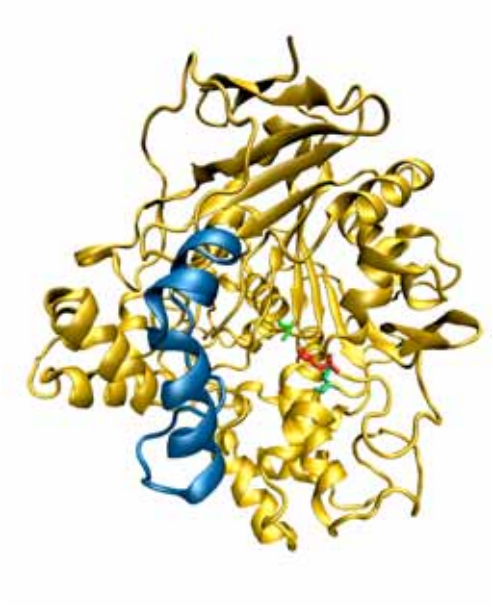

Figure V-14: "Open" lipase B with no water at the end of the simulation.

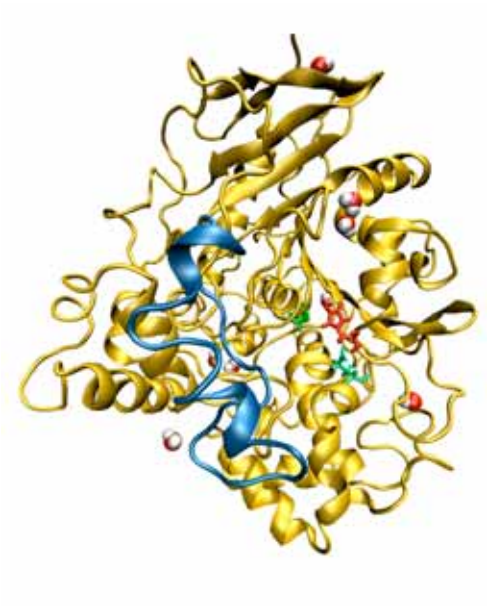

Figure V-15: "Open" lipase B with eight water molecules at the end of the simulation.

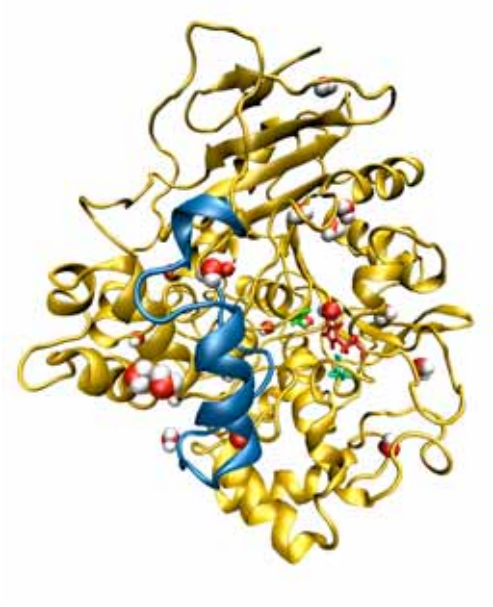

Figure V-16: "Open" lipase B with h 22 water molecules at the end of the simulation.

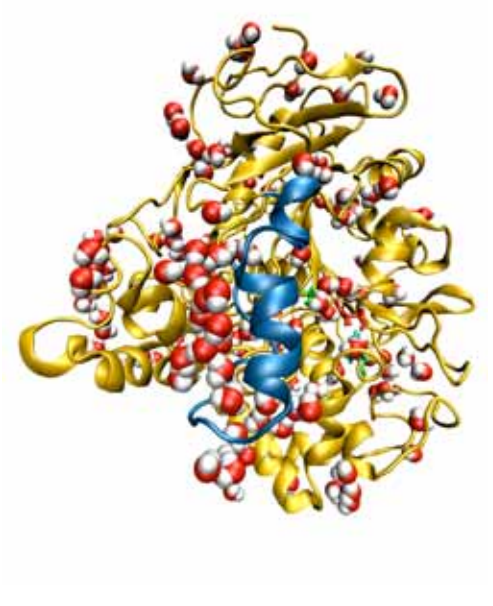

Figure V-17: "Open" lipase B with 158 water molecules at the end of the simulation.

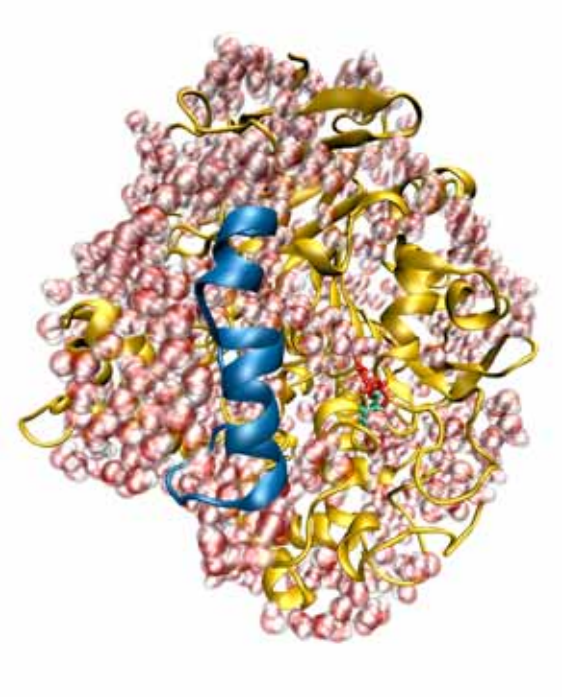

Figure V-18: "Open" lipase B with 634 molecules at the end of the simulation The figures above show that as the hydration level is increased, the water molecules condensed on the "external" side of the flap.

From these pictures, it can be observed that as the amount of water increases, the density of water molecules around the flap and the active site increases particularly. This is in agreement with the particular sensitivity of these two sites to the hydration level. This work gives us some hints on the motions involved in the onset of enzyme activity. However, further analyses have to be performed to give solid conclusions. For instance, the intermediate scattering function could be calculated from the trajectories which on Fourier transform will give the dynamical structure factor, the quantity obtained from the incoherent neutron scattering spectroscopy. The enzyme motions responsible for certain dynamical features observed in the spectrum could be extracted which otherwise would not be possible with experiments.

2.4. Conclusions

MD simulations were used to investigate the global and local dynamics of *C. rugosa* lipase B as a function of hydration. The global dynamics is clearly increased above a hydration level of 0.1 *h* (or 317 water molecules per mol of lipase B). The flap observes the same tendency but it is not the case of the amino acids of the catalytic triad. The active site seems to have higher amplitude

motions at lower hydration and quite irregular. At higher hydration, above 0.1 *h*, the amplitude of the motions remains constant. The higher amplitude of the motions observed at low hydraration and its irregularity as a function of the hydration level might be explained by the location of the "added" water molecules. In fact some might affect more or less the active site. This could also correlate with discrepancies in the enzyme activity at low water content.

3. *Conclusions: the effect of hydration on dynamics*

The global dynamics studies on PLE have revealed the existence of a dynamical transition on a pico-second time scale. The motions observed are faster and activated at higher temperature than usually described. These motions seem to be also of smaller amplitudes than those observed on a nano-second time-scale. The shift to higher temperatures of the dynamical transition as the hydration level decrease might explain why most of the studies do not show dynamical transition in dry samples. In fact, dried enzymes have been shown to have a higher stability and remain active above 350 K when dried. Thus, some studies might not have progressed to sufficiently high temperatures. The amplitude of the motions observed is also consistent with a hydration dependency. The dried PLE sample invested here was dried for a week over P_2O_5, thus it might be expected to have still around 30 water molecules per molecule of enzyme. Nakagawa *et al*. (2008) showed that the boson beak shifted to higher energy upon hydration, implying that hydration affects both the harmonic and anharmonic dynamics behaviour of proteins. This could explain the observation of enzyme activity below the dynamical transition.

Local dynamics of *C. rugosa* lipase B have revealed that the active site was the most sensitive area to hydration as compared to the flap or the whole protein. Small amplitude but fast motions are also observed. The localisation of the water molecules also shows a condensation of water onto the two main important sites for activity, i.e. the flap and the active site. Thus, at very low hydration, the global dynamics would be dominated by the active site dynamics and give an insight into the motions required for the onset of enzyme activity.

From these two studies, we can affirm that "dried" enzymes are not as rigid as previously thought. In addition, in most studies, the proteins were

probably not completely dried. In this work the last nine water molecules bound to lipase B (see Chapter II) could not be removed, and from the MD simulations, it has been observed that the first water molecules added induced major changes in the active site, allowing activity at very low water content.

CHAPTER VI: PROTEIN-PROTEIN INTERACTIONS

1. *Introduction*

Many cell functions involve protein-protein interactions. For instance, depending on the association of a type of cyclin with a cyclin dependent kinase (CDK), a different phase of the cell cycle will be induced. This is only one example of the relevance of the formation or of the breaking of these protein-protein interactions in life. Dynamical studies of proteins have shown the existence of a variety of vibrational motions ranging from high frequency ($\approx 10^{-15}$s) localized oscillations to low-frequency ($\approx 10^{-10}$s) collective modes.

The investigation of low frequency modes has shed light on the presence of the 'Boson peak', which is a broad peak found in the low-frequency region of inelastic neutron and Raman scattering spectra in many glassy materials, including biopolymers at cryogenic temperatures below 200 K. The boson peak is characterized by an excess of spectral density of states as compared to the Debye-frequency law. Joti *et al*. (2005) tried to clarify the origin of the Boson peak, using MD simulations. With the hen egg-white lysozyme as a model and the atomic force field AMBER, they carried out five different simulations and calculated the incoherent dynamic structure factors. They were able to observe the Boson peak only in the case of the simulation in the presence of water. They also correlated the frequency range of the boson peak with one where the diffusive motions are found at room temperature. They hypothesized that the Boson peak originates from the existence of different energy levels. Recently, low frequency modes in proteins were investigated *via* molecular dynamic simulations and normal mode analysis of myoglobin crystals in order to characterise intra and inter-protein vibrations at 150 K (Kurkal-Siebert and Smith, 2006). These studies indicate that the 'Boson peak' originates from $\sim 10^2$ collective harmonic vibrations. Other strong peaks were also found in that region and attributed to harmonic vibrations of proteins relative to each other (Figure VI-1), since in a simulation system containing only one protein the 1 meV peak is absent. Various

other analyses also gave evidence that this peak was a protein-protein intermolecular interaction peak. Experimental demonstration of this peak became an interesting technological challenge.

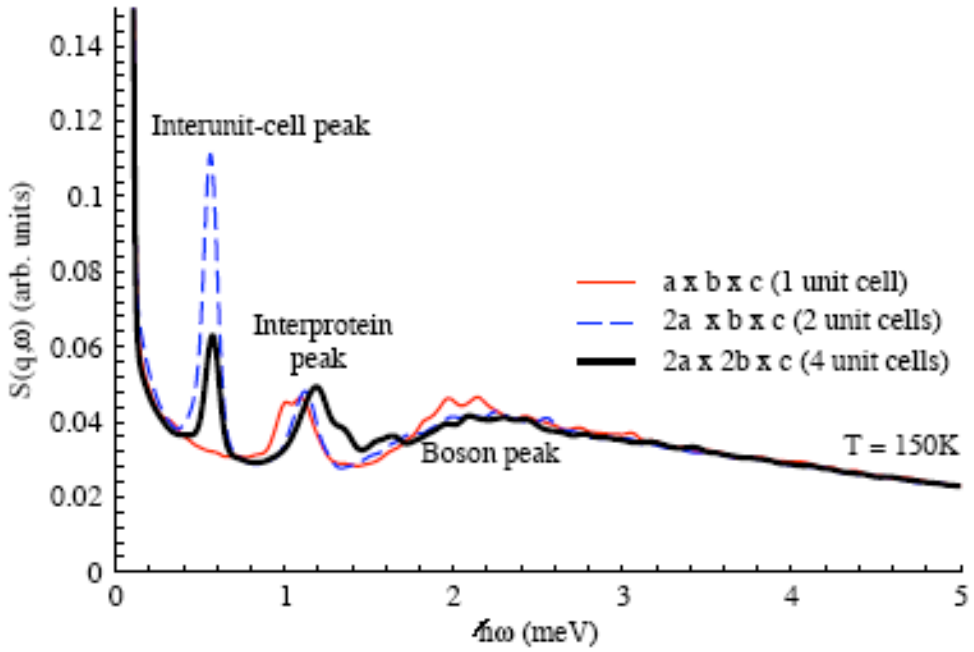

Figure VI-1: Protein-protein intermolecular interaction peak observed at the very low-frequency region of the neutron scattering spectrum calculated from the molecular dynamics simulations.

More recently, the hydration dependence of the dynamical transition in protein-protein interaction has been investigated. MD simulations were performed on low and fully hydrated carboxy-myoglobin crystals. The fully hydrated model presents a dynamical transition above 240 K due to intermolecular fluctuations, which is not present in low hydration models. This transition has also shown to be dominated by the activation of diffusive intermolecular motion (Kurkal-Siebert *et al.*, 2008).

Pig liver esterase (PLE) is found to be active at hydrations as low as 3% (Lind *et al.*, 2004) and the earlier neutron scattering experiments to investigate the correlation between the activity and dynamics of the enzyme powder showed quasi-elastic intensity at all temperatures ranging from 120 K-300 K at all hydrations corresponding to 0%, 3%, 12% and 50% hydrations (Kurkal *et al.*, 2005 ; Kurkal-Siebert *et al.*, 2006).

Having these data sets, the aim became to perform time of flight (tof) neutron scattering experiments of crystals of PLE or lipase B (or some other

protein if this was not possible) to probe the presence of the protein-protein intermolecular interaction peak in the very low-frequency region of the inelastic spectra, to investigate the temperature dependence of the protein-protein intermolecular interaction peak, and to compare the dynamics of disordered (powder) and ordered (crystal) systems.

The first experimental challenge was to produce a large amount of crystalline protein in a deuterated environment. Liu and Sano (1998) have shown for instance how in D_2O the initial aggregation rate of lysozyme is higher than in H_2O. Myoglobin was the first protein ever crystallised (Kendrew, 1950). Since myoglobin is cheap and well characterised, it was chosen as a model protein, with the intention of extending the investigation to PLE and/or Lipase B. PLE has never been crystallised before, however, one step of its purification implies an ammonium sulphate precipitation (Horgan *et al.,* 1966). Lipase B has been crystallised for structure analysis (Grochulski *et al.,* 1994b ; Grochulski *et al.,* 1993 ; Grochulski *et al.,* 1994) but also in large-scale production (Lee *et al.,* 2000).

2. *Materials and Methods*

2.1. Materials

Pig liver esterase (E3019, Sigma) was partially purified as described in Chapter III.2.2.1.2.

Myoglobin (M1882, ≥ 90%, salt free, Sigma) was used without further purification or treatment.

D_2O (99.9 atom %, Aldrich) was used for protein and salt H exchanges.

The crystallisation kits were borrowed from Auckland University.

Deuterated Na-acetate (Cambridge Isotope Laboratories)

2.2. Methods

2.2.1. Protein crystallization

Good introductory concepts on protein crystallisation are related in the book 'Preparation and Analysis of Protein Crystals' (McPherson, 1989).

2.2.1.1 Myoglobin crystallization

A large amount of crystals might be produced using a bulk or a batch method. The bulk crystallisation involves addition of solid salt to a purified protein until the solution develops a barely visible opalescence. The solution is centrifuged and set aside for a few days or weeks. The batch method consists of mixing in small vials the protein solution with a solution containing the precipitating salt at a concentration slightly lower than the one at which the protein will precipitate.

For the first trial analysed at FRM II, 500 mg of myoglobin were D_2O exchanged and dissolved in 50 mL of deuterated sodium acetate (0.1 M). The precipitating reagent used was ammonium sulphate. The hydrogen atoms in the ammonium sulphate were exchanged against deuterium through rotary-evaporation. About 33 g of solid ammonium sulphate were added slowly and mixed to the protein solution until the solution became opalescent. The solution was then set-aside over night in a sealed bottle at room temperature.

For the second trial, the exchangeable protons of myoglobin were not exchanged against deuterium to form larger crystals, as it had been reported that crystals would not grow at deuterium concentrations over 95%. Deuterium affects the protein solubility (Legrand *et al.*, 2001 ; Liu and Sano, 1998). In addition, in many neutron diffraction studies crystals were produced in hydrogenated conditions and soaked into D_2O. In the aim to slightly decrease the percentage of purity of the deuterium oxide and get larger crystals, the exchangeable protons were not exchanged. Thus, myoglobin crystals were formed initially with interactions involving mainly hydrogen atoms, and then the exchangeable protons were slowly exchanged against deuterium. A batch method was used to minimise the amount of salt added to the protein solution and prevent protein precipitation.

It was found that the addition of 75% of a saturated solution of ammonium sulphate was enough to get myoglobin crystals.

2.2.1.2 Pig liver esterase and lipase B crystallization trials

Pig liver esterase (PLE) has never been crystallised. However, purification processes often include an ammonium sulphate precipitation step (Horgan *et al*., 1966). In addition, for the neutron experiment, the crystals have to be grown in deuterium oxide, thus it was decided that for this crystallisation attempt no organic precipitant (which would include non-exchangeable protons) would be used.

The crystallisation method used for the initial screen of conditions was drop evaporation. A 2 μL drop composed of 1 μL of protein solution and 1 μL of the precipitant solution was equilibrated through the vapour phase against 100 μL of the same precipitant solution. Some kits of precipitant solution are available commercially; four of these were used (see the legend of the table VI.1).

The Table below represents the 96 wells of the plate. Each well was designated by a letter (A-H) corresponding to its position within the lines and a number (1-12) corresponding to its position within the columns. The numbers inside the wells corresponded to a specific precipitating solution composition of a specific screen. As different screens were used, different fonts were used to distinguish them.

Table VI-1: Crystallisation conditions solutions investigated for each wells. The wells 'coordinates' are highlighted in grey. The number inside the wells corresponds to a specific condition borrowed from a specific screen (see Tables VI-2 to VI-6).

	1	2	3	4	5	6	7	8	9	10	11	12
A	**1**	**9**	**17**	1	9	17	**3**	**48**	36	**7**	**15**	**23**
B	**2**	**10**	**18**	2	10	18	**7**	9	41	**8**	**16**	**24**
C	**3**	**11**	**19**	3	11	19	**11**	15	**1**	**9**	**17**	**25**
D	**4**	**12**	**20**	4	12	20	**16**	21	**2**	**10**	**18**	**26**
E	**5**	**13**	**21**	5	13	21	**33**	25	**3**	**11**	**19**	**27**
F	**6**	**14**	**22**	6	14	22	**34**	32	**4**	**12**	**20**	**28**
G	**7**	**15**	**23**	7	15	23	**38**	33	**5**	**13**	**21**	**29**
H	**8**	**16**	**24**	8	16	24	**44**	34	**6**	**14**	**22**	**30**

AMMONIUM SULPHATE SCREEN (A1-H3)

Na/K Phosphate screen (A4-H6):

Crystal Screen I (wells A7-A8)

Crystal Screen II (wells B8-B9)

Murielle's screen (wells C9-H12)

The wells A1 to H3 are filled with the precipitating solutions described below by the Table VI-2 corresponding to the ammonium sulphate screen. Different salt and pH conditions are tested. For each condition tested, a number is attributed and reported in this table. The number of the solution used is then reported into the wells of the plate above.

Table VI-2: Ammonium sulphate screen: ammonium sulphate concentration in mol/L (M) and different pH investigated.

	pH	***4***	***5***	***6***	***7***	***8***	***9***
Ammonium sulphate (M)	0.8	19	20	21	22	23	24
	1.6	13	14	15	16	17	18
	2.4	7	8	9	10	11	12
	3.2	1	2	3	4	5	6

Then, from the well A4 to H5, the Na/K phosphate screen was used. The screening conditions are described below in Table VI-3.

Table VI-3: Na/K phosphate screen: Na/K phosphate concentration in mol/L (M) and different pH investigated.

	pH	***5***	***5.6***	***6.2***	***6.8***	***7.4***	***8***
Na/K phosphate (M)	0.8	1	2	3	4	5	6
	1.2	7	8	9	10	11	12
	1.6	13	14	15	16	17	18
	2	19	20	21	22	23	24

Screen kits more complex are also available commercially such as crystal screen™ and crystal screen II™ . Only a few solutions were picked up from these screens, their composition as well as the tube number given by the supplier are reported in Tables VI-4 and VI-5 for crystal screen™ and crystal screen II™ , respectively. The first screen solutions were used to fill the wells from A6 to A8 and the second one for the wells from B8 to B9.

Table VI-4: Description of the solutions kit used from crystal screen™ as described by the supplier.

Solution composition		***Salt***	***Buffer***	***Precipitant***
Tube number	**3**	0	0	0.4 M ammonium dihydrogen phosphate
	7	0	0.1 M Na cacodylate pH 6.5	1.4 M Na acetate trihydrate
	11	0	0.1 M tri-sodium citrate dihydrate pH 5.6	1 M ammonium dihydrogen phosphate
	16	0	0.1 M Hepes-Na pH 7.5	1.5 M tri-lithium sulphate monohydrate
	33	0	0	4 M sodium formate
	34	0	0.1 M Na-acetate trihydrate pH 4.6	2 M sodium formate
	36	0	0.1 M Tris-HCl pH 8.5	8% (W/V) PEG 800
	38	0	0.1 M HEPES-Na pH 7.5	1.4 M tri-sodium citrate dihydrate
	44	0	0	0.2 M magnesium formate
	48	0	0.1 M Tris-HCl pH8.5	

Table VI-5: Description of the solutions kit used from crystal screen II™ as described by the supplier.

Solution composition		**Salt**	**Buffer**	**Precipitant**
Tube number	**9**	0	0.1 M Na-Ac trihydrate pH 4.8	2 M NaCl
	15	0.5 M NH_4SO_4		1.4 M Na acetate trihydrate
	21	0.1 M NaH_2PO_4 0.1 M KH_2PO_4	0.1 M MES pH 6.5	2 M NaCl
	25	0.01 M $CoClH_6$	0.1 M MES pH 6.5	1.8 M NH_4SO_4
	28	0	0	1.6 M Tri-sodium citrate dihydrate pH 6.5
	32	0.1 M NaCl	0.1 M HEPES pH 7.5	1.6 M NH_4SO_4
	33	0	0.1 M HEPES pH 7.5	1.6 M ammonium formate
	34	0.05 M Cadmium sulphate hydrate	0.1 M HEPES pH 7.5	1 M sodium acetate trihydrate
	36	0	0.1 M HEPES pH 7.5	4.3 M NaCl
	41	0.01 Nickel (II) hexhydrate	0.1 M Tris pH8.5	1 M lithium sulfate monohydrate

And finally, a screen of my composition was used to fill the last wells. Three different salts were used: calcium chloride ($CaCl_2$), magnesium sulphate ($MgSO_4$) and ammonium acetate (NH_4Ac). For each salt, two different pH and five different concentrations were tested as described in Table VI-6.

Table VI-6: Content of the precipitating solutions of Murielle's screen.

	$CaCl_2$ concentration (M)	***0.5***	***1***	***1.5***	***2***	***2.5***
pH	6	1	2	3	4	5
	8	6	7	8	9	10
	$MgSO_4$ concentration (M)	***0.5***	***1***	***1.5***	***2***	***2.5***
pH	6	11	12	13	14	15
	8	16	17	18	19	20
	NH_4OAc concentration (M)	***1***	***1.5***	***2***	***2.5***	***3***
pH	4.5	21	22	23	24	25
	8	26	27	28	29	30

The plate was sealed with a plastic film that isolated each well from the others.

Dialysis was also used to crystallise PLE. The PLE (25 mg/mL) was dissolved in HEPES (0.1 M pH 7.5) and placed inside a dialysis button of 50 μL. The button was sealed with a dialysis membrane (molecular weight cut off of 6-8000 M) and placed in the precipitation solution. This solution was a mixture of 0.1 M Tris-HCl at pH 8.5 and 2 M ammonium di-hydrogen phosphate. The button was immersed into 2 mL of the precipitating solution inside a large 6-plate well. A coverslide was fixed onto the top of the well with vacuum grease to isolate the whole system and leave it to equilibrate.

2.3. Neutron scattering measurements

In order to perform these experiments, a week of beam time was initially requested comprising 24 hour runs for lowest temperature (120 K) and highest temperature (room temperature) corresponding to 2 days, as well as 6 hours for each temperature with a step of 10 K temperature ramp from 120 K - 300 K data collection and a day for vanadium and empty can runs. But this method had to be reviewed due to the beam time allocated. At FRMII, the crystals were run at 120 K for 8 hours. At ILL, 6 hours run were performed for each temperature with steps of 40 K temperature ramp from 80K to 290K.

Inelastic, quasi-elastic and elastic scattering analysis will be performed

and the data obtained will be complemented with temperature dependent molecular dynamics simulation study of the protein-protein intermolecular interactions.

2.3.1. FRMII

Only half a day was allocated to this project. An eight hour run was performed at 120 K on a time of flight spectrometer Tof-Tof (refer section V-1.2.3 for description).

2.3.2. ILL

Four days were allocated for this experiment. IN5 is a time of flight spectrometer with a neutron flux at 5 Å of 6.83E5 n/cm^2/s. The resolution is ~100 μeV. A ramp temperature was applied from 80 to 290 K per 40 K every 6 hours.

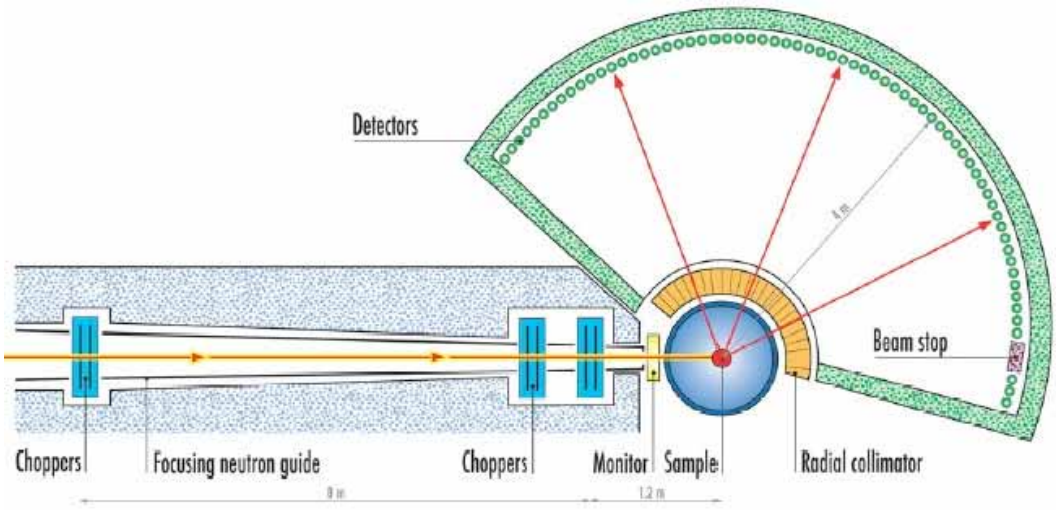

Figure VI-2:Schematic representation of the time of flight spectrometer IN5 from ILL (Grenoble, France)

3. *Results*

3.1. Protein crystallization

The aim of this project was to produce protein crystals for use in neutron scattering experiments. This was an experimental challenge, as PLE had not been crystallised before, and in any case the further use of the crystals for neutron

scattering investigations implied some constraints. In this project we were trying to reproduce experimentally conditions that have been investigated with molecular dynamic simulations, and to adapt them for a demanding neutron scattering investigation. Primarily, the crystals had to be produced on a large scale. Between 100 and 300 mg of protein sample required for neutron scattering analysis. Secondly, the crystals had to be produced in deuterium oxide since we were interested in the protein-protein interaction motions and not those of the solvent; in H_2O the proton signal would mask the signal from the protein protons. The minimisation of a background signal, and of the cost of the sample, limits the choice of the precipitating reagents that can be used; in particular, we needed to use precipitating agents that were relatively neutron transparent. Thirdly, it has been shown that a fully deuterated environment induces the disruption of protein crystals and to sample handling difficulties. And finally, one of the main problems was the "fishing" of the crystals, i.e., the removal of the crystals from the precipitating solution; but it would take ages to fish 200 mg of crystals. In this work we tried to address these constraints.

3.1.1. Myoglobin crystallisation

The initial trial, where all the exchangeable protons were deuterated, led to the formation of two layers of liquid in the bottle. The supernatant was black while the rest of the solution was transparent. The supernatant was examined under a microscope with the x100 objective and revealed the presence of nice brownish microcrystals. The supernatant was loaded into the sample cell used for the neutron scattering investigation. The fact that the crystals were 'floating' might be explained by the fact that hydrogen bonds are more favoured in the presence of protons than deuterons. The supernatant was loaded into a flat sample cell of 3 mm thickness.

The second trial, to produce non-deuterated crystals of myoglobin, was carried out under the supervision of the Prof. Schlichting from the Max Plank Institute of Heidelberg. The non-deuteration of the exchangeable protons of the protein led to the formation of nice and visible myoglobin cystals. However, after a few days, the size of the crystals started to decrease and the crystals started to float on top of the solution. Most of the clear solution was eliminated. The

supernatant was quickly centrifuged but the crystals were still floating. The supernatant was loaded with a 1 mL micropipette (the tip was cut) into a cylindrical sample cell of 3 mm thickness and sealed.

3.1.2. Pig liver esterase (PLE) and lipase B crystallisation

The initial trials were carried out under non-deuterated conditions. These screens revealed some conditions that could be exploited as shown in Tables VI.7 and VI.7.

Table VI-7: Results from the initial crystallisation screen with PLE.

Well	***Precipitating conditions***	***Observations***
C7	0.1 M trisodium citrate dihydrate pH 5.6 1.0 M Ammonium dihydrogen phosphate	Small balls of either needles or crystalline precipitate
A8	0.1 M Tris-hydrochloride pH 8 2.0 M Ammonium dihydrogen phosphate	Small hexagonal crystals
B11	0.1 M phosphate buffer pH 8 0.5 M Magnesium sulphate	Crystalline precipitate and small crystals
A12	2.0 M Ammonium acetate pH 6	Very small crystals

Table VI-8: Results from the initial crystallisation screen with lipase B.

Well	***Precipitating conditions***	***Observations***
C3	0.8 M Ammonium sulphate pH 4	Crystalline precipitate
B7	0.1 M Sodium cacodylate pH 6.5 1.4 M Sodium acetate trihydrated	Crystalline precipitate
B11	0.2 M phosphate buffer pH 8 0.5 M Magnenium sulphate	Crystalline precipitate

None of the conditions investigated seemed to give good results except maybe for the well A8 and PLE. Ideally, for both enzymes the crystalline precipitate should have been examined by powder diffraction to confirm these

results. Conditions inside well B11 seem to have a similar effect on both enzymes, and this result could form the basis of further experiments.

From our best conditions, a scaling up experiment was set up in a dialysis button but the project stopped here since none of the neutron scattering raw data, performed on myoglobin crystals, had been treated, and this was felt to be an essential prerequisite for further work.

3.2. Neutron Scattering

3.2.1. Tof-tof

A raw analysis of the data has been done for the first batch of myoglobin crystals, and did not show any signs of the 1 meV peak. However, the boson peak seems to have moved to higher energy (around 6 meV instead of 3). In fact, inelastic scattering of zeolite crystals gives also a boson peak at 6 meV. This shift might arise from the high salt concentration or the crystal. Thus, it might be hypothesised that 'the 1 meV peak has also shifted to a higher energy level. This hypothesis is supported by recent comparison of low-frequency modes of crystalline and amorphous zeolites. In these studies, the shift of the boson peak is explained by the assimilation of the crystal to a porous system (Greaves *et al.*, 2005). The data analysis is taking longer for our collaborators as it was our first visit at FRM-II and some programmes have to be written to be able to treat them.

3.2.2. IN 5

A raw analysis of the data has been done for the second batch of myoglobin crystals prepared, and did not show any signs of the 1 meV peak either. The density of state confirms the presence of crystals. In addition, the crystals were still swimming inside a lot of precipitating solution. A subtraction of the 'solvent' might give the expected results. A shift of the Boson peak was also observed for the energy range of 3 meV to 6 meV.

4. *Conclusions*

Preliminary results from tof-tof and IN5 showed no evidence for the proposed protein-protein interaction peak. Although its presence cannot be ruled out, for this reason, and because of the difficulties summarised above in obtaining good experimental samples, at this point the experiment moved down the priority list of the research groups, and it has not yet been possible to allocate resources and neutron beam time to complete this work up to the point where this thesis was completed.

However, these results are quite interesting. In fact, Nakagawa *et al.,* (2008) also recently observed a shift of the boson peak to higher energy upon hydration. They concluded that was consistent with a hardening of protein dynamics due to hydrogen bond formation on the protein surface. In addition, water molecules interact strongly with the protein in crystals. The proteins as well as water molecules are constraints. Thus, if the peak observed at 6 meV is the boson peak, it is more reasonable to think that the 1 meV peak might be found around 3 meV.

CHAPTER VII: DISCUSSION

This thesis has had as its objective the determination of whether enzymes require hydration for function, and if so, what level of hydration, and what molecular dynamics might be involved in any linkage of hydration and activity.

Early in the work it became apparent that any hydration required for activity was low, and that to achieve the objectives it would be necessary to examine enzyme activity at very low hydration levels; to determine these low levels of hydration, development of existing water determination methods would be needed. The water quantification work has highlighted the difficulty of achieving a completely anhydrous protein. Despite the drastic drying methods used, the lowest level reached was about three water molecules per molecule of protein for PLE. Although Dolman *et al*. (1997), comparing several methods, found that the 'oxygen 18' method was reliable to ± 2 water molecules per molecule of protein, we cannot assume that complete dryness has been reached. This may indicate the potential existence of internal water molecules that cannot be removed by the methods we have used. Even though we have not been able to reach the objective of unequivocal zero hydration, i. e. 'true' zero water molecule per molecule of enzyme, we have been able to define a pseudo zero hydration level for PLE, i.e., three water molecules plus or minus two water molecules, per molecule of enzyme.

The gas/solid bioreactor presents many advantages to study the effect of hydration on enzyme activity. Firstly, the absence of liquid organic solvent prevents the protein from undergoing denaturation even with water-soluble solvents. Even though the addition of excipient, salt or buffer improves the gas phase activity, it is not essential for activity. Thus, it is possible to isolate the effect of hydration on activity, although the substrates and the products of the reaction still have their own effect that must be accounted for. Secondly, headspace analysis can be very sensitive depending on the column or technique used. In this study, a packed column was used while a capillary column, for instance, although much slower, would have been more sensitive. In spite of this, we were able to detect relatively low amounts of analytes. And finally, the

hydration level can be easily controlled in the solid/gas bioreactor, which is not the case in more elaborate systems. The studies of the effect of hydration on enzyme activity have revealed an increase of the alcoholysis reaction with the hydration level. A closer look at this reaction has shown that the first step of the alcoholysis reaction, which is the formation of the acyl-enzyme intermediate and release of the alcohol product, is hydration dependent while the second one, which corresponds to the transfer of the acyl group to the alcohol, is not. The acyl-enzyme formation is the limiting step (Stoops *et al.,* 1969). These results are in disagreement with those of Bousquet-Dubouch *et al.,* (2001), where water was found to be a competitive inhibitor of the alcohol substrate of the lipase-catalysed alcoholysis reaction. This difference might arise from the protein itself. However, the main difference is that they were measuring the water activity of the gas going through the bioreactor and not the protein hydration. Thus, in this work we are investigating a lower hydration than they did, and it can be envisaged, as our work indicates, that enzymes are able to maintain a basal level of activity even at zero hydration. At a certain hydration level, this activity will be hydration dependent. The second step of the alcoholysis reaction being also dependent of the amount of methanol, a delay might be observed for the hydration dependency of the second step. Although the methanol is able to auto-promote its production, its association with water has a marked effect on the increase of the hydrolysis steps (Greenzaid and Jenks, 1971).

The dynamics investigation revealed that slower motions, on a nano-second timescale, are activated at a lower temperature than the motions observed at a pico-second time scale. Previous experiments highlighted the hydration dependence of the temperature at which the dynamical transition occurred. Present results show that the dynamic behaviour of 'the dry sample' deviates slightly from linearity. This deviation occurs around 295 K. In addition it is known that dehydrated enzymes have increased stability. The dynamics of the dry samples studied in Munich were investigated up to 400 K but the results are not analysed yet. It is quite likely that dried samples show a dynamical transition corresponding to slower motions only at higher temperatures.

Molecular Dynamic simulations on the active site of lipase B have revealed a huge variability of the MSD as a function of the hydration below 0.1 h. The MSD is shown to be sometimes higher than the fully hydrated control. This

variability seems to be in agreement with the experimental data (especially for the rate of propyl butyrate production). An explanation of this variability is that below 0.05 h, the water molecules condense onto the ionic groups of the protein surface. It is a strong interaction, which might lead to major conformational changes. And as the whole system is rigid, these induced motions might be relatively slow. Thus, these same motions could be those investigated on a nano-second time scale. But then how could we explain a basic level of activity? In the case of our enzymes, the presence of the substrate would be enough to cross the energy barrier of another substate probably at the limit with the active state.

This work shows clear evidence that enzyme activity is not necessarily dependent upon hydration (although hydration greatly enhances activity) since, within the limits of the water detection method, activity at zero hydration or very close to it has been achieved. Which is quite a far-reaching result – it implies for example that the main role of water in enzymology (and life?) may be as a solvent and a diffusion medium rather than as an essential or unique structural component. These results show clearly that it is not needed for any surface coverage, but is it need as "structural/internal" water? Indeed the error on the water quantification might be lower than the error calculated by Dolman *et al.*, (1997). The result has been made possible by a careful choice of enzyme, the reaction to be studied, and the experimental system – together with improvements in the measurement of enzyme hydration at very low hydration levels.

Earlier conclusions that activity required about 20% hydration can now be seen as arising mostly from the use of experimental systems which were inevitably diffusion limited (although expressing hydration by mass rather than in a way related to surface coverage (for example) further hindered interpretation).

BIBLIOGRAPHY

Acker, L. (1962). Enzymic Reactions in Foods of Low moisture Content. Advances in Food Research: 263-330.

*Adler, A.J. and G.B. Kistiakowsky (1961). Isolation and Properties of Pig Liver Esterase. Journal of Biological Chemistry **236**(12): 3240-5.*

*Affleck, R., C.A. Haynes and D.S. Clark (1992). Solvent dielectric effects on protein dynamics. The Proceedings of the National Academy of Sciences of the United States of America **89**(11): 5167-70.*

*Affleck, R., Z.F. Xu, V. Suzawa, K. Focht, D.S. Clark and J.S. Dordick (1992). Enzymatic catalysis and dynamics in low-water environments. Proceedings of the National Academy of Sciences of the United State of America **89**(3): 1100-4.*

AQUASTAR Tech Notes Karl Fisher Titration Basics. EMD Chemicals.

*Baker, E.N. and R.E. Hubbard (1984). Hydrogen bonding in globular proteins. Progress in Biophysics and Molecular Biology. **44**(2): 97-179.*

*Barker, D.L. and W.P. Jencks (1969). Pig liver esterase. Some kinetic properties of Pig liver esterase. Physical properties. Biochemistry **8**(10): 3890-7.*

*Barzana, E., A.M. Klibanov and M. Karel (1987). Enzyme-catalyzed, gas-phase reactions. Applied Biochemistry and Biotechnology **15**(1): 25-34.*

*Becker, T., J.A. Hayward, J.L. Finney, R.M. Daniel and J.C. Smith (2004). Neutron frequency windows and the protein dynamical transition. Biophysical Journal. **87**(3): 1436-44.*

*Bée, M. (1992). A physical insight into the elasic incoherent structure factor. Physica B **182**(4): 323-36.*

*Bell, L.N., M.J. Hageman, J.M. Bauer (1995). Impact of moisture on thermally induced denaturation and decomposition of lyophilized bovine somatotropin. Biopolymers **35**(2): 201-9*

*Belton, P.S. and A.M. Gil (1994). IR and Raman spectroscopic studies of the interaction of trehalose with hen egg white lysozyme. Biopolymers **34**(7): 957-61.*

*Bencharit, S., C.C. Edwards, C.L. Morton, E.L. Howard-Williams, P. Kuhn, P.M. Potter and M.R. Redinbo (2006). Multisites Promiscuity in the Processong of Endogenous Substrates by Human Carboxul esterase 1. Journal of Molecular Biology **363**(1): 201-14.*

*Benjamin, S. and A. Pandey (1998). Candida rugosa lipases: molecular biology and versatility in biotechnology. Yeast **14**(12): 1069-87.*

*Berlin, E., P.G. Kliman and M.J. Pallansch (1970). Changes in State of Water in Proteinaceous Systems. Journal of Colloid and Interface science **34**(4): 488-94.*

*Bernard R. Brooks, R.E.B., Barry D. Olafson, David J. States, S. Swaminathan, Martin Karplus, (1983). CHARMM: A program for macromolecular energy, minimization, and dynamics calculations. Journal of Computational Chemistry **4**(2): 187-217.*

*Bernini, A., O. Spiga, A. Ciutti, S. Chiellini, N. Menciassi, V. Venditti and N. Niccolai (2004). On the dynamics of water molecules at the protein solute interfaces. Homeopathy **93**(4): 199-202.*

*Bon, C., A.J. Dianoux, M. Ferrand and M.S. Lehmann (2002). A Model for Water Motion in Crystals of Lysozyme Based on an Incoherent Quasielastic Neutron-Scattering Study. Biophysical Journal **83**(3): 1578-88.*

*Bousquet-Dubouch, M.-P., M. Graber, N. Sousa, S. Lamare and M.-D. Legoy (2001). Alcoholysis catalyzed by Candida antarctica lipase B in a gas/solid system obeys a Ping Pong Bi Bi mechanism with competitive inhibition by the alcohol substrate and water. Biochimica et Biophysica Acta (BBA) - Protein Structure and Molecular Enzymology **1550**(1): 90 - 9.*

*Braco, L., K. Dabulis and A.M. Klibanov (1990). Production of abiotic receptors by molecular imprinting of proteins. Proceedings of the Natural Academy of Science of the United States of America **87**(1): 274-7.*

*Brocca, S., F. Secundo, M. Ossola, L. Alberghina, G. Carrea and M. Lotti (2003). Sequence of the lid affects activity and specificity of Candida rugosa lipase isoenzymes. Protein Science **12**(10): 2312-9.*

*Brooks, B.R., R.E. Bruccoleri, B.D. Olafson, S. D.J., S. Swaminathan and M. Karplus (1983). CHARMM: A Program for Macomolecular Energy, Minimization, and Dynamics Calculations. Journal of computational chemistry **4**(2): 187-217.*

*Bull, H.B. (1944). Adsorption of Water Vapor by Proteins. Journal of the American Chemical Society **66**(9): 1499-507.*

*Bull, H.B. and K. Breese (1968). Protein hydration. I. Binding sites. Archives of Biochemistry and Biophysics **128**(2): 488-96.*

*Careri, G., E. Gratton, P.-H. Yang and J.A. Rupley (1980). Correlation of IR spectroscopic, heat capacity, diamagnetic suceptibility and enzymatic measurments on lysozyme powder. Nature **284**(5756): 572-3.*

*Careri, G. and M. Peyrard (2001). Physical Aspects of the Weakly Hydrated Protein Surface. Cellular and Molecular Biology **47**(5): 745-56.*

*Carpenter, J.F. and J.H. Crowe (1989). An infrared spectroscopoic study of the interactions of carbohydrates with dried proteins. Biochemistry **28**(9): 3916-22.*

*Carpenter, J.F., M.J. Pikal, B.S. Chang and T.W. Randolph (1997). Rational design of stable lyophilised protein formulations: some pratical advice. Pharmaceutical research **14**(8): 969-75.*

*Castillo, B., V. Bansal, A. Ganesan, P.J. Halling, F. Secundo, A. Ferrer, K. Griebenow and G. Barletta (2006). On the activity loss of hydrolases in organic solvents: II. a mechanistic study of subtilisin Carlsberg. BMC Biotechnology **6**: 51-64.*

*Chothia, C. (1974). Hydrophobic bonding and accessible surface area in proteins. Nature **248**(1446): 338-9.*

*Chothia, C. (1975). Structural invariants in protein folding. Nature **254**(5498): 304-8.*

*Cooke, R. and I.D. Kuntz (1974). The properties of water in biological systems. Annual Reviews **3**(0): 95-126.*

*Craig, H. (1961). Isotopic Variations in Meteoric Waters. Science **133**(3465): 1702-3.*

*Daniel, R.M., R.V. Dunn, J.L. Finney and J.C. Smith (2003). The Role of Dynamics in Enzyme Activity. Annual Reviews of Biophysical and Biomolecular Structure **32**: 69-92.*

Daniel, R.M., J.L. Finney, V. Reat, R. Dunn, M. Ferrand and J.C. Smith (1999). Enzyme dynamics and activity: Time-scale dependence of dynamical transitions in glutamate dehydrogenase solution. Biophysical Journal 77(4): 2184-90.

*Daniel, R.M., J.L. Finney and J.C. Smith (2003). The dynamic transition in proteins may have a simple explanation. Faraday Discussion **122**: 163-9.*

*Daniel, R.M., J.C. Smith, M. Ferrand, S. Hery, R.V. Dunn and J.L. Finney (1998). Enzyme activity below the dynamical transition at 220 K. Biophysical Journal **75**(5): 2504-7.*

*de la Casa, R.M., J.M. Sánchez-Montero, R. Rojas and J.V. Sinisterra (1998). Simple determination of the water content in lyophilized isoenzymes of Candida rugosa lipase. Biotechnology Techniques **12**(11): 823-7.*

*de la Casa, R.M., J.V. Sinisterra and J.M. Sanchez-Montero (2006). Characterization and catalytic properties of a new crude lipase from C. rugosa. Enzyme and Microbial Technology **38**(5): 599-609.*

*Dellerue, S., A.J. Petrescu, J.C. Smith and M.C. Bellissent-Funel (2001). Radially softening diffusive motions in a globular protein. Biophysical Journal **81**(3): 1666-76.*

*Demmel, F., W. Doster, W. Petry and A. Schulte (1997). Vibrational frequency shifts as a probe of hydrogen bonds: thermal expansion ans glass transition of myoglobin in mixed solvents. European Biophysical Journal **26**(4): 327-35.*

*Denisov, V.P. and B. Halle (1995). Protein Hydration Dynamics in aqueous Solution: A Comparison of Bovine Pancreatic Trypsin Inhibitor and Ubiquitin by Oxygen-17 Spin Relaxation Dispersion. Journal of Molecular Biology **245**(5): 682-97.*

*Denisov, V.P., B. Halle, J. Peters and H.D. Horlein (1995). Residence Times of the Buried Water Molecules in Bovin Pancreatic Trypsin Inhibitor and Its G36S Mutant. Biochemistry **34**(28): 9046-51.*

*Dolman, M., P.J. Halling, B.D. Moore and S. Waldron (1997). How dry are anhydrous enzymes? Measurement of residual and buried ^{18}O-labeled water molecules using mass spectrometry. Biopolymers **41**(3): 313-21.*

*Dominguez de Maria, P., J.M. Sanchez-Montero, J.V. Sinisterra and A.R. Alcantara (2005). Understanding Candida rugosa lipases: An overview. Biotechnology Advances **24**(2):180-96*

*Doster, W., S. Cusack and W. Petry (1989). Dynamical transition of myoglobin revealed by inelastic neutron scattering. Nature **337**(6209): 754-6.*

*Doster, W. and M. Settles (2005). Protein-water displacement distribution. Biochimica et Biophysica Acta **1749** (2): 173-86.*

*Doster, W. (2008). The dynamical transition of proteins, concepts and misconceptions. European Biophysical Journal **37**(5):591-602*

*Drapon, R. (1985). Enzyme activity as a function of water activity. Properties of water in food. S. D. a. M. J.L., Martinus Nijhoff**:** 171-90.*

*Dravis, B.C., K.E. LeJeune, A.D. Hetro and A.J. Russell (2000). Enzymatic dehalogenation of gas phase substrates with haloalkane dehalogenase. Biotechnology and Bioengineering **69**(3): 235-41.*

*Dudman, N.P.B. and B. Zerner (1975). Carboxyl esterases from Pig and Ox Liver. Methods in Enzymology. J. M. Lowenstein, Academic Press. **XXXV**.*

*Dunn, R.V. and R.M. Daniel (2004). The use of gas-phase substrates to study enzyme catalysis at low hydration. Philosophical Transactions of the Royal Society of London Series B-Biological Sciences **359**(1448): 1309-20.*

*Eisenberg, H. (1990). Thermodynamics and the structure of biological macromolecules. European Journal of Biochemistry **187**(1): 7-22.*

Eisenberg, H. and W. Kauzmann (1969). Properties of Liquid Water. The structure and Properties of Water. Oxford.

*Epstein, S. and T. Mayeda (1953). Variations of O^{18} content of waters from natural sources. Geochimica et Cosmochimica Acta **4**(5): 213-24.*

*Erable, B., I. Goubet, S. Lamare, M.-D. Legoy and T. Maugard (2004). Haloalkan hydrolysis by Rhodococcus erythropolis cells: Comparison of conventional aqueous phase dehaloganation and nonconventional gas phase dehaloganation. Biotechnology and Bioengineering **86**(1): 47-54.*

*Falconer, J.S. (1946). The initial stages in the purification of pig liver esterase. The Biochemical Journal **40**(5-6): 831-4.*

Fanchon, E., E. Geissler, J.-L. Hodeau, J.-R. Regnard and P.A. Timmins (2000). Structure and dynamics of biomolecules: neutron and synchrotron radiation for condensed matter studies. New York, Oxford University Press Inc.

*Farb, D. and W.P. Jencks (1980). Different forms of pig liver esterase. Archives in Biochemistry and Biophysics **203**(1): 214-26.*

*Ferrand, M., A.J. Dianoux, W. Petry and G. Zaccai (1993). Thermal Motions and Function of Bacteriorhodopsin in Purple Membranes - Effects of Temperature and Hydration Studied by Neutron-Scattering. Proceedings of the National Academy of Sciences of the United States of America **90**(20): 9668-72.*

*Ferrand, M., W. Petry, A.J. Dianoux and G. Zaccai (1993). Dynamical Transition of Bacteriorhodopsin in Purple Membranes Revealed by Neutron-Scattering - a Relation between Structure, Dynamics and Function. Physica A **201**(1-3): 425-9.*

*Ferrand, M., G. Zaccai, M. Nina, J.C. Smith, C. Etchebest and B. Roux (1993). Structure and Dynamics of Bacteriorhodopsin - Comparison of Simulation and Experiment. Febs Letters **327**(3): 256-60.*

*Finney, J.L. (1975). Volume Occupation, Environment and Accessibility in Proteins. The Problem of the Protein Surface. Journal of Molecular Biology **96**(4): 721-32.*

*Finney, J.L. (1978). Volume Occupation, Environment, and Accessibility in Proteins. Environment and Molecular area of RNase-S. Journal of Molecular Biology **119**(3): 415-41.*

*Finney, J.L., B.J. Gellatly, I.C. Golton and J. Goodfellow (1980). Solvent effects and polar interactions in the structural stability and dynamics of globular protein. Biophysical Journal **32**(1): 17-30.*

*Fishman, A. and U. Cogan (2003). Bio-imprinting of lipases with fatty acids. Journal of molecular Catalysis B: Ezymatic **22**(3-4): 193-202.*

Fitter, J., T. Gutberlet and J. Katsaras (2006). Neutron Scattering in Biology: techniques and applications. Heidelberg, Springer Berlin Heidelberg New York.

Fontes, N., J. Partridge, P.J. Halling and S. Barreiros (2002). Zeolite Molecular sieves Have Dramatic Acid-Base Effects on Enzymes in Nonaqueous media. Biotechnology and Bioengineering 77(3): 296-305.

*Francks, F. (1993). Storage stabilisation of proteins. Protein Biotechnology. F. Francks, Humana Press Inc**:** 489-531.*

*Franks, F. (1993). Protein hydration. Protein Biotechnology: isolation, characterisation and stabilisation. F. Franks. Totowa, N.J.: Humana Press, inc. 1993**:** 437-65.*

*Fujita, Y. and Y. Noda (1981). Effect of hydration on the thermal stability of protein as measured by differential scanning calorimetry. International Journal of Peptides and Protein Research **18**(1):12-7*

*Gabel, F., D. Bicout, U. Lehnert, M. Tehei, M. Weik and G. Zaccai (2003). Protein dynamics studied by neutron scattering. Quarterly Reviews of Biophysics **35**(04): 327-67.*

*Gais, H.J., M. Jungen and V. Jadhav (2001). Activation of pig liver esterase in organic media with organic polymers. Application to the enantioselective acylation of racemic functionalized secondary alcohols. Journal of Organic Chemistry **66**(10): 3384-96.*

*Garcia-Alles, L.F. and V. Gotor (1998). Lipase-catalysed transesterification in organic media: solvent effects on equilibrium and individual rate constanta. Biotechnology and Bioengineering **59**(6): 684-94.*

*Gates, R.E. (1979). Shape and accessible surface area of globular proteins. Journal of Molecular Biology **127**(3): 345 - 51.*

*Gellatly, B.J. and J.L. Finney (1982). Calculation of Protein Volumes: an Alternative to the Voronoi Procedure. Journal of Molecular Biology **161**(2): 305-22.*

*Gentili, A., R. Curini, E. Cernia, G. D'Ascenzo.(1997) Thermal stability of Candida cylindracea lipase. Journal of Molecular Catalysis B: Enzymatic **3**(1-4):43-9*

*Gonzalez-Navarro, H. and L. Braco (1997). Improving lipase activity in solvent-free media by interfacial activation-based by molecular bioimprinting. Journal of Molecular Catalysis B: Ezymatic **3(**1-4): 111-9.*

*Gonzalez-Navarro, H. and L. Braco (1997). Improving lipase activity in solvent-free media by interfacial activation-based molecular imprinting. Journal of molecular Catalysis B: Ezymatic **3**: 111-9.*

*Gorman, L.A. and J.S. Dordick (1992). Organic solvents strip water off enzymes. Biotechnology Bioengineering **39**(4): 392-7.*

*Graber, M., M.-P. Bousquet-Dubouch, S. Lamare and M.-D. Legoy (2003). Alcoholysis catalyzed by Candida antarctica lipase B in a gas/solid system: effects of water on kinetic parameters. Biochimica et Biophysica Acta (BBA) - Proteins & Proteomics **1648**(1-2): 24 - 32.*

*Graber, M., M.-P. Bousquet-Dubouch, N. Sousa, S. Lamare and M.-D. Legoy (2003). Water plays a different role on activation thermodynamic parameters of alcoholysis reaction catalyzed by lipase in gaseous and organic media. Biochimica et Biophysica Acta (BBA) - Proteins & Proteomics **1645**(1): 56-62.*

*Greaves, G.N., F. Meneau, D.G. Jones and J. Taylor (2005). Identifying vibritions that destabilize crystals and characterize the glassy state. Science **308**(1299): 1299-302.*

*Green, J.L. and C.A. Angell (1989). Phase relation and verification in saccharide-water solutions and the trehalose anomaly. The Journal of Physical Chemistry **93**(8): 2880-2.*

*Greenspan, L. (1977). Humidity fixed points of binary saturated aqueous solutions. Journal of Research of the National Bureau of Standards - A Physics and Chemistry **81 A**(1): 89-96.*

*Greenzaid, P. and W.P. Jencks (1971). Pig liver esterase. Reactions with alcohols, structure-reactivity correlations, and the acyl-enzyme intermediate. Biochemistry **10**(7): 1210-22.*

*Grochulski, P., F. Bouthillier, R.J. Kazlauskas, A.N. Serreqi, J.D. Schrag, E. Ziomek and M. Cygler (1994b). Analogs of reaction intermediates identify a unique substrate binding site in Candida rugosa lipase. Biochemistry **33**(12): 3494-500.*

*Grochulski, P., Y. Li, J.D. Schrag, F. Bouthillier, P. Smith, D. Harrison, B. Rubin and M. Cygler (1993). Insights into interfacial activation from an open structure of Candida rugosa lipase. Journal of Biological Chemistry. **268**(17): 12843-7.*

*Grochulski, P., Y. Li, J.D. Schrag and M. Cygler (1994). Two conformational states of Candida rugosa lipase. Protein Science **3**(1): 82-91.*

*Gronenborn, A. and M. Clore (1997). Water in and around proteins. The biochemist **19**: 18-21.*

*Guinn, R.M., P.S. Skerker, P. Kavanaugh and D.S. Clark (1991). Activity and flexibility of alcohol dehydrogenase in organic solvents. Biotechnology and Bioengineering **37**(4): 303-8.*

*Hacking, M.A.P.J., H. Akkus, F. van Rantwijk and R.A. Sheldon (1999). Lipases and esterases-catalysed acylation of hetero-substituted nitrogen nucleophiles in water and organic solvents. Biotechnology and Bioengineering **68**(1): 84-90.*

*Halling, P.J. (1990). High-affinity binding of water by proteins is similar in air and in organic solvents. Biochim Biophys Acta **1040(**2): 225-8.*

*Hammes-Schiffer, S. (2002). Impact of Enzyme Motion on Activity. Biochemistry **41**(45): 13335-43.*

*Hayward, J.A. and J.C. Smith (2002). Temperature Dependence of Protein Dynamics: Computer Simulation Analysis of Neutron Scattering Properties. Biophysical Journal **82**(3): 1216-25.*

*Henchman, R.H. and J.A. McCammon (2002). Structural and dynamics properties of water around acetyl chilinesterase. Protein Science **11**(9): 2080-90.*

*Henry, W.M., G. Nickless and F.H. Pollard (1967). The reaction of phosphorus pentoxide with water. Journal of inorganic nuclear chemistry **29**: 2479-80.*

*Heymann, E. and W. Junge (1979). Characterization of the isoenzymes of pig-liver esterase. 1. Chemical Studies. European Journal of Biochemistry **95**(3): 509-18.*

*Horgan, D.J., J.R. Dunstone, J.K. Stoops, E.C. Webb and B. Zerner (1969). Carboxylesterases (EC 3.1.1). The molecular weight and equivalent weight of pig liver carboxylesterase. Biochemistry **8**(5): 2006-13.*

*Horgan, D.J., J.K. Stoops, E.C. Webb and B. Zerner (1969). Carboxylesterases (EC 3.1.1). A large-scale purification of pig liver carboxylesterase. Biochemistry **8**(5): 2000-6.*

*Horgan, D.J., E.C. Webb and B. Zerner (1966). A large scale purification of cristalline pig liver carboxyesterase. Biochemical and Biophysical Research Communications **23**(1): 18-22.*

*Hutcheon, G., P.J. Halling and B.D. Moore (1994). Measurements and Control of Hydration in Nonaqueous Biocatalysis. Enzyme and Microbial Technology **16**(178): 465-72.*

*Isengard, H.-D. (2001). Water content, one of the most important properties of food. Food Control **12**(7): 395-400.*

*Jensen, R.G., F.A. deJong and R.M. Clark (1983). Determination of lipase specificity. Lipids **18**(3): 239-52.*

*Joti, Y., A. Kitao and N. Go (2005). Protein boson peak originated from hydration-related multiple minima energy landscape. Journal of the American Chemical Society **127**(24): 8705-9.*

*Kandori, H. (2000). Role of internal water molecules in bacteriorhodopsin. Biochimica et Biophysica Acta **1460**(1): 177-91.*

*Karplus, M. and G.A. Petsko (1990). Molecular dynamics simulations in biology. Nature **347**(6294): 631-9.*

*Kendrew, J.C. (1950). The crystal structure of Horse Met-myoglobin. I. general features: The arrangement of the polypeptide chains. Proceedings of the Royal society of London. Series A, Mathematical and Physical Sciences **201**(1064): 62-89.*

*Kim, J., D.S. Clark and J.S. Dordick (1999). Intrinsic effects of solvent polarity on enzymic activation energies. Biotechnology and Bioengineering **67**(1): 112-6.*

*Kim, S.Y., J.H. Sohn, Y.R. Pyun and E.S. Choi (2007). Variations in protein glycosylation in Hansenula polymorpha depending on cell culture stage. Journal of Microbial Biotechnology **17**(12): 1949-54.*

*Klibanov, A.M. (1989). Enzymatic catalysis in anhydrous organic solvents. Trends in Biochemical Sciences **14**(4): 141-4.*

*Klibanov, A.M. (2001). Improving enzymes by using them in organic solvents. Nature **409**(1): 241-6.*

*Kneller, G.R. and J.C. Smith (1994). Liquid-like side-chain dynamics in myoglobin. Journal of Molecular Biology **242**(3): 181-5.*

Kolb, B. and L.S. Ettre (1997). Static Headspace-Gas Chromatography: theory and practice. New York, John Wiley & Sons Inc.

*Kornblatt, J. and J. Kornblatt (1997). The role of water in recognition and catalysis by enzyme. The biochemist **19**: 14-7.*

*Kossiakoff, A.A. (1985). The Application of Neutron Crystallography to the Study of Dynamic and Hydration Properties of Proteins. Annual Reviews of Biochemistry **54**: 1195-227.*

Kostorz, G. and S.W. Lovesay (1979). Treatise on materials science and technology. New York, Academic Press.

*Krisch, K. (1966). Reaction of a microsomal esterase from hog-liver with diethyl rho nitro phenyl phosphate. Biochimica et Biophysica Acta **122**(2): 265-80.*

*Kudryavtsev, A.B., G. Christopher, C.D. Smith, S.B. Mirov, W.M. Rosenblum and L.j. DeLucas (2000). The effect of hydration of internal watwer in thaumatin and lysozyme crystals as revealed by Raman method. Journal of Crystal Growth **219**(1): 102-14.*

*Kuntz, I.D. and W. Kauzmann (1974). Hydration of proteins and polypeptides. Advances in protein chemistry. **28:** 239-345.*

*Kurkal, V., R.M. Daniel, J.L. Finney, M. Tehei, R.V. Dunn and J.C. Smith (2005). Enzyme activity and flexibility at very low hydration. Biophysical Journal **89**(2): 1282-7.*

*Kurkal-Siebert, V., R. agarwal and J.C. Smith (2008). Hydration-dependent dynamical transition in protein: Protein interactions at 240 K. Physical Review Letters **100**(13): 138102-4.*

*Kurkal-Siebert, V., R.M. Daniel, J.L. Finney, M. Tehei, R.V. Dunn and J.C. Smith (2006). Enzyme hydration, activity and flexibility: A neutron scattering approach. Journal of Non-Crystalline Solids **352**(42-49): 4387-93.*

*Kurkal-Siebert, V. and J.C. Smith (2006). Low-temperature protein dynamics: a simulation analysis of interprotein vibrations and the Boson peak at 150 K. Journal of the American Chemical Society **128**(7): 2356-64.*

*Lamare, S., B. Caillaud, K. Roule, I. Goubet and M.-D. Legoy (2001). Production of natural esters at the pre-industrial scale by solid/gas biocatalysis. Biocatalyst and biotransformation **19**(5-6): 361-77.*

*Lamare, S. and M.-D. Legoy (1993). Biocatalyst in the gas phase. Trends in Biotechology **11**(10): 413-8.*

*Lamare, S. and M.-D. Legoy (1995). Working at Controlled Water Activity in a Continuous Process: The Gas/Solid System as a Solution. Biotechnology and Bioengineering **45**(5): 387-97.*

*Lange, S., A. Musidlowska, C. Schmidt-Dannert, J. Schmitt and U.T. Bornscheuer (2001). Cloning, functional expression, and characterization of recombinant pig liver esterase. Chembiochem **2**(7-8): 576-82.*

Leach, A.R. (2001). Molecular Modelling: priciples and applications. London, Pearson Education Limited.

*Lee, B. and F.M. Richards (1971). The interpretation of protein structures: Estimation of static accessibility. Journal of Molecular Biology **55**(3): 379-80.*

*Lee, M.-Y. and J.S. Dordick (2002). Enzyme activation for nonaqueous media. Current Opinion in Biotechnology **13**(4): 376-84.*

*Lee, S.B. and K.-I. Kim (1995). Effect of Water on enzyme Hydration and Enzyme Reaction Rate in Organic Solvents. Journal of Fermentation and Bioengineering **79**(5): 473-8.*

*Lee, T.S., J.D. Vaghjiani, G. Lye, J. and M.K. Turner (2000). A systematic approach to the large-scale production of protein crystals. Enzyme and Microbial Technology **26**(8): 582-92.*

*Legrand, L., I. Rosenman, F. Boue and M.C. Robert (2001). Effect of the substitution of light by heavy water on lysozyme KCl and $NaNO_3$ solubility. Journal of Crystal Growth **232**(6):244-9*

*Letisse, F., S. Lamare, M.-D. Legoy and M. Graber (2003). Solid/gas biocatalysis: an appropriate tool to study the influence of organic components on kinetics of lipase-catalyzed alcoholysis. Biochimica et Biophysica Acta (BBA) - Proteins & Proteomics **1652**(1): 27 - 34.*

*Levy, M. and P.R. Ocken (1969). Purification and properties of pig liver esterase. Archives in Biochemistry and Biophysics **135**(1): 259-64.*

*Liao, Y.-H., M.B. Brown, A. Quader and G.P. Martin (2002). protective mechanism of stabilizing excipients against dehydration in the freeze-drying of proteins. Pharmaceutical research **19**(12): 1854-61.*

*Liltorp, K., K.L. Jakobsen, O.F. Nielsen, H. Ramlov and P. Westh (2001). Bound water and cryptobiosis: Thermodynamic properties of water at biopolymer surfaces. Zoologischer Anzeiger **240**(6): 557-62.*

*Lind, P.A., R.M. Daniel, C. Monk and R.V. Dunn (2004). Esterase catalysis of substrate vapour: enzyme activity occurs at very low hydration. Biochimica et Biophysica Acta-Proteins and Proteomics **1702**(1): 103-10.*

*Liu, X.Q. and Y. Sano (1998). Effect of Na^+ and K^+ ions on the initial crystalization process of lysozyme in the presence of D_2O and H_2O. Journal of Protein Chemistry **17**(5): 479-84.*

*Longhi, S., F. Fusetti, R. Grandori, M. Lotti, M. Vanoni and L. Alberghina (1992). Cloning and nucleotide sequences of two lipase genes from Candida cylindracea. Biochimica et Biophysica Acta **1131**(2): 227-32.*

*Lopez, C., N.P. Guerra and M.L. Rua (2000). Purification and characterization of two isoforms from Candida rugosa lipase B. Biotechnology Letters **22**(16): 1291-4.*

*Ma, L., M. Pesson and P. Adlercreutz (2002). Water activity dependence of lipase catalysis in organic media explains successful transesterification reactions. Enzyme and Microbial Technology **31**(7): 1024-9.*

*MacKerell, A.D. (1998). Developments in the CHARMM all-atom empirical energy function for biological molecules. Abstracts of Papers of the American Chemical Society **216**: U696-U.*

*Makarov, V.A., B.K. Andrews, P.E. Smith and B.M. Pettitt (2000). Residence Time of Water Molecules in the Hydration sites of Myoglobin. Biophysical Journal **79**(6): 2966-74.*

*Martinelle, M., M. Holmquist and K. Hult (1995). On the interfacial activation of Candida antartica lipase A and B as compared with Humicola lanuginosa lipase. Biochimica et Biophysica Acta **1258**(3): 272-6.*

*Martinelle, M. and K. Hult (1995). Kinetics of acyl transfer reactions in organic media catalysed by Candida antartica lipase B. Biochimica et Biophysica Acta **1251**(2): 191-7.*

*May, J.C., R.M. Wheeler, N. Etz and D. Grosso (1991). Measurement of final container residual moisture in freeze-dried biological products. Developments in Biological Standardisation **74**: 153-64.*

McCammon, J.A. and S.C. Harvey (1987). Dynamics of proteins and nucleic acids. New York.

McPherson, A. (1989). Preparation and analysis of protein crystals., John Wiley & sons.

*Meiering, E.M. and G. Wagner (1995). Detection of Long-lived Bound Water Molecules in complexes of human Dihydrofolate Reductase with Methotrexate and NADPH. Journal of Molecular Biology **247**(2): 294-308.*

*Merzel, F. and J.C. Smith (2002). Is the first hydration shell of lysozyme of higher density than bulk water? Proceedings of the National Academy of Sciences of the United States of America **99**(8): 5378-83.*

*Meyer, E. (1992). Internal Water-Molecules and H-Bonding in Biological Macromolecules - a Review of Structural Features with Functional Implications. Protein Science **1**(12): 1543-62.*

*Miller, S., J. Janin, A.M. Lesk and C. Chothia (1987). Interior and surface of monomeric proteins. Journal of Molecular Biology **196**(3): 641 - 56.*

*Mingarro, I., C. Abad and L. Braco (1995). Interfacial activation-based molacular bioimprinting of lipolytic enzymes. Proceedings of the Natural Academy of Science of the United States of America **92**(8): 3308-12.*

*Mitra, S.P. and D.K. Chattoraj (1978). Thermal Stability & Excess Free Energy of Hydration of Bovine Serum Albumin in the Presence of Neutral Salts. Indian Journal of Biochemistry & Biophysics **15**(4): 239-44.*

*Modig, K., E. Liepinsh, G. Otting and B. Halle (2004). Dynamics of protein and peptide hydration. Journal of the American Chemical Society **126**(1): 102-14.*

*Nakagawa, H., Y. Joti, A. Kitao and M. Kataoka (2008). Hydration affects both harmonic and anharmonic nature of protein dynamics. Biophysical Journal **95**(6):2916-23*

*Nie, K., F. Xie and T. Tan (2006). Lipase-catalyzed methanolysis to produce biodiesel: Optimization of the biodiesel production. Journal of molecular Catalysis B: Ezymatic **43**(1-4): 142-7.*

*O'Brien, M.A. (1948). The control of humidity by saturated salt solution. Journal of Scientific Instruments **25**: 73-6.*

*Parak, F. and E.W. Knapp (1984). A consistent picture of protein dynamics. Proceedings of the National Academy of Science of the United States of America. **81**(22): 7088-92.*

*Parker, M.C., B.D. Moore and A.J. Blacker (1995). Measuring enzyme hydration in nonpolar organic solvents using NMR. Biotechnology and Bioengineering **46**(5): 452-8.*

*Partridge, J., P.R. Dennison, B.D. Moore and P.J. Halling (1998). Activity and mobility of subtilisin in low water organic media: hydration is more important than solvent dielectric. Biochimica Et Biophysica Acta-Protein Structure and Molecular Enzymology **1386**(1): 79-89.*

*Phillips, G.N.J. and B.M. Pettitt (1995). Structure and dynamics of the water around myoglobin. Protein Science **4**(2): 149-58.*

*Poole, P.L. and J.L. Finney (1983). Hydration-induced conformational and flexibility changes in lysozyme at low water content. International Journal of Biological Macromolecules **5**(5): 308-10.*

*Provencher, L. and J.B. Jones (1994). A Concluding Specification of the Dimensions of the Active-Site Model of Pig-Liver Esterase. Journal of Organic Chemistry **59**(10): 2729-32.*

*Provencher, L., H. Wynn, J.B. Jones and A.R. Krawczyk (1993). Enzymes in Organic-Synthesis .51. Probing the Dimensions of the Large Hydrophobic Pocket of the Active-Site of Pig-Liver Esterase. Tetrahedron-Asymmetry **4**(9): 2025-40.*

*Rasmussen, B.F., A.M. Stock, D. Ringe and G.A. Petsko (1992). Crystalline ribonuclease A loses function below the dynamical transition at 220 K. Nature **357**(6377): 423-4.*

*Reat, V., R.V. Dunn, M. Ferrand, J.L. Finney, R.M. Daniel and J.C. Smith (2000). Solvent dependence of dynamic transitions in protein solutions. PNAS **97**(18): 9961-6.*

*Rich, J.O., V.V. Mozhaev, J.S. Dordick, D.S. Clark and Y.L. Khmelnitsky (2002). Molecular imprinting of enzymes with water-insoluble ligands for nonaqueous biocatalysis. Journal of the American Chemical Society **124**: 5254-5.*

*Roh, J.H., J.E. Curtis, S. Azzam, V.N. Novikov, I. Peral, Z. Chowdhuri, R.B. Gregory and A.P. Sokolov (2006). Influence of hydration on the dynamics of Lsozyme. Biophys J. **91**(7): 2573-80.*

*Roh, J.H., V.N. Novikov, R.B. Gregory, J.E. Curtis, Z. Chowdhuri and A.P. Sokolov (2005). Onsets of anharmonicity in protein dynamics. Phys Rev Lett. **95**(3): 038101.*

*Ru, M.T., J.S. Dordick, J.A. Reimer and D.S. Clark (1998). Optimizing the salt-induced activation of enzymes in organic solvents: effects of lyophilisation time and water content. Biotechnology and Bioengineering **63**(2): 233-41.*

*Rua, L., T. Diaz-Maurino, V.M. Fernandez, C. Otero and A. Ballesteros (1993). Purification and characterization of two distinct lipases from Candida cylindracea. Biochimica et Biophysica Acta **1156**(2): 181-9.*

*Rua, M.L., T. Diaz-Maurino, C. Otero and A. Ballesteros (1992). Isoenzymes of lipase from Candida cylindracea. Studies related to carbohydrate composition. Ann N Y Acad Sci. **672**: 20-3.*

*Rupley, J.A. and G. Careri (1988). Enzyme hydration and function. The enzyme catalysis process: Energetics, Mechanism and Dynamics. A. Cooper. Glasgow, Plenum Press**:** 223-34.*

*Rupley, J.A. and G. Careri (1991). Protein hydration and function. Advances in protein chemistry. **41:** 37-172.*

*Rupley, J.A., E. Gratton and G. Careri (1983). Water and globular proteins. Trends in Biochemical Sciences **8**(1): 18-22.*

*Rupley, J.A., P.-H. Yang and G. Tollin (1980). Thermodynamic and Related Studies of Water Interacting with Protein. Water in polymers. S. P. Roland, American Chemical Society. **ACS symposium series 127:** 111-32.*

*Russell, A.J. and A.M. Klibanov (1988). Inhibitor-induced enzyme activation in organic solvents. The Journal of Biological Chemistry **263**(24): 11624-6.*

*Russo, D., G. Hura and T. Head-gordon (2004). Hydration dynamics near a model protein surface. Biophysical Journal **86**(3): 1852-62.*

*Sei, Y., S. Shimotakahara, J. Ishii, H. Shindo, H. Seki, K. Yamaguchi and M. Tashiro (2005). Observation of water molecules bound to a protein using cold-spray ionization mass spectrometry. Analytical Sciences **21**(4): 449-51.*

*Seligmann, E.B.J. and J.F. Farber (1971). Freeze drying and residual moisture. Cryobiology **8**(2): 138-44.*

*Shibata, M., N. Muneda, K. Ihara, T. Sasaki, M. Demura and H. Kandori (2004). Internal water molecules of light-driven chloride pump proteins. chemical physics letters **392**(4-6): 330-3.*

*Shnyrov, V.L., L. Diez Martinez, M.G Roig, A.E. Lyubarev, B.I. Kurganov, E. Villar (1999). Irreversible thermal denaturation of lipase B from Candida rugosa. Thermochimica Acta **325**(7):143-9.*

*Skujins, J.J. and A.D. McLaren (1967). Enzyme Reaction Rates at Limited Water Activities. Science **158**(3808): 1569-70.*

*Slade, C.J. (2000). Molecular (or bio-) imprinting of bovine serum albumin. Journal of molecular Catalysis B: Ezymatic **9**: 97-105.*

*Smith, A.L., H.M. Shirazi and S.R. Mulligan (2002). Water sorption isotherms and enthalpies of water sorption by lysozyme using the quartz crystal microbalance/heat conduction calorimeter. Biochimica et Biophysica Acta (BBA) - Protein Structure and Molecular Enzymology **1594**(1): 150-9.*

*Smith, J.C., F. Merzel, C.S. Verma and S. Fischer (2002). Protein hydration water: Structure and thermodynamics. Journal of Molecular Liquids **101**(1-3): 27-33.*

*Steim, J.M. (1965). Differential Thermal Analysis of Protein Denaturation in Solution. Archives in Biochemistry and Biophysics **112**(3): 599-604.*

*Stevens, E. and L. Stevens (1979). The effect of restricted hydration on the rate of reaction of glucose-6-dehydrogenase, phosphoglucose isomerase, hexokinase and fumarase. Biochemitry J. **179**: 161-7.*

Stryer, L. (1999). Biochemistry. New York, W.H. freeman and Company.

*Suzuki, M., J. Shigematsu and T. Kodama (1996). Hydration Study of Proteins in Solution by Microwave Dielectric Analysis. Journal of Physical Chemistry **100**(17): 7279-82.*

*Svergun, D.I., S. Richard, M.H.J. Koch, Z. Sayers, S. Kuprin and G. Zaccai (1998). Protein hydration in solution: Experimental observation by x-ray and neutron scattering. Proceedings of the National Academy of Sciences of the United States of America **95**(5): 2267-72.*

*Takano, K., J. Funahashi, Y. Yamagata, S. Fuji and K. Yutani (1997). Contribution of Water in the Interior of a Protein to the Conformational Stability. Journal of Molecular Biology **274**(1): 132-42.*

*Teller, D.C. (1976). Accessible area packing volumes and interaction surfaces of globular proteins. Nature **260**(5553): 729-31.*

*Tournier, A.L., V. Reat, R. Dunn, R. Daniel, J.C. Smith and J. Finney (2005). Temperature and timescale dependence of protein dynamics in methanol: water mixtures. Physical Chemistry Chemical Physics **7**(7): 1388-93.*

*Tournier, A.L., J.C. Xu and J.C. Smith (2003). Translational hydration water dynamics drives the protein glass transition. Biophysical Journal **85**(3): 1871-5.*

*Toussignant, A. and J.N. Pelletier (2004). Protein Motions Promote Catalysis. Chemistry & Biology **11**(8): 1037-42.*

*Trusell, F. and H. Diehl (1963). Efficiency of Chemical Desiccants. Analytical Chemistry **35**(6): 674-7.*

*Tsai, A.M., D.A. Neumann and L.N. Bell (2000). Molecular Dynamics of Solid-State Lysozyme as Affected by Glycerol and Water: A Neutron Scattering Study. Biophysical Journal **79**(5): 2728-32.*

*Turner, N.A., E.C. Needs, J.A. Khan and E.N. Vulfson (2001). Analysis of conformational states of Candida rugosa lipase in solution: implications for mechanism of interfacial activation and separation of open and closed forms. Biotechnology and Bioengineering **72**(1): 108-18.*

*Valivety, R.H., P.J. Halling and A.R. Macrae (1992). Reaction rate with suspended lipase catalyst shows similar dependence on water activity in different organic solvents. Biochimica et Biophysica Acta **1118**(3): 218-22.*

*Valivety, R.H., P.J. Halling and A.R. Macrae (1992). Rhizomucor miehei lipase remains highly active at water activity below 0.0001. Febs Letters **301**(3): 258-60.*

*Valivety, R.H., P.J. Halling, A.D. Peilow and A.R. Macrae (1992). Lipases from different sources vary widely in dependence of catalytic activity on water activity. Biochimica et Biophysica Acta **1122**(2): 143-6.*

*Williams, M.A., J.M. Goodfellow and J.M. Thornton (1994). Buried Waters and Internal Cavities in Monomeric Proteins. Protein Science **3**(8): 1224-35.*

*Wood, K., U. Lehnert, B. Kessler, G. Zaccai and D. Oesterhelt (2008). Hydration dependence of active core fluctuations in bacteriorhodopsin. Biophysical Journal **95**(1): 194-202.*

*Yang,C.R., B.E. Shapiro, E.D. Mjolsness and G.W. Hatfield (2005). An enzyme mechanism language for the mathematical modeling of metabolic pathways. Bioinformatics **21**(6):774-780.*

*Yang, F.X. and A.J. Russell (1995). The Role of Hydration in Enzyme Activity and Stability: 1. Water Adsorption by Alcohol Dehydrogenase in a Continuous Gas Phase Reactor. Biotechnology and Bioengineering **49**(6): 700-8.*

*Yang, F.X. and A.J. Russell (1996). The role of hydration in enzyme activity and stability .2. Alcohol dehydrogenase activity and stability in a continuous gas phase reactor. Biotechnology and Bioengineering **49**(6): 709-16.*

*Yang, P.-H. and J.A. Rupley (1979). Protein-water interactions. Heat Capacity of the Lysozyme-water system. American Chemical Society **18**(12): 2654-61.*

*Zaccai, G. (1999). Neutron scattering in Biology in 1998 and beyond. Journal of Physics and Chemistry of Solids **60**(8-9): 1291-5.*

*Zaccai, G. (2000). Biochemistry - How soft is a protein? A protein dynamics force constant measured by neutron scattering. Science **288**(5471): 1604-7.*

*Zacharis, E., P.J. Halling and G. Rees (1999). Volatile buffers can override the "pH memory" of subtilisin catalysis in organic media. Proceedings of the Natural Academy of Science of the United States of America **96**(4): 1201-5.*

*Zaks, A. and A.M. Klibanov (1988). Enzymatic catalysis in nonaqueous solvents. The Journal of Biological Chemistry **263**(7): 3194-201.*

*Zanotti, J.M., M.C. Bellissent-Funel and J. Parello (1999). Hydration-coupled dynamics in proteins studied by neutron scattering and NMR: The case of the typical EF-hand calcium-binding parvalbumin. Biophysical Journal **76**(5): 2390-411.*